PL ISSN 0028-3894

STOWARZYSZENIE
NEUROPATOLOGÓW POLSKICH

NEUROPATOLOGIA POLSKA

TOM 20 1982 ZESZYT 1—2

WROCŁAW · WARSZAWA · KRAKÓW · GDAŃSK · ŁÓDŹ
ZAKŁAD NARODOWY IM. OSSOLIŃSKICH
WYDAWNICTWO POLSKIEJ AKADEMII NAUK

NEUROPATOLOGIA POLSKA

KWARTALNIK

TOM 20 1982 ZESZYT 1—2

ADRES REDAKCJI

Centrum Medycyny Doświadczalnej i Klinicznej Polskiej Akademii Nauk,
ul. Dworkowa 3, 00—784 Warszawa, tel. 49-82-79, 49-70-18

Wydano z pomocą finansową Polskiej Akademii Nauk

The present issue of "Neuropatologia Polska" contains the papers read at the IVth Conference of the Polish Association of Neuropathologists, held in Poznań. It was intended initially to publish these materials separately as "Conference Proceedings". Unfortunately, for reasons beyond the editor's control, this could not be achieved. Therefore, and considering the papers as still retaining their scientific value, the editors have decided to publish them in a current issue of "Neuropatologia Polska". The editors express their apologies to the authors for the regretful delay.

NEUROPAT. POL., 1982, 20, 1—2
PL ISSN 0028—3894

MIECZYSŁAW WENDER, MIROSŁAW KOZIK, OLGA MUSZYŃSKA

HISTOCHEMISTRY OF NEUROGLIAL ENZYMES IN THE DEVELOPING RABBIT OPTIC NERVE *

Institute of Diseases of the Nervous System and Sensory Organs, School of Medicine, Poznań

The optic nerves are known for their particular sensitivity towards the action of various noxious agents, as evidenced by the high frequency of changes occuring there in the course of various demyelinating lesions. The elucidation of the selectively high sensitivity fibres of the optic nerves cells for a through understanding of events connected with the process of myelinogenesis in this very structure of the central nervous system.

From the evidence obtained from various regions of the brain it appears that myelination gliosis, the event preceding and accompanying myelinogenesis, is characterised by a considerable increase of activity of various phosphatases and in some species also of oxidoreductases involved in glycolysis, the citric acid cycle and the pentose phosphate shunt (Wender, Kozik, 1968; Wender et al., 1970; 1975). On the other hand, Blunt et al. (1971) were unable to demonstrate a positive correlation between the increase of activity of various oxidoreductases in the optic nerves of kittens and its myelination or the differentiation of glial cells belonging to the oligodendroglial line. It thus would appear that data pertaining to the process of myelinogenesis in other cerebral structures is not necessarily applicable in every detail to events occurring in the optic track.

Hence, we have undertaken a systematic study of morphological and chemical events occurring in the optic tract of the maturating brain. Histochemical investigations concerned with the activity of various phosphatases, esterases and oxidoreductases in the developing optic nerve constituted an essential part of this study, and their results are presented and discussed below.

---

* This investigation was supported by NIH PL 480, Research Agreement No. 05—092—N.

MATERIAL AND METHODS

Investigations were performed on Chinchilla rabbits of both sexes. The experimental animals were divided into 5 age groups, each consisting of 6 rabbits, i.e. into animals aged 3, 12, 30, 70 and 180 days postnatal.

The animals were killed by decapitation, the brain being removed instantly and the optic nerves dissected and subjected to investigations. Histological and histoenzymatic examinations were performed on sections fixed for 18 h at 4°C in Baker's solution. Oxidative enzyme assays were performed on fresh cryostat sections, 12 μm in thickness.

Activities of the following oxidoreductases were assayed: glycerol-3-phosphate dehydrogenase (1-glycerol-3-phosphate: NAD oxidoreductase — E.C.1.1.1.8.) — incubation time 20 min., lactate dehydrogenase — LDH (1-lactate: NAD oxidoreductase — E.C.1.1.1.27.) — incubation time 50 min., 3-hydroxybutyrate dehydrogenase (D-3-hydroxybutyrate: NAD — oxidoreductase — E.C.1.1.1.30.) — incubation time 60 min., glucose-6-phosphate dehydrogenase (D-glucose-6-phosphate: NAD P oxidoreductase — E.C.1.1.1.49.) — incubation time 30 min. succinate dehydrogenase (succinate: acceptor-oxidoreductase — E.C.1.3.99.1.) — incubation time 30 min. threo-D-isocitrate: NAD — E.C.1.1.1.41. (decarboxylating--iso-citric-dehydrogenase) — incubation time 35 min., reduced NADP: tetrazolium dehydrogenase (reduced NADP: acceptor-oxidoreductase — E.C.1.6.99.1.) — incubation time 30 min., reduced NAD: tetrazolium dehydrogenase (reduced NAD: acceptor-oxidoreductase — E.C.1.6.99.3.) — incubation time 35 min.

The individual dehydrogenase activities, were assayed in the basal incubation medium described by Pearse (1960) with Nitro BT tetrazolium salt and appropriate substrate as recommended by Niweliński (1963). Activities of the following hydrolases were studied using 15 μm thick frozen sections. The activities of acid phosphatase (acP, orthophosphoric monoester phosphohydrolase — 3.1.3.2.) and of alkaline phosphatase (alkP, orthophosphoric monoester phosphohydrolase — 3.1.3.1.) were assayed according to the Gomori method (1953). Thiamine pyrophosphatase (TPP-ase, thiamine phosphate pyrophosphgorylase — 2.5.1a) was demonstrated using the Novikoff and Goldfischer method (1961) and adenosinetriphosphatase (ATP-phosphohydrolase — 3.6.1.3.) with the Wachstein and Meisel method (1957). For estimation of unspecific esterase (carboxyl-ester hydrolase — 3.1.1.1.) the Barnett and Seligman method (1951), as modified by Holt (1956) was employed. Acetylcholinesterase (AChE — 3.1.1.7.) as well as unspecific cholinesterase (ChE — 3.1.1.8.) were assayed according to Koelle as modified by Gerebtzoff (1953).

RESULTS

Developmental changes of oxidoreductases

Glycerophosphate dehydrogenase (GDP). In the optic nerve of 3 day animals GDP could not be demonstrated. In the next experimental group, however, distinct intracytoplasmic GDP activity was detectable in a good many glial cells of the optic nerve. The intensity of staining as well as the number of reactive cells were increased in still older animals (30- and 70-day rabbits), but in the latter group of animals,it was the interfascicular oligodendroglia which showed GDP activity (Fig. 1). In adult animals (180 days), activity was demonstrable in a certain part of glial cells of the optic nerve and even then these cells were considerably less reactive than those of the younger animals.

Fig. 1. Rabbit optic nerve, 70 days postnatal. Generalized reaction for α-glycerophosphate dehydrogenase in the interfascicular oligodendroglia and in capillary walls. × 90

Glucose-6-phosphate dehydrogenase (G-6-PDH). Neuroglial activity of G-6-PDH could only be demonstrated in the optic nerve of adult rabbits (180 days). The preceding developmental stages, including the period of active myelination were without influence on this enzyme activity. The capillary walls of the optic nerve were distinctly reactive with respect to G-6-PDH independently of the age of the donor animal.

Isocitrate dehydrogenase (ICDH). The histoenzymatic reaction for ICDH performed on the optic nerve of 3 and 12 day rabbits was negative. The specimens of the 30-day animals instead displayed considerable activity of ICDH in the neuroglia (Fig. 2). The optic nerves of 70-day animals showed a positive reaction for ICDH, which was distributed both in the epitelium of capillaries and in the neuroglia. Staining observed in the neuroglia was of considerable intensity. The optic nerves of adult animals displayed a histoenzymatic pattern comparable to that observed in the former age group.

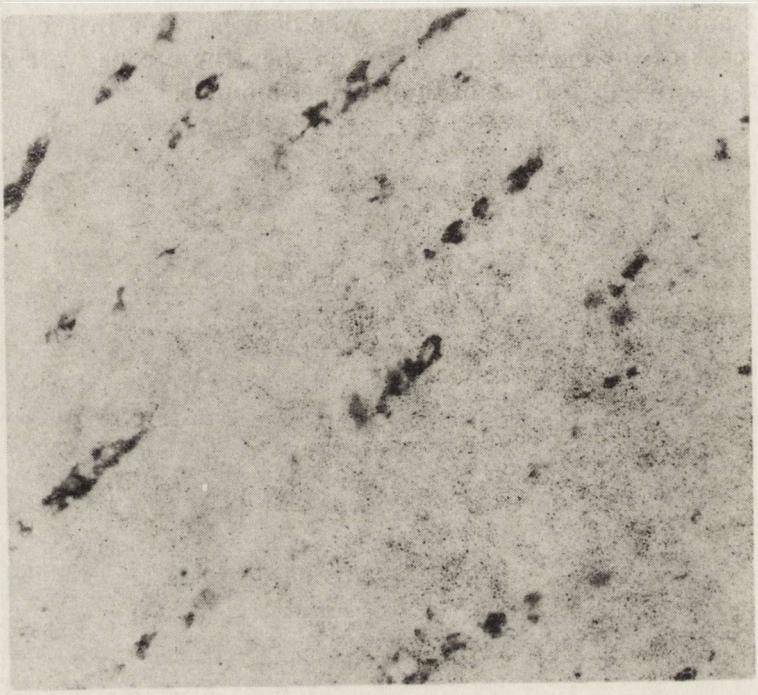

Fig. 2. Rabbit optic nerve, 30 days postnatal. Many neuroglial cells show isocitrate dehydrogenase activity of variable intensity. × 250

Succinate dehydrogenase (SDH). The neuroglia of the optic nerves of 3-day old rabbits did not react to SDH. In the next two age groups (12- and 30-day animals) weak staining for SDH was seen in the neuroglia of the optic nerves, but with advancement of the animals' age the altogether weak neuroglial SDH activity seemed to disappear completely. However, single oligodendroglial cells had a distinctly stronger reaction than the remainder, thus standing out from their surroundings.

Hydroxybutyrate dehydrogenase. In neuroglia of the optic nerve hydroxybutyrate dehydrogenase could not be demonstrated in any of the investigated age groups of animals.

NADH-tetrazolium dehydrogenase. A positive reaction was first ob-

served in the neuroglia of the optic nerve of 12-day old animals. In the younger animals (3-day) neuroglia was unreactive. With the advance of the postnatal age the activity of neuroglia towards NADH dependent reduction of tetrazolium salts tended to increase until the age of 30 days (Fig. 3) to remain at this level until adulthood. A positive reaction was and seen also in capillary walls.

Fig. 3. Distribution of reduced NAD-dependent tetrazolium dehydrogenase activity in the rabbit optic nerve, 30 days postnatal. Enzyme reaction products located in capillary walls and in many neuroglial cells. × 100

NADP-H: tetrazolium dehydrogenase. The activity and distribution of NADP-H dependent tetrazolium dehydrogenase in the developing rabbit optic nerve was entirely comparable to that observed for the NADH — dependent enzymic reaction.

Developmental changes of hydrolytic enzyme activities

Acid phosphatase (acP). The neuroglia of the rabbit optic nerve did not react to acP throughout the whole period of investigation.

Alkaline phosphatase (alkP). In the 3-day old animals age group, alkP was not demonstrable in the optic nerve. At the age of 12 days postnatal, reaction products for alkP were demonstrable within neuronal axons, the neuroglia remaining unreactive. A similar distribution of

alkP activity was observed in the optic nerves of older animals, where distinct enzyme activity was located in myelinated axons, the neuroglia instead lacking any reaction products.

Adenosinetri phosphohydrolase (ATP-ase). In the optic nerves of 3-day old rabbits ATP-ase activity could not be demonstrated. At the age of 12 days postnatal, a positive reaction was displayed by capillary walls, the neuroglia remaining still unreactive. In the nerves of 30-day old animals — a slight ATP-ase activity was also demonstrable in the neuroglia. The neuroglial reaction for ATP-ase in 70-day old rabbits was decidedly higher, than that observed in the younger animals (Fig. 4). However, at the age of 180 days postnatal, the glial cells of the optic nerve were again unreactive.

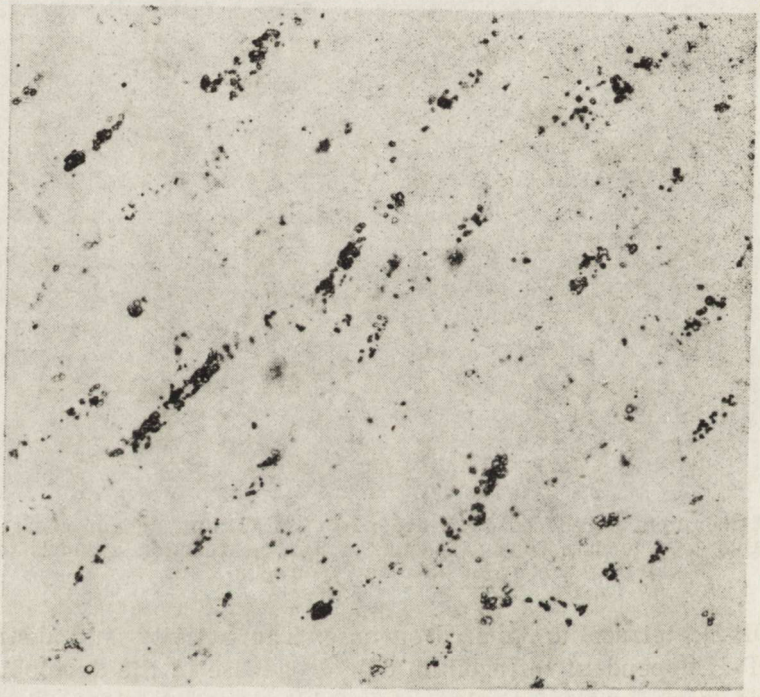

Fig. 4. Rabbit optic nerve, 70 days postnatal. Neuroglial cells showing an intense staining for ATP-ase. × 100

Thiamine pyrophosphatase (TPP-ase). TPP-ase activity was not demonstrable until the age of 12 days postnatal, when distinct enzyme activity was seen in both the capillary walls and in the differentiating neuroglia. The neuroglial TPP-ase activity of the optic nerve of animals aged 30 days was distinctly higher compared with the younger age group (Fig. 5) and remained at comparable level in 70-day old animals. The neuroglial histoenzymic reaction for TPP-ase in the optic nerve of adult rabbits, however, was markedly lessened, showing only a weak

staining. In contrast to this, the capillary walls were intensely stained.

Nonspecific esterase. The neuroglia of the optic nerve remained unreactive with respect to nonspecific esterase throughout the whole period of investigation. Microgranular deposits of enzyme reaction products were located along the nerve fibres.

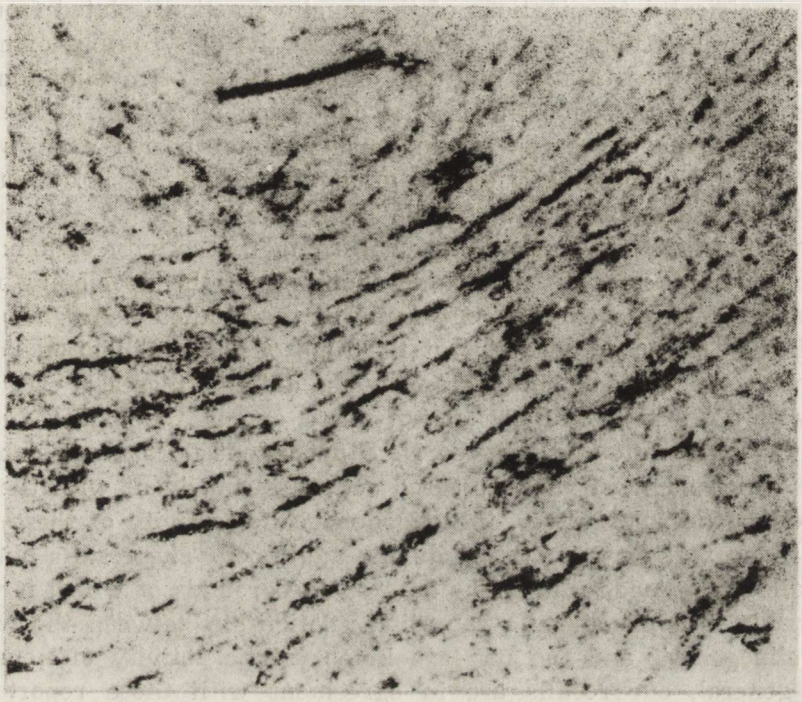

Fig. 5. Histoenzymic reaction for TPP-ase. Rabbit optic nerve, 30 days postnatal. Strong enzymic activity in capillary walls, the neuroglia considerably less reactive. × 90

Acetylcholinesterase (AChE). AChE activity could not be demonstrated in the rabbit optic nerve.

Butyrylcholinesterase. Glial cells of the rabbit optic nerve lacked butyrylcholinesterase activity. The myelinated nerve fibres instead were positively, though weakly, stained in 12-days old animals. In rabbits aged 30 days the reaction for the enzyme was still high.

DISCUSSION

Blunt et al. (1971) found that myelinated nerve fibres appear in the kitten optic nerve significantly preceding the differentiation of the oligodendroglia, and also in advance of the increased oxidoreductase activity accompanying glial differentiation.

Ultrastructural studies performed by Śniatała-Kamasa (1978) on the rabbit optic nerve showed that at the age of 3 days postnatal only

unmyelinated axons of small diameter may be seen. In 12-day old rabbits the axons of the optic nerve are enveloped by a few loosely adhering myelin lamellae. Further development is characterized by enlargement of the axonal diameter and increase of the number of surrounding myelin lamellae. A quantitative evaluation of the process of myelin deposition was attempted by Pankrac (1978), who on the base of gravimetrical determinations of the myelin fraction isolated from the developing rabbit optic nerve, tried to assess the daily output of myelin formation and thus to determine the onset and top of myelination. The results of her study have shown that deposition of myelin in the optic nerve takes place over the whole developmental period even beyond adulthood, the highest daily output of myelin formation, i.e. the top of myelination falling to the age of 30 days postnatal.

From the histoenzymatic study concerning the activity of a number of phosphatases, esterases and oxidoreductases of the developing rabbit optic nerve it appeared that only some of the studied neuroglial enzymes showed enhanced activities at the time of the myelination peak.

Among the various phosphatases — a definite increase was noted only with respect to TPP-ase activity, and among the oxidoreductases there were isocitrate and reduced NAD-dependent tetrazolium dehydrogenase which demonstrated increased activities coincident with the peak of myelinogenesis. However, the oligodendroglial activity of these enzymes had no tendency to decline during adulthood. The results obtained thus failed to provide convincing data on the grounds of which it would be possible to demonstrate a causative relationship between the process of myelinogenesis and the increase in enzymatic activity of neuroglia.

In general, our results are in agreement with those reported by Blunt et al. (1971) for the optic nerve of kittens. Our results, however, have demonstrated considerable differences in the neuroglial histoenzymatic activity during the process of myelinogenesis between the optic nerve and other brain regions. The differentiating cells of myelination gliosis of the rabbit white matter displayed distinctly increased activity of oxidoreductive enzymes compared to the immature neuroglia of the very early period of postnatal development, without however, any prevalence of enzymes acting within a particular metabolic pathway as pentose shunt, glycolysis or Krebs cycle (Wender et al., 1975). The same may be stated with respect to the activity of various phosphatases. Unlike the optic nerve, the neuroglial cells of the developmental myelination gliosis showed distinctly increased reactivity with respect to acP, ATP-ase and TPP-ase (Wender et al., 1969).

These findings point to the optic nerve as a structure of the central nervous system which differs from other brain regions with respect to histoenzymatically detectable events accompanying the process of myelinogenesis.

This conclusion, however, is difficult to understand in the light of morphological developmental studies. The optic nerve of mammals originates in the course of embryonic development as a diverticulum projecting from the lateral part of the diencephalon. The lumen of the optic stock is composed from stem cells, forming a neuroectodermal matrix layer yielding all the glia of the optic nerve (Vaughn, 1969). The matrix cells of the fetal optic nerve resemble closely those found in other parts of the immature brain (Lyser, 1961; Wechsler, 1966), and those of the developing optic nerves give rise to both astrocytes and oligodendrocytes. However, some small glioblasts are retained in fully mature optic nerves as the third type of neuroglia. Also the most acceptable concept of myelinogenesis in the optic nerve does not differ from that acknowledged for other parts of the central nervous system. According to this view the mature or immature glial cells of the oligodendrocyte line send out numerous cytoplasmic extensions of their plasma membranes and connect with numerous axons (Peters, 1964; Peters, Proskaner, 1969). The only exception from this viewpoint is that raised by Wendell-Smith and co-workers (1966), according to which, in the optic nerve of kittens lacking oligodendroglial cells, this is the astrocyte population of lamina cribrosa which is responsible for the formation of myelin sheaths in this particular region. On the other hand, there are suggestions (Vaughn, 1969) that there exist morphological differences between active and mature oligodendrocytes. The dispersed appearances of nuclear chromatin may reflect high levels of synthetic activity in active oligodendrocytes during myelinogenesis.

Based on our studies performed on several animal species and human beings we would like to advocate this view, adding that one of the most significant exponents of the active oligodendroglia is its enzymatic pattern characterised by the marked enhancement of activity of several phosphatases and oxidoreductases. This was not the case in the course of myelinogenesis in the optic nerve. In our previous works we have stressed species differences in the enzymatic pattern of active neuroglial cells in the course of myelinogenesis. From the actual studies it may be inferred that regional differences should also be taken into account when discussing the problem of enzymic activity of neuroglial cells during active myelination of nervous fibres.

REFERENCES

1. Barnett R., Seligman A.: Histochemical demonstration of esterases by production of Indigo. Science, 1951, 194, 2970—2971.
2. Blunt M., Paisley P., Wendell-Smith C.: Oxidative enzyme histochemistry of immature neuroglia during myelination. J. Anat., 1971, 110, 421—433.
3. Gerebtzoff M.: Recherches histochimiques sur les acétylcholine et choline esterase. Acta anat., 1953, 19, 336—339.

4. Gomori G.: Microscopic histochemistry. The University of Chicago Press, Chicago 1953.
5. Holt S.: The value of fundamental studies of staining reactions enzyme in histochemistry, with reference to indoxyl methods for esterases. J. Histochem. Cytochem., 1956, 4, 94—99.
6. Lyser K.: Early differentiation of motor neuroblasts in the chick embryo as studied by electron microscopy. Develop. Biol., 1968, 17, 117—142.
7. Niweliński J.: Dehydrogenazy. In: Script of histochemical methods. Warszawa 1963, 171—198.
8. Novikoff A., Goldfischer B.: Nucleoside diphosphatase activity in the Golgi apparatus and its usefulness for cytological studies. Proc. Nat. Acad. Sci., 1961, 47, 802—810.
9. Pankrac J.: The deposition of myelin in the developing rat brain with special reference to late periods of postnatal development. Abstracts of IV Neuropathological Conference, Poznań, 1978, 101.
10. Pearse A.: Histochemistry, theoretical and applied. Churchill, London 1960.
11. Peters A.: Observations on the connexions between myelin sheaths and glial cells in the optic nerve of young rats. J. Anat. (Lond.), 1964, 98, 125—134.
12. Peters A., Proskauer C.: The ratio between myelin segments and oligodendrocytes in the optic nerve of the adult rat. Anat. Rec., 1969, 163, 243.
13. Śniatała-Kamasa M.: Ultrastructural picture of the optic nerve in the rabbit during ontogenic development. Abstracts of the IV Neuropathological Conference, Poznań 1978, 127.
14. Vaughn J.: An electron microscopic analysis of gliogenesis in rat optic nerves. Z. Zellforsch., 1969, 94, 293—324.
15. Wachstein M., Meise E.: Histochemistry of hepatic phosphatases of a physiologic pH, with special reference to the demonstration of bile canaliculi. Amer. J. Clin. Pathol., 1957, 27, 13—23.
16. Wechsler W.: Feinstruktur des Neuralrohres und der neuroektodermalen Matrixzellen am Zentralnervensystem von Hühnerembryonen. Z. Zellforsch., 1966, 70, 240—268.
17. Wendell-Smith C., Blunt M., Baldwin F.: The ultrastructural characterisation of macroglial cell types. J. comp. Neurol., 1966, 127, 219—240.
18. Wender M., Kozik M.: Histochemistry of cerebral white matter in relation to myelination of mouse brain. J. Hirnforsch., 1968, 10, 83—92.
19. Wender M., Kozik M., Mularek O.: Histochemistry of oxidative enzymes in the neuroglia in course of myelination. Acta anat., 1975, 91, 83—96.
20. Wender M., Kozik M., Owsianowski M.: A histoenzymatic study of neuroglia during myelination of the rabbit brain. Folia Histochem. Cytochem., 1969, 7, 135—150.
21. Wender M., Kozik M., Wojciechowski T.: Contribution to the enzyme histochemistry of the cerebral white matter in the developing human brain. Biol. Neonate, 1970, 15, 8—18.

The authors' address: Prof. M. Wender — Department of Neurology, School of Medicine. 49 Przybyszewski Str., 60—355 Poznań, Poland

NEUROPAT. POL., 1982, 20, 1—2
PL ISSN 0028—3894

MARIA ŚNIATAŁA-KAMASA

ULTRASTRUCTURAL PICTURE OF THE OPTIC NERVE IN RABBIT DURING ONTOGENETIC DEVELOPMENT *

Institute of Diseases of Nervous System and of Sensory Organs, School of Medicine, Poznań

The optic nerve, similar to the olfactory nerve, is not a real nerve but an expansion of the brain alone and appears as a fibre pathway ranging from the retina to the diencephalon. It runs from the orbit throughout the canalis opticus and enters the cranium cavity.

It was reported previously that the optic nerve in rats is devoid of myelin and oligodendroglia at the birth. Myelin formation in this region is not complicated by the migration of undifferentiated glia from a distant germinal matrix and the outgrowth of axons from neurons other than those in the retina. Vaughn (1969) emphasized that a glial cell can be readily identified in this area because all of the undifferentiated cells are presumably glial precursors.

The studies on gliogenesis and myelinogenesis performed in rats (Vaughn, 1969; Hirose, Bass, 1973; Skoff et al., 1976) have shown that the optic nerve is a useful model for both ultrastructural and biochemical investigations. In our laboratory comparative studies were undertaken on the optic nerve in another animal namely in the rabbit. The purpose of this investigations is to abtain data which could become the framework for the examination of experimental models in which the myelin sheath of the optic nerve is damaged.

MATERIAL AND METHODS

Intracranial portions of the rabbit optic nerve taken on the 3rd, 12th, 30th and 70th day after birth were fixed by immersion in glutaraldehyde and paraformaldehyde solution according to Karnovsky's fixative (1965) and postfixed in osmium tetroxide. The specimens were

* This investigation was supported by NIH PL 480. Research Agreement No. 05-092-N.

dehydrated in a graded series of ethanol and embedded in Epon. Ultrathin sections were counterstained with uranyl acetate and lead citrate and examined in a JEM-7A electron microscope.

RESULTS

By the 3rd postnatal day the elements of the rabbit optic nerve consist of astroblasts, undifferentiated glial cells and unmyelinated axons of small diameters (Fig. 1). Astroblasts have a large pale nucleus, in which chromatin does not form heavy aggregations. The cytoplasm of these cells has an electron lucent appearance and contains few filaments, scanty microtubules, free polyribosomes, few short cisterns of rough endoplasmic reticulum and mitochondria. Long-shaped mitochondria often appear in this type of cell. Axons of small diameter are abundantly present. Glioblast processes divide axons into bundles. Giant axons occur accidentally. Their diameter is many times greater than that of other axons. They are wrapped by several (as many as five) — loosely arranged myelin lamellae (Fig. 2). Cytoplasm of glioblasts con-

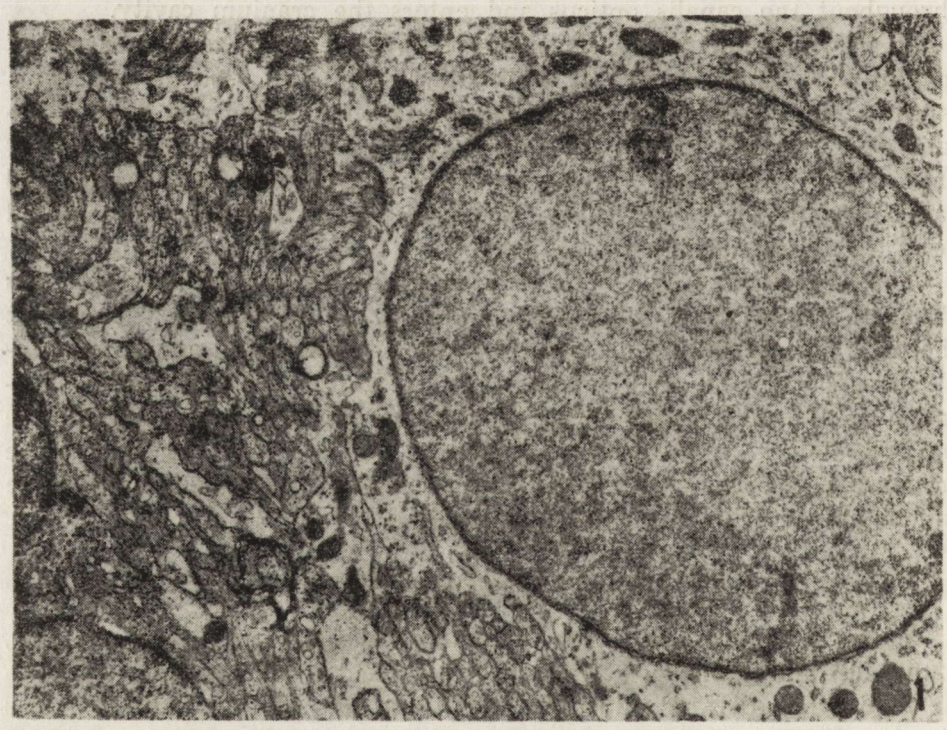

Fig. 1. 3 days postnatal. Astroblast with large, pale nucleus in which heterochromatin does not form heavy aggregations. Their cytoplasm with an electron-lucent appearance and few filaments, single microtubules, free polyribosomes, few short cisternae of rough endoplasmic reticulum and mitochondria. Unmyelinated axons of a small size. × 8 000

Fig. 2. 3 days postnatal. Giant axons in the neighbourhood of two glioblasts. Giant axons are wrapped by several — as many as five — loosely arranged myelin lamellae. × 8 000

tains numerous free polyribosomes, few rough endoplasmic reticulum, filaments, microtubules and Golgi apparatus. Their nuclei are oval and folded; clumped chromatin masses are not seen. Astroglial end-feet are distributed around blood vessels the walls of which are composed of endothelial cells and narrow basement membrane. The layer of astroglial end-feet is narrow in some areas and wide in others (Fig. 3).

Glial elements in 12-day old rabbits include astroglia and oligodendroglia cells, which are in various stages of differentiation. Most axons have no myelin sheath in this period. But considerable increase of the axon diameters in comparison with those in 3-day old animals is evident (Fig. 4). Greater axons are wrapped by several (from two to five) loosely arranged myelin lamellae. There are differences between the electron density of the nucleus and the cytoplasm of oligodendroglial and astroglial cells, as well as in the content of cytoplasmic organelles (Fig. 5). In the astroglial cell the cisternae of rough endoplasmic reticulum are scanty and located mainly in the perinuclear area.

The oligodendroglial cells have pronounced endoplasmic reticulum in the cytoplasm and dense clusters of chromatin in the nuclei similar to a mature oligodendroglial cell. The extensions of the cytoplasm of immature oligodendroglia are in direct contact with the myelinating

Fig. 3. 3 days postnatal. Blood vessel composed of endothelial cells and narrow basement membrane. Astroglial end-feet distributed around the blood vessel. The layer of astroglial end-feet is narrow in some areas and wide in others. × 9 200

axons. It is worth noting that outer mesaxons, are of high electron density. The filaments and microtubules are very delicate in 12-day old animals.

Astroglial end-feet form a layer dividing glial elements of the optic nerve from the pial space in which fibroblasts, cross sections of collagen and the endothelium can be seen (Fig. 6). The myelin sheath in the 12-day old rabbit has loosely arranged lamellae.

On the 30th day of life myelin has compact formation similar to mature animals. But the width of the myelin sheath, although greater than in the group of younger animals, is smaller than in the mature ones. Axons usually show four to seven compactly wrapped myelin membranes. There is a further increase of the axon volume (Fig. 7). In the cytoplasm of oligodendrocytes, which forms short extensions, rows of long, narrow cisternae of the rough endoplasmic reticulum appear at this stage and the microtubules often form bundles. This fact proves that these organelles become more organized during development. Astrocytes show several, wide stellate processes which radiate from the perikarya. The processes contain bundles of filaments and scanty polyribosomes. In the perikarya there are free polyribosomes and only some

Fig. 4. 12 days postnatal. Most axons have no myelin sheath. Myelinating axons are visible in close contact with the cytoplasm of oligodendroglia cell. × 10 800.

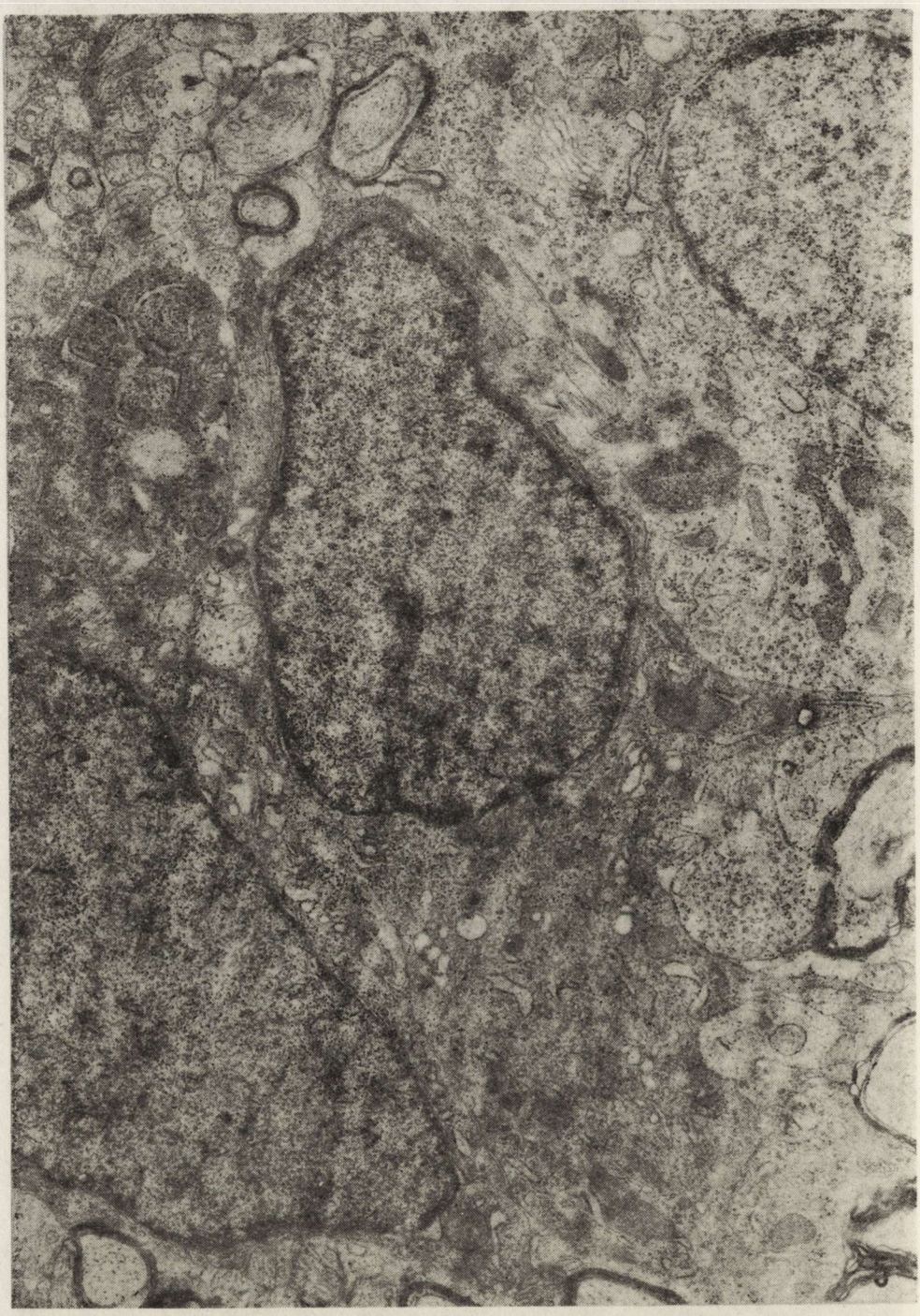

Fig. 5. 12 days postnatal. Oligodendroglial and astroglial cells. The differences between electron density of the nucleus and the cytoplasm of these two cell types are evident as well as the difference in the content of cytoplasmic organelles. × 12 600.

of them are connected with the short, wide-bore cisternae of the rough endoplasmic reticulum. Smooth endoplasmic reticulum is also sparse. Moreover the filaments, small and great mitochondria and dense bodies are scatered throughout the astrocytic cytoplasma (Fig. 8). Another characteristic feature of this type of glia are puncta adherentia.

In principle, glial cells in the rabbit optic nerve on the 70th day postnatal life are morphologically similar to those on the 30th day (Figs 9, 10). Only the cytoplasm volume appears to decrease. Glial cells and their processes expand in such a way that they aggregate myelinated axons into bundles (Figs 11, 12).

DISCUSSION

The investigations on gliogenesis performed by Vaughn (1969) in the optic nerve of the rat have lead the author to the conclusion that the development of oligodendroglia and the formation of myelin took place after birth. Skoff et al. (1976), by employing the autoradiographic method with (^{3}H) thymidine, proved that in the developing optic nerve in rats astroglial cells are formed throughout embryonic and early postnatal development, whereas oligodendrocytes are generated only during the postnatal period. Our investigations on the optic nerve in rabbits confirm these findings. In the first group of animals (3 days postnatal) astroblasts and undifferentiated glial cells are seen. Their processes form a supporting net for the axons of retinal ganglion cells. Astroglial end-feet are distributed around blood vessels and at the pial surface. In the latter region they act as glia limitans separating neural elements from endothelial cells and the subarachnoid space. Skoff's investigations (1976) have given ample evidence that oligodendroglia in rats begin to undergo their final cell division at five days of postnatal age, that is 1—2 days before the onset of myelin formation. A great majority of these cells are produced after the onset of myelination with the peak period occurring between 10 and 14 days postnatal.

By the 12th postnatal day one can recognize oligodendroblasts with a great number of organelles in the rabbit optic nerve. It is well known that morphological features denote biochemical activity. Hirose and Bass (1973) showed that a rapid accumulation of cholesterol and cerebrosides coincided with oligodendroglial differentiation. According to Skoff et al. (1976), the numerous organelles in the cytoplasm of labelled oligodendroblasts suggest that they can produce certain specific cell proteins and lipids for myelin membranes although these cells are in the early stages of differentiation. During this period loosely arranged myelin lamellae appear around the largest axons.

Our observations show that oligodendroblasts send out cytoplasmic extensions of their plasma membranes, which appear to be continuous

Fig. 6. 12 days postnatal. Astroglial end-feet form the layer dividing glial elements of the optic nerve from the pial space in which fibroblasts, cross section of collagen and the endothelium can be seen. × 8 000

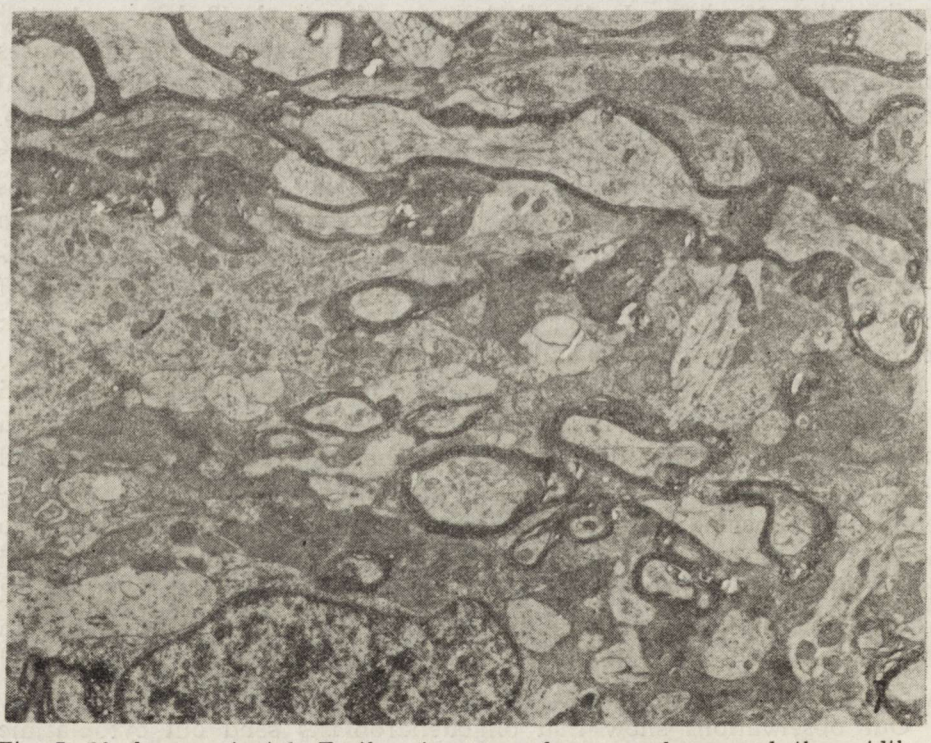

Fig. 7. 30 days postnatal. Further increase of axon volume and the width of myelin sheath. Myelin has a compact formation. × 5 100

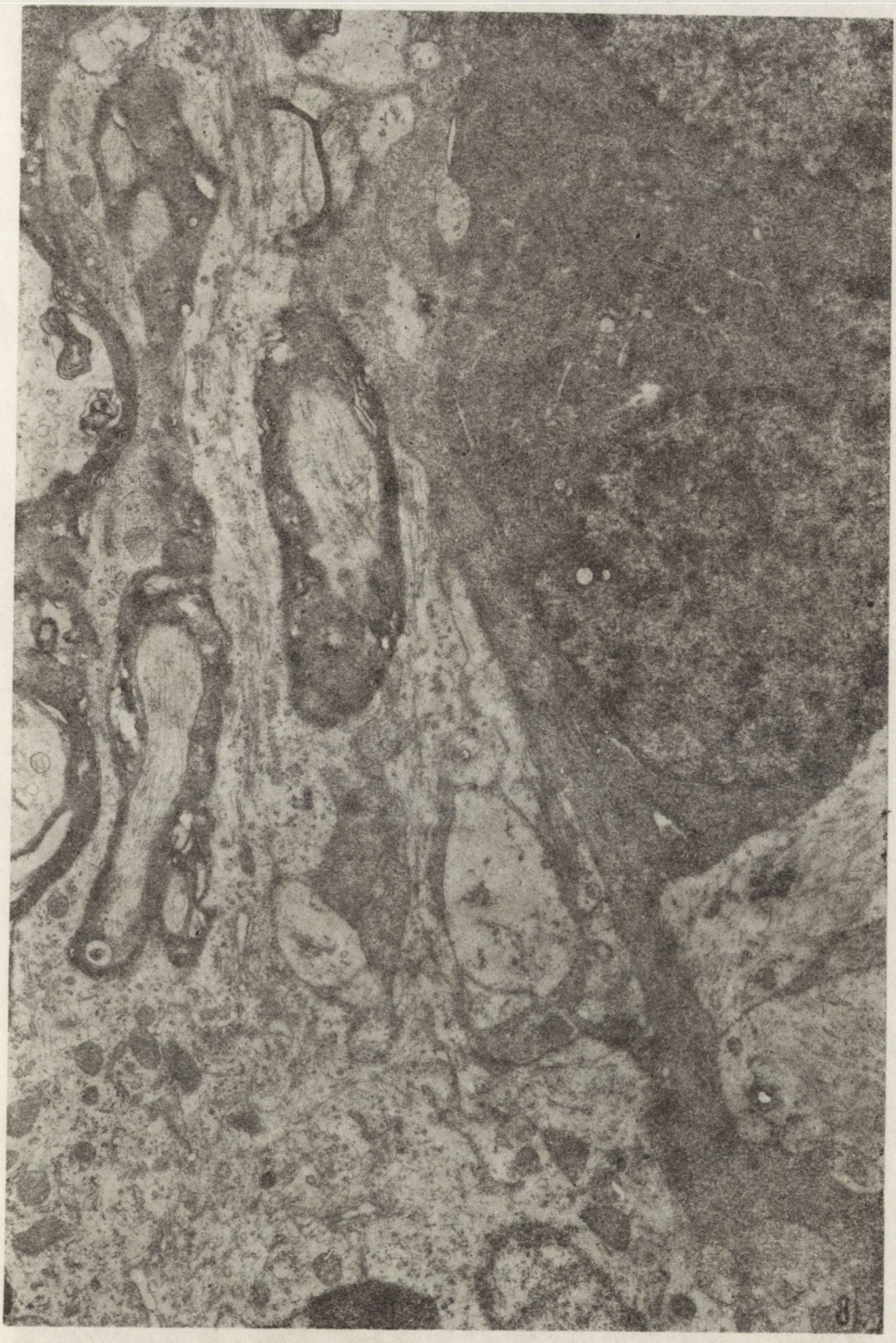

Fig. 8. 30 days postnatal. Astrocyte located near the oligodendrocyte, the cytoplasm of which forms short extensions and contains rich rough endoplasmic reticulum arranged in parallel rows. This cell forms wide, stellate processes and filaments; small and great mitochondria and dense bodies are scattered throughout the astrocytic cytoplasm. × 8 900

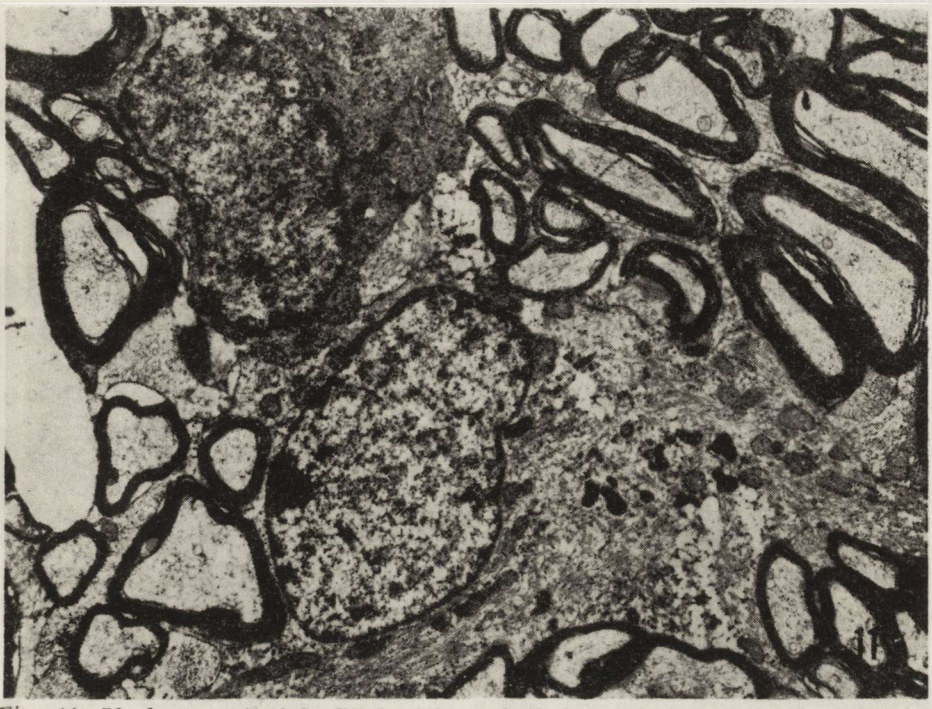

Fig. 11. 70 days postnatal. Glial cells and their processes form rows between bundles of myelinated axons. Short processes of oligodendroglia cell in contact with the surface of axons. × 5 300

with the outer lamellae of larger axons. The earliest appearance of myelin around axons with the largest diameters confirms the assumption that axons must reach a certain diameter before they begin to be myelinated (Matthews, Duncan, 1971).

The characteristic feature of astroglial cells in 12-day old rabbits is the fact that they have only occasional clusters of filaments within their cytoplasm. Beside wide-bore cysterns of endoplasmic reticulum, dense bodies and puncta adherentia are visible.

There are also unidentifiable cells in this age group. It is possible to classify them as differentiating oligodendroglia or astroglia.

The number of myelinated axons in the rabbit optic nerve continues to increase and by the 30th postnatal day a great majority of axons are myelinated. Axons with small diameters are now also involved in

---

Fig. 9. 70 days postnatal. Longitudinal section through the blood vessel of the optic nerve. There are no free spaces between endothelial cells, basement membrane, astroglial end-feet and glial components in the normal optic nerve. The processes of fibrous astrocytes show great differences in electron density. Some of the end-feet contain fewer filaments and have a light appearance and others contain abundant filaments and have a dark appearance. × 8 000

Fig. 10. 70 days postnatal. Puncta adherentia, typical for astrocytes are visible between the cell body of astrocyte with the smaller amount of filaments and the process of astrocyte rich in filaments. × 8 500

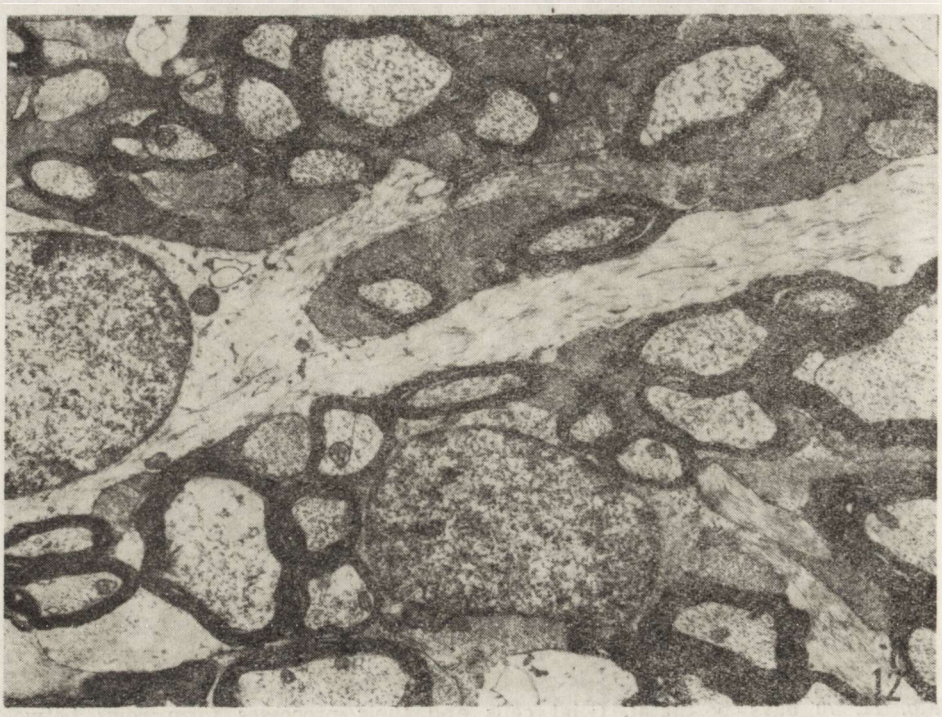

Fig. 12. 70 days postnatal. The axons wrapped by wide, compact myelin sheaths composed of about 10—20 lamellae. × 6 800

this process. The larger the fiber, the greater the number of lamellae to be observed. It is worth noting that the myelin is tightly compact. Basic protein and proteolipid protein appear at this time and it had been suggested that they may be necessary for the compaction of myelin (Morell et al., 1972). Recently the investigations made by Tennekoon et al. (1977) suggest that the appearance of myelin basic protein correlates more closely with the compaction of myelin than does proteolipid protein. Glial cells in 30-day old animals show further qualitative and quantitative morphological changes in comparison with the earlier age group. Oligodendrocytes are mature cells and constitute more than half of the cell population in the optic nerve. Astrocytes are characterized now by numerous, distinctly outlined filaments, which often form bundles.

Our data indicate that both morphology and cell population by the time the rabbit is 70 days old are similar to those found in the 30-day old rabbits. Glial cells and their processes are arranged in rows lying between bundles of myelinated axons. Astrocytes are stellate. Several cytoplasmic processes radiate from their perikarya and interlace with other processes. The cytoplasm of oligodendrocytes contains more polyribosomes than that of astrocytes and frequently shows clusters of microtubules and stucks of the cisternae of endoplasmic reticulum. How-

ever, the appearance of myelinated fibers is markedly different and it is easy to distinguish it from that seen in 30-day old animals. The compact myelin sheath is wide now and it is usually composed of 10—20 lamellae.

Our studies on the developing optic nerve in rabbits do not confirm the suggestions of some investigators (Bensted et al., 1957; Blunt et al., 1965; Schonbach et al., 1968) who believe that the proliferation of oligodendroglia precedes myelinogenesis in the central nervous system and an adult complement of oligodendroglia is reached before the period of myelin formation.

Skoff et al. (1976) on the basis of the investigations performed in the rat optic nerve are of the opinion that the proliferation of oligodendroglia occurs mainly during early stages of myelinogenesis. This agrees with the results of our investigations which lead to the conclusion that not only adult oligodendroglia take part in the myelination of the rabbit optic nerve, because the division and differentiation of oligodendroblasts occur simultaneously with the myelin formation.

REFERENCES

1. Bensted J. P. M., Dobbing J., Morgan R. S., Reid R. T. W., Payling-Wright G.: Neuroglia development and myelination in the spinal cord of chick embryo. J. Embriol. exp. Morph., 1957, 4, 428—431.
2. Blunt M. J., Wendell-Smith C. P., Paisley P. G., Baldwin T.: Glial nerve fibre relationships in mammalian optic nerve. J. Anat. (Lond.), 1965, 99, 1—11.
3. Hirose G., Bass N.: Maturation of oligodendroglia and myelinogenesis in rat optic nerve: a quantitative histochemical study. J. comp. Neurol. 1973, 152, 201—210.
4. Karnovsky M. H.: A formaldehyde-glutaraldehyde fixative of high osmolality for use in electron microscopy. J. Cell Biol., 1965, 27, 137A.
5. Matthews M. A., Duncan D.: A quantitative study of morphological changes accompanying the initiation and progress of myelin production in the dorsal funiculus of the rat spinal cord. J. comp. Neurol., 1971, 142, 1—22.
6. Morell P., Greenfeld S., Constantine-Ceccarini E., Wiśniewski H.: Changes in protein composition of mouse brain myelin during development. J. Neurochem., 1972, 19, 2545—2554.
7. Schonbach J., Hu K. H., Friede R. L.: Cellular and chemical changes during myelination; histologic, autoradiographic and biochemical data on myelination in the pyramidal tract and corpus callosum of the rat. J. Comp. Neurol., 1968, 134, 21—38.
8. Skoff R. P., Price D. L., Stocks A.: Electron microscopic autoradiographic studies of gliogenesis in rat optic nerve. I. Cell proliferation. J. comp. Neurol., 1976, 169, 291—312.
9. Tennekoon G. I., Cohen S. R., Price D. L., McKhan G. M.: Myelinogenesis in optic nerve. J. Cell Biol., 1977, 72, 604—616.
10. Vaughn J. E.: An electron microscopic analysis of gliogenesis in rat optic nerves. Z. Zellforsch. Mikrosk. Anat., 1969, 94, 293—324.

Author's address: Department of Neurology, School of Medicine, 49, Przybyszewski Str., 60—355 Poznań, Poland

NEUROPAT. POL., 1982, 20, 1—2
PL ISSN 0028—3894

JADWIGA PANKRAC

MYELIN FORMATION IN DEVELOPING RAT BRAIN WITH PARTICULAR REFERENCE TO THE LATE MATURATION PERIOD

Department of Neurology, Institute of Nervous System and Sensory Organs' Diseases, School of Medicine, Poznań

Myelin formation in the brain in early periods of life has been described by a number of authors investigating this process both in animal and human brains. Results of investigations concerning myelin formation and the peak of myelination of the rat brain (Norton, Poduslo, 1973: Adamczewska, 1978), of the optic nerve in rabbit (Adamczewska-Goncerzewicz, 1978), of the brain and optic nerve in rabbit and rat brain (Pankrac, 1976; 1978) indicate that accumulation of myelin does not end at the moment when the animal reaches sexual maturity, but continues further.

In the light of these findings it seemed useful to follow myelin formation in the later period of extrauterine life.

MATERIAL AND METHODS

The experiments were performed on Wistar rats of both sexes aged from 14 days to 18 months. From young animals 14—28-day old about 20 brains were taken for one determination and from the group of animals aged more than two months one brain for each measurement. Brains of young animals were examined on 14th, 17th, 21st, 25th and 28th day of life, whereas in the animals 2—12-month old investigations were performed at 30-day intervals. The last group consisted of rats aged 18 months.

The experimental animals were sacrified by decapitation under superficial ether anesthesia, their brains were weighed accurately and ho-

mogenized in a homogeniser with a teflon piston. The myelin fraction was isolated by differential centrifugation in a discontinous sucrose gradient after Horrocks (1967; 1968) and the myelin was weighed. After weight determination the yield of myelin (mg/brain) was determined.

RESULTS

If we assume that the amount of myelin recovered is a constant fraction of its amount present in the brain, it may be supposed that myelination is a continuous process, at least in the period under study (Norton, Poduslo, 1973). Therefore myelin accumulation is presented in the diagrams (Fig. 1, 2) as the logarithmic function of extrauterine age. Figure 1 shows myelin accumulation in the rat brain from the 14th to the 160th day of life.

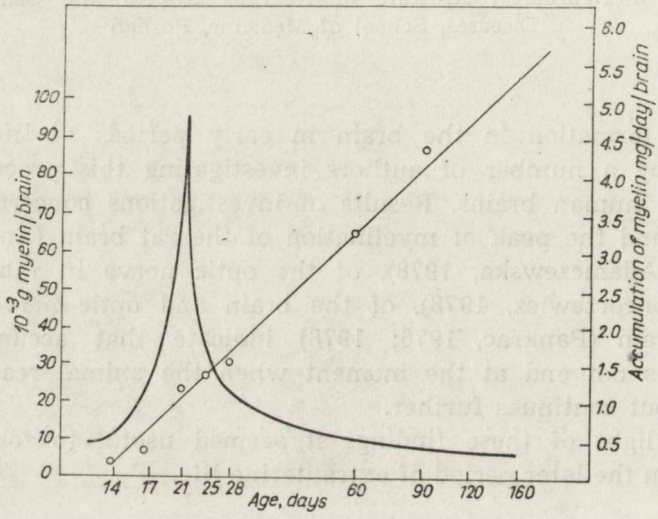

Fig. 1. The accumulation of myelin in rat brain as logarithmic function of postnatal age; o — represents yields of myelin in mg/brain (left ordinate); the rate of accumulation is plotted as a thick curve in mg myelin/day/brain (right ordinate)

The presented data indicate that the peak of rat brain myelination occurs on the 21st day of extrauterine life. On this day 4.7 mg of myelin is accumulated although at this time there is only 17.6 per cent of myelin in the brain. It also results from the data presented in the diagram that the absolute increase in myelin content is proportional to the animal's age and extends in time far beyond the period of active myelinogenesis. Figure 2 is a continuation of the preceding one. It takes into account myelin accumulation in the later life periods and at the

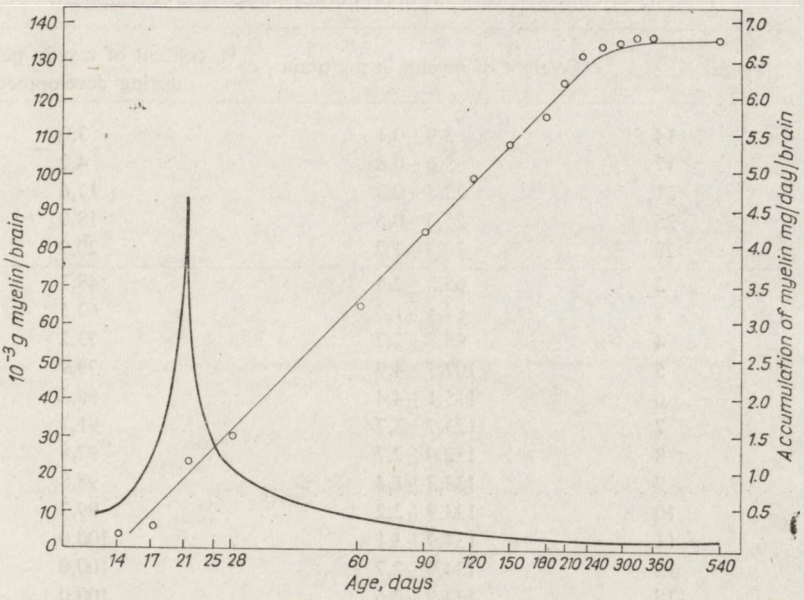

Fig. 2. The accumulation of myelin in rat brain as logarithmic function of postnatal age; o — represents yields of myelin in mg/brain (left ordinate); the rate of accumulation is plotted as a thick curve in mg myelin/day/brain (right ordinate)

same time illustrates the course of rat brain myelination beginning with che 14th day of life and up to the moment of reaching 18 months of age.

As seen from the diagram, the increase in myelin content progresses, beginning with the 14th day of life up to maturity and it extends beyond the period of active myelinogenesis up to the 330th day of life of the animal. Thereafter to the 18th month of life the level remains the same.

It also results from the diagram that after the myelination peak in the rat brain falling to day 21 of extrauterine life rate of myelin increase slows down, and at later periods it is only slight.

The amount of accumulated myelin deposited in the particular periods of extrauterine life is shown as percentage in Table 1.

When the rat reaches the age of 11 months the myelin amount stabilises. Its weight at this time is assumed as 100 per cent and the percentage of myelin accumulated in earlier life periods is calculated in reference to this value.

It results from the data here presented that up to the 14th day of extrauterine life of the rat 3 per cent of myelin is accumulated, up to the peak day of myelination, that is the 21st day of life 17.6 per cent

Table 1. Myelinogenesis of rat brain during ontogenetic development

	Age	Weight of myelin in mg/brain	% content of myelin per brain during development
Day	14	3,9±0,1	3,0
	17	5,6±0,8	4,2
	21	23,7±0,3	17,6
	25	25,5±0,5	18,9
	28	28,3±1,2	20,9
Month	2	65,2±2,5	48,3
	3	84,4±1,4	62,5
	4	98,8±2,7	73,2
	5	107,7±4,9	79,9
	6	115,1±4,4	85,3
	7	123,7±3,7	91,7
	8	132,0±2,7	97,8
	9	133,3±1,4	98,8
	10	133,9±2,2	99,3
	11	134,9±3,1	100,0
	12	134,9±2,7	100,0
	18	134,9±2,6	100,0

and up to the end of the second month of life 48.3 per cent. In later life periods, beginning with 3 months up to eleven, myelin is further accumulated, but with each month the rate of its deposition decreases.

DISCUSSION

The present results agree with the observations of Horrocks (1973), Rawlins and Smith (and Norton and Poduslo (1973). These investigators basing on studies of the basic components of the myelin sheath, that is brain lipids and proteins in such rodents as mice, rats and guinea pigs, established that the myelin content in the brains of these animals increases up to 2 years of life, that is in late periods of development. These authors also report that in these animal species, in later developmental periods the contents of galactolipids, cholesterol and sfingomyelin increase, thus, of those components which are generally considered as basic components of the myelin sheath lipids. In some brain regions an increase was observed of the content of the particular myelin lipids as late as in two-year-old animals.

According to Horrocks (1973), the increased myelin content in the developing brain is due to the increasing amount of myelin lipids. Rawlins and Smith (1971) affirms that the increase in lipid content in the rat brain after the second month of life is probably caused by myelin accumulation. The observation of Horrocks (1974) also seems of importance, namely, that the increase in myelin content in the brain is associated with an increase of weight of the latter.

Merat and Dickerson (1973), Pankrac (1976) in their reports on myelin deposition in rabbit and rat brain state that the time at which myelination ends depends on the brain region.

Thus results for myelin obtained from the brain as a whole are a resultant of myelination processes in the particular brain regions.

REFERENCES

1. Adamczewska Z.: Myelin lipids in the developing rat brain. Neuropat. Pol., 1978, 16, 11—23.
2. Adamczewska-Goncerzewicz Z.: Lipidy mieliny nerwu wzrokowego królika w czasie ontogenezy. Streszcz. ref. IV Konf. Stow. Neuropat. Pol., Poznań 1978, 3.
3. Horrocks L. A.: Composition of myelin from peripheral and central nervous system of the squirrel monkey. J. Lipid Res., 1967, 8, 569—576.
4. Horrocks L. A.: Composition of mouse brain myelin during development. J. Neurochem., 1968, 15, 483—488.
5. Horrocks L. A.: Composition and metabolism of myelin phosphoglycerides during maturation and aging. Progress in Brain Research, Neurobiological Aspects of Maturation and Aging. 1973, 40, 383—395.
6. Horrocks L. A., Sun G. Y., D'Amato R. A.: Changes in brain lipids during aging. Neurobiology of Aging. Book available from: Plenum Publishing Corporation, 1974, 359—367.
7. Merat A., Dickerson J. W. T.: The effect of development on the gangliosides of rat and pig brain. J. Neurochem., 1973, 20, 873—880.
8. Norton W. T., Poduslo S. E.: Myelination in brain: changes in myelin composition during brain maturation. J. Neurochem., 1973, 21, 759—773.
9. Pankrac J.: Oznaczanie przyrostu mieliny oraz szczytu mielinizacji w mózgu w rozwoju ontogenetycznym. Streszcz. ref. XI Dzień Neuroch. Klin., Zielona Góra 1976, 8—9.
10. Pankrac J.: Odkładanie mieliny w rozwijającym się mózgu ze szczególnym uwzględnieniem późnego okresu dojrzewania. Streszcz. ref. IV Konf. Stow. Neuropat. Pol., Poznań 1978, 100.
11. Rawlins F. A., Smith M. E.: Myelin synthesis in vitro. A comparative study of central and peripheral nervous tissue. J. Neurochem., 1971, 18, 10.

NEUROPAT. POL., 1982, 20, 1—2
PL ISSN 0028—3894

ANDRZEJ GONCERZEWICZ, WIESŁAWA BICZYSKO, WIESŁAW CITOWICKI

WALLERIAN DEGENERATION IN THE MYELINATING RABBIT OPTIC NERVE *

Department of Neurology, Institute of Biostructures and Department of Otolaryngology, School of Medicine, Poznań

Many ultrastructural studies of Wallerian degeneration (WD) of the adult optic nerve have been published (Luse, McCamman, 1957; Krugger, Maxwell, 1969; Vaughn, Pease, 1970; Vaughn et al., 1970; Cook, Wiśniewski, 1973; Goncerzewicz, 1982). Few details of this process are as yet known in the central nervous system (CNS) degeneration of immature tissue (Aldskogius, 1974; Cook et al., 1974; Reier, Webster, 1974). One of the most important questions is the origin of phagocytic cells in the degenerating CNS, which has been reviewed by Russell (1962) and Bunge (1968). In the WD various cell types have been detected as being phagocytic: Bignami and Ralston (1969) describe these cells as macrophages derived from unknown sources; Daniel and Strich (1969) and Aldskogius (1974) interpret cells acting in this way as microglia. Cook and Wiśniewski (1973) stress the principal phagocytic role of oligodendroglia and Vaughn et al. (1970) are of the same opinion about multipotential glia cells, although they do not deny some participation of astroglia (Vaughn, Pease, 1970) in the phagocytosis. In more recent literature (Fernnado, 1973; Reier, Webster, 1974; Nathaniel, Nathaniel, 1977) astroglia cells are claimed to be the only phagocytes in WD.

In the face of this controversy we decided to perform an ultrastructural study of WD in the optic nerve of young rabbits.

The aim of this study was: to reevaluate the type of cell involved in phagocytosis and to compare the pattern of Wallerian degeneration in young animals with that in adults.

---

* This investigation was supported by NIH PL 480. Research Agreement No. 05-027-N.

MATERIAL AND METHODS

Unilateral (right) eye enucleation of 8-day old Chinchilla rabbits was performed under Nembutal anesthesia. Special care was taken to avoid the stretching of the optic nerve. Material for light and electron microscopy after 4, 8, 16, 24, 32, 48 and 80 days survival was taken. Each group was represented by 4 animals. Control material contained 14 animals in parallel groups and will be described separately. Under general Nembutal anesthesia the skull was opened and the optic nerves were exposed to paraformaldehyde-glutaraldehyde pH 7.4 Karnovsky fixative. After 10 min of immersion fixation the right and left optic nerves were dissected from the chiasma, each one being 4 mm long and were placed in Karnovsky fixative solution for 4 h at room temperature. After overnight washing in 0.1 M cacodylate buffer samples were post-fixed in 1% osmium tetroxide in 0.1 M cacodylate buffer pH 7.4 at +4°C. Dehydration was made in graded concentrations of ethanol. The sections were subsequently embedded in Epon. During embedding location, orientation and proximo-distal sequence of the blocks from each optic nerve were maintained.

Beginning from the chiasma 1 μm serial sections were used to trace the extent of degeneration and characterization. Semithin and ultrathin section were cut with Reichert OmU_3 ultramicrotome. Ultrathin sections were stained with uranyl acetate and with lead citrate. Electron microscopy pictures were taken with a JEM 7A microscope.

RESULTS

Examination of the optic nerve four days after the operation (d.a.o.) revealed almost all myelinating and myelinated axons as being edematous with swollen and broken microtubules and with flocullent material inside. Some of the axons contained myelin-like electron dense material. Only few axons retained their normal appearance. The myelin surrounding swollen axons had enlarged spaces between its sheath and myelin membranes were often broken (Fig. 1).

The differentiation of glial cells in the left, undissected optic nerve of 12-day old rabbits was proper to the age (Śniatała-Kamasa, 1979). According to electron microscopic criteria fibrillary astrocytes, few protoplasmic astrocytes, oligodendrocytes, astroblasts and oligodendroblasts were clearly recognized. In the right optic nerve the majority of fibrillary astrocytes contained nuclei with invaginated nuclear envelope, with heterochromatine located beneath it and also spread inwards into the euchromatine territory (Fig. 2). Besides in the sectioning plane, nucleoli with mixed fibrillary and granular compartments were present. The number of perichromatine granules was increased. Perichromatine granules were present on the border line between hetero- and euchroma-

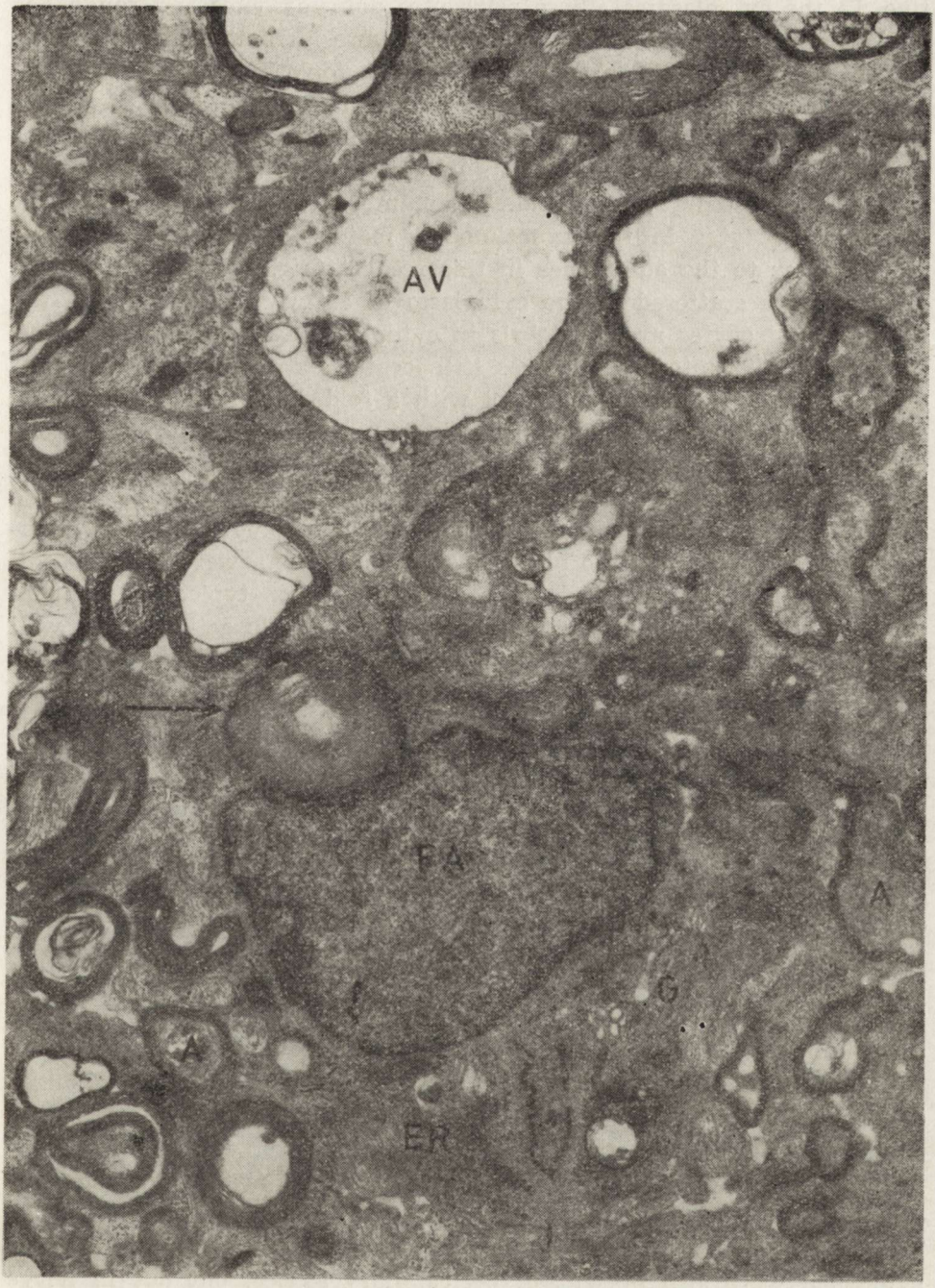

Fig. 1. 4th day after the operation. Fibrous astrocytes (FA) contains in cytoplasm ingested myelin (arrow), enlarged Golgi apparatus (G) and numerous ergastoplasmic channels (ER). The axons have either swollen appearance (AV), or condensation of axoplasm with the presence of filamentous material (A). Myelin surrounding swollen axons shows advanced stage of disintegration. × 8 000

tine. In the cytoplasm of these astrocytes polirybosomes and rough endoplasmic reticulum channels perceptibily were increased. In comparison to control material the number of rough endoplasmic channels in the experimental material was markedly higher, but the number of polirybosomes was lower (Fig. 2). The Golgi area contained many dictyosomes and was spread in the cytoplasm. In close vicinity to the Golgi area numerous lysosomes were noted. The number of glial filaments in fibrillary astrocytes in the experimental material was high; the cells were similar to the adult ones in this respect (Fig. 3). A few glycogen rosettes were scattered in the cytoplasm of astrocytes. In some of the described astrocytes myelin debris in cytoplasm was present. However, most of the disrupted myelin was still located extracellulary. Oligodendrocytes contained irregular nuclei with a folded nuclear envelope and with heterochromatine located beneath it. In their cytoplasm numerous polirybosomes and rough endoplasmic reticulum channels were present. In some oligodendrocytes round lipid droplets in small numbers were visible, and some ingested myelin was occasionally noted. Single astroblasts, some of them in the phase of mitotic division, were also present. Blood capillaries were lined by a single layer of typical endothelial cells. In the endothelium cytoplasm micropinocytotic activity was well marked. Perivascular space in all experimental material was slightly enlarged and contained pericytes. Extracellular space in the nerve tissue was narrow, very similar to the normal condition.

Eight days after the operation (16th day of extrauterine life) morphologically normal axons were no longer visible. Axons with dark flocullent material or with empty spaces in their axoplasm surrounded by shell-like myelin were present in the material. The gradual dissapearance of myelin debris and axons was apparent, leaving extracellular space between astroglial process (Fig. 4). Fibrous astrocytes look essentially similar to those decribed in the previous group, with the exception of dark lipid bodes present in their cytoplasm together with ingested myelin. Fibrous astrocytes and their processes contained an increased number of glycogen rosettes.

Analysis of semithin sections revealed a reduced number of oligodendroglial cells. In the electron microscopic studies these cells appeared similar to normal, with the exception of the electron lucent lipid droplets in their cytoplasm. Phagocytosis of disrupted myelin by oligodendroglial cells was not observed in this period. Single mononuclear cells, histiocytelike cells, probably of blood origin with lipid droplets in their cytoplasm were also present in pericapillary spaces, but not in nerve parenchyma.

Capillary blood vessels showed normal endothelial cells and were surrounded by enlarged perivascular space, in which pericytes and single collagen fibers were noted.

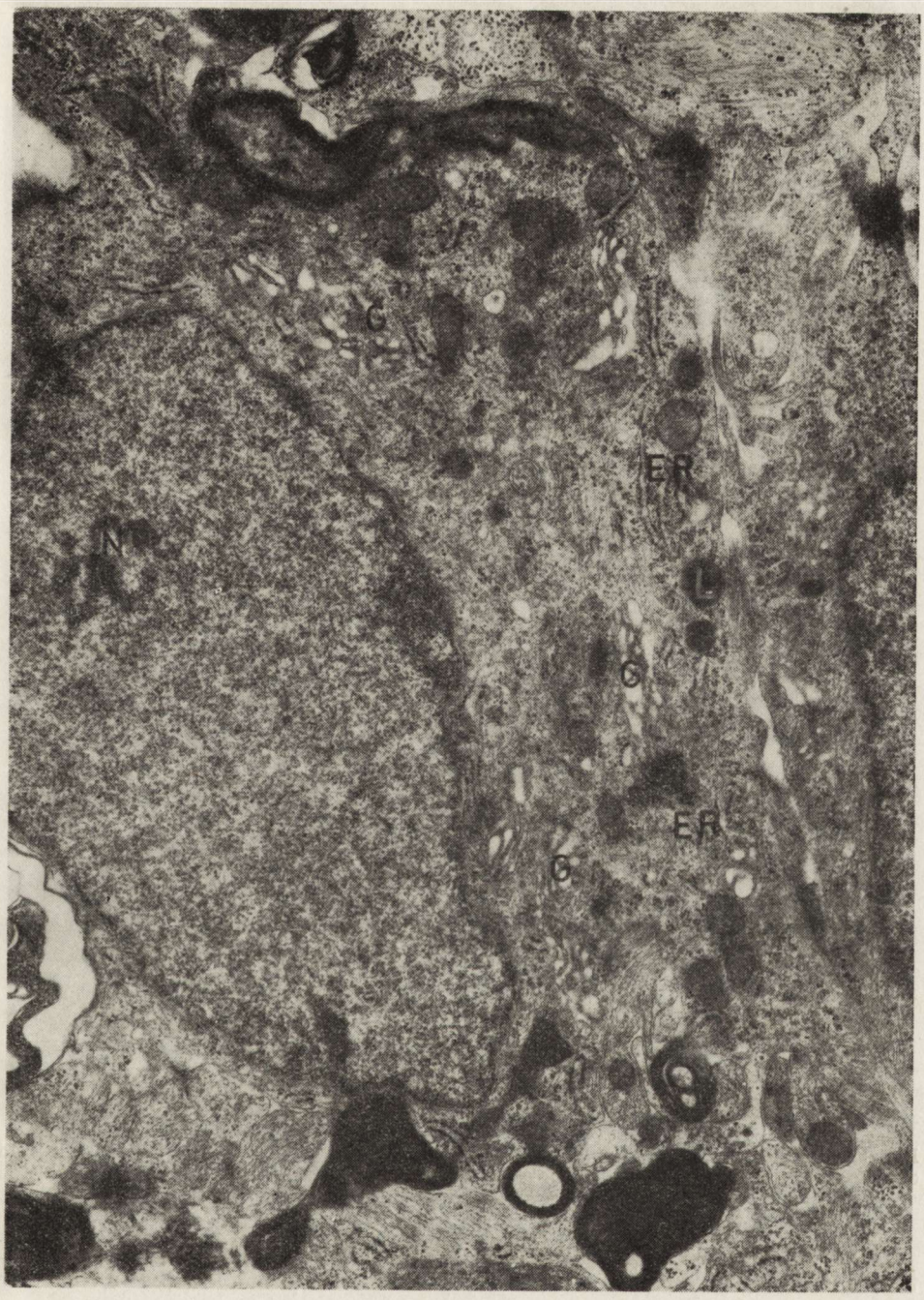

Fig. 2. 4th d.a.o. Fibrous astrocyte with the nucleus of irregular outline and prominent nucleolus (NL). Cytoplasm shows extended Golgi apparatus (G), numerous lysosomes (L) and rough endoplasmic reticulum channels (ER). × 14 000

Fig. 3. 4th d.a.o. Astrocytic processes with fair number of gliofilaments surround degenerating axons (A), which contain filamentous material and some disrupted myelin. × 16 500

In the group of animals investigated 16 days after the operation, the optic nerve was built mainly of fibrillary astrocytes with few oligodendrocytes present. Extracellulary lying myelin debris and degenerated axons were very few. Extracellular space was scattered myelin and electron-dark lipid droplets. The latter were also present in the perinuclear cytoplasm of fibrillary astrocytes (Fig. 5). The number

Fig. 4. 8th d.a.o. Numerous myelin debris (M) are visible in slightly enlarged extracellular space. Some of processes of fibrous astrocytes contain lipid droplets (x). Arrows show degenerating myelin being encircled by astrocyte processes. × 10 000

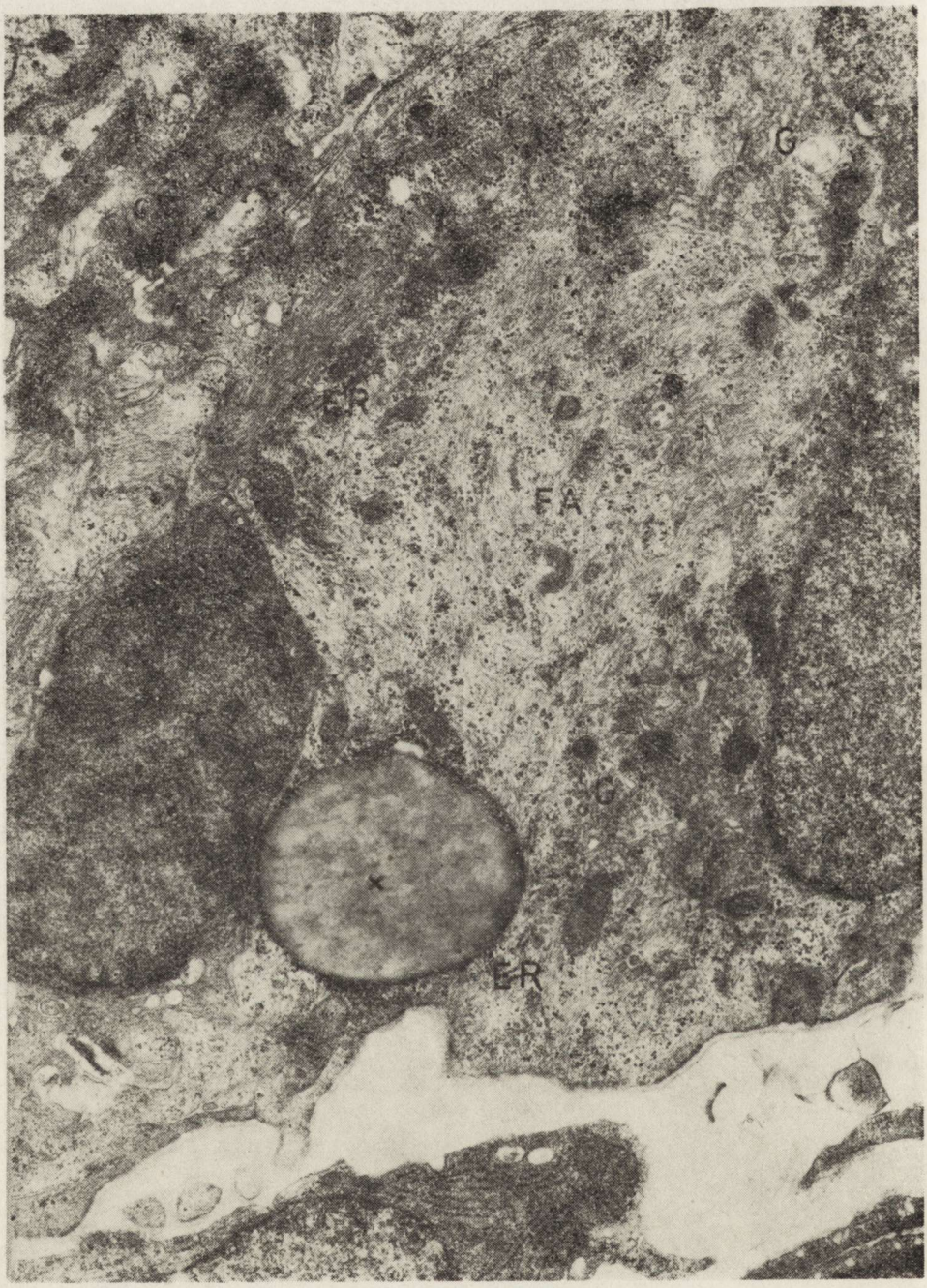

Fig. 5. 16th d.a.o. Cytoplasm of fibrous astrocyte (FA) contains large lipid droplets (x), extended Golgi apparatus (G) and a small number of ergastoplasmic channels (ER). × 7 800

Fig. 6. 16th d.a.o. Oligodendrocyte (O) enwrapped by some myelin leaflets. Myelin debris (M) in extracellular space is visible but most of the area of the section is filled by processes of fibrous astrocytes. × 12 000

Fig. 7. 32nd d.a.o. Glial scar, which is exclusively built from cell bodies and processes of fibrous astrocytes. × 10 000

and structure of oligodendroglial cells in this group was similar to the previous one. Macrophages loaded with lipid droplets were rarely seen in perivascular space which was enlarged and contained pericytes and collagen fibers.

At this stage of the experiment the cicatrization process was greatly developed and generated by fibrillary astrocytes and their processes. Some of the oligodendroglial cells were wrapped by few (2 or 3) myelin leaflets (Fig. 6). Such myelin leaflets surrounding cell processes were also seen.

Electron microscopic pictures of animals, taken for investigation between 24 and 32 days after the operation were similar. In the areas covered by fibrillary astrocytes scar (Fig. 7) single astrocytes containing ingested myelin were present. Myelin fragments associated with lipid droplets were found in their cytoplasm. In this period of experiment very few oligodendrocytes were present. Their cytoplasm and nuclei were regular and devoid of myelin debris.

Extracellular space in some areas was very narrow, just as in the normal optic nerve. It was present as an irregular, fairly large, electron lucent space in some areas. Perivascular space was as described previously; enlarged and containing pericytes and numerous collagen fibers.

In animals taken for investigation after 48 and 80 days after the removal of the eye bulb, almost total scarification of nerve tissue was observed.

DISCUSSION

Axonal and myelin changes were the first phenomena observed in experimental material. Four days after eye-bulb removal flocullation and condensation as well as watery degeneration of the axoplasm appeared. This applies to axons of all sizes. Myelin surrounding these axons was also heavily altered. As early as 16 days after the operation these degenerated exons were very few and they disappeared completely from the injured nerve between 16 and 24 days after the operation.

Cook et al. (1974) have described similar alteration of axons, but watery degeneration was limited to the larger axons only. Goncerzewicz (1982) has shown only slight changes of axoplasmic density and initial splitting of myelin lamellae in adult rabbits 4 days after eye-bulb removal. In our experiment degeneration seems to appear much earlier than in adult animals. Considerable difference between the rats as far as degeneration in young and adult optic nerve fibers was concerned, was noted by Cook and Wiśniewski (1973) and Aldskogius (1974). Pecci Saavedra (1969) attributed the faster degeneration in young animals to more rapid axoplasmic transport for its slow and fast components. The different pace of degeneration may also be related to earlier release of

autolytic enzymes within the axon. Cook et al. (1974) was of the opinion that faster removal of axonal debris may be due to greater metabolic activity of immature tissue.

In normal optic nerves of 12-day old rabbits (Śniatała-Kamasa, 1979) compact myelin sheaths were present around axons of greater diameter, only a few lamellae being visible around smaller ones. In our material the first experimental group (4 days after the operation, i.e. 12-day old animals) showed enlargement of the spaces between the myelin leaflets and also distortion of its regular structure. The last remnants of distorted myelin sheath persisted extracellularly only till 24 d.a.o. The process of the removal of myelin debris was also much faster in young animals in comparison with the observation of Goncerzewicz (1982) in adult rabbits. A similar pattern of disruption and ingestion has been observed by Reier and Webster (1974) in developing tadpole optic nerve.

The main problem elaborated in literature on the central Wallerian degeneration concerned the type of cell acting as phagocytes of the remnants of disrupted myelinated axon. In our study disrupted myelin fragments were generally seen, within the cytoplasm of fibrous astrocytes, differing from the normal ones in their shape and the structure of nuclei and cytoplasm. These cells showed enlargement of nucleoli and an increased number of perichromatin granules, which were morphological indicators of increased RNA synthesis. The increased number of polyribosomes and rough endoplasmic reticulum channels may correspond to these nuclear changes as well as being subsequent to phagocytic activity of these cells. These fibrous astrocytes resembled in some respect immature forms. Vaughn and Pease (1970) and Fernando (1973) on the basis of cytoplasmic structure found similarities between immature astrocytes and those present in the optic nerve during Wallerian degeneration. In our opinion immature and reactive forms of astrocytes might be similar in respect of shape and structure of nuclei and of the amount of rough endoplasmic reticulum and polyribosomes; nevertheless, they differed in the number of glial filaments, the number and structure of lysosomes and of the extent of the Golgi area. In our first experimental group differentiation and maturation of glia cells was not completely finished, since we could see some mitotic figures. These immature cells possessed cytoplasm with few glial filaments and were almost devoid of lysosomes. In contrast, all the cells involved in phagocytosis of myelin were mature forms with a great amount of glial filaments, number of lysosomes and extended Golgi area.

In the late stages of the experiment large quantities of round electron lucent vacuoles were seen in close connection with phagocytosed myelin fragments. There is evidence (Bignami, Ralston, 1969), that these vacuoles, present within the cytoplasm of phagocytic cells, represent the product of chemical myelin breakdown. All the authors describing

central Wallerian degeneration are of the same opinion regarding the sequence of myelin intracellular degradation, but they differ in their opinions of the type of cell acting in this process. Our observations showing the presence of myelin debris and lipid vacuoles within the cells possessing gliofibrills are in accordance with data obtained by Reier and Webster (1974), Fernando (1974), Nathaniel (1977) and also Goncerzewicz (1982) for Wallerian degeneration in the optic nerve and in the other regions of CNS. Different observations in Wallerian degeneration in the optic nerve, presented by Vaughn and Pease (1970) and by Cook and Wiśniewski (1973), who atributted the main phagocytic role to multipotential glia cells and oligodendroglia, respectively, may have their source in species differences. In spite of this controversy it seems evident that the process of myelin digestion and degradation is much faster in young animals than in adults. All the authors describing central Wallerian degeneration in the mature nervous system stress the very slow rate of myelin degradation. It is especially true for comparison with Goncerzewicz's (1982) results in the same species. In the adult rabbit optic nerve intracellular lipid vacuoles appeared for the first time on 32 d.a.o. — in the same period in young animals the degradation of myelin debris is almost complete. The same difference between young and adult tissue is shown for scarification process, which in this experiment, started at 16 and were completed at 48 d.a.o. — in the period when in the adult tissue only hypertrophy of astroglial processes is developed as the initial stage of scarification.

In our experiment there is little evidence for the role of oligodendroglia as well as microglia in phagocytosis. In fact there were few oligodendroglia cells visible in some of the first experimental groups possessing small amounts of lipid droplets. This phenomenon may be related to the apparent inhibition of myelination following nerve injury. Lipids still synthetised by oligodendroglia cells cannot be used for myelination because of the destruction of axons which can be myelinated (Pecci Saavedra et al., 1969; Cook, Wiśniewski, 1973). The potential capacity of these cells is expressed in the formation of topographically aberrant myelin. Moreover, the small number of reactive oligodendroglia cells present in our material was difficult to distinguish from miccoglial cells. The same problem was taken up by Cook et al. (1974) who found that reactive oligodendrocytes may show various shapes of nucleoli, arrangements of chromatin and extent of rough endoplasmic reticulum, which are common criteria, used for distinguishing between oligocytes and microglia. Therefore, they believed that so-called microglia cells are in fact reactive oligodendrocytes. Cells resembling microglia were seen within degenerating myelin whorls in early stages of direct and indirect Wallerian degeneration of the hypoglossal nerve, and also outside myelin in the later stage of this process by Aldskogius (1974).

These cells had a similar appearance to phagocytes described in the other model of Wallerian degeneration in adult tissue. The opposite results relating to oligodendroglia and microglia were published by Vaughn and Pease (1970), who stressed that there was no evidence of phagocytosis performed by oligodendroglia and no dramatic changes in these cells beyond formation of aberrant myelin during the later stages. Also, much less activity of oligodendrocytes during Wallerian degeneration have been described by Reiner and Webster (1974).

In contrast, Cook and Wiśniewski (1974) during Wallerian degeneration of the optic nerve in kittens found oligodendroglia as the most active cells in phagocytosis of degenerating myelin. In our material the reactive forms of fibrous astrocytes predominated in phagocyte population and it is consistent with morphological and histochemical evidence of phagocytosis in adult optic nerve degeneration described by Goncerzewicz (1982) in rabbits.

In the face of this controversy we can assume that in central Wallerian degeneration phagocytes may derive from different sources, depending on the region investigated and species used for the experiment.

REFERENCES

1. Aldskogius H.: Indirect and direct Wallerian degeneration in the intramedullary root fibres of the hypoglossal nerve. An electron microscopical study in the kitten. Adv. Anat. Embryol. Cell Biol., 1974, 50, 7—78.
2. Bignami A., Ralston H. J., III: The cellular reaction to Wallerian degeneration in the central nervous system of the cat. Brain Res., 1969, 13, 444—461.
3. Bunge R. P.: Glial cells and the central myelin sheath. Physiol. Rev., 1968, 48, 197—251.
4. Cook R. D., Ghetti B., Wiśniewski H. M.: The pattern of Wallerian degeneration in the optic nerve of newborn kittens: an ultrastructural study. Brain Res., 1974, 75, 261—275.
5. Cook R. D., Wiśniewski H. M.: The role of oligodendroglia and astroglia in Wallerian degeneration of the optic nerve. Brain Res., 1973, 61, 191—206.
6. Daniel P. M., Strich S. J.: Histological observations on Wallerian degeneration in the spinal cord of the baboon, Papio papio. Acta neuropath. (Berl.), 1969, 12, 314—328.
7. Fernando D. A.: An electron microscopic study of the neuroglial reaction in Wallerian degeneration of the corticospinal tract. Acta anat., 1973, 86, 459—473.
8. Goncerzewicz A.: Electron microscopic study of astrocytic reaction in Wallerian degeneration of the rabbit optic nerve. Neuropat. Pol., 1982, 20, 47—60.
9. Kruger L., Maxwell D. S.: Wallerian degeneration in the optic nerve of a reptile: an electron microscopic study. Am. J. Anat., 1969, 125, 247—270.
10. Luse S. A., McCamman R. E.: Electron microscopy and biochemistry of Wallerian degeneration in the optic and tibial nerves. Am. J. Path., 1957, 53, 586.

11. Nathaniel E. J. H., Nathaniel D. R.: Astroglial response to degeneration of dorsal root fibers in adult rat spinal cord. Exper. Neurol., 1977, 54, 60—76.
12. Pecci Saavedra J., Vaccarezza O. L., Masciti T. A.: Degeneration in the parvocellular portion of the lateral geniculate nucleus of the cebus monkey. A light and electron microscope study. Z. Zellforsch., 1969, 93, 164—181.
13. Reier P. J., Webster H. deF.: Regeneration and remyelination of Xenopus tadpole optic nerve fibers following transection or crush. J. Neurocytol., 1974, 3, 591—618.
14. Russell G. V.: The compound granular corpuscle or gitter cell: a review, together with notes on the origin of this phagocyte. Texas Rep. Biol. Med., 1962, 20, 338—351.
15. Śniatała-Kamasa M.: Ultrastructural picture of the optic nerve in rabbit during ontogenic development. Neuropat. Pol., 1982, 20, 11—23.
16. Vaughn J. E., Hinds P. L., Skoff R. P.: Electron microscopic studies of Wallerian degeneration in rat optic nerves. I. The multipotential glia. J. comp. Neurol., 1970, 140, 175—206.
17. Vaughn J. E., Pease D. C.: Electron microscopic studies of Wallerian degeneration in rat optic nerves. II. Astrocytes, oligodendrocytes and adventitial cells. J. comp. Neurol., 1970, 140, 207—226.

Author's address: Department of Neurology, Academy of Medicine, 49, Przybyszewski Str., 60—355 Poznań, Poland

NEUROPAT. POL., 1982, 20, 1—2
PL ISSN 0028—3894

ANDRZEJ GONCERZEWICZ

ELECTRON MICROSCOPIC STUDY OF ASTROCYTIC REACTION IN WALLERIAN DEGENERATION OF THE RABBIT OPTIC NERVE *

Department of Neurology, Institute of Diseases of the Nervous System and Sensory Organs, School of Medicine, Poznań

Astroglial cells are known to react to various noxious agents by means of hypertrophy and/or proliferation. These cells are also able to acquire phagocytic properties in some pathological conditions. This latter function in Wallerian degeneration in the optic nerve is confirmed by several authors (Reier, Webster, 1974; Nathaniel, Nathaniel, 1977), but others consider it as secondary to oligodendroglial (Cook, Wiśniewski, 1973) or multipotential glia cells (Vaughn et al., 1970) phagocytosis. This work is a contribution to the discussion of the above presented problem.

MATERIAL AND METHODS

Forty two adult Chinchilla rabbits were used in the experiment. In Nembutal anesthesia the right optic nerve was cut with scissors immediately behind the eye. Special care was paid to avoid stretching the nerve when dissected. The eye bulb was subsequently removed. Material for electron microscopic studies was taken on the 4th, 8th, 16th, 24th, 32nd, 48th and 80th day after the operation. In Nembutal anesthesia, efficient circulatory action being still present the skull was surgically opened, the frontal lobes were pushed aside and excess of fixative (Karnovsky, 1965) was applied onto the exposed optic nerves. After 10—15 min fixation in situ, a 10 mm long portion of the nerve nearest to the optic chiasma was removed. Small pieces obtained by cutting the tissue with a razor blade were left to fix in Karnovsky solution at room temporature for 8 h (for morphological studies) and for 60—90 min (for studying the activity of some hydrolytic enzymes).

* This investigation was supported by NIH PL 480. Research Agreement No. 05-027-N.

These latter sections were carefully washed in 0.2 M cacodylate buffer and incubated in media for acid phosphatase (Miller, Palade, 1964) and for thiamine pyrophosphatase (Novikoff, Goldfischer, 1961). After incubation the sections were rinsed for 15 min in veronal-acetate buffer (pH 7.4).

Following this procedure, these sections were processed similarly to those for morphological studies. All the experimental material was stored overnight in cacodylate buffer and fixed in 1% osmium tetroxide for 1 h, washed in veronal-acetate buffer for 15 min, dehydrated and embedded in Epon. Both semithin and ultrathin sections were cut on Reichert ultramicrotome: Ultrathin sections were counterstained on grids with uranyl and lead salts (the latter was omitted in the case of sections from enzyme-incubated material) prior to examination in JEM 7A electron microscope.

RESULTS

On the 4th day after the operation only slight changes of axoplasmic density and initial splitting of myelin lamellae was noted. At the same time an increase in the number of lysosomal structures in the astrocytic perikarya and in their processes penetrating between the groups of axons was observed (Fig. 1). Some of these lysosomal bodies revealed a multilamellated internal structure (Fig. 1, insert). AcP-ase activity was confined to larger lysosomes (Figs. 2, 3), only occasionally enzyme activity was observed in cysterns of the Golgi system.

Several axons, mainly larger ones, displayed more distinct degenerative changes during this period. More advanced splitting of lamellae and contraction or watery appearance of the axoplasm could be seen. Some myelin sheaths were collapsed showing no traces of axoplasm inside. It seemed that they had lost their connections with the supporting oligodendroglia cells, as inner and outer loops were no longer observable. Processes of fibrous astrocytes with a fair number of polyribosomes and granular endoplasmic reticulum (GER) structures were visible surrounding degenerated myelin sheaths, which still retained their periodical structure (Fig. 4).

On the 8th day after the operation much more advanced degeneration of myelinated axons was observed. Concomitantly with gradual loss of neurotubules and neurofilaments, spectrum of various density of condensation and flocullation of axoplasm were noted as well as shell-like and telescopic patterns of collapsed myelin. Most of the astroglia population displayed voluminous, organellae-rich perikarya and broad, fibril-containing processes (Fig. 5). A small number of astroglial processes of much less density were also seen.

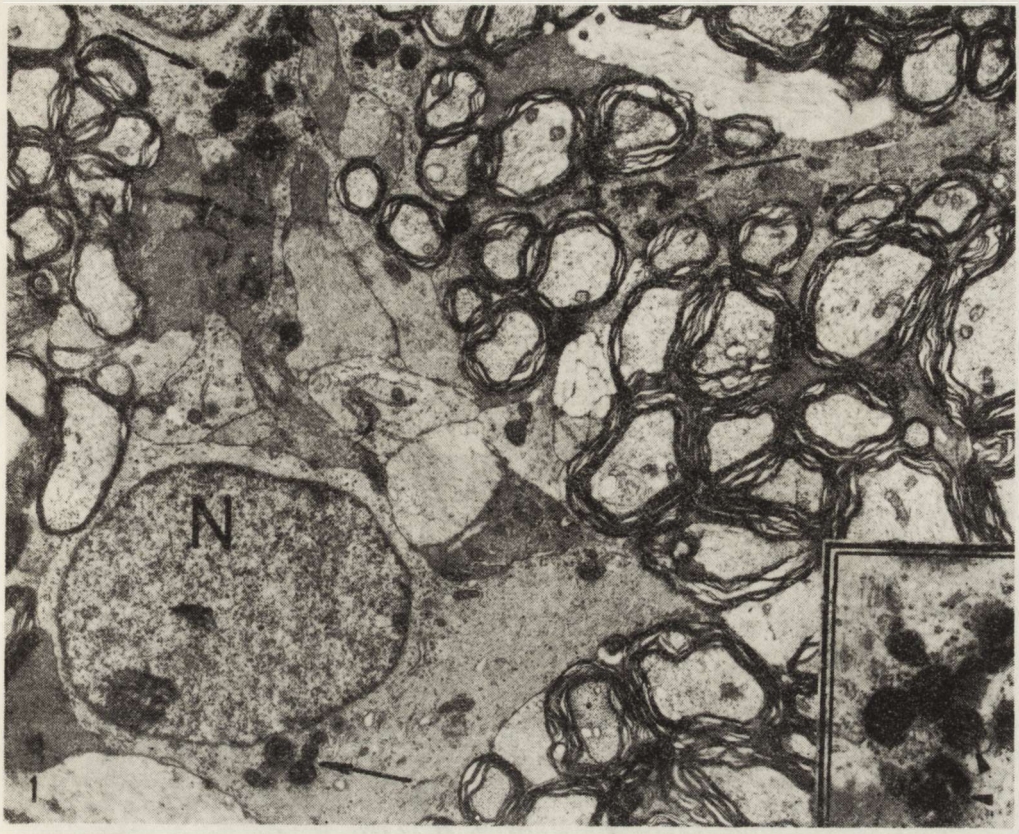

Fig. 1. (4th day after operation). Nucleus of fibrous astrocyte (N) shows an increased number of perichromatin granules. Perikarya and processes of astrocytes contain abundant conglomerates of lysosomal bodies (arrows). Insert reveals multilamellated internal structure of these lysosomes (arrowheads). Note also initial splitting of myelin lamellae, concomitant with a slight increase of axoplasmic density (asterisks). × 4 500; insert × 8 200

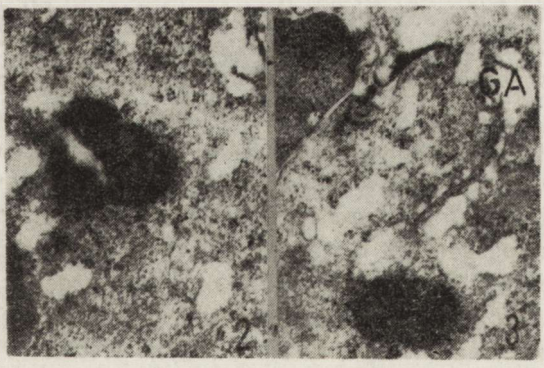

Fig. 2. (4th day after operation). Lysosome visible in the astrocytic cytoplasm contains. AcP-ase reaction product. × 31 000

Fig. 3. (4th day after operation). AcP-positive lysosome is situated in perinuclear cytoplasm of fibrous astrocyte. Neighbouring Golgi structures (GA) are devoid of enzyme reaction product. × 24 000

Fig. 4. (4th day after operation). Astrocytic process (Ap) tends to surround collapsed myelin sheath, which partially retains its periodical structure (arrows). Groups of lysosomes (L) of different size and shape in the other astrocytic process are visible. × 15 600

For the first time more pronounced changes in astroglial nuclei and cytoplasm were noted. Typical features of these cells were: invaginations of nuclear membrane, increased number of perichromatin granules and nucleoplasmic density much greater than in normal astroglia, comparable density of the cytoplasm due to numerous free and membrane--bound ribosomes, and the presence of wide, short cisterns of GER. Their processes containing gliofibrils embraced degenerated axons and, in the case of subpially located cells, formed glia limitans (Fig. 5).

In these reactive astrocytic cells the activity of AcP-ase was surprisingly low and was confined to the typical, round or oval lysosomes of 1—1.5 μm in size. The presence of enzyme reaction product in the Golgi system appeared to be extremely rare, but this structure was highly reactive for TPP-ase. Profuse reaction product was present in the outermost part of the Golgi system, but not inside the Golgi stacks (Fig. 6). In some instances diffuse reaction product filled to capacity large Golgi saccules (Fig. 7). It is worth noting that, on the 8th and 16th day after operation TPP-ase activity was much more pronounced in the astroglia of lighter rather than of darker cytoplasmic background (Fig. 8).

Fig. 5. (8th day after operation). Astrocytes (A) different in their nucleoplasmic and cytoplasmic densities. Their processes constitute glial limitans (arrows). Bundles of fibrils (f) and wide profiles of granular endoplasmic reticulum (GER) visible in their cytoplasm predominate in the "darker" cell. Axons in various stages of degeneration are present. Some of them are in close contact with the processes of astroglia (asterisks). × 4 200

On the 24th day after nerve transection a fair number of degenerated axons were situated intracellularly. The way in which engulfing progressed is shown in Fig. 9, where the process of fibrous astrocyte completely surround the axon with disintegrated axoplasm but with still retained periodicity of the myelin sheath. The normal structure of myelin, even engulfed, persisted usually as long as it was sequestrated from the cytoplasm by the trilaminar membrane. On 32nd and 48th day of experimental injury intracellular digestion of myelin debris proceeded, but many degenerated axons were still observable lying extracellulary. In these cases small and irregular clefts of extracellular space were visible in close vicinity of the split and collapsed myelin (Fig. 10). For the first time conglomerations of rounded, electron-lucent vacuoles appeared in the astrocytic cytoplasm (Figs. 10—12). As a rule, they were delineated by a thin rim of a structureless electron-dense substance- but in some cases no definite borders could be traced (Fig. 12). Vacuoles were closely associated with the ingested myelin frag-

Fig. 6. (16th day after operation). TPP-ase reaction product is localized in the outer part of the Golgi apparatus of fibrous astrocyte. × 54 000

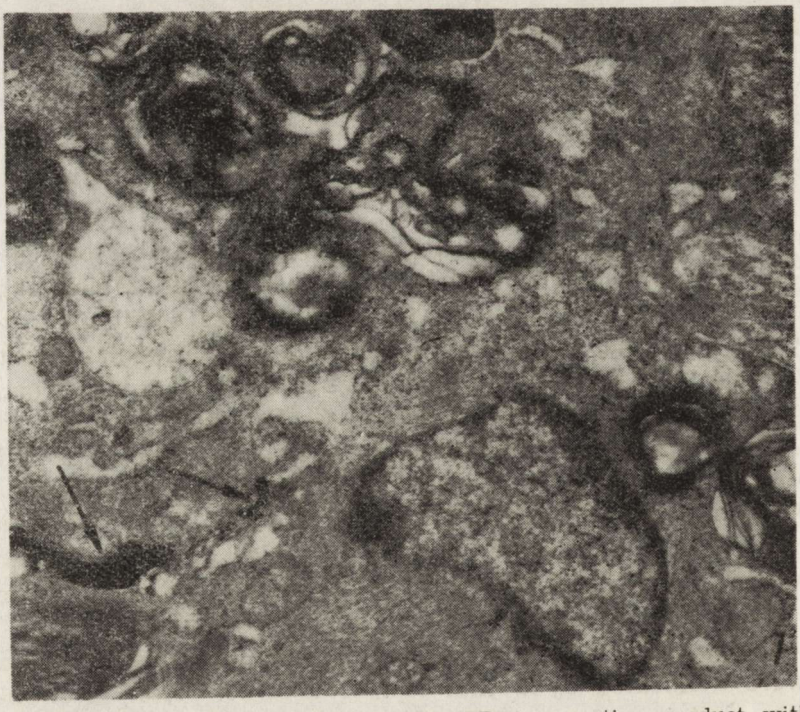

Fig. 7. (16th day after operation). Profuse TPP-ase reaction product within the Golgi structures of fibrous astrocyte (arrows). Groups of degenerating axons are situated in close vicinity to the cell. × 23 000

Fig. 8. (16th day after operation). Two fibrous astrocytes of different cytoplasmic density (compare with Fig. 5). The TPP-ase reaction product is present in the Golgi structures (arrows) of the "lighter" cell, whereas their counterparts of the "darker" one are empty (arrowhead). × 8 100

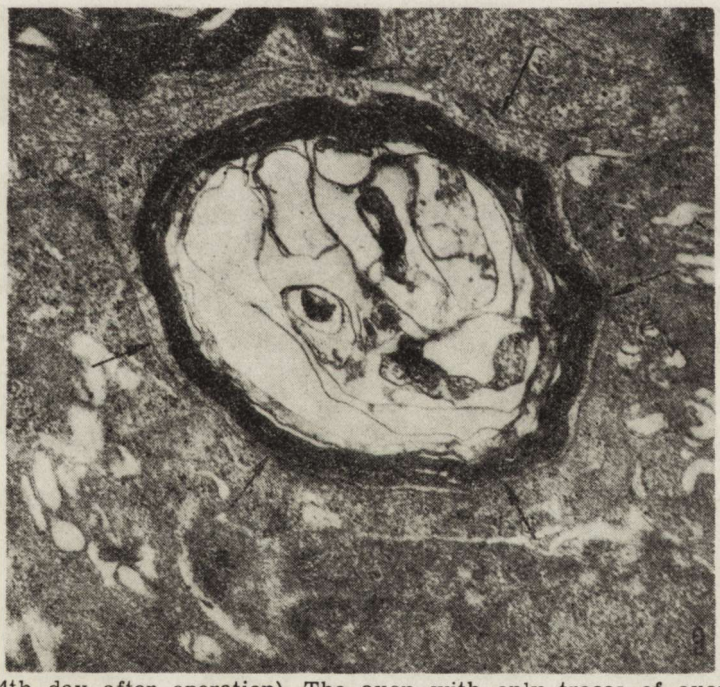

Fig. 9. (24th day after operation). The axon with only traces of axoplasm, but rather well preserved myelin sheath, is completely encircled with astrocytic process (its plasma membrane is shown by arrows). Another astrocyte with enlarged Golgi system is visible in the lower part of the picture. × 26 300

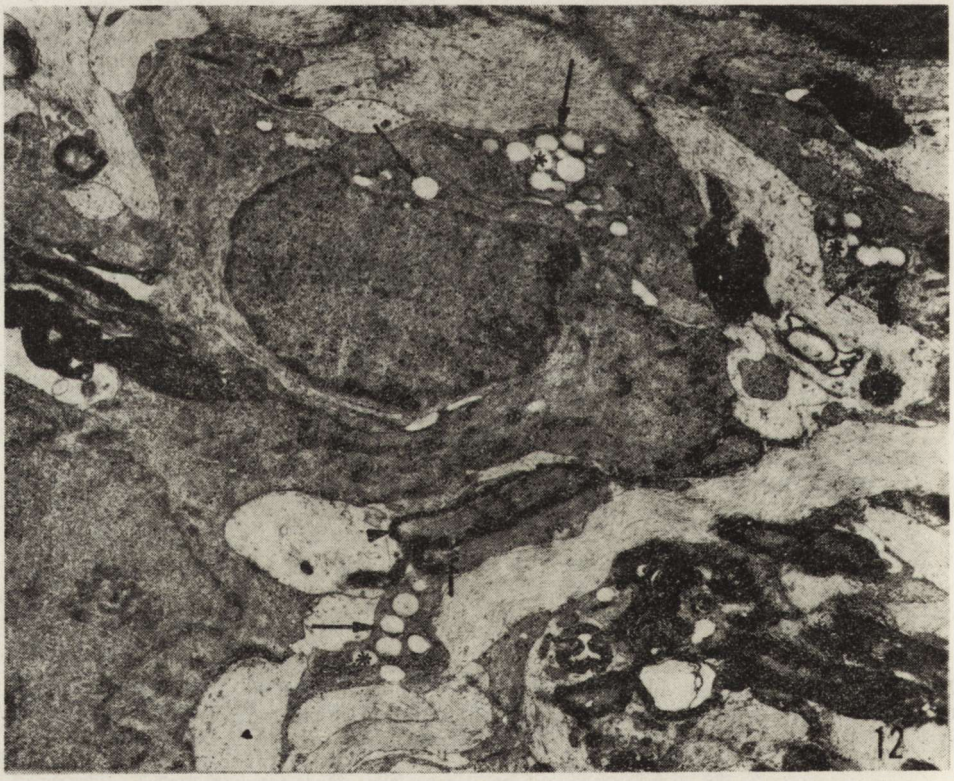

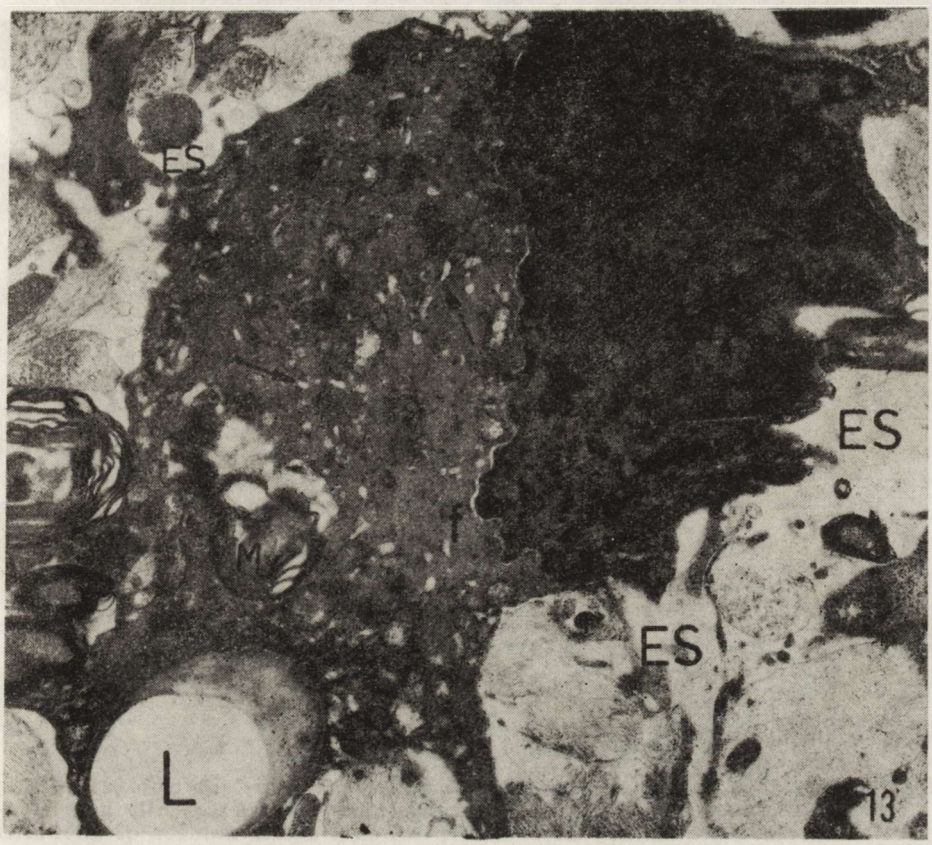

Fig. 13. (80th day after operation). The cell of irregular outline, thin processes and dark cytoplasm contains gliofibrils (f) and wide profiles of GER (arrows). Degenerating myelin (My) and huge lipid vacuole (L) partially filled with an amorphous substance are present within the cytoplasm. Considerable amount of extracellular space (ES) between intact plasma membranes is visible. × 16 100

Fig. 10. (32nd day after operation). Astrocytic process containing lipid vacuoles (L) associated with ingested myelin fragments (My). This process almost completely surrounds a relatively normal-looking axon (asterisk), leaving small clefts of extracellular space (arrows). × 17 200

Fig. 11. (32nd day after operation). Phagocytosed myelin fragments (My) with its structure becoming effaced — compare with the myelin surrounding the axon just being ingested (asterisk). Light lipid vacuoles are bordered by a rim of structureless substance (arrows). × 22 000

Fig. 12. (32nd day after operation). Round, electron-lucent vacuoles are visible in the astrocyte perikaryon and processes (arrows). One of these processes containing gliofibrils (f) and vacuoles is closely associated with the degenerating axon (arrowhead). Most of vacuoles are bordered by a thin rim of the electron dense substance, but some (asterisks) have no definite borders. × 6 600

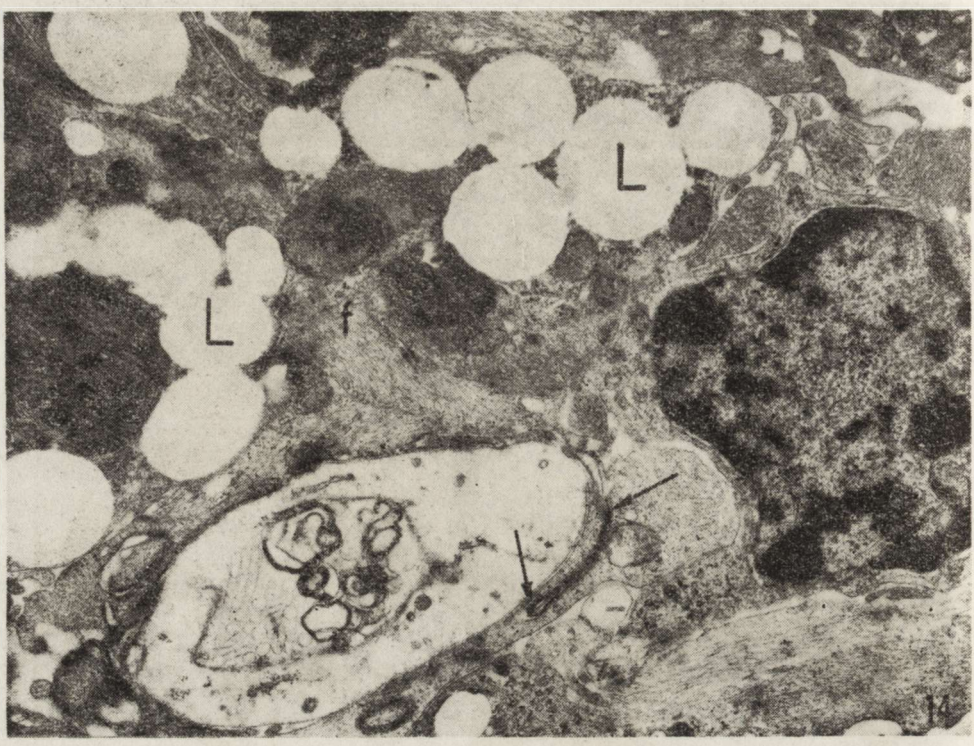

Fig. 14. (80th day after operation). Myelin ovoids (asterisks) in close connection with large, electron-lucent vacuoles (L) which tend to coalesce. All these structures are present within the cell process possessing a fair number of gliofibrils (f). Note also aberrant myelin (arrows) between closely apposed astrocytic processes. × 17 300

ments, which gradually loose their normal periodicity, as they were no longer separated from the cytoplasm (Fig. 11). Many wide GER channels were seen in the area of vacuole accumulation, but there was no evidence of distending of these structures to form vacuoles.

On 80th day after nerve transection the fibrous scar involved the majority of nerve tissue. In some places astrocytic processes were closely packed, in others a fairly large extracellular space appeared with no evidence of being artifactual — plasma membranes were usually intact (Fig. 13). Some degenerated axons were still lying extracellulary and in those cases their myelin sheath partially retained its normal structure. When myelin was closed in an astrocyte body, it lost its structure and was transformed into ovoids closely associated with lipid vacuoles (Fig. 14). All the structures mentioned above were situated within the cells possessing bundles of gliofibrils (Figs. 13—15). The cytoplasm of these cells radically changed its morphology, when compared with normal astroglia. Their dark nuclei of irregular outline sometimes possessed an increased number of perichromatin granules, and

Fig. 15. (80th day after operation). The irregularly shaped cell contains bundles of gliofibrils, a large, electron-lucent vacuole (L) and myelin ovoids (asterisks). The astrocyte process in the left upper part enclose numerous lipid vacuoles either outside or inside the phagocytized myelin just becoming effected (arrows). Considerable amounts of extracellular space is visible. × 18 900

the wide cisterns of GER were still present within the dark cytoplasm (Fig. 13) — which caused their similarity to earlier described reactive forms. The great overall density and the presence of long, thin processes would suggest categorizing these cells to microglia type, but the presence of gliofibrils would invalidate this (Fig. 13, 15).

DISCUSSION

The above presented data show that in Wallerian degeneration of the rabbit optic nerve parallel to massive, but relatively slow disintegration of myelinated axons considerable morphological changes of astroglial cells are present. In the earliest stage of the pathological process, when only slight changes in axoplasm and myelin are to be observed a fair number of lysosomal, AcP-positive structures appear within the perikara and processes of astroglia cells. Beginning from the 8th day after nerve transection, when almost all axons undergo disintegration to various extent, astrocytic cytoplasm becomes much more voluminous than in normal conditions and contains a greater number of wide cisternae of GER, many lysosomal structures of vari-

ous size and shape, and enlarged Golgi complexes showing high TPP-ase activity. These cells meet either morphological (Vaughn, Pease, 1970; Nathaniel, Nathaniel, 1977) or histochemical (Wender, Kozik, 1971) criteria for reactive forms.

Simultaneously cells which also contain wide channels of GER, but with much greater density of cytoplasm due to an increased number of free and membrane-bounded ribosomes, and with nucleus of irregular outline containing an increased number of perichromatin granules, may be seen. The overall aspect of these cells strongly suggested their ability to fibril protein synthesis (Vaughn, Pease, 1970). Therefore, in spite of the rather low activity of hydrolytic enzymes, these cells may be also recognized as reactive forms of increased metabolic activity.

Broad processes filled with bundles of glial filaments are common for the two types of reactive astroglia presented above. It is impossible to decide, whether these cellular forms exist parallelly, or undergo transformation one to the other. It seems unjustified to consider reactive astroglia as primitive, dedifferentiated forms, as Fernando (1973) suggests. Instead, analysis of dynamic cellular changes in the early stages of degeneration indicates that mature astrocytes gradually changed their morphology on account of the new functions they have to fulfill in the injured nerve. These new functions are: producing glial scar and phagocytosis. Both these processes require large amounts of protein produced by the cell itself; therefore mature, reactive astrocyte bears, in some respect, a resemblance to early or late astrocytoblasts.

The sequence of events in phagocytosis of degenerated myelin is just the same, as has been described by Bignami and Ralston (1969). The cell process surrounds the extracellulary lying, misshapen myelin sheath which, however, retains its periodicity for some time after being engulfed. Intracellular lytic action results in the loss of the characteristic structure of myelin, and in turn gives rise to large ovoids and round electron-lucent vacuoles. But contrary to the claim of these authors, the phagocytic function is, in this experimental model, performed exclusively by astroglia. The only criteria which were used for the identification of the phagocytes as astroglia is the presence of gliofibrils Such a simple, but unquestionable criterion is especially useful, when the cell containing myelin disintegration products bears superficial resemblance to a classical microglia cell (see Fig. 15). Other evidence to support identification of lipofages as astroglia has been drawn from many similarities in the cytoplasmic pattern of phagocytes and of dark, reactive astroglia, which in the early period of degeneration directed their processes to the group of degenerating axons.

All the phagocytes observed in the rabbit optic nerve in the course of Wallerian degeneration reveal bundles of gliofibril which can exclude oligodendrocytes, microglia, adventitial cells, multipotential glial

cells and also cells of hematogenous origin as a source of lipophages. This is contrary to the claim of many investigators examining central Wallerian degeneration. A possible explanation is offered by regional and species differences. Another one would be drawn from Vaughn and Pease's statement (1970): "phagocytic cells might derive from several different sources, ... numbers of phagocytes depend upon the extent of neural degeneration and the degree of inflammation involved".

However, the lack of sufficient criteria for cellular identification in injured nervous tissue should also be taken into consideration as a possible source of an old controversy on the origin of macrophages in general. In this experiment only one, certain criterion, appears to be sufficient for proper identification of the cell type, which in the course of time changes its functions and, consequently, also its morphology--bearing a superficial resemblance to quite different cellular elements. The other way, leading to proper cellular identification in pathological conditions seems to be a step by step study of tissue morphology in the course of time with the intention of constructing the dynamic picture of cellular changes. This has been done in this experiment for structural and histochemical analysis of reactive astroglia cells.

I wish to acknowledge the skillful technical assistance given by Miss Mieczysława Kwiatkiewicz.

REFERENCES

1. Bignami A., Ralston H. J., III: The cellular reaction to Wallerian degeneration in the central nervous system of the cat. Brain Res., 1969, 13, 444—461.
2. Cook R., Wiśniewski H. M.: The role of oligodendroglia and astroglia in Wallerian degeneration of the optic nerve. Brain Res., 1973, 61, 191—206.
3. Fernando D. A.: An electron microscopic study of the neuroglial reaction in Wallerian degeneration of the corticospinal tract. Acta anat., 1973, 86, 459—473.
4. Karnovsky M. J.: A formaldehyde-glutaraldehyde fixative of high osmolarity for use in electron microscopy. J. Cell Biol., 1965, 27, 137A—138A.
5. Miller F., Palade G. E.: Lytic activities in renal protein absorption droplets. An electron microscopical cytochemical study. J. Cell Biol., 1964, 23, 519—532.
6. Nathaniel E. J. H., Nathaniel D. R.: Astroglial response to degeneration of dorsal root fibers in adult rat spinal cord. Exp. neurol., 1977, 54, 60—76.
7. Novikoff A. B., Goldfischer S.: Nucleoside-diphosphatase activity in the Golgi apparatus and its usefulness for cytological studies. Proc. Natl. Acad. Sci. USA, 1961, 47, 802—810.
8. Reier P. J., Webster H. deF: Regeneration and remyelination to Xenopus tadpole optic nerve fibres following transection or crush. J. neurocytol., 1974, 3, 591—618.
9. Wender M., Kozik M.: Aktywność enzymów neurogleju w okresie mielinizacji i demielinizacji. Neurol. Neurochir. Pol. 1971, 5, 617—622.

10. Vaughn J. E., Hinds P. L., Skoff R. P.: Electron microscopic studies of Wallerian degeneration in rat optic nerves. I. The multipotential glia. J. comp. Neurol., 1970, 140, 175—206.
11. Vaughn J. E., Pease D. C.: Electron microscopic studies of Wallerian degeneration in rat optic nerves. II. Astrocytes, oligodendrocytes and adventitial cells. J. comp. Neurol., 1970, 140, 207—226.

Author's address: Department of Neurology, School of Medicine, 49, Przybyszewski Str., Poznań 60—355, Poland

NEUROPAT. POL., 1982, 20, 1—2
PL ISSN 0028—3894

PIOTR B. KOZŁOWSKI

PATHOMECHANISM OF PERIVENTRICULAR WHITE MATTER NECROSIS IN NEWBORNS

PRELIMINARY REPORT

Laboratory of Developmental Neuropathology, Medical Research Centre, Polish Academy of Sciences, Warszawa

White matter necrosis in the immature brain has been known for a long time, but its morphological features are still being discussed, and pathogenesis remains speculative. Its first description was given by Virchow in 1867 (quoted after Friede, 1975) and interpreted as congenital encephalitis. Later, white matter necrosis, as a part of inflammatory changes of brain tissue was separated from non inflammatory white matter lesions. Many damaging factors resulting in this kind of changes were suggested by different authors. Most of them emphasize the role of anoxia (Banker, Larroche, 1962; Terplan, 1967; Larroche, 1977; Ferrer, Navarro, 1978). Schwarz's concept (1956; 1961) accepts venous stasis and stagnant anoxia as the most common cause of the leukomalacia in newborns. Periventricular foci of coagulative necrosis separated by Banker and Larroche (1962) from the whole group of white matter necrosis of different types under the name of "periventricular leukomalacia" are considered by Larroche (1977) as the effect of local ischemia.

The other types of lesions such as edema, colliquative focal or extensive necrosis leading to caval destruction of the immature white matter provoke more controversy (Towbin, 1970; Schwartz, 1972; Friede, 1975; Terplan, 1976).

Many experiments were carried out to find possible explanation of the effect of general hypoxia, asphyxia, local ischemia, shock, infection and other factors that might be responsible for the white matter damage in immature brain. The white matter abnormalities very similar to those observed in human neonatal brains were obtained by Abramowicz (1964) in adult cats, in which basilar artery and one or both Sylvian arteries were occluded. Vascular network of the cat's brain in many respects is very similar to this in the human fetal brain. How-

ever, in human newborns this kind of occlusions provokes quite different lesions and in cases with periventricular necrosis occlusions or narrowings of those vessels can rarely be seen. Analysis of particular autopsy cases is complicated by frequent occurrence of different concomitant factors which may be responsible for the damage of the newborn's brain. Further investigations of large groups of cases seem to be necessary for establishing the real correlation between the type of the particular factor and an exact form of white matter lesion. A large autopsy material from one obstetric hospital was available in our Laboratory and this inclined us to analyse the problem of coexistence of white matter lesion with various pathologic factors both in the mother and in the newborn child.

MATERIAL AND METHODS

Investigations were performed on 33 cases of premature infants and newborns with necrotic changes in white matter. This group was selected from 419 brains of newborns who died in the first days of life in the Obstetric Clinic of Medical School in Warsaw during a 10-year period from 1963 to 1974. In all the newborns who died in this Clinic, general autopsy and microscopical examination of the internal body organs were routinely performed. All the brains from those cases were studied both macroscopically and microscopically. The light microscopy was performed on the material stained with the routine neuropathological techniques.

Cases with inflammatory changes in white matter were excluded. In the selected group of 33 cases with the white matter necrosis the analysis included the morphological abnormalities in the brains, their developmental age, and changes in all body organs. Data concerning gestation and delivery were also taken into consideration.

RESULTS

Analysis of clinical data reveals that complications of gestation such as diabetes and gestosis, complications of delivery-requiring cesarean sections or instrumental intervention (vacuum extractor, forceps) and deliveries diagnosed as infected were more frequent in cases with periventricular lesions of the newborn brain than in all 419 newborns under study (Table 1).

In the neuropathological examination coagulative necrosis was seen in 8 cases of the series. In the light microscopy the necrotic areas took the forme of a cellular, homogeneous foci, lightly stained with hematoxylin-eosin and deeply PAS-positive (Fig. 1). These foci were irregular in shape and surrounded by rarefied tissue. In cases with a longer duration the cavities were formed with macrophages and hypertrophic

Table 1. Frequency of gestation and delivery complications

Gestation and delivery complication	Cases with the white matter lesions 33 cases — 100%	Total material 419 cases — 100%
Diabetes	12%	8,6%
Gestosis	36%	8%
Cesarean section	24,2%	11,7%
Vacuum extractor, forceps	22%	1,7%
Infected delivery	11%	6,3%

glial cells on their periphery (Fig. 2).

Another type of damage was marked focal edema observed in 15 cases. Rarefaction of tissue without macrophagic reaction but with numerous reactive hypertrophic or swollen glial cells was the most typically pathological features of such foci (Fig. 3). This type of the white matter abnormality was considered as an initial stage of the colliquative necrosis.

Colliquative necrosis was presented in 10 cases. Its foci were characterized by dissolution and disintegration of while matter with macrophages, reactive astrocytes and gemistocytes filling the whole necrotic areas (Fig. 4). Concomitance of coagulative and colliquative necrosis was found in only one case. Necroses and focal edematous changes were either uni- or bilateral and then not always symmetrical. Coagulative necrosis occurred exclusively in the periventricular region, frontally to anterior horns of lateral ventricles, in corona radiata of parietal lobes and laterally to occipital horns. Areas of colliquative necrosis and severe edema with rarefaction and disintegration of white matter were also seen in the periventricular regions, but as a role they occupied larger areas. In only one case small foci of necrosis were located in the central parts of cortical gyri.

The intensity of hypoxic changes in the analysed brains should be pointed out. The features of generalized anoxic encephalopathy in the form of diffuse neuronal lesions in all the grey structures, predominantly in the cortex, were found in 15 cases. Peri- and intraventricular hemorrhages, subarachnoid hemorrhages and focal neuronal loss which are the other results of prolonged hypoxia were observed in 26 cases. Inflammatory changes took the form of macrophagic leptomeningitis, in two cases with shallow infiltration of cortex, but in none of these brains inflammatory process was present in the white matter.

Developmental age of analyzed brains, which was taken as an indication of the development of the newborn, in 20 cases was 36 weeks or more, in 7 cases was 32—36 weeks and only in 6 cases were less. Within the group of cases with coagulative necrosis there was no case with a developmental age of the brain younger than 34 weeks.

Fig. 1. Early stage of coagulative necrosis with congestion and small hemorrhagic foci around the necrotic area. H—E. × 60

Fig. 2. The lesion of a longer duration. Small cavity surrounded by numerous glial cells and few macrophages. H—E. × 100

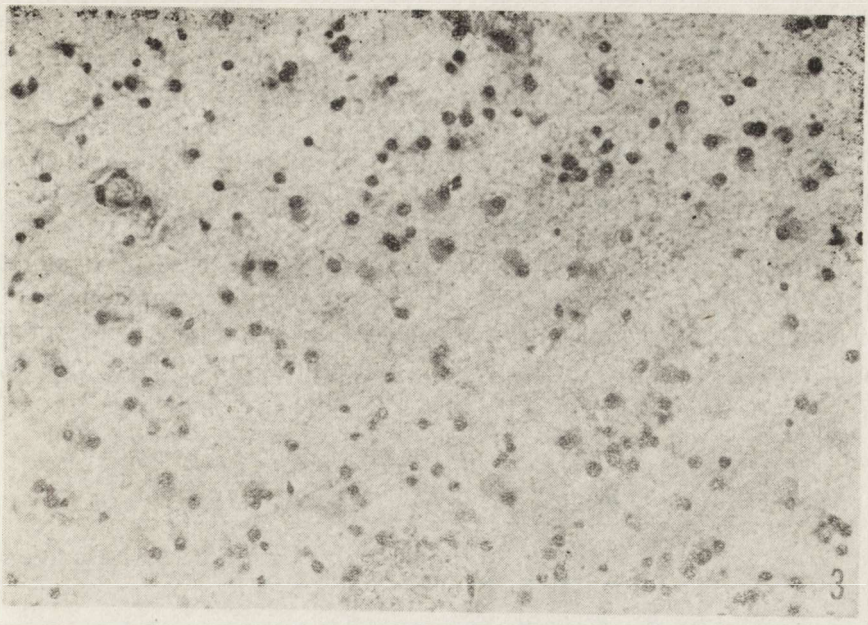

Fig. 3. Focal edema. Hypertrophic glial cells lying within rarefied edematous background. H—E. × 150

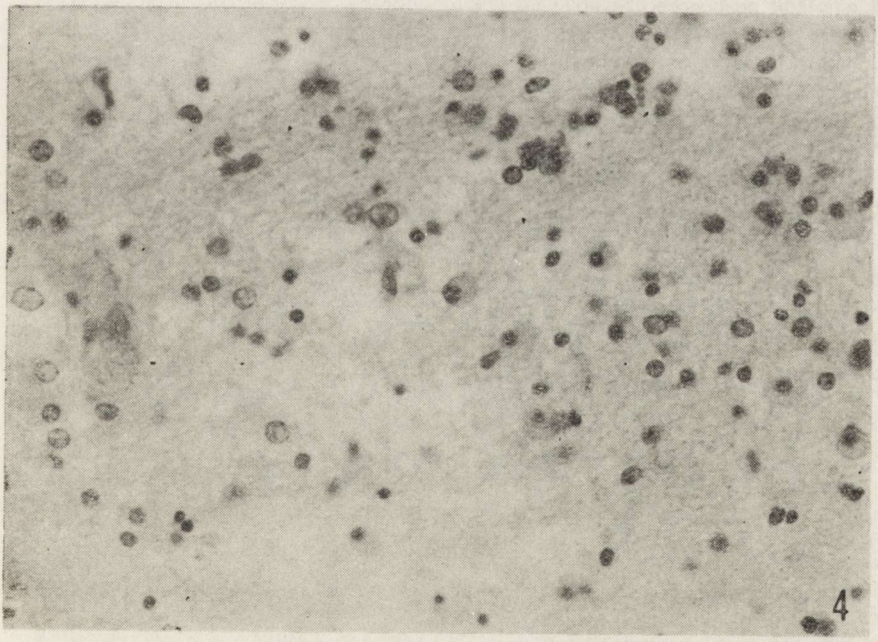

Fig. 4. Fresh colliquative necrosis. Numerous macrophages in liquefied white matter. H—E. × 330

The microscopic examination of the internal body organs revealed that massive, confluent pneumonia was by far the most frequent finding (15 cases). Hyaline membranes were present in lungs of 8 cases (in 3 of them together with pneumonia), hypopneumatosis and hemorrhages without pneumonia and hyaline membranes in other 8 cases. Features of generalized anoxia were found in 21 newborns and generalized infection in 5 cases.

In the placenta and in the umbilical cord in 6 cases inflammatory infiltrations were found, and in 19 ones various placental abnormalities which might have damaged maternal-fetal exchange were present. These were pathological changes of placental villi, villous vessels, or infarcts.

Table 2. Anoxic and inflammatory changes

Type of changes	Cases with the white matter lesions 33 cases — 100%	Total material 419 cases — 100%
Peri- and intraventricular hemorrhages	30%	37%
Subarachnoid hemorrhages	36%	37,4%
Anoxic encephalopathy	39,4%	25,5%
Features of generalized anoxia of newborn	63,6%	69,9%
Meningitis and meningoencephalitis	21,2%	6,1%
Pneumonia	45,4%	39,4%
Inflammatory changes in placenta	18,2%	6,3%
Generalized infection of newborn	15,1%	2,7%
Infected delivery	10%	6,3%

The pathologic changes described above indicated that in nearly all cases with white matter lesions hypoxic changes and features of infection occurred. They were much more frequent in this group than in all 419 newborns under study (Table 2). The combined analysis of clinical data and postmortem examination proved the occurrence of both generalized hypoxia and infection in more than half cases (54%) of analized group (Table 3).

Table 3. Anoxic and inflammatory changes

Type of changes	Number of cases
Features of anoxia and infection	18
Anoxic changes without infection	11
Infection without anoxic changes	2
Neither infections nor anoxic changes	2

DISCUSSION

Neuropathological analysis of periventricular brain lesions in perinatal period combined with clinico-pathological correlation clearly indicates that hypoxia and infection play a very important role in the pathogenesis of this type of brain damage. It is a generally known fact that infections, mostly pneumonias in newborns and particularly prematures, generalize very quickly, leading to bacteriemia and endotoxemia (Głuszcz, 1961). Obviously infections and hypoxia may supplement each other. Pneumonia which was found in 15 of 17 infected newborns could have deepen hypoxic condition by altering blood oxidation in lungs (Dąmbska et al., 1977). Therefore it seems that concommitans of hypoxia and infection was one of the most important pathogenetic factors responsible for the brain lesions in the examined material.

Relatively higher metabolic rate of the myelinating periventricular white matter makes this region more vulnerable to insufficient blood supply, and it may lead to relatively more severe damage of white matter than the grey structures in the developing brain. A very high water content (90—92%) in immature brain may be the cause of local edema and necrosis more or less widespread in the white matter in cases of local circulatory disturbances (Rucka, 1970).

The special conditions of blood supply make the periventricular region specially vulnerable. Areas around the frontal horn of lateral ventricle, those located laterally to posterior horns in parieto-occipital region and laterally to temporal horns, are the border zones between the ventriculopetal and ventriculofugal arteries (De Reuck, 1971; 1977). Larroche (1977) postulated that coagulative necrosis (periventricular leukomalacia) in this region results from local ischemia in these "end

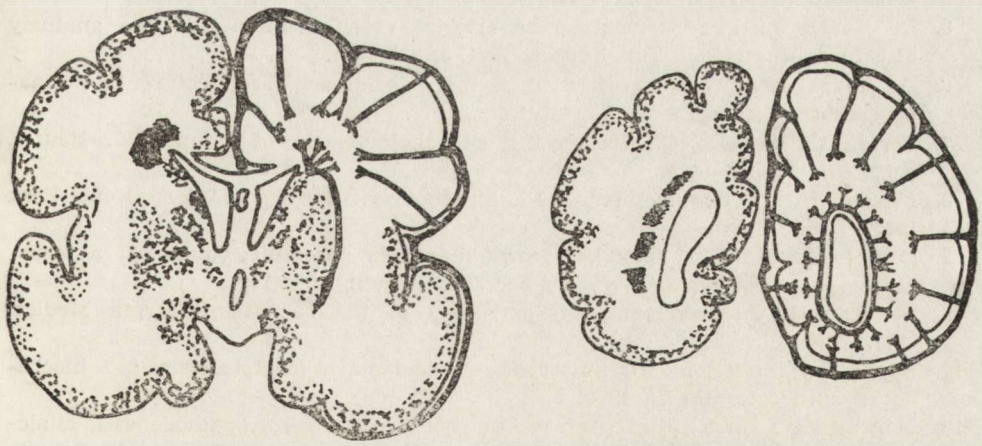

Fig. 5. Topography of periventricular necroses and vascularisation of the periventricular region (after Larroche, 1977)

zones". Friede (1975) used the term "periventricular infarcts" to indicate this type of brain lesion. The topography of lesions, not only coagulative necrosis but also colliquative and focal edematous damage, in the examined cases corresponds very well with the topography of periventricular border zones (Fig. 5).

Both the nature of the brain lesions and their topography indicate that local ischemia may be the most probable pathogenic factor responsible for their appearance.

In the absence of thrombosis in pial vessels, their constriction may be discussed as the cause of insufficient blood perfusion of the deep border zones. However, vasoconstriction in this condition seems rather improbable, because asphyxia (acidotic hypoxia), which is more common in perinatal pathology than hypocapnia, produces vasodilatation (Auer, 1978).

Our findings rise the question as to whether both generalized hypoxia and infection-may lead to such pathological process which could disturbe the blood supply in periventricular arterial border zones in the developing brain. This problem needs further investigation.

REFERENCES

1. Abramowicz A.: The pathogenesis of experimental periventricular cerebral necrosis and its possible relation to the periventricular leukomalacia of birth trauma. J. Neurol. Neurosurg. Psychiat., 1964, 27, 85—95.
2. Auer L.: Pial arterial reactions to hyper- and hypocapnia: a dynamic experimental study in cats. Eur. Neurol., 1978, 17, 351—362.
3. Banker B. Q., Larroche J. C.: Periventricular leukomalacia of infancy. Arch. Neurol. (Chic.), 1962, 7, 386—410.
4. Dąmbska M., Dydyk L., Liebhardt U., Roszkowski I., Szamborski J.: Zmiany w mózgach noworodków w następstwie uszkodzenia zespołu płód-łożysko. Neuropat. Pol., 1977, 15, 119—128.
5. De Reuck J.: The periventricular arterial vascularisation and the anatomy of cerebral infarction. Eur. Neurol., 1971, 5, 321—334.
6. De Reuck J. L.: The significance of the arterial angioarchitecture in perinatal cerebral damage. Acta Neurol. Belg., 1977, 77, 65—94.
7. Ferrer I., Navarro C.: Multicystic encephalomalacia of infancy. J. Neurol. Sci., 1978, 38, 179—189.
8. Friede R. L.: Developmental Neuropathology. Springer, Wien, New York 1975.
9. Głuszcz A.: Rozsiana okołokomorowa martwica posocznicowa mózgu a toksoplazmoza u wcześniaków. Wydz. Łódz. Tow. Nauk., Łódź 1961.
10. Larroche J. C.: Developmental pathology of the neonate. Excerpta Medica, 1977.
11. Rucka R.: Obrzęk mózgu noworodka w badaniach morfologicznych i biochemicznych. Doctor thesis. 1970.
12. Schwartz P.: Birth injuries of the newborn: morphology, pathogenesis, clinical pathology and prevention of birth injuries of the newborn. Arch. Pediat., 1956, 73, 429—450.

13. Schwartz P.: Birth injuries of the newborn. S. Karger, Basel 1961.
14. Schwartz P.: Birth injuries. In: Pathology of the nervous system. Mc Grow-Hill, vol. 2, 1972.
15. Terplan K. L.: Histopathologic brain changes in 1152 cases of the perinatal and early infancy period. Biol. Neonate, 1967, 11, 348—366.
16. Towbin A.: Central nervous system damage in the human fetus and newborn infant. Am. J. Dis. Child 1970, 119, 529—542.

Author's address: Laboratory of Developmental Neuropathology Medical Research Centre Polish Academy of Sciences, 3 Pasteur str., 02—093 Warszawa.

NEUROPAT. POL., 1982, 20, 1—2
PL ISSN 0028—3894

JOACHIM LEHMANN

POLYMICROGYRIA AND PORENCEPHALY AFTER INTRAUTERINE CYTOMEGALY VIRUS INFECTION

Department of Neuropathology, Pathological Institute, Karl-Marx-University, Leipzig

Maternal cytomegaly virus (CVM) infection occurs in about 6 per cent of pregnancies (Friede, 1975). The frequency of nonsymptomatic infection of the salivary glands in children amounts from 10 to 32 per cent (Weller, Hanshaw, 1962). Generalized disease was found in 1 or 2 per cent in autopsy series (Seifert, Oehme, 1957). In approximatively 10 per cent of cases with in acute fatal course, the central nervous system is involved (Medearis, 1957).

The pattern of cerebral lesions in the acute cases is different. In most cases picture typical of necrotizing meningoencephalitis is seen. The pathological changes consist mainly in tissue necrosis, bleeding, and mineralization, further typical inclusion bodies, type A. The preferential site of these changes are the walls of lateral ventricles, and less frequently the walls of the third and fourth ventricle (Haymaker et al., 1954).

The incidence of cerebral affections after intrauterine CMV infections in survivors appears to be much higher (Thalhammer, 1967; Friede, 1975). A definite connection — usually unrecognized — between CMV infection and cerebral damage is difficult to prove. But serological tests, performed in children with microcephaly and healthy controls showed significantly higher titer levels of antibodies against CMV in microcephalic children (Peller, Goetz, 1978). The early intrauterine infection leads to cortical malformations above all to widespread polymicrogyria of the neocortex, variably associated with porencephalic defects (Diezel, 1954; Nissen, 1969).

A case of a 12-year old girl with polymicrogyria and porencephaly after CMV infection is presented.

CASE REPORT

The patient was the first born child of a 19-year old mother who denied any infection or other complications during pregnancy. The mature born girl showed a distinct microcephaly. The clinical course was characterized by a severe mental and motor retardation, spastic pareses, epileptic seizures, and intermittent infections. The diagnosis of cytomegalic-inclusion disease was confirmed on the basis of detection of inclusion-bearing cells in the saliva and urine of the patient at the age of 10 and 12 weeks postnatal. At the age of 12 months a swelling of lymph nodes and a hepatosplenomegaly was detected. The girl died at the age of 12 years after intermittent respiratory infection. The general autopsy revealed multiple limb deformaties secondary to contractures, severe scoliosis, generalized dystrophy and pneumonia. Chronic nonspecific inflammation was found in the parotid glands with periductal lymphocytic infiltrations and proliferation of the ductal epithelium.

The main gross brain finding was microencephaly accompanied by a marked polymicrogyria of the frontal, parietal and temporal lobes, which however, did not involve the paleocortex. On the coronal section through the basal ganglia a porencephalic cavity, destroying particularly nucleus lentiformis and internal capsule on the left side was seen (Fig. 1).

The cortical malformation was characterized by an abnormal ar-

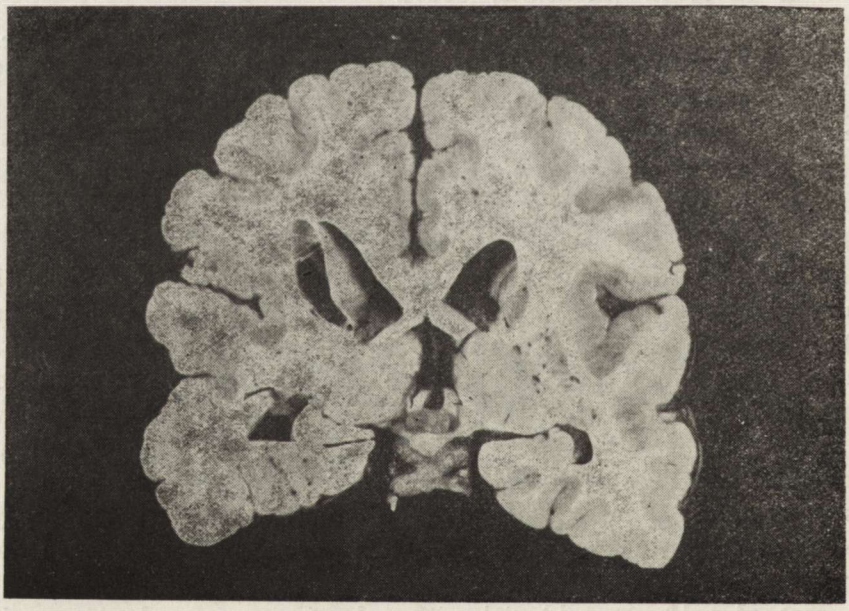

Fig. 1. Coronal section through the basal ganglia: marked polymicrogyria and paraventricular porencephalic cavity at the left side

rangement of all layers and an excessive folding of all of the upper layers and an absence of separation of the individual gyri due to the fusion of their surfaces. The usual pattern was a four-layered cortex associated with small heterotopias in the white matter. In some poly-

Fig. 2. Abnormal subpial plexus of myelinated fibers in a polymicrogyric area. × 52

Fig. 3. Cerebellar microgyria: fusion between folia, ectopic neurons in the molecular layer, and irregular formation of the internal granule cell layer. × 83

microgyric areas the cortex was a normal six layered one. These polymicrogyric regions show in parts an abnormal subpial plexus of myelinated tangential fibers (Fig. 2). Small areas of mineralization were scattered periventricularly.

In both cerebellar hemispheres small zones of microgyria were found. Fusion between folia, ectopic neurons in the molecular layer and irregular formation of the internal granular cell layer can be seen in these regions (Fig. 3).

COMMENT

The largest review of literature which we discovered about the association of cytomegalic inclusion disease with cerebral lesions was that by Nissen (1969). He listed 28 cases. The constellation of findings in these cases were as follows: 1) malformations (microgyria, pachygyria, heterotopias, microcephaly, cerebellar hypoplasia) associated with defects (porencephaly or hydranencephaly) and inflammatory changes: 7 cases; 2) malformations without other pathological changes: 3 cases; 3) defects without other pathological changes: 1 case; 4) inflammatory changes without other lesions: 10 cases; 5) malformations associated with inflammatory changes: 6 cases; 6) defects associated with inflammatory changes: 1 case.

The oldest patient died at the age of 1.4 years (Oehme, 1957). In all cases the cerebral lesions were connected with a viscerale manifestation of cytomegalic inclusion disease. The teratogenetic determination period in these cases ranged from the 4th to the 6th gestation month (Nissen, 1969). The viscerale manifestation in each of the cases implies that intrauterine CMV infections are chronic with a continuance to the postnatal life.

The significance of fetal CMV infection for causing malformation in the present case is not certain. But the typical constellation of findings and the detection of inclusion-bearing cells during the first three months of life suggest that there is such a connection.

Williams et al. (1976) after investigations with Golgi impregnation emphasized that the classical microgyric cerebral cortex is composed of typical six layers. There are no subcortical masses of heterotopic neurons. These observations indicate that microgyria is consequence of a pathological process acting after cellular migration to the cortex is completed yet before the final gyral pattern is established, that is approximately the 6th gestation month. The cortex of our case shows partly embryonal four-layered microgyric portions with subcortical heterotopic neurons. It seems to be the effect of an infection during the 5th to the 6th fetal month.

The histological features of cerebellar microgyria in the present case

confirm to De León's interpretation of this malformation (De León, 1972; De León et al., 1976). The author described cerebellar microgyria as a secondary fusion of pre-existent folia. According to his concept microgyria seems to result from a pathological process involving the external granule cell layer during a relatively late period of cerebellar development.

In the present case the combination of polymicrogyria, porencephaly and cerebellar microgyria supports the view of a continuation of the infection during the second half of pregnancy.

This report documents the difficulties in the teratogenic and etiologic interpretation of complex cerebral lesions in later stages.

REFERENCES

1. De León G. A.: Observations on cerebral and cerebellar microgyria. Acta neuropath. (Berl.), 1972, 20, 278—287.
2. De León G. A., Grover W. D., Mestre G. M.: Cerebellar microgyria. Acta neuropath. (Berl.), 1976, 35, 81—85.
3. Diezel P. B.: Mikrogyrie infolge cerebraler Speicheldrüsenvirusinfektion im Rahmen einer generalisierten Cytomegalie bei einem Säugling. Virchows Arch., 1954, 325, 109—130.
4. Friede R. L.: Developmental neuropathology. Springer, Wien, New York 1975.
5. Haymaker W., Girdany B. R., Stephens J., Lillie R. D., Fetterman G. H.: Cerebral involvement with advanced periventricular calcification in generalized cytomegalic inclusion disease in the newborn. J. Neuropath. exp. Neurol., 1954, 13, 562—586.
6. Medearis D. N.: Cytomegalic inclusion disease: analysis of clinical features based on literature and six additional cases. Pediatrics, 1957, 19, 467—480.
7. Nissen P.: Über zerebrale Zytomegalie. Inaug. Diss. Univ. Göttingen, 1969.
8. Oehme J.: Cerebrale Verlaufsform der Cytomegalie. Mschr. Kinderheilk., 1957, 105, 366—367.
9. Peller P., Goetz O.: Zerebralschäden und Zytomegalievirusinfektion. Dtsch. med. Wschr., 1978, 103, 265—267.
10. Seifert G., Oehme J.: Pathologie und Klinik der Cytomegalie. Abhandl. Gebiet. prakt. Kinderheilk., Vol. 2, Thieme, Leipzig, 1957.
11. Thalhammer O.: Pränatale Erkrankungen des Menschen. Thieme, Stuttgart, 1967.
12. Weller T. H., Hanshaw J. B.: Virologic and clinical observations on cytomegalic inclusion disease. New Engl. J. Med., 1962, 266, 1233—1244.
13. Williams R. S., Ferrante R. J., Caviness V. S.: The cellular pathology of microgyria. A Golgi analysis. Acta neuropath. (Berl.), 1976, 36, 269—283.

Authors address: Dr. J. Lehmann, Abteilung für Neuropathologie, Pathologisches Institut der Karl-Marx-Universität, DDR-701 Leipzig, Liebigstr. 26

NEUROPAT. POL., 1982, 20, 1—2
PL ISSN 0028—3894

MARIA DĄMBSKA, DANUTA MAŚLIŃSKA

EFFECT OF DICHLORVOS (DDVP) INTOXICATION OF RABBIT BRAIN

Laboratory of Developmental Neuropathology Medical Research Centre, Polish Academy of Sciences, Warszawa

Dichlorvos (DDVP) — a phosphoorganic pesticide has been proved to exert a toxic effect on brain metabolism (Pachecka et al., 1975; Sitkiewicz, Zalewska, 1975). Previous studies revealed that intoxication by DDVP among others leads to the damage of myelinated nerve fibers (Zelman, 1977). These observations suggest that this intoxication may evoke even more severe damage during myelination and produce abnormalities in the formation of myelin sheaths. The present work was undertaken to test this hypothesis on the developing brain in rabbits.

The studies were performed on 24 rabbits from 6 litters. Nine mg/kg body weight per day of DDVP were administered orally in 1 m oil between the 5th and 16th day of life to a half of each litter. The remaining animals represented a control group.

Morphological, histochemical (light microscopic) and ultrastructural investigations of the brain tissue were performed on 16- and 32-day old animals.

Samples for morphological studies were taken from the brain on the level of optic chiasm, embedded in paraffin and stained by Klüver method. Histochemical investigations were done on criostat sections and comprised the brain regions situated rostraly from the chiasm. Histoenzymatic investigations dealt with the activities of succinic dehydrogenase (Pearse, 1972), acid phosphatase (Gomori method and Barka, Anderson method, 1965; modified by Burston, with AS-TR as a substrate), acetylcholinesterase (Karnovsky, Roots, 1964; with iso-OMPA as inhibitor in the concentration of 1×10^{-5} M). They were performed on 16-day old animals. Histochemical reaction for phospholipids by OTAN reaction according to Adams (1965) and reaction for plasmalogen after Hayes as modified by Adams (1965) were performed on the brains of 32-day old animals. Tissue samples for electron microscopic examina-

tion comprising the central part of the corpus callosum were prepared according to the methods used for ultrastructural studies and examined in Tesla 500 BS electron microscope. Electron microscopic examination was performed on slices from the corpus callosum on the 16th and the 32nd day of life.

RESULTS

Morphological observations on sections stained by the Klüver method showed lack of myelin sheaths in corpus callosum of intoxicated animals in the 16th day of life and an evidently paler staining of this structure in the 32nd day of life (Fig. 1a, b).

Histochemical studies showed a decrease of acetylocholinesterase activity (AChE) in all brain regions of the intoxicated animals. This enzyme activity could not be detected in the corpus callosum and the internal capsule.

In the brains of control rabbits formazan grains indicating the SDH activity were found to accumulate in glial cells of corpus callosum on the poles of cytoplasm on both sides of the nuclei. These glial cells formed chains of different lengths along the myelinating fibers. In the brains of the intoxicated group the amount of formazan grains was decreased and the chain-glial arrangement was much less pronounced.

The acid phosphatase activity was very high in the cytoplasm of the glial cells in 16-day old control animals, but very weak in the brains of intoxicated rabbits (Fig. 2a, b).

OTAN reaction and reaction for plasmalogens in the corpus callosum fibers of 32-day old intoxicated animals were weaker in comparison to the control brains (Fig. 3a, b).

In the corpus callosum on the 16th day of life myelin had just begun to be formed. The number of fibers in the stage of myelination was smaller in the intoxicated animals than in the control group. In this structure some of the mitochondria were enlarged, their cristae tended to be on the periphery of the structure and fine-granular degenerative changes were visible in the matrix (Fig. 4). The damaged mitochondria were particularly abundant in the glial processes around the vessels. Astrocytic cytoplasm was electron-lucent and contained a few organelles and enlarged endoplasmic channels (Fig. 5). Mitochondria of this type were also visible in the perikarya of myelinating glia cells, often in the vicinity of the myelinating fibers.

In the 32nd day of life numerous glial cells contained altered mitochondria. Their degeneration was more advanced than in the 16th day (Fig. 6). Only a few cristae were present at the periphery of the large mitochondrial structure with fine granular degeneration. The cells with damaged mitochondria also showed other pathological changes. They

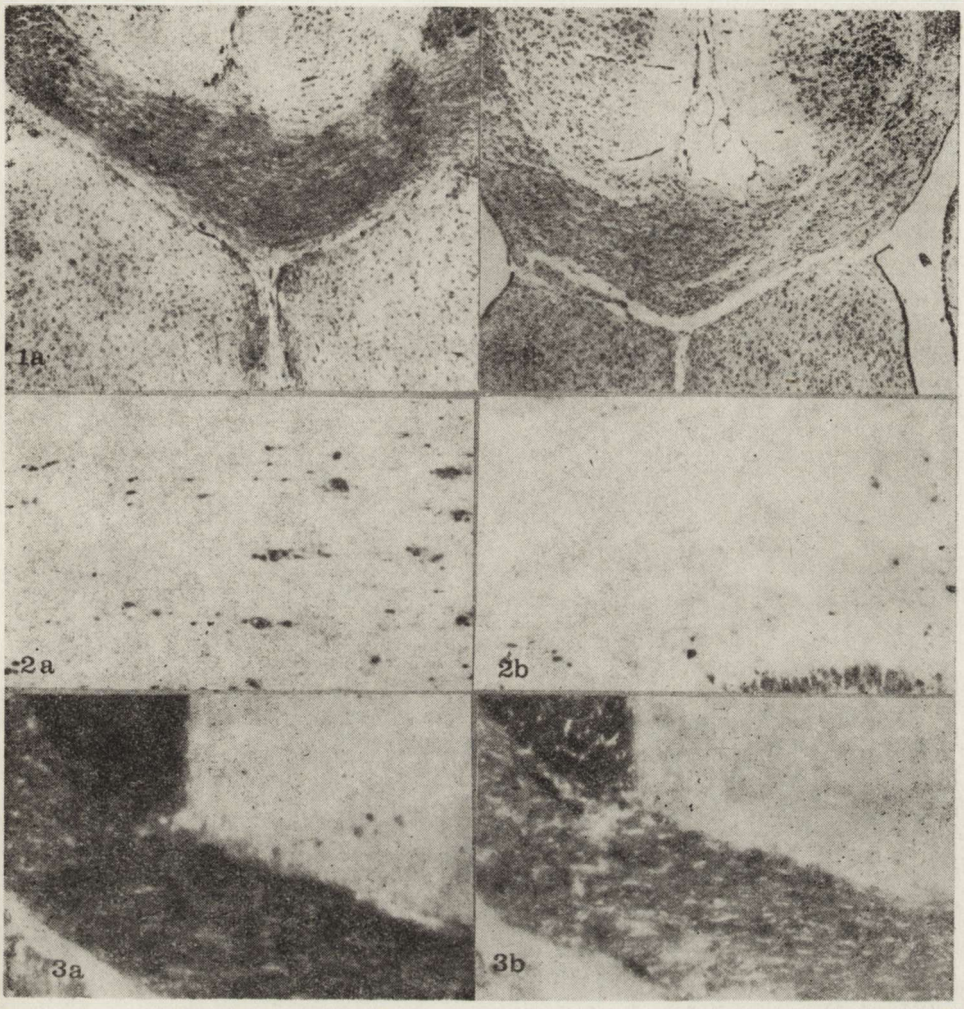

Fig. 1. The degree of myelination of the corpus callosum in a 32-day old rabbit: a) control, b) experimental group. Klüver. × 20

Fig. 2. Acid phosphatase activity in corpus callosum in a 16-day old rabbit: a) control, b) experimental group. Burston. × 100.

Fig. 3. The OTAN reaction in corpus callosum of a 32-day old rabbit: a) control, b) experimental group. × 30

had pale cytoplasm, poor in other organelles (Fig. 7). Lamellar mitochondrial degeneration was sporadically observed (Fig. 8). Generally, the processes of myelination of corpus callosum was present, but it was less advanced than in the animals of the control group. In some myelinating axons degenerative changes were found (Fig. 9). Between myelinating fibers an abnormal position of inner lamellae was present (Fig. 10).

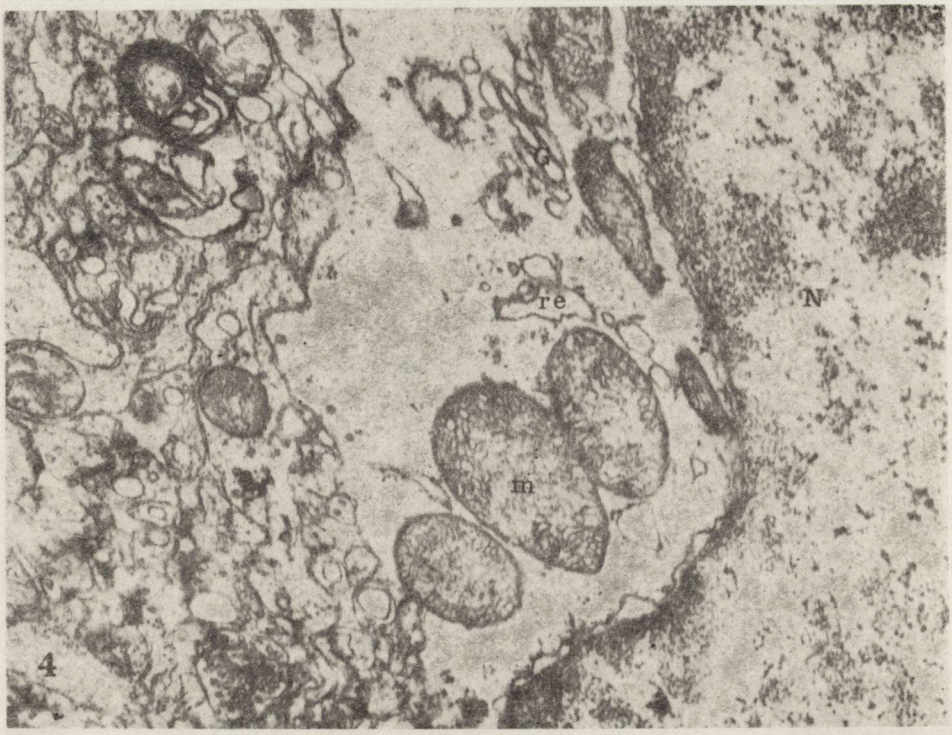

Fig. 4. Glial cell from corpus callosum of a 16-day old rabbit. Enlarged mitochondria (m) with granular changes in the matrix. N — nucleus, G — Golgi apparatus, re — endoplasmic reticulum. × 14 000

Fig. 5. Perivascular astrocytic process in corpus callosum of a 16-day old rabbit. Large, damaged mitochondria (m) in electron lucent cytoplasm. Endoplasmic reticulum enlarged. ep — endothelial process, A — astrocyte. × 7 000

Fig. 6. Corpus callosum of a 32-day old rabbit. Damaged mitochondria (m) with granular degeneration of matrix partially distended cristae situated at the periphery on astrocyte. Arrows — gliofibrile. × 14 000

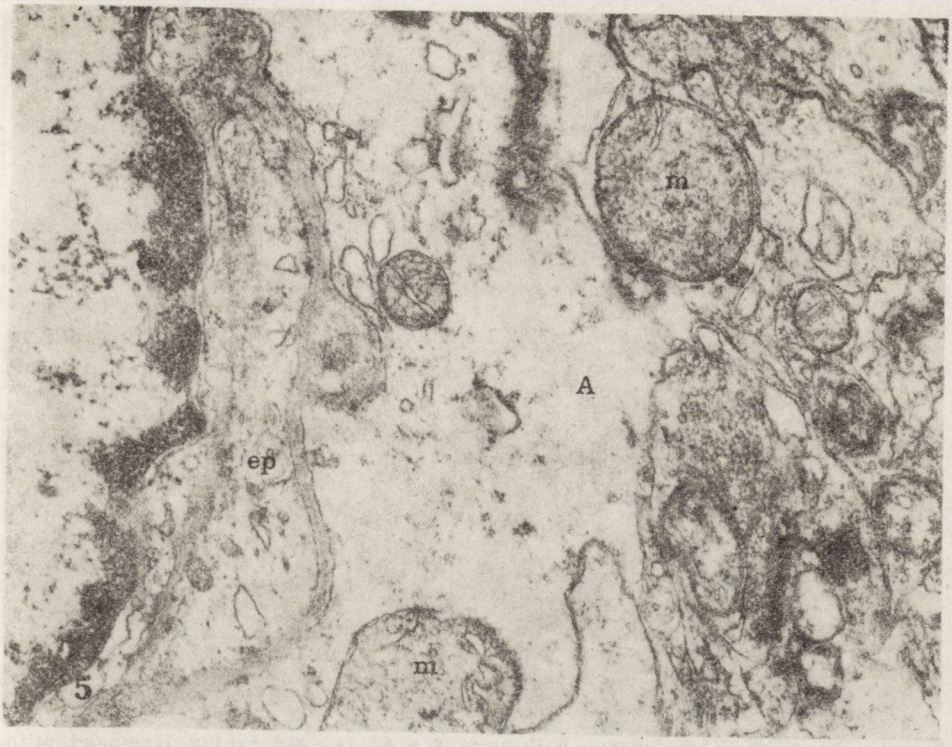

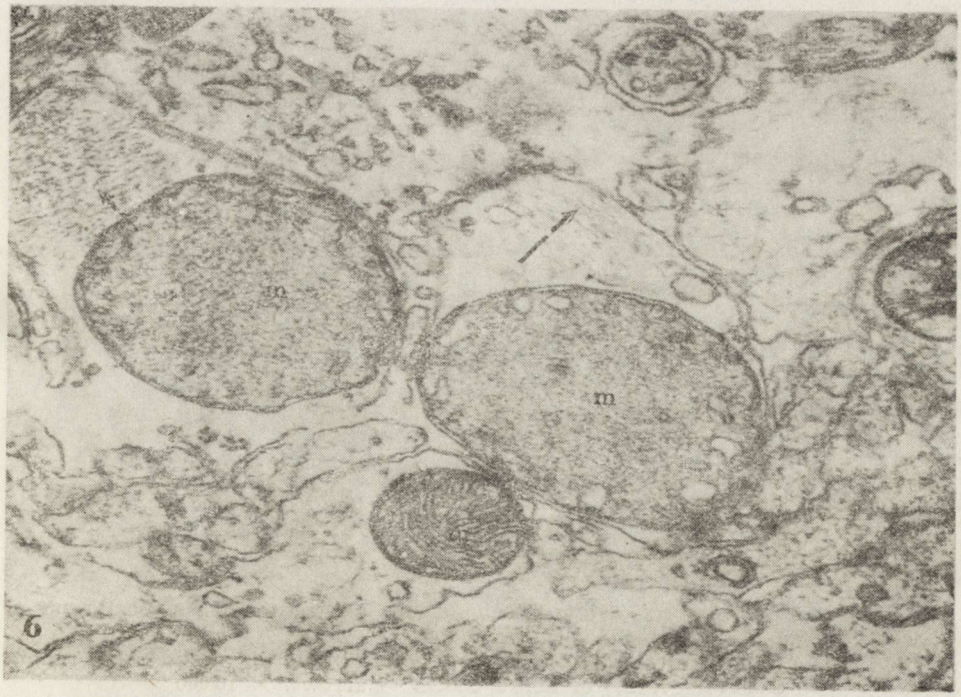

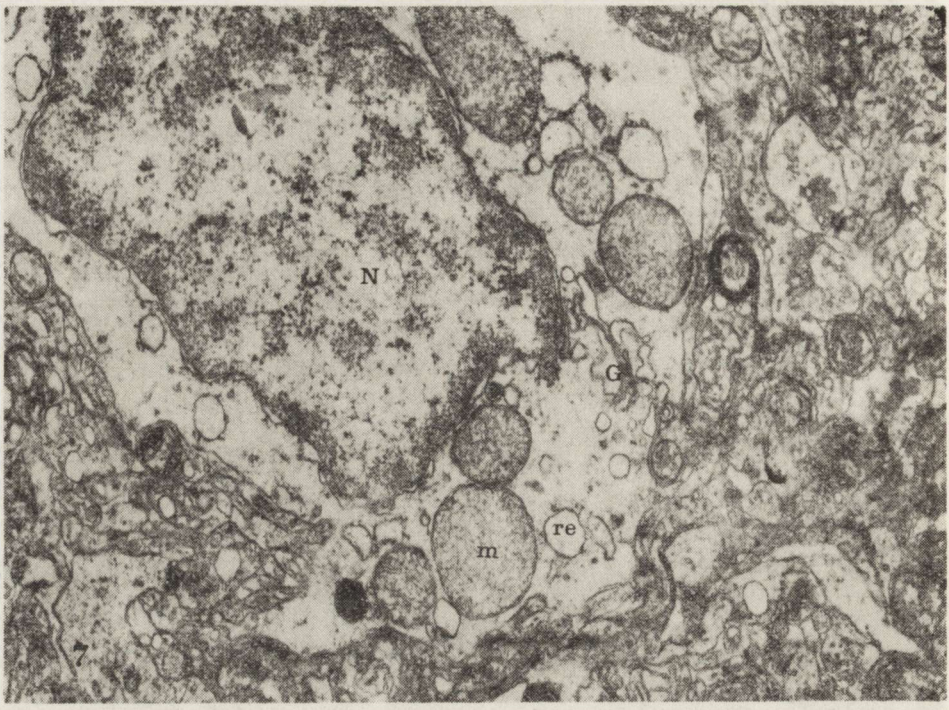

Fig. 7. The glial cell in corpus callosum of a 32-day old rabbit. Damaged mitochondria (m) in electron-lucent cytoplasm, enlarged endoplasmic reticulum (re) and Golgi apparatus (G) are seen. N — nucleus. × 5 000

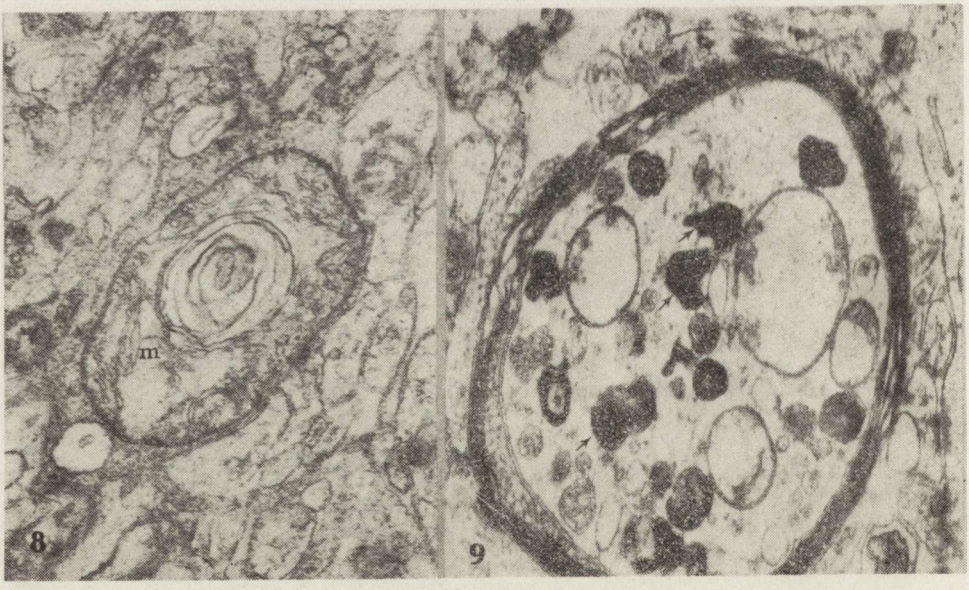

Fig. 8. Lamellar degeneration of mitochondrium (m) in the corpus callosum of a 32-day old rabbit. × 7 000

Fig. 9. Degeneration of myelinated axon in corpus callosum of a 32-day old rabbit. Different forms of dense bodies — arrows. × 10 000

Fig. 10. Degeneration features in the myelinating axon in the corpus callosum of a 32-day old rabbit. Oberrant inner myelin lamellae. Changed mitochondria (m) in the axon and enlarged dense mitochondrium (m) in the neuropil. × 7 000

DISCUSSION

The obtained results suggest that DDVP impairs the physiological development of the brain in the period of myelination. Abnormalities in the histochemical reactions in the intoxicated animals corresponded well to ultrastructural changes observed.

In accordance with previous studies (Zalewska et al., 1977; Maślińska, Zalewska, 1978 a, b) DDVP developed an inhibitory effect on AChE and some other enzyme activities. Poor histochemical reaction for SDH activity in glial cells is well explained by ultrastructural changes in mitochondria. Less myelinated fibers of corpus callosum of intoxicated animals observed in light and electron microscope corresponded to decreased reactions for OTAN and plasmalogen.

Ultrastructural studies suggest that the toxic effect of pesticide is focused on the mitochondria of glia cells leading to the damage of mitochondrial structure and function. This intoxication provoked swelling in glial cells (Trump, Arstila, 1975). The consequence of this may be the abnormal myelination and even degeneration of particular fibers.

REFERENCES

1. Adams C. W. M.: Histochemistry of lipids. In: Neurohistochemistry. Ed. C. W. M. Adams, Elsevier Publ. Comp., Amsterdam, London, N. York 1965, 57—58.

2. Barka T., Anderson P. J.: Histochemistry Theory, Practice and Bibliography — Hoeber Medical Division. Harper and Row, Publ. Inc., N. York, Evanston, London 1965, 245.
3. Gomori G.: An improved histochemical technic for acid phosphatase. Stain Technol., 1950, 25, 81.
4. Karnovsky M. J., Roots L.: A "direct-coloring" thiocholine method for cholinesterases. J. Histochem. Cytochem., 1964, 12, 219—220.
5. Maślińska D., Zalewska Z.: Activity of some mitochondrial enzymes in the progeny of rabbits treated with dichlorvos in the gestation period. Folia Histochem. Cytochem., 1978, 16, 139—146.
6. Maślińska D., Zalewska Z.: Effect of the dichlorvos administered to the pregnant rabbits on the cholinesterases activity in the progeny. Folia Histochem. Cytochem., 1978, 16, 335—342.
7. Pachecka J., Suliński A., Ziółkowska G.: The activities of some esterases of the rat brain after intoxication by organophosphate insecticides dichlorvos and trichlorphon. Neuropat. Pol., 1975, 13, 455—462.
8. Pearse A. G. E.: Histochemistry Theoretical and Applied. Churchill Livingstone, Edinburgh and London 1972, p. 1343.
9. Sitkiewicz D., Zalewska Z.: Effect of organophosphate insecticides on some oxidoreductase in rat brain mitochondria. Neuropat. Pol., 1975, 43, 463—469.
10. Trump B. F., Arstila A. U.: Cellular reaction to injury. In: Principles of Pathobiology, Eds: LaVia MF, Hill RB, New York Oxford University Press, 1975, p. 9.
11. Zalewska Z., Wolna B., Sitkiewicz D., Bicz W.: Effect of dichlorvos on some enzyme activities of the rat brain during postnatal development. II. Oxidoreductases. Neuropat. Pol., 1977, 15, 367—372.
12. Zelman I. B.: Patomorfologia mózgu szczura w doświadczalnym zatruciu fosforoorganicznym pestycydem dichlorfosem (DDVP). Neuropat. Pol., 1977, 15, 515—522.

Author's address: Laboratory of Developmental Neuropathology Medical Research Centre, Polish Academy of Sciences: 3, Pasteur Str., 02—093 Warszawa

NEUROPAT. POL., 1982, 20, 1—2
PL ISSN 0028—3894

ZUZANNA KRAŚNICKA

EFFECT OF SERUM FROM PATIENTS WITH UREMIC SYNDROME AND OF EXOGENOUS UREA AND CREATININE ON ORGANOTYPIC NERVE TISSUE CULTURE

Department of Neuropathology, Medical Research Centre, Polish Academy of Sciences

The pathological changes in the nervous system occurring in uremia have been known for a long time (Bodechtel, Erbslöh, 1958). It is also known that they are resulting from complex metabolic disturbances involving particularly protein metabolism. Owing to the defect of renal function numerous products of protein origin are retained in the organism, above all urea and guanidine compounds to which creatinine also belongs. The relation has not been so far elucidated between urea and guanidine derivaties retention and the uremic syndrome (Wilson, 1971).

Morphological changes in the central nervous system are unspecific and the frequent coexistence of complications of vasogenic origin makes difficult the evaluation of the influence of an increased content of nitrogen substances on the state of the nervous tissue (Olsen, 1961; Osetowska, Mossakowki, 1963). For this reason it seemed purposeful to use a model of tissue culture for the investigation of the immediate influence of blood serum from patients with the uremic syndrome or of the particular pathogenic agents contained in it on the morphological picture of the nerve tissue.

MATERIAL AND METHODS

The investigations were performed on 3-week cultures of newborn rat cerebellum. The experiments were run in four groups.

In group I serum from patients with the uremic syndrome, in group II urea and in group III creatinine were used. Group IV consisted of control cultures. The pathogenic agent was added for a period of 3 days.

The sera applied in group I were taken from patients with chronic

glomerulo nephritis. All patients were subjected to periodical extrasystemic dialysis. Blood samples for culture were collected before dialysis in the period of increase in the urea and creatinine levels.

In group II in which to the standard nutrient medium exogenous urea was added, two subgroups were distinguished with different urea concentrations (100 and 200 mg%). Group III was similarly differentiated and exogenous creatinine (Sigma) was added: in subgroup one creatinine concentration was 5 mg% and in the second one 10 mg%.

The culture was observed under a light and electron microscope. The cultures were stained by routine methods, Sudan black B and PAS and the enzymic activity of succinate, glutamate and glucose-6-phosphate dehydrogenases was tested according to the methods described by Mossakowski et al. (1970). The cultures for electron microscopy were prepared in a standard way and embedded in Epon. Ultrathin sections were contrasted with uranyl acetate and lead citrate and photographed with the use of a JEM 7A electron microscope.

RESULTS

Group I: The cultures subjected to the action of sera from patients with the uremic syndrome show distinct structural abnormalities as compared with control cultures.

Observations in the light microscope show considerable swelling of glial and nerve cells. The cell dimensions are increased and their processes thickened. Neurones usually exhibit features of tigrolysis. The highest degree of swelling was noted in the astrocytes (Fig. 1). The cytoplasm of the most astroglial cells contains numerous vacuoles. In the growth zone microglial proliferation is observed quite frequently. The number of cell divisions in the glial population is markedly lower than in the control cultures. In cultures stained with Sudan black B swelling of the myelin sheaths is visible, sometimes also their disintegration with the formation of myelin spheres (Fig. 2). The changes in myelin structure are accompanied by excessive accumulation of sudanophilic substances, mostly in the oligodendrocyte cytoplasm. The nerve cells as well as both types of neuroglia accumulate in the perikaryal cytoplasm granular PAS-positive substance, much more abundant than in the corresponding control cultures.

The activity of the examined dehydrogenases also shows considerable abnormalities as compared with that in the control material. The histochemical reaction is the weakest in tests for succinic dehydrogenase, it is also weak when revealing glutamine dehydrogenase. The activity of glucose-6-phosphate dehydrogenase is characterised by a slightly weakened reaction. The swollen glial cells give a weaker reaction than the remaining nerve tissue cells.

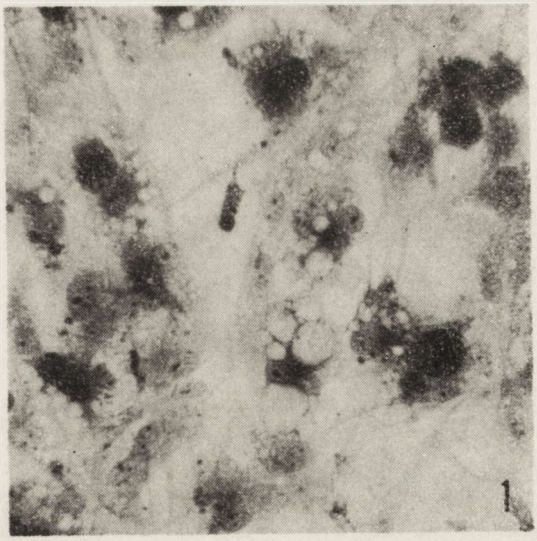

Fig. 1. Group I. Vacuolar degeneration and swelling of cells. Nissl. × 400

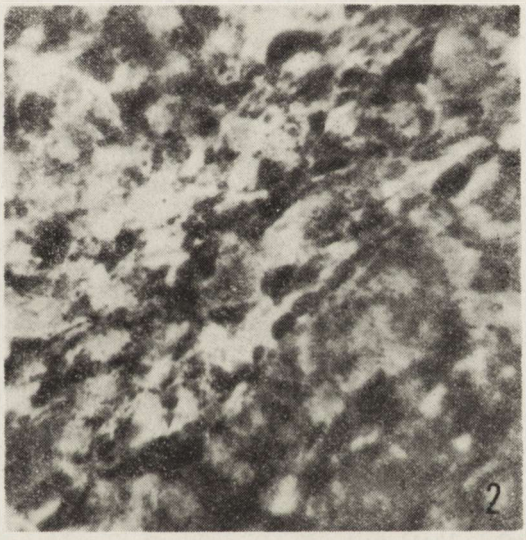

Fig. 2. Group I. Swelling and fragmentation of myelin sheath. Sudan black B. × 400

Electron microscopic observations of the group I culture show striking changes in the Purkinje cells, consisting in disappearance of the rough endoplasmic reticulum, reduction in number of ribosomes and polyribosomes and in widening of the Golgi apparatus canaliculi. The mitochondria of these cells are swollen, their matrix is clear and cristae fragmented (Fig. 3). Small neurones corresponding to the cells of the granular layer are less impaired. Their endoplasmic reticulum is usually well developed and preserves the typical arrangement of canaliculi

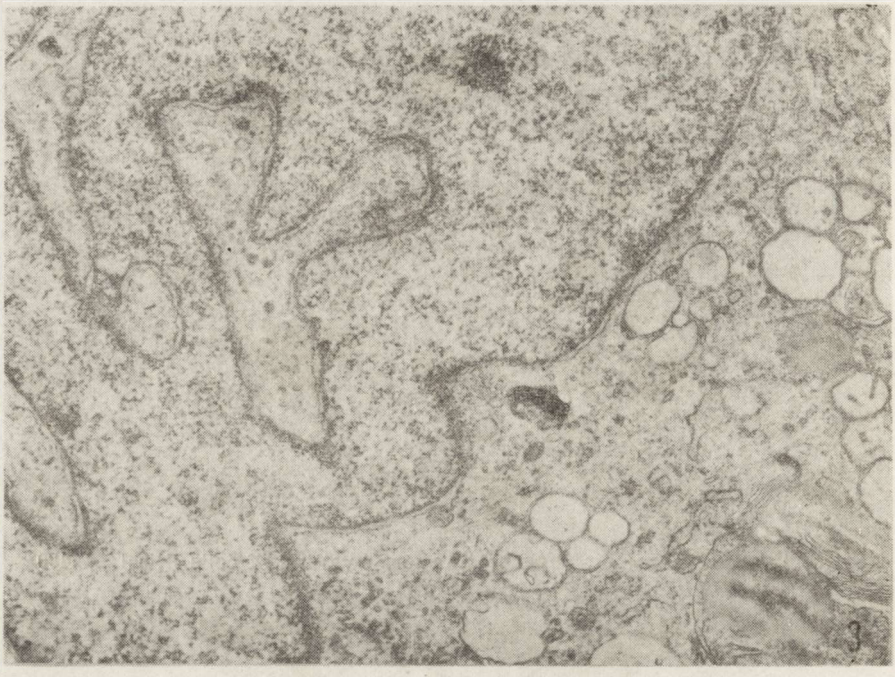

Fig. 3. Group I. Fragment of Purkinje cell with swollen mitochondria (M) and fragmented rough endoplasmic reticulum. × 15 000

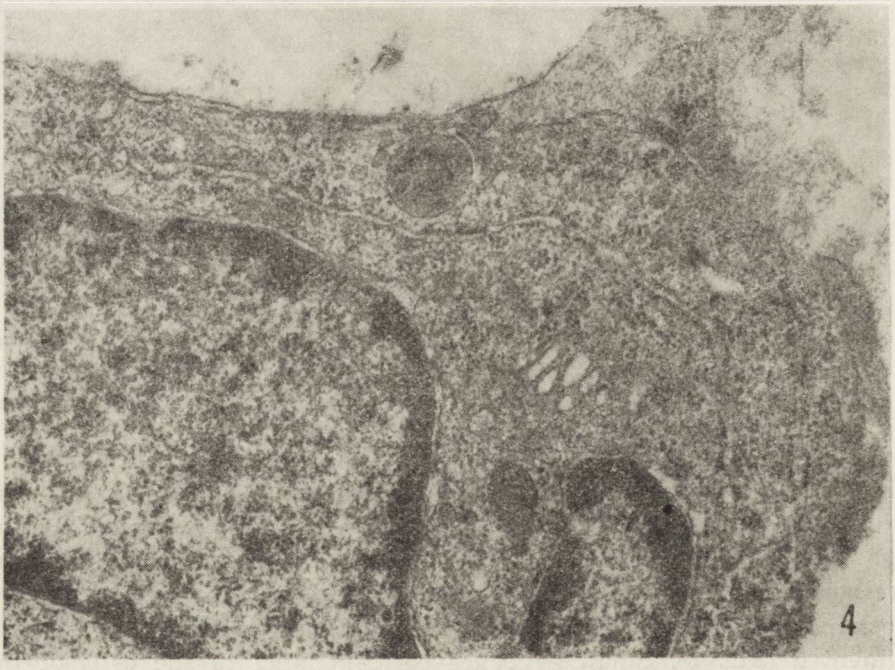

Fig. 4. Group I. Fragment of nerve cell from granular layer. Well preserved rough endoplasmic reticulum. Golgi apparatus with features of hypertrophy. × 12 000

Fig. 5. Group I. Structural changes in myelin sheath: splitting of lamellae and partial obliteration of lamellar structure; axoplasm of low density with flake-like material. × 15 000

Fig. 6. Group I. Fragment of oligodendrocyte with numerous lipid drops. × 15 000

Fig. 7. Group I. Fragment of astrocyte. Very pronounced dilatation of the rough endoplasmic reticulum channels (ER). Swollen mitochondria completely depleted of cristae (M). × 27 000

(Fig. 4). Numerous minute mitochondria show a mostly normal structure, only some of them are swollen, however, to a smaller extent than the mitochondria of the Purkinje cells. The Golgi apparatus shows features of hypertrophy. The nuclear envelope and chromatin system of large and small neurones are normal.

The axons of the most nerve cells show degenerative changes, they are frequently deprived of typical organelles. In only few axons neurotubules are visible. The myelin structure shows major abnormalities consisting in splitting and a certain obliteration of its laminar structure (Fig. 5).

The cytoplasm of oligodendrocytes contains great numbers of lysosomes and lipid droplets (Fig. 6). The rough endoplasmic reticulum is built of short canaliculi. The Golgi apparatus is usually well developed. Minute mitochondria with normal structure are not numerous. The oligodendrocyte nuclei show characteristic chromatin patterns and a normally developed nuclear envelope. Astrocytes show the most pronounced ultrastructural changes. The rough endoplasmic reticulum ca-

naliculi are greatly dilated, they form vacuoles on the periphery of which small groupings of ribosomes are visible (Fig. 7). In some cells considerable delamination of the outer layer of the nuclear envelope is observed. The mitochondria are mostly swollen with matrix of low density and frequently deprived of cristae. The number of lysosomes is usually increased. The Golgi apparatus shows a varying degree of hypertrophy in the particular cells. The microglial cells do not show major abnormalities in the picture of their nuclei and cytoplasm.

Group II: Cultures subjected to the action of exogenous urea in a 100 mg% concentration show slight morphological changes as compared to the control ones. Observations in the light microscope reveal a low degree swelling of the cell involving almost exclusively astroglia. Accumulation of PAS-positive granules in the cytoplasm of glial cells is less pronounced than in group I, although greater than in the control cultures. Staining with Sudan black B does not reveal abnormalities in the picture of nerve fibres. Histochemical studies reveal weakened reactions demonstrating the activities of succinate and glutamate dehydrogenase, whereas the reaction for glucose-6-phosphate dehydrogenase does not show any difference as compared with that in control cultures.

Cultures subjected to the action of urea in a 200 mg% concentration show more pronounced morphological changes and their picture resembles the abnormalities described in group I. In this subgroup considerable swelling of the cytoplasm of nerve and glial cells is observed. Most distinct vacuolar degeneration features are seen in astrocytes. Accumulation of PAS-positive granular material is very abundant in the cytoplasm of nerve and glial cells. Frequently segmental swelling of the myelin sheaths is noted, sometimes with severe damage to them. Histochemical reactions revealing succinate and glutamate dehydrogenase activity are very weak. A somewhat stronger reaction manifests glucose-6-phosphate activity.

Electron microscope observations of cultures treated with urea in a 100 mg% concentration show slight alterations as compared with the control one. The structure of granular and Purkinje cells is mostly normal. Neither does the axoplasm show any changes. On the other hand, abnormalities are noted in the myelin structure around numerous axons. They consist above all in laminar splitting leading to the formation of irregular spaces between the laminae.

Oligodendrocytes, like in group I contain an increased number of lysosomes and lipid droplets (Fig. 8). The Golgi apparatus is distinctly spread in the cytoplasm of these cells. The astrocytes are swollen. The mitochondria of these cells only sometimes show features of swelling

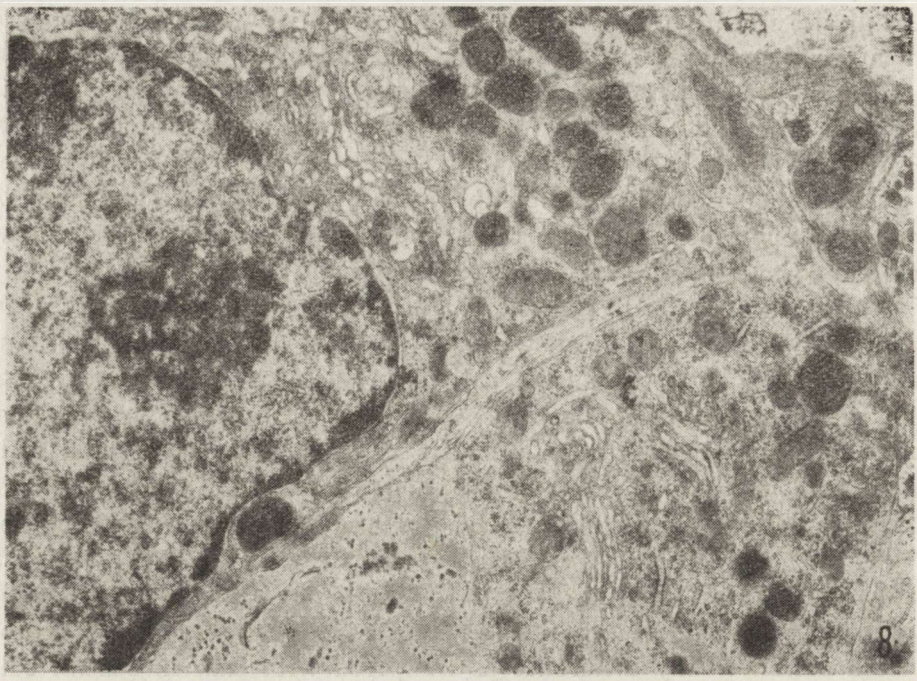

Fig. 8. Fragment of culture of group II. Two fragments of oligodendrocytes with numerous lysosomes, lipid drops and dilatated cisterns of Golgi apparatus. × 12 000

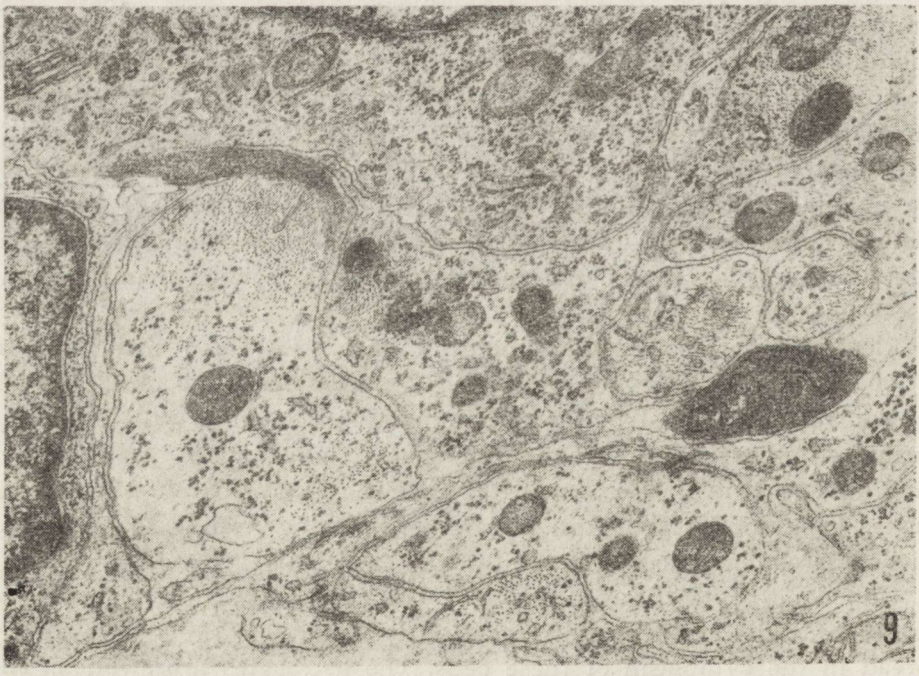

Fig. 9. Fragment of culture of group II. Swollen astrocytic processes with abundant glycogen grains. × 13 000

most of them have a normal structure. The cytoplasm of the perikarya and astrocytic processes contains lysosomes of various sizes and a large amount of glycogen granules (Fig. 9). The gliofibril content varies in the particular cells.

An increased urea concentration (200 mg%) in the medium causes a slight intensification of the above described impairments of the cell cytoplasm. The changes are more generalised and involve a large number of glial cells.

Group III: Creatinin introduced into the nutrient medium in a 5 mg% concentration produces changes similar in character and intensity to the abnormalities developing under the action of urea in a 100 mg% concentration. Swelling of the cytoplasm of glial cells is observed, mainly astrocytes as well as an increase in the number of glycogen granules and depression of the intensity of enzymatic reactions of the tested dehydrogenases (particularly succinate and glutamate). The picture of the myelin sheaths does not show differences as compared with that of control cultures.

When creatinine is applied in a 10 mg% concentration the pathological changes are more pronounced and similar to those found under the action of urea in a 200 mg% concentration. In preparations stained by the Nissl method considerable swelling of the cytoplasm of nerve and glial cells is observed. Features of degeneration appear mostly in the astroglia. The succinate and glutamate dehydrogenase activities are markedly depressed and the reaction for glucose-6-phosphate dehydrogenase is only slightly weaker as compared with that in the control.

Electron microscope investigations in this experimental group show most essential changes in the glial cell population. Oligodendrocytes exhibit an increased number of lysosomes and numerous lipid droplets. The astrocyte cytoplasm is generally swollen and contains numerous glycogen granules. The neurones do not show major alterations as compared with the control group. Only mitochondria in some cells are swollen. On the other hand changes are pronounced in the myelin structure. They consist its swelling and widening of the interlaminar space.

DISCUSSION

The here presented results obtained with the use of the light and electron microscopes are concordant and show an identical pattern of changes in the three experimental groups. The highest intensity of changes in group I may be explained by the summation of the actions of urea and creatinine and also by the presence of other toxic substances in the serum of patients with uremia. To these belong aliphatic and aromatic amines, peptides, organic acids, indoles and phenols (Hicks et al., 1962; Mütting, Dishuk, 1967; Fishman, 1970; Gulyassy et al., 1970).

In this experimental group, beside intensive changes in the glia, changes are noted in the neurones, consisting in swelling of the mitochondria and axoplasm disintegration. Impairment of myelin observed by us in the light microscope has its counterpart in the electronmicroscopic patterns of all the three experimental groups. It is most pronounced, however, in group I with serum from patients with the uremic syndrome.

Treatment of the nerve tissue culture with one pathogen (urea and creatinine caused changes in the structure of neuroglial cells, but no major abnormalities were observed in the microglia structure. The different reaction of microglia is known from clinical neuropathology and other experimental models in vitro such as, among others, hypoxia or hyperoxia (Kraśnicka, Renkawek, 1969). The presence of glycogen granules in astrocytes observed in groups II and III seems to indicate a less severe metabolic damage to the tissue than in the group with serum from patients with the uremic syndrome.

Electronmicroscopic studies point to the different character of the degenerative changes in astrocytes and oligodendrocytes. This difference can be seen in all the experimental groups, notwithstanding the concentration of the pathogenic factors. Oligodendrocytes contain an increased amount of lipid substances and astrocytes exhibit a tendency to cytoplasm swelling with a marked dilatation of the rough endoplasmic reticulum canaliculi. The differences observed in the structure of astro- and oligodendroglia are not specific for uremic toxins. Similar changes were observed after hypoxia (Kraśnicka et al., 1973, 1976), after poisoning with carbon oxide (Korthals et al., 1973) and as the consequence of intoxication with cyaninates (Mossakowski, Gajkowska, 1976). It would seem, therefore, that the reaction of glial cells to noxious agents depends above all on the type of cell and on its function.

We have not found in the available literature any data concerning ultrastructural changes in the brain in the course of uremia, but biopsy material from peripheral nerves of uremic patients has been examined in the electron microscope. Appenzeller et al. (1971) and Cervos-Navarro et al. (1974) demonstrated similar lesions in segments of peripheral nerves in electronmicroscopic analysis. The main changes consisted in segmental demyelination, damage to axons, proliferation of Schwann cells and increased amounts of glycogen and lipid bodies in their cytoplasm. If the differences between biopsy material and experimental material from tissue culture are taken into account, the similar character of the changes evoked by the toxic agents present in the case of uremia should be stressed, above all the similarity of reaction of cells responsible for myelination in the peripheral and central nervous systems, that is Schwann cells and oligodendrocytes.

In the light of the data here presented it may be concluded that the agent responsible for the lesions in the central nervous system in ure-

mia are present in the blood serum. This role may be played both by urea and creatinine. The opinions on their pathogenic significance in uremia are controversial. Gilboe and Javid (1964) attribute the appearance of toxic symptoms in uremia to urea retention. They demonstrated that urea undergoes transformation to cyanates and that both urea and cyanates exacerbate the uremic symptoms and accelerate the death of experimental animals. Urea proved to be an inhibitor of a number of enzymatic systems, among them of monoamino and xanthine oxidases (Rajagapalan et al., 1961; Giordano, 1963). Giovanetti et al. (1970) and Balestri et al. (1970) demonstrated a dependence between urea concentration and inhibition of glucose uptake in uremia.

At present most authors attribute the basic pathogenic influence to the action of guanidine derivatives to which creatinine belongs. An unequivocal correlation has been demonstrated between the high creatinine concentration in the blood serum and the intensity of uremic symptoms (Olsen, 1961; Giordano, 1963; Giovanetti et al., 1969). It seems, therefore, justified to accept the role of urea and creatinine as pathogens in lesions of the central nervous system in uremia, as indicated by the here presented investigations, although the mechanism of action of these compounds still remains obscure.

REFERENCES

1. Appenzeller O., Kornfeld M., Mac Gee J.: Neuropathy in chronic renal disease. A microscopic, ultrastructural and biochemical study of sural nerve biopsis. Arch. Neurol., 1971, 24, 449—461.
2. Balestri P. L., Biagini M., Rindi P., Giovanetti S.: Uremic toxins. Arch. Intern. Med., 1970, 126, 843—845.
3. Bodechtel G., Erbslöh F.: Die Veränderungen des Zentralnervensystems bei Nierenkrankheiten. In: Handbuch der speziellen pathologischen Anatomie und Histologie. Springer, 1958, XIII, 2B, 1392—1427.
4. Cervos-Navarro J., Matakas F., Stoltenburg G.: Elektronenmikroskopische Untersuchungen in urämischen Neuropathie. Neuropat. Pol., 1974, 12, 291—298.
5. Gilboe D. D., Javid M. J.: Breakdown products of urea and uremic syndrome. Proc.Soc.Exp.Biol.,Med., 1964, 115, 633—637.
6. Giordano G.: Use of exogenous and endogenous urea for protein synthesis in normal and uremic subjects. J. Lab. Clin. Med., 1963, 62, 231—246.
7. Giovanetti S., Biagini M., Balestri P. L., Navalesi Giagnoni P., Matteis A., Ferro-Milone P., Perfitti C.: Uremialike syndrome in dogs chronically intoxicated with methylguanidine and creatinine. Clin.Sci., 1969, 36, 445—452.
8. Giovanetti S., Balestri P. L., Biagini M., Menichini G., Rindi P.: Implications of dietary therapy. Arch.Intern.Med., 1970, 126, 900—905.
9. Gulyassy P. F., Aviram M., Peters J. H.: Evaluation of amino acid and protein requirements in chronic uremia. Arch.Intern.Med., 1970, 126, 855—859.
10. Fishman R. A.: Permeability changes in experimental uremic encephalopathy. Arch.Intern.Med., 1970, 126, 835—837.

11. Hicks J. M. Young D. S., Wootton I. D. P.: Abnormal blood constituents in acute renal failure. Clin.Chim.Acta, 1962, 7, 623—633.
12. Korthals J., Hoppe B., Karwacka H.: Badania mikroskopowo-elektronowe nad toksycznym wpływem tlenku węgla na tkankę glejową hodowaną in vitro. Neuropat.Pol., 1973, 11, 315—322.
13. Kraśnicka Z., Gajkowska B., Mossakowski M. J.: Effect of shortlasting anoxia on in vitro culture of cerebellum. Neuropat.Pol., 1976, 14, 11—22.
14. Kraśnicka Z., Renkawek K.: Morfologia i histochemia mikrogleju w hodowli tkankowej w warunkach prawidłowych i patologicznych. Neuropat.Pol., 1969, 9, 73—90.
15. Kraśnicka Z., Renkawek K., Gajkowska B.: Wpływ krótkotrwałej anoksji na obraz ultrastrukturalny komórek glejowych hodowanych in vitro. Neuropat. Pol., 1973, 11, 398—404.
16. Mossakowski M. J., Gajkowska B.: Obraz mikroskopowo-elektronowy uszkodzeń gleju wywołanych cyjankiem sodu w hodowli pozaustrojowej. Neuropat. Pol., 1976, 14, 441—449.
17. Mossakowski M. J., Renkawek K., Kraśnicka Z., Śmiałek M., Pronaszko A.: Morphology and histochemistry of Wilsonian and hepatogenic gliopathy in tissue culture. Acta Neuropath. (Berl.), 1970, 16, 1—16.
18. Mütting D., Dishuk B. D.: Free amino acids in serum, cerebrospinal fluid and urine in renal disease with and without uremia. Proc.Soc.Exp.Biol.Med., 1967, 126, 754—758.
19. Olsen S.: The brain in uremia. Acta Psych.Neurol.Sand., 1961, 36, Suppl. 156, 1—126.
20. Osetowska E., Mossakowski M. J.: Zmiany w ośrodkowym układzie nerwowym w stanach mocznicowych. Neuropat.Pol., 1963, 1, 101—122.
21. Rajagapalan K. V., Fridovich I., Handler P.: Competitive inhibition of enzyme activity by urea. J.Biol.Chem., 1961, 236, 1059—1065.
22. Wilson D. M.: Metabolic abnormalities in uremia. Med.Cl.North.Am., 1971, 55, 1381—1396.

Author's address: Department of Neuropathology, Medical Research Centre, Polish Academy of Sciences, 3, Dworkowa Str., 00—784 Warszawa, Poland

NEUROPAT. POL., 1982, 20, 1—2
PL ISSN 0028—3894

ZBIGNIEW STELMASIAK

EFFECT OF ISCHEMIA ON MONOAMINE METABOLISM. BRAIN MONOAMINE METABOLITES IN CEREBROSPINAL FLUID OF PATIENTS WITH RECENT CEREBRAL INFARCTION

Department of Clinical Neurology, Institute of Diseases of the Nervous System, School of Medicine, Lublin

It was found that the 5-hydroxyindoleacetic acid (5-HIAA) and homovanillic acid (HVA) concentrations in cerebrospinal fluid (CSF) were decreased in patients with Parkinson disease (Bernheimer et al., 1966; Godwin-Austen et al., 1971; Papeschi et al., 1972), in patients with disseminated sclerosis (Claveria et al., 1974), in some patients with epilepsy (Papeschi et al., 1972; Shaywitz et al., 1975) and in patients after head injury (Vecht et al., 1975).

It is known from experimental work that after cerebral ischemia the metabolism of monoamines can be disturbed in brain (Wurtman, Zervas, 1974; Chikvaidze, Melitauri, 1974; Gadamski et al., 1976; Mrsulja et al., 1976; Stelmasiak, 1976).

Increase of serotonin and noradrenaline concentration and increase of cyclic AMP in CSF of patients with stroke was also found (Berzin et al., 1969; Misra et al., 1967; Meyer et al., 1974; Southern, Christoff, 1962; Welch et al., 1975).

HVA reflects dopamine turnover in the brain but 5-HIAA — partly cerebral and partly spinal serotonin turnover (Moir et al., 1970). Because there are no reports in literature dealing with the systemic determination of HVA and 5-HIAA concentration in CSF of patients with recent cerebral infarction it was decided to examine it.

MATERIAL AND METHODS

HVA and 5-HIAA concentration was determined in CSF collected from 50 patients with recent cerebral infarction before starting treatment, between 2—48 hrs, on average 19 hrs after cerebral stroke and from 30 patients without central nervous system diseases, mostly with lumbar radiculopathy in remission period of disease, who served as

a control group. All patients were treated in the Department of Clinical Neurology in Lublin.

The age of patients with cerebral infarction was between 41—85 (average — 66 years) and in the control group it was between 34—70 (average — 47 years). There were 27 women and 23 men in the stroke group and 12 women and 18 men in the control group.

In the group of patients with cerebral infarction middle cerebral artery thrombosis was diagnosed in 34 patients and middle cerebral artery embolism in 16 remaining patients. Diagnosis was based on typical clinical symptoms and in 7 patients it was verified with biopsy. In all patients CSF and blood routine examinations: EEG, ECG, X-rays were performed *.

Blood hypertension in 22 (44%), atrial fibrillation in 13 (26%), consciousness disturbances in 12 (24%), hemiplegia in 28 (56%), hemiparesis in 22 (44%) patients were found.

In patients with cerebral infarction concentration of protein in CSF was 26—99; on average 45 mg%, and glucose concentration was 50—77; on average 59 mg%. There were no cells, CSF were always clear, water like and without blood contaminations.

There were no abnormalities detected in CSF or in blood of patients in the control group.

In patients with cerebral infarction blood glucose concentration was on average 95 mg%, urea—43 mg%, total protein — 7.05 g%, total cholesterol — 212 mg%.

Approximately 8 ml of CSF was taken by lumbar puncture and stored at 20°C until determinations of HVA and 5-HIAA were performed (Godwin-Austen et al., 1971). Contemporary with each test tube, 2 blank tubes with redestilled water and 2 with different standard solution concentrations (BDH standards) were used. Extinctions were read at 320/450 nm for HVA and at 365/495 nm for 5-HIAA on the Farrand type fluorimeter in the Scientific Research Centre of the School of Medicine in Lublin.

RESULTS

The results obtained in the control group (Table 1) were similar to those reported in the literature as normal (Claveria et al., 1974; Curzon, 1972; Moir et al., 1970; Papeschi et al., 1972).

In 21 patients with recent cerebral infarction HVA concentration in CSF was higher than the highest control value and in 29 patients it was between the range of the control values. The average value was decreased in patients with cerebral infarction by 0.033 μg/ml as compared with an average control value and the difference was statistically significant ($p<0.001$) (Table 1).

* In some of them an additional cerebral angiography was done.

Table 1. HVA and 5-HIAA concentration (μg/m) in CSF of patients with recent cerebral infarction

Substance examined	Control group (n = 30)	Patients with cerebral infarction (n = 50)	p
HVA	0.049±0.013 (0.012–0.080)	0.016±0.009 (0.002–0.059)	< 0.001
5-HIAA	0.039±0.013 (0.004–0.067)	0.060±0.029 (0.021–0.137)	< 0.001
	1.36±0.53 (0.69–2.85)	0.31±0.21 (0.02–1.23)	< 0.001

In 18 patients with recent cerebral infarction 5-HIAA concentration was higher than the highest control value and in 32 patients it was between the range of the control values. The average value in patients with cerebral infarction was higher by 0.021 μg/ml than an average control value and the difference was statistically significant ($p<0.001$).

In all patients with recent cerebral infarction HVA : 5-HIAA index values were lower than the lowest control value. An average index value was lower by 1.07 and the difference was statistically significant ($p<0.001$) (Table 1).

The average HVA concentration in CSF 2 hours after cerebral infarction was decreased by 0.040 μg/ml compared with an average control value, in CSF collected between 2—24 hours after stroke it was decreased by 0.032 μg/ml, and in CSF collected between 24—48 hours after stroke it was decreased by 0.031 μg/ml. All these differences were statistically significant ($p<0.001$).

The average HVA concentration in CSF collected between 24—48 hours after stroke was higher by 0.009 μg/ml than an average HVA concentration in CSF collected 2 hours after stroke and the difference was statistically significant ($p<0,02$) (Fig. 1).

The average 5-HIAA concentration in CSF collected 2 hours after cerebral infarction was higher by 0.002 μg/ml than an average control value ($p>0.05$), in CSF collected between 2—24 hours after stroke it was higher by 0.021 μg/ml and in CSF collected between 24—48 hours after stroke it was higher by 0.037 μg/ml and these both differences were statistically significant ($p<0,001$).

The average 5-HIAA concentration in CSF collected between 24—48 hours after stroke was by 0.035 μg/ml higher than an average 5-HIAA CSF concentration 2 hours after stroke and the difference was statistically significant ($p<0.02$) (Fig. 1).

The average HVA : 5-HIAA index value in CSF collected 2 hours after cerebral infarction was lower by 1.09 than an average control value, in CSF collected between 2—24 hours after stroke it was lower

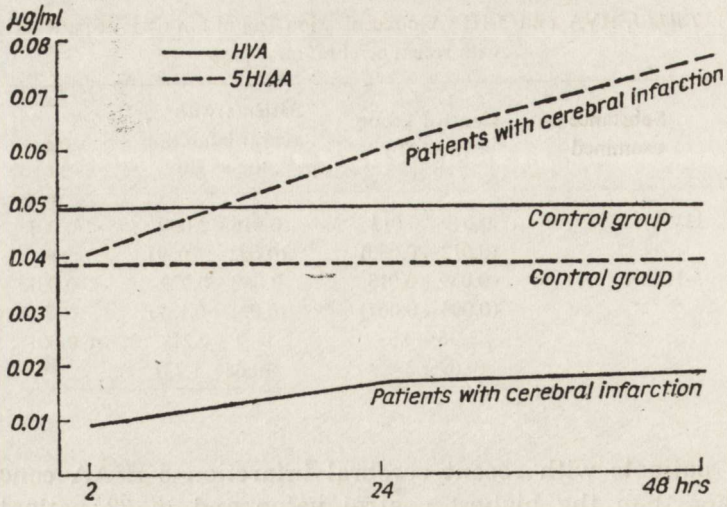

Fig. 1. Changes of HVA and 5-HIAA concentration in CSF of patients with recent cerebral infarction and duration of disease

by 1.03, in CSF collected between 24—48 hours after stroke it was lower by 1.08 and all these differences were statistically significant ($p<0.001$).

The average HVA : 5-HIAA index value in CSF collected from patients with cerebral infarction did not differ significantly 2 hours and between 24—48 hours after stroke ($p>0.05$).

In patients with recent cerebral infarction with hemiparesis HVA CSF concentration in 19 patients was lower than the lowest control value and in 3 patients it was between the range of the controls; 5-HIAA CSF concentration in 11 patients was higher than an average control value and in 11—it was in the range of the controls; HVA : : 5-HIAA index values in all of 22 patients was lower than the lowest control value.

In patients with hemiparesis the average HVA concentration in CSF was decreased by 0.028 µg/ml ($p<0.001$), of 5-HIAA — it was increased by 0.027 µg/ml ($p<0.02$) and the HVA : 5-HIAA index value was decreased by 0.97 ($p<0.001$) compared with the average values in the control group (Table 2).

In 25 patients with hemiplegia HVA concentration in CSF was lower than the lowest control value and in 3 — it was between the range of the controls. In 5 patients with hemiplegia 5-HIAA concentration in CSF was higher than the highest control value and in 23 — it was between the range of the controls. In all of 28 patients with hemiplegia HVA : 5-HIAA index values in CSF were lower than the lowest control value.

In patients with hemiparalysis the average concentration of HVA

Table 2. Concentration of HVA and 5-HIAA in the CSF in patients with a recent cerebral infarction

Monoamines	Control group (n = 30)	Patients with hemiparesis (n = 22)		Patients with hemiparalysis (n = 28)	
HVA	0.049±0.013 (0.028–0.080)	0.021±0.009 (0.002–0.045)	p<0.001	0.011±0.008 (0.002–0.028)	p<0.001
5-HIAA	0.039±0.013 (0.004–0.067)	0.066±0.31 (0.016–0.137)	p<0.02	0.056±0.027 (0.021–0.118)	p<0.01
HVA / 5-HIAA	1.36±0.53 (0.69–2.85)	0.39±0.21 (0.04–1.23)	p<0.001	0.24±0.18 (0.02–0.76)	p<0.001

in CSF was decreased by 0.038 μg/ml ($p<0.001$), of 5-HIAA — it was increased by 0.017 μg/ml ($p<0.01$) and HVA : 5-HIAA index value — was decreased by 1.12 ($p<0.001$) compared with an average value in the control group (Table 3).

Table 3. HVA and 5-HIAA concentration in CSF of patients with recent cerebral infarction and duration of disease and degree of paresis of the limbs

Clinical data	HVA		5-HIAA		HVA / 5-HIAA	
Duration of disease	+0.19	p< 0.05	+0.34	p < 0.02	0	–
Degree of paresis	−0.49	p < 0.001	−0.13	p > 0.05	0.83	p < 0.001

In patients with recent cerebral infarction correlation coefficient values between the time of disease with HVA CSF concentration was +0.19 ($p>0.05$), and with 5-HIAA — it was +0.34 ($p<0.02$) (Table 3). Correlation coefficient values between degree of paresis with HVA CSF concentration was —0,49 ($p<0.001$), with 5-HIAA it was —0.13 ($p>>0.05$), with HVA : 5-HIAA index value it was —0.83 ($p<0.001$). Correlation coefficient value between HVA and 5-HIAA CSF concentration in patients with cerebral infarction was +0.28 ($p>0.05$).

DISCUSSION

Statistically significant decrease of HVA concentration in cerebrospinal fluid of patients with recent cerebral infarction was found which is in agreement with the experimental results obtained in baboons with middle cerebral artery occlusion, where significant decrease of HVA content in the ischemic area in striatum was found 2 hours after cerebral infarction (Stelmasiak, 1976; Stelmasiak et al., 1978).

Decrease of HVA concentration in CSF of patients with recent cerebral infarction seems to reflect low concentration of this metabolite of dopamine and probably the decrease of dopamine turnover in striatum also, as a consequence of ischemia of this structure.

Decrease of HVA concentration in cerebrospinal fluid of patients with head injury was found during the first days and remained decreased for an extended period (Vecht et al., 1975), so it is possible that decrease of dopamine content in striatum is dependent on similar mechanisms of disturbances of monoamine metabolism as caused by different nonspecific factors like ischemia, trauma, degenerative changes (Wurtman, Zervas, 1974). In ischemia, trauma or hypoxia noradrenaline and serotonin may be abnormally released with extraneuronal accumulation and diffusion to cerebrospinal fluid (Wurtman, Zervas, 1974; Kogure et al., 1975). It has been suggested that altered monoamine metabolism might be implicated to the pathophysiology of cerebral infarction or progression of infarction because such factors as reduced cerebral blood flow, disturbances of cerebral metabolism and cerebral edema are common in patients with cerebral infarction (Wurtman, Zervas, 1974; Meyer et al., 1974,, Kogure et al., 1975; Mršulja et al., 1976).

Extracerebral consequences of stroke connected with hyperactivity of hypothalamus-hypophysis-suprarenal gland axis and stress reaction after stroke (Kawiak, Stelmasiak, 1967; Kawiak, 1969; Selye, 1970) can affect monoamine metabolism. Elevated cortisol concentration found in the blood of baboons after experimental cerebral infarction (Stelmasiak, 1976) can disturb monoamine enzymes activity (Curzon, 1972).

Elevated free tryptopharn (TP) concentration in plasma and TP concentration in CSF found in patients after cerebral infarction (Stelmasiak, 1978) lead to increase of tryptophan content and probably to increase of serotonin turnover in brain, since it is known that free plasma TP only can penetrate blood-brain-barrier so it is the only known source of brain tryptophan (Curzon, 1972). Increase of TP concentration in plasma is not specific and it was found after different stress situations (Curzon, 1972; Stelmasiak, Curzon, 1974).

Tyrosine (dopamine precursor) was only slightly reduced in blood and in CSF of patients after cerebral infarction (Stelmasiak, 1978).

In the present study it was interesting to find a significant negative correlation between HVA concentration in cerebrospinal fluid and index value of HVA : 5-HIAA with degree of paresis of the limbs. The results are in agreement with those which Claveria et al. (1974) found in CSF of patients with disseminate sclerosis: low HVA and 5-HIAA concentrations were found in patients with paralysis of the limbs and in patients bedridden.

Clinic-biochemical correlations dealing with monoamines were also shown by other investigators. Meyer et al. (1974) found that noradrenaline and serotonin levels were in high concentration in cerebrospinal fluid of patients with cerebral infarction and with severe neurological deficit. Papeschi et al. (1970) suggested that HVA and 5-HIAA concentration in the brain and in cerebrospinal fluid is an index of

dopamine and serotonin turnover correlated with movement activity in patients with Parkinson disease, where decrease of HVA concentration in CSF was negatively correlated with general rigidity and poor movement activity. It is interesting also, that Vecht et al. (1975) did not find significant correlation between decreased HVA and 5-HIAA concentration in CSF of patients after head trauma and with degree of disturbances of consciousness.

In the present study 5-HIAA concentration in CSF of patients with recent cerebral infarction did not change significantly in the early period after cerebral infarction but later a progressive increase occurred partly reflecting increase of serotonin turnover in the brain. This observation is similar to that made by Meyer et al. (1974), who found an increase of noradrenaline concentration in the CSF of patients during first 2 weeks after stroke and to that noticed by Kawiak (1968), who found decrease of urinary excretion of 5-HIAA during first 2 days after stroke and later a progressive increase in the excretion of this metabolite of serotonin during next days, in paralell with the clinical improvement.

In the present study, age and sex of patients with cerebral infarction were similar to those in the control group partly eliminating the effect of atherosclerosis but some link between blood hypertension and brain monoamine metabolism seems to be possible (Meyer et al., 1974).

The results obtained in the present study, in patients after cerebral infarction and those which were found in baboons with experimental middle cerebral artery occlusion (Stelmasiak, 1976) showed a decrease of dopamine turnover and less decrease of serotonin turnover in the ischemic area in the early period after cerebral infarction and showed a progressive increase of serotonin turnover in the neurons far from the ischemic area.

Intracerebral and extracerebral consequences of stroke seem to be responsible for disturbances of monoamine metabolism found.

REFERENCES

1. Bernheimer H., Birkmayer W., Hornykiewicz O.: Homovanillinsäure in Liquor cerebrospinalis: Untersuchungen beim Parkinson-Syndrom und anderen Erkrankungen des ZNS. Wien.Kin.Wschr., 1966, 78, 417—419.
2. Berzin Y. E., Auna Z. P., Brezhinsky G. Y.: The significance of blood serotonin and CSF in the clinical picture and pathogenesis of acute cerebral circulatory disturbance. Zh. Nevropat. Psikhiat., 1969, 69, 1011—1015.
3. Chikvaidze V. N., Melitauri N. N.: Effect of ischemia on the regional distribution of biogenic amines in the brain of rabbits. Neuropat. Pol., 1974, 4, 671—682.
4. Claveria L. E., Curzon G., Harrison M. J. G., Kantamaneni B. D.: Amine metabolites in the CSF of patients with disseminated sclerosis. J. Neurol. Neurosurg. Psychiatry, 1974, 37, 715—718.
5. Curzon G.: Brain amine metabolism in some neurological and psychiatric

disorders. In: Biochemical Aspects of Nervous Diseases, J. N. Cumings. Plenum Press, London, New York 1972.
6. Gadamski R., Szumańska G., Sikorska M.: Effect of circulatory hypoxia on rabbit brain catecholamines. Histochemical and fluorescence study. Neuropat. Pol., 1976, 1, 23—30.
7. Godwin-Austen R. B., Kantamaneni B. D., Curzon G.: Comparison of benefit from L-dopa in Parkinsonism with increase of amine metabolites in the CSF. J. Neurol. Neurosurg. Psychiatry, 1971, 34, 219—223.
8. Kawiak W.: Investigations on urinary excretion of 5-hydroxyindoleacetic acid (5-HIAA) in patients after cerebral stroke. Pol. Med. J., 1968, 4, 974—979.
9. Kawiak W.: The studies on activity of the hypothalamus-hypophysis-suprarenal gland axis and on some regulation mechanisms of metabolism in early period of acute disturbances of blood circulation in brain. DSc. Thesis. Library of the School of Medicine, Lublin, Poland, 1969.
10. Kawiak W., Stelmasiak Z.: Investigations on glucose metabolism in patients with cerebrovascular accidents. II. Insulin and epinephrine loading tests in patients after cerebral stroke. Pol. Med. J., 1967, 4, 950—956.
11. Kogure K., Scheinberg P., Matsumoto A., Busto R., Reinmuth O. M.: Catecholamines in experimental brain ischemia. Arch. Neurol., 1975, 32, 21—24.
12. Meyer J. S., Welch K. M. A., Okamoto S., Shimazu K.: Disordered neurotransmitter function- Demonstration by measurement of norepinephrine and 5-hydroxytryptamine in CSF of patients with recent cerebral infarction. Brain, 1974, 97, 655—664.
13. Misra S. S., Singh K. S., Bhargava P.: Estimation of 5-hydroxytryptamine (5-HT) level in CSF of patients with intracranial or spinal lesions. J. Neurol. Neurosurg. Psychiatry, 1967, 30, 163—165.
14. Moir A. T. B., Ashcroft G. W., Crawford T. B. B., Eccleston D., Guldberg H. C.: Cerebral metabolites in cerebrospinal fluid as a biochemical approach to the brain. Brain, 1970, 93, 357—368.
15. Mršulja B. B., Mršulja B. J., Spatz M., Klatzo I.: Brain serotonin after experimental vascular occlusion. Neurology (Minneap.), 1976, 26, 785—787.
16. Papeschi R., Molina-Negro P., Sourkes T. L., Erba G.: The concentration of HVA and 5-HIAA in ventricular and lumbar CSF. Neurology (Minneap.), 1972, 11, 1151—1159.
17. Selye H.: The evolution of stress concept. Stress and cardiovascular disease. Amer. J. Cardiol., 1970, 26, 289—299.
18. Shaywitz B. A., Cohen D. J., Bowers M. B. Jr.: Reduced cerebrospinal fluid 5-hydroxyindoleacetic acid and homovanillic acid, in children with epilepsy. Neurology (Minneap.), 1975, 25, 72—79.
19. Southern A. L., Christoff N.: CSF serotonin in brain tumor and other neurological disorders determined by spectrophotofluorimetric method. J. Lab. clin. Med., 1962, 59, 320—326.
20. Stelmasiak Z.: Monoamines and their metabolites content in brain, CSF, blood and internal organs in recent cerebral infarction. Experimental and clinical examinations. DSc. Thesis. Library of the School of Medicine. Lublin, Poland, 1976.
21. Stelmasiak Z.: Tryptophan and tyrosine concentration in plasma and CSF of patients with recent cerebral infarction. Neurol. Neurochir. Pol., 1979, 1, 1—6.
22. Stelmasiak Z., Curzon G.: Effect of electroconvulsive therapy on plasma unesterified fatty acid and free tryptophan concentrations in man. J. Neurochem., 1974, 22, 603—604.

23. Vecht Gh. J., Woerkom T. C. A. M., Teelken A. W., Minderhoud J. M.: HVA and 5-HIAA CSF levels. Arch. Neurol., 1975, 32, 792—797.
24. Welch K., Meyer J. S., Chee A. N. C.: Evidence for disordered cyclic AMP metabolism in patients with cerebral infarction. Europ. Neurol., 1975, 2, 144—153.
25. Wurtman R. J., Zervas N. T.: Monoamine neurotransmitters and the pathophysiology of stroke and central nervous system trauma. J. Neurosurg., 1974, 40, 34—36.

Author's address: Department of Clinical Neurology. School of Medicine. 8, Dr Jaczewskiego Str., 20—090 Lublin, Poland

KOMUNIKAT

INTERNATIONAL SOCIETY OF CEREBRAL BLOOD FLOW AND METABOLISM

IInd Satellite Symposium on
"Effects of Aging on Regulation
of Cerebral Blood Flow and Metabolism"
San Remo, June 30—July 1st, 1983

SCIENTIFIC COMMITTEE

C. Fieschi, C. W. Loeb, A. Agnoli, L. Amaducci, L. Angelucci, M. Baldy-Moulinier, A. Bés, A. Carpi, G. Crepaldi, P. Fiorani, D. H. Ingvar, G. L. Lenzi, E. T. Mackenzie, J. Seylaz

The Symposium will be held in San Remo (Italy) on June 30 — July 1st, 1983. The dead-line for abstracts is January 31, 1983.

Preliminary Program

June 30th

8^{30}—11^{30} Aging Brain: Cerebral Blood Flow and Metabolism regulation in experimental animals.

11^{30}—13^{00} Local Cerebral Energy Metabolism in experimental animals as related to function.

16^{00}—18^{00} Experimental Pharmacology of CBF and Metabolism in Aging Brain.

18^{00}—19^{30} Round Table and final Discussion on Experimental Studies.

July 1st

8^{30}—10^{30} Human Studies in the Aging Brain: CBF and Metabolism in Normal Subjects and in Age-related Pathology.

11^{00}—13^{00} Physiological Activation of CBF and Metabolism in Normal and Abnormal Aging.

16^{00}—18^{00} Therapeutical manipulation of the Age-related changes in CBF and Aging.

18^{00}—19^{30} Round Table and final Disscussion on Human Studies.

Scientists interested in further information may apply to the Organizing Secretariat c/o GIBI s.a.s. Mrs Maria Paola Gerini, 7 via Olona 00198 Roma.

NEUROPAT. POL., 1982, 20, 1—2
PL ISSN 0028—3894

WERNER JÄNISCH, DIETER SCHREIBER, HERMANNFRIEDRICH GERLACH

ANEURYSMS OF THE BASAL ARTERIES AS THE CAUSE OF INTRACEREBRAL CIRCULATORY DISTURBANCES

(ANALYSIS OF AUTOPSY MATERIAL)

Institute of Pathology of the Martin-Luther-University, Halle
Institute of Pathology of the Medical Academy, Erfurt

The main clinical symptom of ruptured aneurysms of the basal arteries of the brain is subarachnoid hemorrhage. Analysis of the clinical course and of *post-mortem* examinations demonstrates, that it is possible for a patient to survive even a severe subarachnoid hemorrhage and that death is the consequence of intracerebral and/or ventricular hemorrhages in a large number of patients. The frequency of intracerebral and ventricular hemorrhages depends mainly on the localization of the aneurysms (Jänisch, 1963; Schreiber et al., 1977). For further evaluation of the problem the necropsies of two Institutes of Pathology were analyzed.

MATERIAL AND METHODS

92 602 necropsies, performed at the Institutes of Pathology of the Martin-Luther-University Halle (1960—1976) and the Medical Academy Erfurt (1960—1977), were evaluated (Table 1). The consequences of rupture of aneurysms were studied in 332 cases, where no operation took place. The aneurysms were divided into three groups according to their localization:

Anterior group: at the arteria cerebri anterior or the ramus communicans anterior;

Medial group: at the intracranial segment of the internal carotid artery, the arteria cerebri media or the adjacent parts of the rami communicantes posteriores;

Posterior group: at the intracranial extensions of the vertebral arteries, the arteria basilaris, the posterior cerebral arteries and the adjacent parts of the rami communicantes posteriores.

Table 1. Intracranial aneurysms in 92 602 necropsies

Type and state of aneurysm	Number of cases
With a single aneurysm	379
With multiple aneurysms	19
among them with two aneurysms	13
with three aneurysms	6
Total number of aneurysms	423
ruptured aneurysms without operation	332
ruptured aneurysms operated upon	30
non-ruptured aneurysms	61

The consequences of rupture were divided into groups according to the type of hemorrhage and its severity:

Subarachnoid hemorrhage (s.h.): Severe s.h. occupied at least the subarachnoid space at the base of the brain, extending from the frontal lobes up to the pons and the basis of the cerebellum and involving the basal cisterns. An additional extension of the s.h. along the convexity of the cerebral and cerebellar hemispheres was present in many

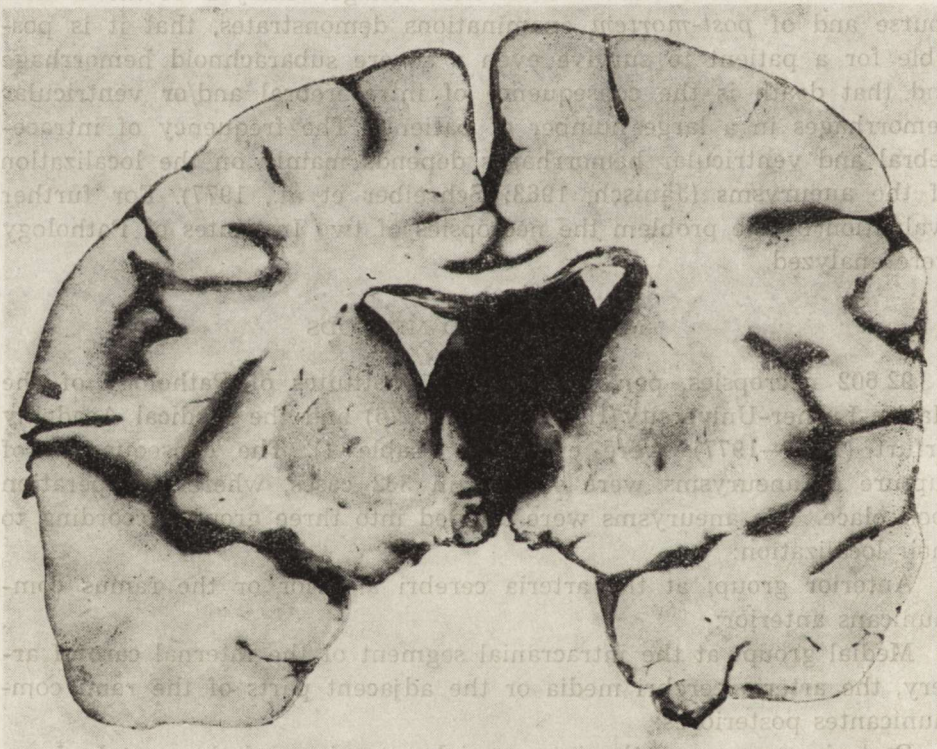

Fig. 1. Ruptured aneurysm of the ramus communicans anterior. Subarachnoid hemorrhage perforating the lamina terminalis and penetrating into the right lateral ventricle. Female, 48 (Nr 344/77, Inst. Path. Halle)

cases. The s.h. was considered to be moderate, when smaller patches of hemorrhage were present or when the cisterna cerebello-medullaris contained blood originating from a ventricular hemorrhage;

Severe ventricular hemorrhage (v.h.) filled all or most of the ventricles of the brain with clotted blood, the latter forming casts of the sligthly dilated ventricles. Some admixture of blood in the CSF in one or several ventricles was regarded as insignificant v.h.;

Cerebral hemorrhage (c.h.) was recorded when the newly formed blood-filled cavity in the brain tissue had a diameter of at least 2 cm. According to this definition the penetration of a hemorrhage through the lamina terminalis into the lateral ventricle (Fig. 1) was not regarded as a c.h.

The combination of several types of hemorrhage in a single patient was a common finding. Each type was independently counted.

RESULTS

Rupture occurs mainly in the 6th and 7th decade of life (Table 2). Most of the ruptured aneurysms are less than one centimeter in diameter (Table 3). It has to be taken into consideration, however, that the size of an aneurysm somewhat decreases after death due to the lack of blood pressure. 46.1 per cent of the ruptured aneurysm belong to the anterior, 39.8 per cent to the medial and 14.1 per cent to the posterior group. Severe subarachnoid hemorrhage is present at death in about 80 per cent of the patients with insignificant differences between the three groups (Table 4).

The average incidence of intracerebral hemorrhage (inh.) amounts to 60 per cent. However, the differences between the groups are considerable. Aneurysms of the anterior group cause in 70 per cent, those of the posterior group in 25 per cent of the patients. A similar tendency

Table 2. Age at necropsy of 332 patients with ruptured intracranial aneurysms

Decades of life	Number of patients	In per cent of the 332 cases
0 < 10	4	1.2
10 < 20	3	0.9
20 < 30	18	5.4
30 < 40	37	11.1
40 < 50	70	21.1
50 < 60	79	23.8
60 < 70	86	25.9
70 < 80	34	10.3
> 80	1	0.3
total	332	100,0

Table 3. Size of 332 ruptured intracranial aneurysms

Largest diameter	Number of aneurysms	In per cent of the 332 cases
up to 1 cm	223	67.2
1 cm – 2 cm	80	24.1
2 cm – 4 cm	9	1.2
size not reported	16	4.8

Table 4. Type of hemorrhage in 332 patients with ruptured intracranial aneurysms. Figures in brackets indicate the percentage in relation to the number of aneurysms of the group concerned

Localization and number of aneurysms	Subarachnoid severe	Subarachnoid moderate	Intracerebral	Ventricular severe	Ventricular moderate
anterior group 153	124 (81%)	29	107 (61%)	72 (45%)	34
medial group 132	103 (76%)	21	83 (61%)	35 (26%)	31
posterior group 47	38 (81%)	8	12 (25%)	6 (12%)	22

exists with the ventricular hemorrhages. They occurred in 45 per cent of the patients who died from aneurysms of the anterior group, whereas this complication only occurred in 12 per cent of the patients with aneurysms of the posterior group. A ruptured aneurysm was clinically diagnosed or at least suspected in 15 per cent of the patients only (Table 5). In 25 per cent of the patients no clinical diagnosis was given or the diagnosis a disease outside the CNF was made.

Table 5. Clinical diagnoses in 332 patients with ruptured intracranial aneurysms

Clinical diagnosis	Number of patients	In per cent of the 332 patients	
aneurysm	51	15.4	
subarachnoid hemorrhage	86	25.9	
stroke	75	22.6	77.4
brain tumor	18	5.4	
meningitis, encephalitis, brain abscess	10	3.0	
other intracranial diseases	17	5.1	
myocardial infarction, coronary insufficiency	30	9.0	
pulmonary artery embolism	7	2.1	22.6
other diseases or no diagnosis	38	11.5	

DISCUSSION

Ruptured aneurysms of the circle of Willis are to be considered in the differential diagnosis of intracranial hemorrhages, if severe subarachnoid hemorrhage is present, and the patient is young.

Our evaluation of necropsies demonstrates, however, that rupture of intracranial aneurysms occurs mainly in old persons. Only 20 per cent of the patients were younger than 40 years. Another explanation for the high percentage of wrong diagnoses of ruptured aneurysms (Table 5) is the large number of severe ventricular hemorrhages in aneurysms of the anterior group. The rupture leads to perforation of the lamina terminalis in most of the cases and the blood reaches the lateral ventricle. The resulting quick deterioration of the patient does not permit detailed clinical investigation. This explains the great number of tentative diagnoses of infarction of the myocardium or acute coronary disease. In many patients with aneurysms of the anterior or medial groups hemorrhage occurs first in the frontal or temporal lobes, causing hematomas of the brain, thus imitating the clinical symptoms of a stroke. Especially in old patients the stroke is assumed to be the result of hypertension and no further investigations by arteriography have been made. The high blood pressure occurring in many cases seems to lend support hypertension hypothesis.

Clinicians have to take into consideration, however, that increased blood pressure may be the consequence and not the cause of the hemorrhage, since the increased intracranial pressure due to the intracerebral hemorrhage may induce a reflex rise of the blood pressure.

REFERENCES

1. Jänisch W.: Zur Frage intrazerebraler Blutungen bei rupturierten Hirnbasisaneurysmen. Frankfurt. Z. Path., 1963, 73, 111—117.
2. Schreiber D., Jänisch W., Peschel R.: Rupturierte Hirnbasisaneurysmen. Eine Analyse des Obduktionsgutes aus 2 pathologischen Instituten. Zbl. allg. Path. path., Anat. 1977, 121, 11—21.

Author's address: Prof. W. Jänisch, Pathologische Institutes der Martin-Luther Universität, 402 Halle, Leninallee 14, PSF 545, DDR

KOMUNIKAT

ESTABLISHMENT OF AN INTERNATIONAL REGISTER OF FAMILIAL BRAIN TUMOURS

An International Register of Familial Brain Tumours (IRFBT) has been established at the Comprehensive Cancer Centre, Leyden, The Netherlands, following the publication of an initial register (Tijssen et al., 1982). The IRFBT is engaged in the active search for new cases of familial brain tumours and would like to invite clinicians worldwide to submit cases, either published or unpublished to this register. Care will be taken to update the register at appropriate times.

C. C. Tijssen, M. D.
M. R. Halprin, M. D.
L. J. Endtz, M. D.

Address: IRFBT, Comprehensive Cancer Centre, Vondellaan 47, 2332 AA Leyden, The Netherlands.

Reference: TIJSSEN C. C., HALPRIN M. R., and ENDTZ L. J. 1982. Familial Brain Tumours, a Commented Register. Martinus Nijhoff Publishers, The Hague, The Netherlands.

NEUROPAT. POL., 1982, 20, 1—2
PL ISSN 0028—3894

JÓZEFA DĄBROWSKA

CHOROID PLEXUSES IN CEREBRAL ATHEROSCLEROSIS

(PRELIMINARY COMMUNICATION)

Neurological Clinic, Institute of Nervous System and Sensory Organs Diseases, School of Medicine, Wrocław

During fetal and individual life the choroid plexus undergoes morphological and histochemical changes (Shuangshoti, Netsky, 1966). In mature and old age it is frequently impossible to distinguish between the normal and the pathological structure of the plexus. Usually in the 4th—5th decade of life degenerative changes appear in the cells of the epithelium layer and stroma of the plexus (Shuangshoti, Netsky, 1970; Oksche, Müller, 1972). In 1928 Zandowa called attention to the changes in the vessels and connective tissue of the stroma as well as the epithelial layer of the plexus which accompany atherosclerosis of the cerebral vessels. Since, then no comprehensive work has appeared dealing with atherosclerosis of the cerebral vessels and the pathomorphology of the choroid plexus.

The present study was undertaken to gain a better knowledge on the morphology of the choroid plexuses in elder subjects and to establish whether the degenerative changes in the latter depend solely on the age of the individual or else are due to atherosclerosis of the cerebral vessels.

MATERIAL AND METHODS

In material consisted of choroid plexuses of the lateral ventricles and the arterial circles of the brain base from 40 brains. Ten of them served as controls. These brains showed no atherosclerotic changes of the vessels. They were taken from persons who died suddenly at the age of 42—77 years because of trauma (5 cases), drowning (2 cases), alcohol intoxication (2 cases), rupture of aneurysm at brain base (1 case). The remaining 30 cases consisted of brains with atherosclerosis of the larger vessels of brain base and vasogenic changes (malacia 25, hemorrhage 5) from subjects who died at the age of 49—85 years of stroke.

For describing the degree of advancement of atherosclerosis qualitative and quantitative methods were used. Quantitative evaluation of the extent of atherosclerosis was based on Aftandilow's method (1961; 1970), of simple planimetry in the present autor's own modification. The prepared out arterial circle was placed on a glass plate with millimetre scale, the contours were traced and the points corresponding to atherosclerotic changes on the surface were marked. The percentual extent of the changed area corresponded to the degree of atherosclerosis. Three degrees were distinguished: the first (I) — macroscopically visible atherosclerotic changes (plaques) visible through the relatively thin vascular wall, occupying up to 24 per cent of the vessel surface; the second (II) — 25—50 per cent of the vessel surface; the third (III) — occupying more than 50 per cent of the vascular surface.

Evaluation of the quality and advancement of the changes was based on routine microscopic examination of the arteries. Four phases were distinguished: for phase 1 the characteristic feature is swelling proliferation and lipid infiltration of vascular endothelium, reaction of the muscle cells and fibroblasts, the internal elastic lamina being preserved; in phase 2 the latter undergoes partial fragmentation, atherosclerotic plaques develop protruding into the vascular lumen or penetrating into the media. In the atheromatous plaque, and sometimes beyond it in the media degenerative changes of hyaline-fibrous type appear. Phase 3 of atherosclerosis is characterised by a fibrous organisation of the plaque or its ulceration. The media shows hyaline degeneration, hypertrophy or atrophy. Changes in the internal elastic lamina become severer, leading to considerable defects. In the advanced phase (4) the changes develop further so that as a rule complete disappearance of the internal elastic lamina is noted and the atheromatous plaque undergoing hyaline degeneration or calcified fills a large part of the vascular lumen or vascular wall. Sometimes extravasations from the newly formed "own" vessels and paramural thromboses are observed. The media atrophies or becomes hypertrophied.

The choroid plexuses of the lateral ventricles and segments or arteries of the Willis circle were fixed with formalin and embedded in paraffin. The preparations were stained by H-E, van Gieson, Von Kossa and Langeron methods. The state of the epithelium, stroma and plexus vessel was estimated.

RESULTS

The choroid plexus in the control group (Table 1) did not show any changes (Fig. 1), or only slight ones. The epithelium of the plexus was unchanged, that is single-layered, cubic with well developed nuclei. Some (focal) proliferation of epithelial cells was found in only two cases, desquamination of single epithelial cells in three cases, cytoplasmic va-

Table 1. Control group; Morphology of choroid plexuses of ventricles

No.	Case no.	Age Sex	Epithelium	Stroma	Vessels
1	430/77	59 M	single-layer, cubic with well developed nuclei, single vacuoles	focal calcifications, no other changes	thin-walled with wide lumen
2	458/77	45 M	structure normal	thin with cell reaction, no major changes	no changes (as in case)
3	465/77	43 M	desquamation of single cells, no other changes	no changes	no changes
4	468/77	45 M	structure normal	single calcifications, no other changes	no changes
5	49/78	54 M	focal cell proliferation, no other changes	no changes	no changes
6	88/78	51 F	no changes	moderately hypertrophic, single psammomatous bodies	no changes
7	394/77	52 M	single desquamation foci	single psammomatous bodies	no changes
8	170/76	42 M	no changes	moderately hypertrophied	considerable hyalinisation of walls
9	434/77	77 M	desquamation of single cells	moderately hypertrophied and hyalinised	no changes
10	74/78	44 M	minute cell proliferation foci, no other changes	no changes	no changes

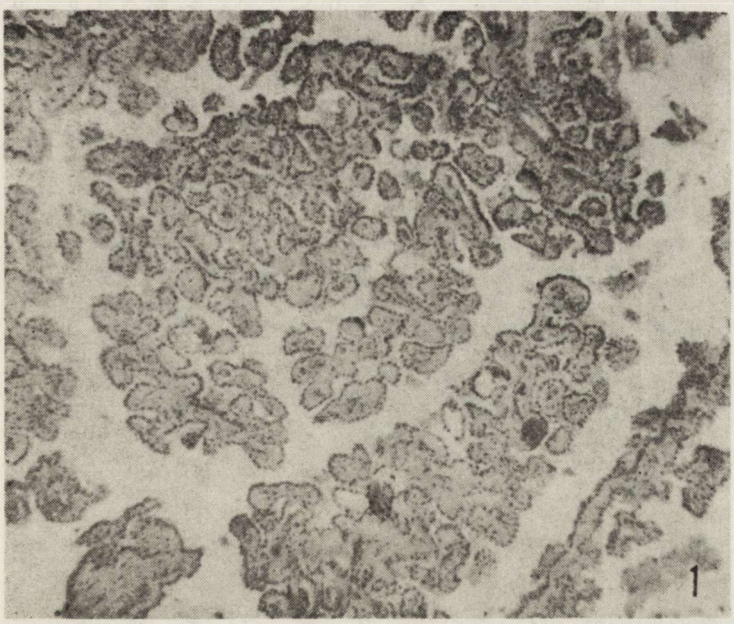

Fig. 1. Normal picture of the choroid plexus. H—E. × 80

Table 2. Morphology of choroid plexuses

No.	Case no.	Age Sex	Degree and phase of atherosclerosis	Epithelium	Stroma	Vessels
1	1122/77	49 F	I/1	profusely desquamating, single proliferation foci	single foci of fibrosis and calcification	intervillous fine, in glomus thick hyalinised
2	1106/76	60 F	I/4	well preserved	hypertrophied, fibrosis, calcification and pseudo calcium foci	with narrowed lumen
3	1044/75	76 F	II/2	profusely desquamating, cytoplasmic vacuoles	well developed, particularly around villous vessels	well preserved
4	1162/77	64 M	II/2	flat, desquamating profusely	thin, fibrous numerous psammomatous bodies	thick, fibrous delaminated
5	920/72	85 F	II/3	moderately desquamous, single foci of cell proliferation, vacuoles	thin, calcification foci, numerous psammomatous bodies	thick with hyaline-fibrous changes
6	1039/75	69 M	II/3	flat, desquamating profusely (large defects)	hypertrophied, hyalinised	thick, delaminated
7	1172/78	64 F	II/3	well preserved	hypertrophied, hyalinised, partly calcified	thick, hyalinised
8	897/72	59 M	II/4	flat, desquamating profusely vacuoles and foam-like cells present	fibrosed, calcified, numerous psammomatous bodies	thick, fibrosed delaminated
9	1022/74	64 F	II/4	flat, desquamating profusely	moderately hypertrophied, hyalinised, psammomatous bodies	well preserved
10	906/72	56 M	III/1	well preserved, vacuoles present and foci of cell proliferation	thick hypertrophied, calcified, fibrosed, numerous psammomatus bodies	thick, hyaline
11	1100/74	66 F	III/1	profusely desquamating, vacuoles present	numerous calcifications and psammomatous bodies	without major changes
12	898/72	77 M	III/2	desquamating moderately	hypertrophied, numerous calcifications	thick, hyaline
13	904/72	58 M	III/2	considerable defects	hypertrophied, fibrosed, calcified, cysts with pseudocalcium	in villi focally calcified others thick, hyaline

14	981/73	74 M	III/2	considerable defects	hypertrophied, foci of hyalinisation, calcifications	thick, hyaline
15	985/74	72 M	III/2	desquamating profusely	hypertrophied, numerous hyalinisation and calcification foci	thick, delaminated
16	1080/76	68 F	III/2	proliferation foci	hypertrophied with numerous fibrosis and calcification foci	thick, hyaline and calcified walls
17	1095/76	68 F	III/3	well preserved	hypertrophied, no other changes	well preserved
18	881/71	68 M	III/3	well preserved with proliferation	hypertrophied, hyalinisation features	well preserved
19	896/72	66 M	III/3	desquamating profusely, vacuoles present	hypertrophied, numerous psammomatous bodies	well preserved
20	903/72	55 M	III/3	desquamating profusely	hypertrophied with hyalinisation features	thick, fibrosed and calcified
21	919/72	51 M	III/3	desquamating profusely	fibrosed and calcified	thick, hyaline
22	1075/76	78 F	III/3	profusely desquamated, numerous foam-like cells	hypertrophied, fibrosed and calcified	thick, delaminated
23	1076/76	67 M	III/3	plexus structure obliterated, particular	components difficult to distinguish	thick, hyalinised walls their structure undergoing obliteration
24	1115/76	76 F	III/3	well preserved, numerous cell proliferation foci	thin, with fibrosis features	thick, fibrosed walls, numerous calcification foci in villous vessels
25	1160/77	76 F	III/3	foam-like cells present, mostly well preserved	hypertrophied numerous foci of hyalinisation and fibrosis and calcification	thick, hyaline
26	1165/77	62 F	III/4	has disappeared almost completely	hypertrophied, hyalinised, calcified	thick, hyaline walls
27	1120/77	70 F	III/4	well preserved	with hyalinisation features	mostly thick, hyaline delaminated
28	1136/76	75 F	III/4	mostly well preserved	thin with hyalinisation features	well preserved
29	1146/77	72 F	III/4	desquamated on large areas	hypertrophied, structure obliterated	thick, obliterated structure
30	1150/77	65 M	III/4	desquamated on large areas, has almost disappeared	thin, disappearing	with thick walls and obliterated structure

cuoles in one case. The connective tissue of the stroma was in five cases moderately hypertrophied with only some hyalinisation foci or calcifications. The presence of concentric bodies was demonstrated in two cases. In one case the vessels showed features of hyalinisation, the remaining ones did not exhibit any changes.

The results of examination of the choroid plexuses from 30 brains with atherosclerotic changes in arteries of the Willis circle are summarized in Table 2.

Among the brains with atherosclerosis I° (2 cases) phase 1 of atherosclerosis was recognised in one case. In the plexus epithelium profuse desquamating cells and focal proliferation could be seen. In the stroma single foci of fibrosis and calcification were present. The walls of the vessels in glomus choroideus were thicker and hyalinised. In the second case the atherosclerotic changes indicated phase 4. The epithelial layer of the plexus was well preserved, the stroma hypertrophied, particularly around the vessels of villi. There were, moreover, foci of calcification, fibrosis and pseudocalcium depositions.

From among the seven cases of atherosclerosis II° two were classified to phase 2; three to phase 3, two to phase 4. The epithelium of the plexus was well preserved only in one case, in five it was flattened and desquamating, in one case it had almost disappeared. The presence of cytoplasmic vacuoles was noted in three cases, single foam-like cells (detached from the epithelial layer) and swollen in two cases. Connective

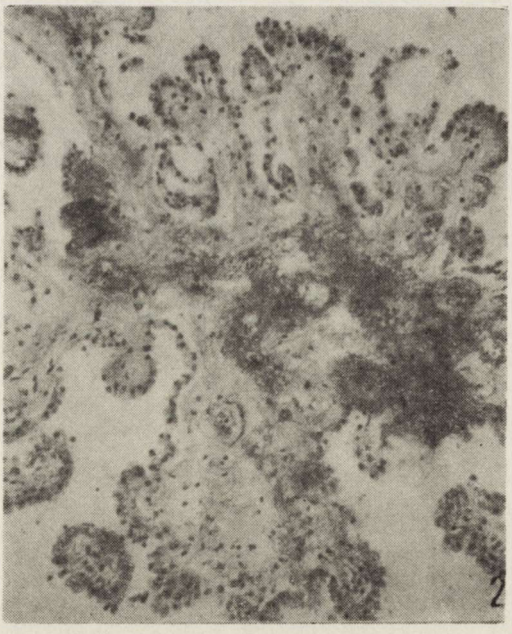

Fig. 2. Hypertrophia, hyalinosis and calcification of the plexus stroma. H—E. × 200

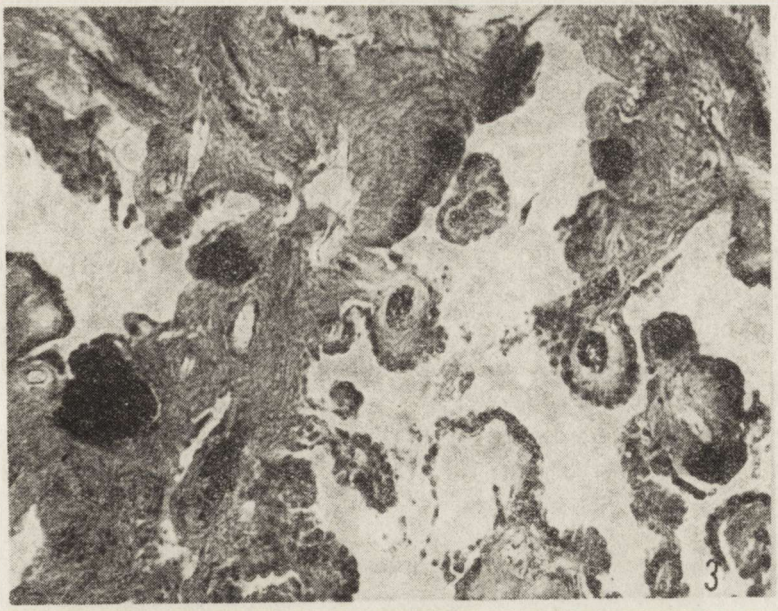

Fig. 3. Slight desquamating of the epithelial cells and focal calcification are present. Langeron. × 200

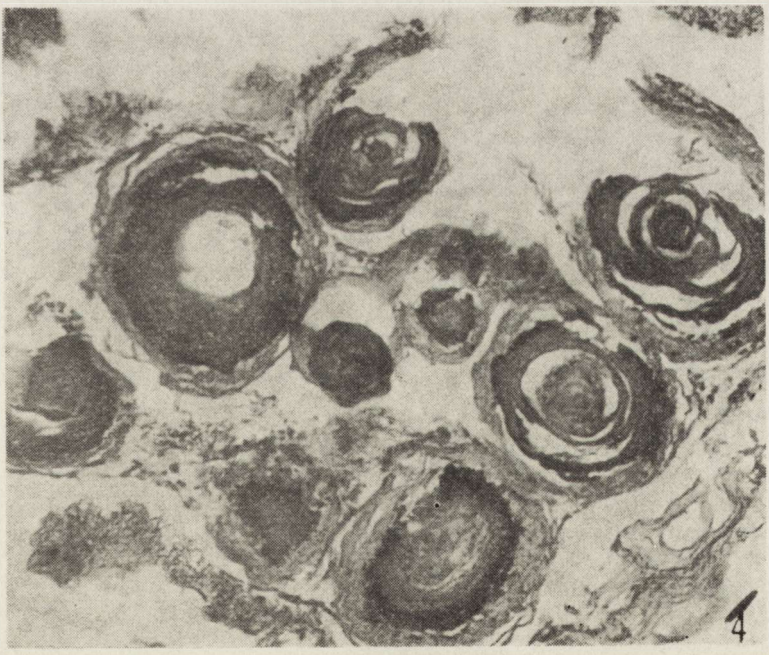

Fig. 4. Psammoma bodies in the choroid plexus. von Kossa. × 500

tissue of the plexus was in three cases greatly hypertrophied (Fig. 2) and in these cases numerous hyalinisation and calcification foci were observed. In three cases numerous concentric bodies were present without hypertrophy of the stromal connective tissue. The vessels were well preserved in two cases, in the remaining five there were hyaline-fibrous changes and in one focal calcification. Delamination of vessel walls was noted in three cases.

Atherosclerosis III° (21 cases) was classified as follows: two cases to phase 1, five to phase 2, ten to phase 3, four to phase 4. The epithelium of the plexus was well preserved in seven cases, in three of these focal cell proliferation and vacuoles were observed and in one case foam-like cells. In 12 cases the cells were flat and desquamated to a large extent and in five they had disappeared. The stromal connective tissue of the plexus showed proliferation in 15 of the 21 cases. Hypertrophy of the

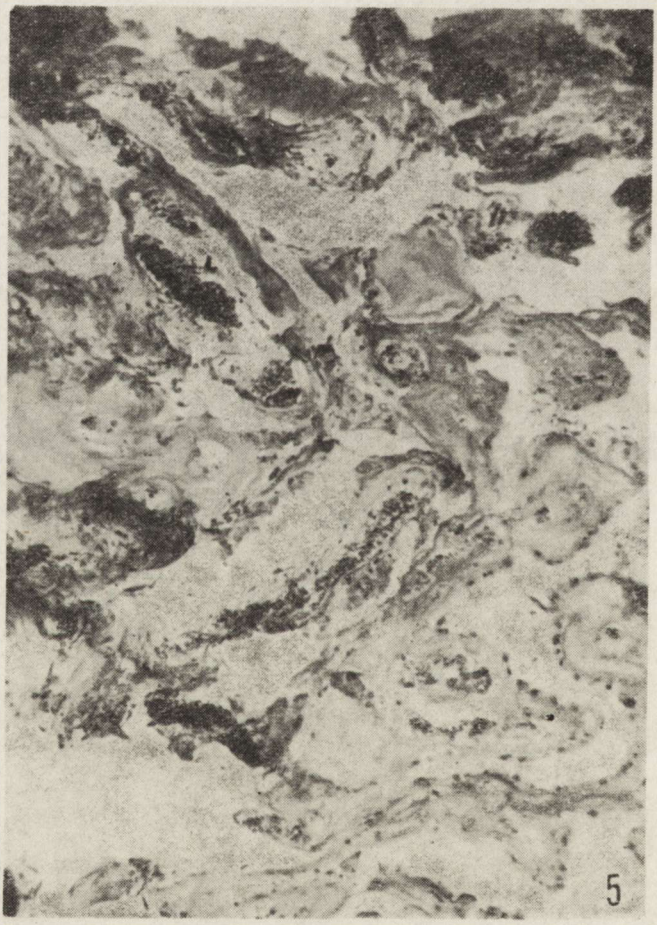

Fig. 5. Absence of the epithelial cells, degeneration of the stroma, hypertrophy and hyalinosis of blood vessels. van Gieson. × 200

stroma was associated with degenerative changes such as focal or extensive hyalinisation of the stroma, fibrosis and calcification (Fig. 3). In four cases the presence of cysts filled with pseudocalcium was observed (Fig. 4). The plexus exhibited considerable regressive changes (Fig. 5). Degenerative vascular changes (hyalinisation, fibrosis, thickening and delamination of walls) were found in 16 cases, whereas in five the plexus vessels did not show major abnormalities.

CONCLUSIONS

1. In the 5th to 8th life decade the choroid plexus of the lateral ventricles in the brains without atheromatosis of larger arteries are not changed significantly.

2. In a similar age group the choroid plexuses of lateral ventricles in the brains with atheromatosis of larger arteries exhibit marked degenerative changes.

3. It would seem that atherosclerosis of brain vessels, and not the age of the subject is responsible for these degenerative changes.

4. There probably exists a relation between the degree of advancement of brain atherosclerosis and the intensity of changes in the plexus.

REFERENCES

1. Aftandiłow G. G.: Dinamika atieroskleroticzeskogo processa u czełowieka. Medicine, Moskwa 1970.
2. Aftandiłow G. G.: Płanimietriczeskoje liniejki dla koliczestwiennoj ocenki artieroskleroticzeskich porażenij sosudow. Arch. Patoł., 1961, 4, 89—90.
3. Oksche A., Müller W.: Zytobiologie der Plexus choroidei als Grenzfache der Blutbahn und Liquor cerebrospinalis. Anat. Anz. Bd., 1972, 131, 433—447.
4. Shuangshoti S., Netsky M.: Human choroid plexus: morphologic and histochemical alterations with age. Am. J. Anat., 1970, 128, 73—96.
5. Shuangshoti S., Netsky M.: Histogenesis of choroid plexus in man. Am. J. Anat., 1966, 118, 283—316.
6. Zandowa N.: Splot naczyniasty. Polskie Towarzystwo Naukowe, Warszawa 1928.

Author's address: 118 Traugutt Str., 50—420 Wrocław, Poland

NEUROPAT. POL., 1982, 20, 1—2
PL ISSN 0028—3894

HERMANN HAGER, PAUL ZIMMERMANN

MORPHOLOGY AND CYTOMETRY OF SURAL NERVE IN TANGIER DISEASE

Institute of Neuropathology, Neurological Centre of Justus-Liebig University, Giessen

A 5-year old boy and his 6-year old sister from the Chesapeak Bay Island, Tangier presenting grossly enlarged, yellow-orange tonsils were the first reported cases with an α-lipoprotein deficiency (Frederickson et al., 1961). In some patients a disturbance of peripheral nerve function developed. The first electron microscopic study of peripheral nerve changes in Tangier disease was published by Kocen et al. (1973). In our case of an adult-onset Tangier disease combined light, electron-microscopical and cytometric studies on sural nerve biopsy were performed.

CASE REPORT

A 55-year old man (O.M.) suffered from a neuropathy over several years. In October 1974 an α-1-lipoprotein deficiency was found (Genetic Institute, University Marburg) and a Tangier disease was suggested. In July 1975 the patient was admitted to the Medical Department of the University Giessen suffering from an excessive weakness of hands and legs. On examination he showed, besides the signs of a severe polyneuropathy, yellowish-orange plaques on the tonsils. Histology of the tonsils and of a rectal biopsy revealed many cells with foamy cytoplasm; These results confirmed the diagnosis of the Tangier disease.

RESULTS

Light-microscopy

Transverse sections of the sural nerve showed an inhomogeneous loss of nerve fibres. Small fibres dominated. In some axons small dense droplets of unknown origin were observed in combination with a degeneration of the myelin sheath. In longitudinal sections through sural nerve fibres a segmental disintegration of myelin was found. In some fibres axonal degeneration was observed within an intact Schwann cell sheath. An extensive endoneural collagenization was also evident. These results speak in favour of a chronic neuropathy.

Electron microscopy

In addition to the myelinated axons, very few unmyelinated axons were present in the sural nerve. Most of the Schwann cell processes were with axons. The most striking abnormalities were multiple vacuoles within the Schwann cell cytoplasm. These vacuoles had a clear cut boundary apposed by a small rim of electrondense homogeneous deposits. In some Schwann cells the nuclei were deformed by attached vacuoles. Some unmyelinated fibres showed "globules" caused by enlarged vacuoles. The process of demyelination was characterized by the disintegration of the myelin sheath into droplets and myelin figures. These "fingerprint-like" bodies were noted in the vicinity of the axon, displacing it. Destruction of the axon was minimal. Sometimes vacuoles surrounded by a double membrane mitochondrial origin indicating were found. In the paranodal region irregular inward protrusions of myelin lamella containing electrondense material and small myelin bodies were often seen. Vesicular and tubular organelles associated with dense bodies were observed in the paranodal region of the axon. The amount of endoneural collagen was excessive.

Cytometry

The density of myelinated fibres was grossly reduced to 3.814/mm² as compared with a control value of 4.800/mm² (Sluga, 1974). The fibre size distribution of this sural nerve biopsy is shown in Figure 1. The

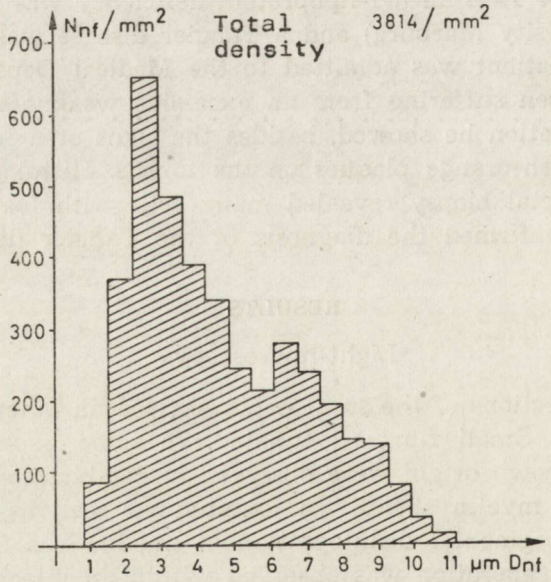

Fig. 1. Density distribution of myelinated fibres of sural nerve (N_{nf}/mm²). D_{nf} — Total diameter of myelinated nerve fibre. N_{nf} — Number of myelinated nerve fibres

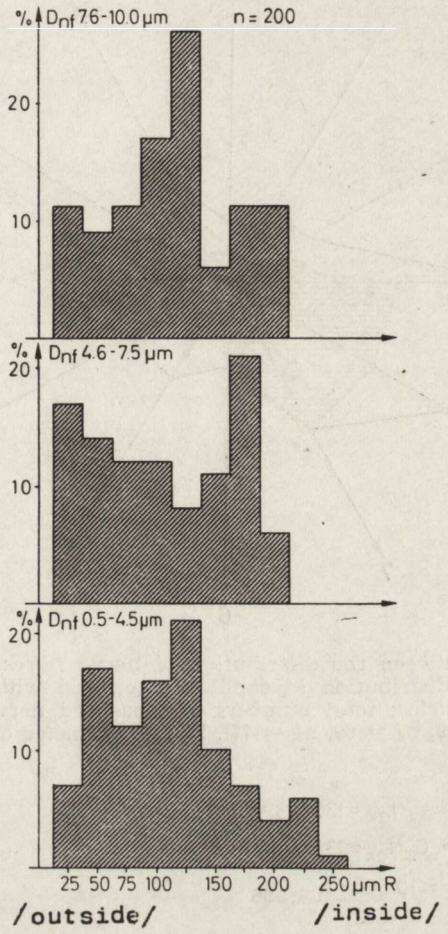

Fig. 2. Relationship between fibre diameter and distance from the fascile boundary (R)

normal bimodal distribution was lost and there was also a loss of fibres with a diameter of less than 6 µm (normal value 800—900/mm² for fibre diameters between 2—3 µm; Sluga, 1974). For quantifying relationships between the capillary system and the fascicle structure we correlated the fibre-type distribution with the fibre distance from the fascicle surface and from the endoneural capillaries. In Figure 2 it is demonstrated that small myelinated fibres (diameter 0.5—4.5 µm) and the largest myelinated fibres (diameter 7.6—10 µm) accumulate in a distance of up to 125 µm from the fascicle boundary. The number of myelinated fibres with diameter between 4.6 and 7.5 µm increased in the middle of the fascicle (distance from the fascicle boundary 150—200 µm). Figure 3 shows the methodical approach and the results of quantifying capillary-nerve fibre interrelationships. A test screen with

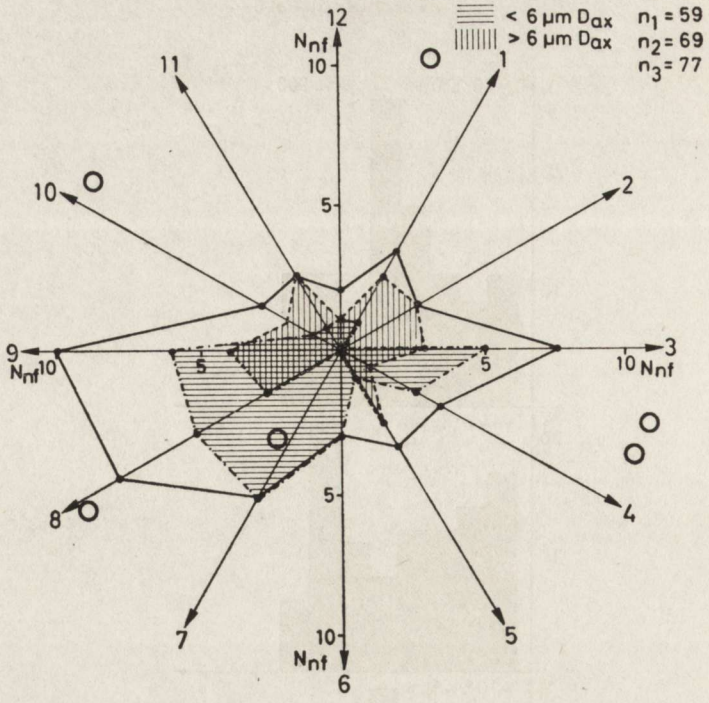

Fig. 3. Relationship between the distribution of nerve fibres along the radial test lines (1—12) and the distribution of capillaries (circles) within the nerve fascicle (mean value of 3 fascicles; total numbers of measured nerve fibres per fascicle: $n_1 = 59$, $n_2 = 69$, $n_3 = 77$). D_{ax} — Diameter of axon

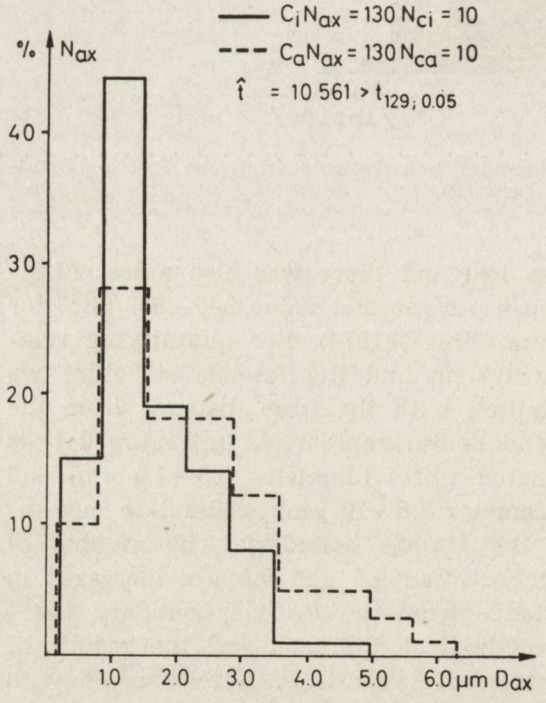

Fig. 4. Distribution of nerve fibre diameter up to a distance of 50 µm from 10 peripherally and 10 centrally placed endoneural capillaries. N_{ax} — Total number of measured axons

radial lines was projected over the fascicle. Then the capillaries were localized in the different segments of the test screen. The diameter of myelinated nerve fibres was measured along the test lines. The capillaries were differentiated according to their distance from the test lines and the fascicle boundary. Fibres with diameters over 6 μm were associated with capillaries that were distributed within the fascicle. This was confirmed by measurements of the distribution of nerve fibres up to a pericapillary distance of 50 μm (Fig. 4).

DISCUSSION

In our case complaints indicating a slowly progressive polyneuropathy were impressive in an early phase of the disease. Other typical signs of Tangier disease were diagnosed later, i.e. α-lipoprotein deficiency, accumulation of lipid inclusions in tonsils and in rectal mucosa.

Light-microscopic examination revealed a slowly progressive neuropathy. Under the electron-microscope multiple vacuoles were found in the cytoplasm of Schwann cells. According to Kocen et al. (1973) these deposits seem to be lipid inclusions and relatively characteristic of Tangier disease. Many bands of Büngner indicated axonal degeneration. But it is known that vacuolated inclusions in Schwann cell cytoplasm combined with axonal degeneration is also characteristic of primary axonal neuropathies (Schlaepfer, Hager, 1964). The ultrastructural appearance of vacuoles in the paranodal processes of Schwann cells seems to be an interesting observation since the internodal myelin sheath appeared intact. There results speak in favour of a progressive disintegration of the myelin sheath starting in the paranodal region which is later followed by axonal degeneration. Kocen et al. (1973) did not report any paranodal lesions and believe in a primary axonal neuropathy in Tangier disease, although they found less of axons without signs of severe axonal degeneration. Therefore, the basis for the suggested primary axonal degeneration is poorly understood.

Cholesterol seems to be the main product within the vacuoles of Schwann cells. These deposits could arise during a defect of intracellular cholesterol transport which was discussed by Kocen et al. (1973). Assuming that transport processes are disturbed in Tangier disease it was tried to quantify interrelationships between the vascular system and the Schwann cell-axon-complex. Small nerve fibres (total diameter < 6 μm) accumulated around endofascicular capillaries (Fig. 4). These nerve fibres may regenerate along the preexisting capillaries. Nerve fibres with diameters > 6 μm were not so intimately related with capillaries. It is assumed that large myelinated nerve fibres have a higher rate of lipid metabolism than axons surrounded by a thinner myelin

sheath. Therefore, the loss of nerve fibres is more prominent in fibre classes with diameters > 6 μm in Tangier disease — a disease of lipid metabolism.

REFERENCES

1. Frefrickson D. S., Altrocchi P. H., Avioli L. V., Goodmann D. S., Goodmann H. C.: Tangier disease. Ann. intern. Med., 1961, 55, 1016—1031.
2. Kocen R. S., King R. H. M., Thomas P. K., Haas L. F.: Nerve biopsy findings in two cases of Tangier disease. Acta neuropath. (Berl.), 1973, 26, 317—327.
3. Schlaepfer W., Hager H.: Ultrastructural studies of I. N. H. induced neuropathy in rats. II. Alteration and decomposition of the myelin sheath. Am. J. Path., 1964, 45, 423—433.
4. Sluga E.: Polyneuropathien. Typen und Differenzierung. Ergebnisse bioptischer Untersuchungen. Schriftenreihe Neurologie, Springer. Berlin—Heidelberg—New York, 1974. Bd. 14.

Author's address: Neuropathologisches Institut am Zentrum für Neurologie des Klinikums der Justus-Liebi-Universität, D-6300 Giessen, Arndtstrasse 16, Bundesrepublik Deutschland

NEUROPAT. POL., 1982, 20, 1—2
PL ISSN 0028—3894

MARGIT GALLAI

PERONEAL MUSCULAR ATROPHY. ELECTRONMICROSCOPIC STUDIES

National Institute for Nervous and Mental Disease, and Postgraduate Medical School, Electronmicroscopic Laboratory, Budapest

Peroneal muscular atrophy (PMA) is a slowly progressive hereditary disease, characterized by weakness of the muscles, which are innervated by the peroneal nerve. Weakness of the intrinsic muscles of the feet and hands and some sensory loss in the distal aspects of the lower limbs are frequently associated with it.

In recent years new classifications have been recommended on the basis of new types of examinations: nerve conduction velocity measuring and the biopsy of the sural nerve. We had the opportunity to make

Table 1. Report of cases

Clinical data		Cases			
		Z.J.	I.J.	Sz.M.	A.A.
Age in years	examination	61	71	53	39
	onset of complaints	13	55	12	36
Pes cavus	patient	+	+	+	right
	family members	+	+	?	ø
Weakness and atrophy	dorsiflection of feet	+	+	+	right
	hand muscles	+	+	+	+
Absence of deep tendom reflexes	lower limbs	+	+	+	right
	upper limbs	+	+	ø	ø
Abnormal superficial sensation	lower limbs	+	+	ø	ø
	upper limbs	ø	ø	ø	ø
Heel-Shin dyssinergia		+	+	ø	ø
Leg cramps and aches		ø	+	ø	+
Tremor of hands		ø	+	ø	+

electronmicroscopic examinations on the sural nerves of 4 patients, suffering from peroneal muscular atrophy. Clinical and electronmicroscopic data are summarized and the most important morphological alterations documented (Table 1).

Motor nerve conduction velocity was reduced significantly in the 1st and 2nd patients and preserved or only slightly reduced in the 3rd and 4th. The data are summarized in table 2.

Table 2. Motor nerve conduction velocities (NCV) in m/sec. and distal motor latencies (DML) in msec/cm

Nerve	Cases – NCV/DML			
Cases:	Z.J.	I.J.	Sz.M.	A.A.
Radial nerve	22.7	19.6	57.0	61.6
	1.46	1.71	0.55	0.57
Ulnar nerve	18.0	10.0	66.0	i.u.
	1.21	1.38	0.50	
Peroneal nerve l.d.	n.r.	14.5	50.8	47.9
		1.83	0.56	0.72
Peroneal nerve l. sin.	n.r.	i.u.	50.4	52.0
			0.50	0.67

n. r.-not recordable i. u.-information unavailable

On semithin sections of the sural nerves in the 1st and 2nd cases a severe reduction in the density of the large myelinated axons are observed (Fig. 1). The larger axon diameters are 6—7 μm instead of 9—10 μm. Concentric layers around large myelinated axons of the type of onion bulb formations are present. In case 3, there is no onion bulb, the large myelinated axons are somewhat sparser than in the normal nerves (Fig. 2). In case 4 semithin sections do not reveal any pathological alterations.

The fine structure of the sural nerves of the first two patients are similar to each other. Onion bulbs are composed of Schwann cell processes around a central myelinated axon (Fig. 3). It may be normal, hypermyelinated or disintegrated. The axon survives the segmental loss of its myelin and a new sheet is built up by Schwann cells (Fig. 4). There are many more collagen bundles surrounded by Schwann cells, than in normal condition (Fig. 5). These bundles are thought to occupy the place of impaired unmyelinated axons.

The third case, characterized clinically by a slightly diminished rate of nerve conduction velocity, does not show onion bulb formations and loss or reconstruction of myelin sheaths. The most apparent feature is shrinkage of the largest axons. Redundant loops of myelin, partly degenerated fill the adaxonal space (Fig. 6). Clusters of myelinated fibres

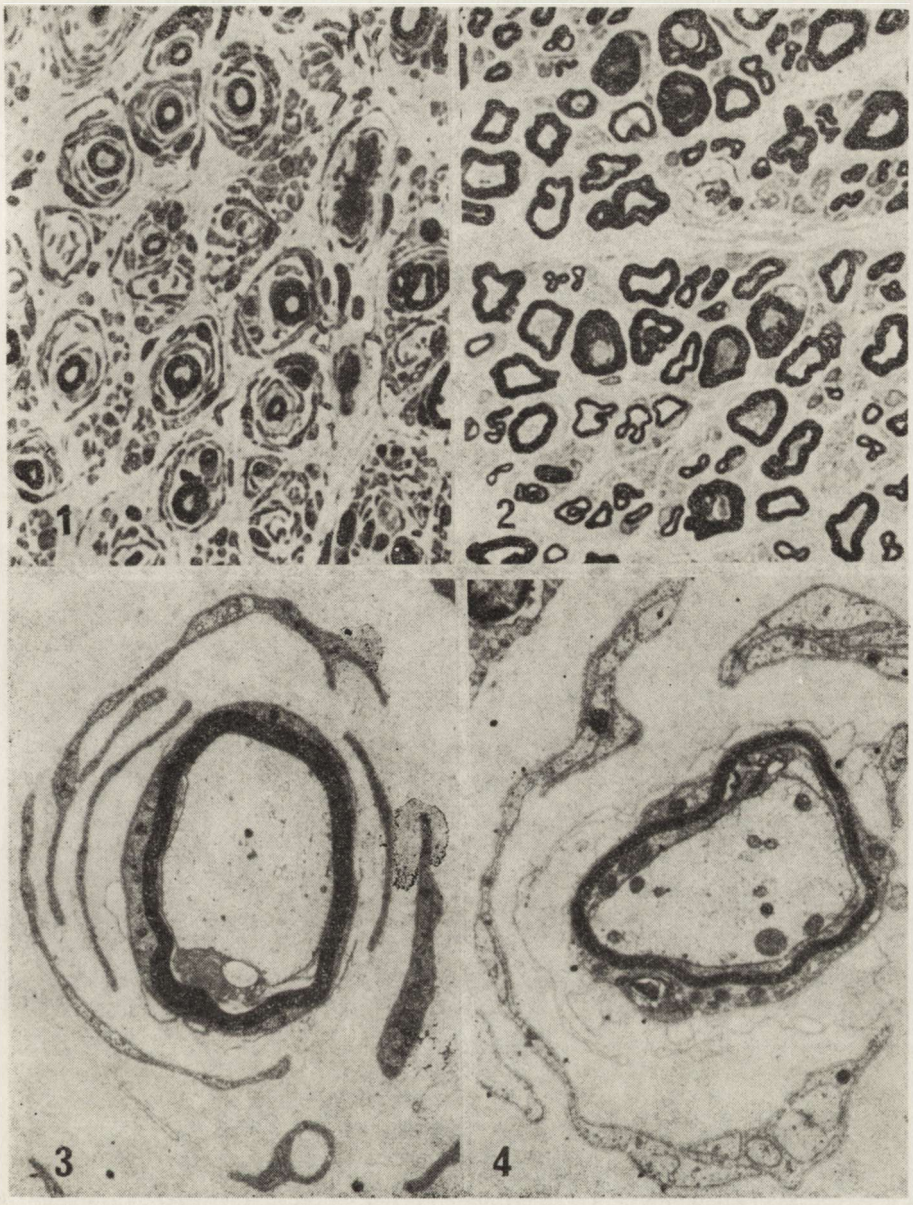

Fig. 1. Onion-bulb formations, reduction of the diameters and density of large myelinated fibres in the sural nerve of case 2. Semithin section, toluidine blue. × 640

Fig. 2. Case 3. The largest fibres are of normal diameter and density. Structural changes in many axons. Semithin section, toluidine blue. × 640

Fig. 3. Case 2. Cross section of an onion bulb. × 6000

Fig. 4. Case 2. The central nerve fibre of the onion bulb is surrounded by a loose band of basement membrane myelin sheath is very thin. These are considered as signs of demyelination and remyelination. × 8800

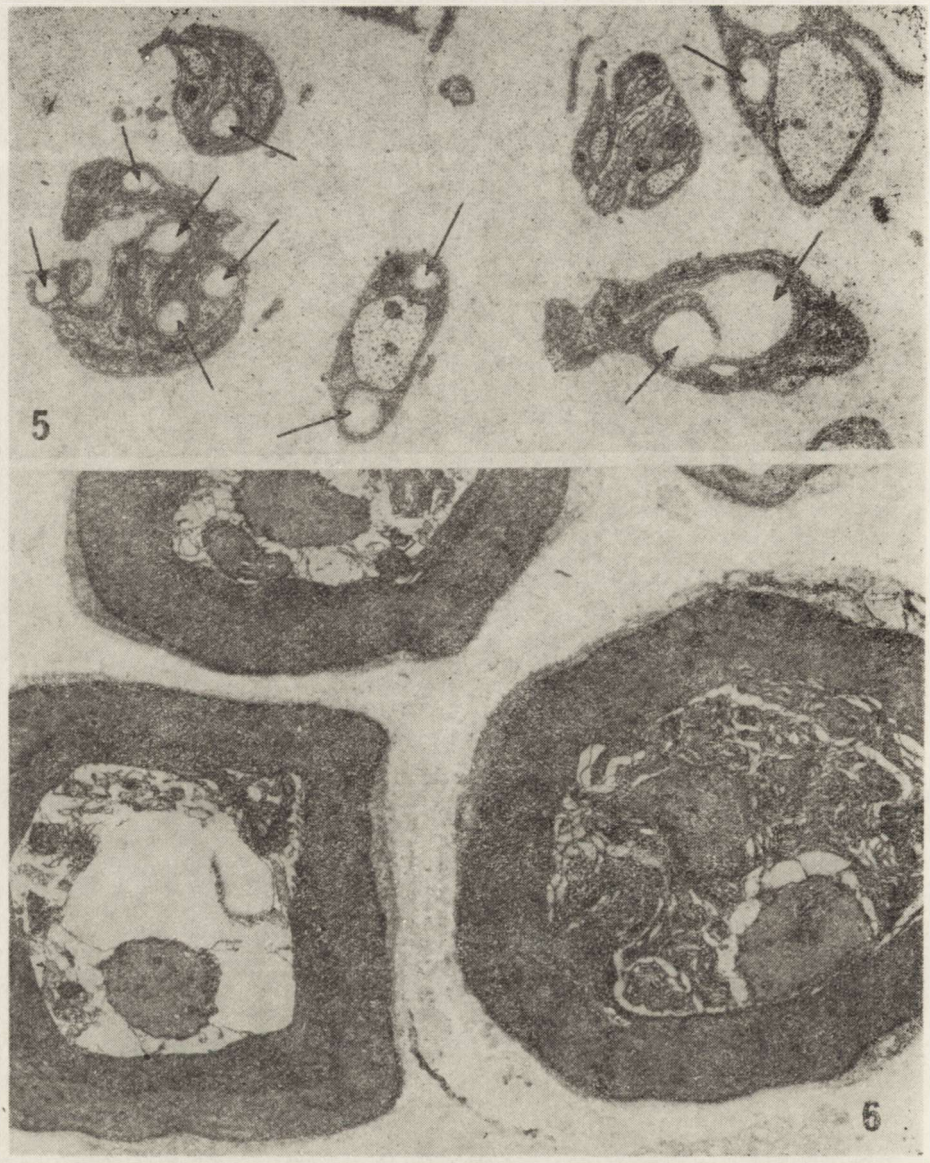

Fig. 5. Case 2. Schwann cells encasing collagen bundles (arrows). Extensive deposition of collagen in the intercellular space. × 8800

Fig. 6. Case 3. Shrinkage of axons, loops and bands of myelin in the adaxonal space. Myelin sheaths are only moderately altered. × 6600

and numerous unmyelinated axons of unusually small diameters present are regenerating elements (Fig. 7).

The fine structure of the sural nerve from case 4 was similar to those obtained from normal human subjects.

Fig. 7. Case 3. "Cluster" of small, regenerating unmyelinated fibres. × 7600

DISCUSSION

Clinical characteristics and classification of PMA are summarised by Behse and Buchtal (1977) and by Bradley et al. (1977). Dyck, Thomas and Lambert (1975) used another terminology, namely that of hereditary motor and sensory neuropathy (HMSN).

Patients suffering from PMA can be divided into two groups on the basis of nerve conduction velocity (NCV). One group demonstrates significant reduction in speed, the other shows normal or nearly normal conduction data. Since the publication of Dyck and Lambert (1977) and that to Behse and Buchtal (1977) appeared, we have known, that there is a strong correlation between NCV and pathomorphology of the peripheral nerves. In cases with a 50% or more reduction in velocity speed segmental demyelination and onion bulb formation are generally found. With normal, or only slightly diminished NCV neurons show degenera-

tion, either in the whole, or in the distal part of the axon. If there are no sensory disturbances, the case may be classified as a spinal type. In this type of PMA the NCV is normal or near to normal and the sural nerves do not show pathological alterations.

The most striking clinical features of all inherited neuropathies are pes cavus (high instep or arches) and hammer toes, they occur in more than 90 per cent of all cases. First symptoms are usually abnormalities of gait in consequence of muscle weakness and atrophy in the foot and leg muscles. Atrophy of leg and distal thigh muscles produces an inverted bottle effect. Enlargement of peripheral nerves may be observed in some hypertrophic type cases, but exact differentiation between hypertrophic, neuronal and spinal type requires the examination of NCV and sural nerve biopsy.

Onion bulbs are easily seen in the light microscopy. They are characteristic of the hypertrophic type of PMA (HMSN type I). They are the consequences of repeated segmental demyelinations and remyelinations. The number of myelinated and normal unmyelinated fibres decreases, the amount of endoneural collagen is greater than in normal nerves. Hypertrophic neuropathy is not restricted to inherited diseases, it occurs in some exogenous neuropathies too. Our 1st and 2nd cases reveal a positive family history, typical clinical signs and diminished NCV. Therefore we classify them as a hypertrophic type of PMA.

In case 3, Schwann cells and myelin sheaths are almost normal, the most pronounced electronmicroscopic alteration is the axonal atrophy of the large myelinated nerves. Adaxonal myelin alterations seem to be secondary, filling the space resulting from the shrinkage of the axon. Clusters of myelinated and unmyelinated fibres are the signs of regeneration activity. This axonal atrophy with regeneration and with a normal NCV ascertains, that case 3 represents the neuronal type of PMA (HMSN type II).

In the 4th case peripheral motor system was seriously impaired, however, neither clinical signs of sensibility disturbances, nor electrophysiological alterations were found. The sural nerve morphology was also normal. Consequently this case was classified as a spinal type of PMA.

In conclusion, the morphologic examination of the sural nerve is a useful method for differentiating inherited neuropathies.

REFERENCES

1. Behse F., Buchthal F.: Peroneal muscular atrophy (PMA) and related disorders. II. Histological Findings in Sural Nerves. Brain, 1977, 100, 67—85.
2. Bradley W. G., Madrid R., Davis C. J. F.: The peroneal atrophy syndrome. Clinical genetic, Electrophysiological and Nerve Biopsy Studies. Part 3. Clinical, Electrophysiological and Pathological Correlations. J. Neurol. Sci., 1977, 32, 123—136.

3. Buchthal F., Behse F.: Peroneal muscular atrophy (PMA) and related disorders. I. Clinical Manifestation as Related to Biopsy Findings. Nerve Conduction and Electromyography. Brain, 1977, 100, 41—66.
4. Dyck P. J., Thomas P. K., Lambert E. H.: Peripheral neuropathy. W. B. Sounders Company, Philadelphia—London—Toronto 1975.
5. Dyck P. J., Lambert E. H.: Lower motor and primary sensory neuron diseases with peroneal muscular atrophy. I. Neurologic, Genetic and Electrophysiologic Findings in Hereditary Polyneuropathies. Arch. Neurol., 1977, 18, 603—618.

Author's address: Postgraduate Medical School, Electronmicroscopic Laboratory, Budapest XIII, Szaboks u. 35

DZIAŁ KRONIKI I INFORMACJI

W dniu 20 kwietnia 1982 r., w szóstą rocznicę śmierci prof. dr. med. Anatola Dowżenki, wieloletniego kierownika I Kliniki Neurologicznej Instytutu Psychoneurologicznego, została w tejże Klinice odsłonięta, ufundowana przez pracowników Instytutu, tablica pamiątkowa ku Jego czci.

*

W dniu 12 czerwca 1982 r. odbyła się w Krakowie uroczystość odnowienia dyplomu Doktora prof. dr. hab. med. Adamowi Kunickiemu, z okazji 50 rocznicy uzyskania przez Niego dyplomu Doktora Nauk Medycznych.

*

W dniu 22 września 1982 r. odbyła się w Instytucie Psychoneurologicznym uroczystość osiemdziesięciolecia urodzin prof. dr. med. Zygmunta Kuligowskiego, pierwszego i wieloletniego Dyrektora Instytutu i Przewodniczącego jego Rady Naukowej

*

W dniu 14 października 1982 r. odbyło się w Łodzi uroczyste posiedzenie Polskiego Towarzystwa Neurologicznego z okazji 90-lecia urodzin nestora neurologii polskiej prof. dr. h. c. nauk med. Eufemiusza Hermana.

*

W dniu 29 października 82 r. Rada Państwa nadała doc. dr. hab. med. Jerzemu Kulczyckiemu, kierownikowi I Kliniki Neurologicznej Instytutu Psychoneurologicznego w Warszawie, tytuł profesora nadzwyczajnego.

*

Następujący koledzy uzyskali ostatnio stopień naukowy doktora habilitowanego:

— dr med. Janusz Alwasiak, kierownik Pracowni Neuropatologii Katedry Onkologii AM w Łodzi, na podstawie rozprawy pt. „Współzależność między cechami morfologicznymi i klinicznymi w gwiaździakach i skąpodrzewiakach nadnamiotowych mózgu". Stopień został nadany przez Radę Wydziału Lekarskiego AM w Łodzi w dniu 15 XII 1981 r.,

— dr med. Jolanta Borowska-Lehman, na podstawie rozprawy pt. „Niektóre aspekty odczynowości komórkowej w nowotworach śródczaszkowych". Stopień został nadany przez Radę Wydziału Lekarskiego AM w Gdańsku w dniu 5 III 1982 r.,

— dr med. Lubomira Dydyk, adiunkt Pracowni Mikroskopii Elektronowej CMD i K PAN w Warszawie, na podstawie rozprawy pt. „Wpływ normobarycznej hyperoksji na korę mózgu w okresie jej rozwoju z uwzględnieniem zmian płucnych". Stopień został nadany przez Radę I Wydziału Lekarskiego AM w Warszawie w dniu 14 IV 1982 r.

*

W dniu 8 września 1982 r., w czasie trwania IX Międzynarodowego Kongresu Neuropatologii w Wiedniu, odbyło się Walne Zgromadzenie Międzynarodowego Towarzystwa Neuropatologicznego, na którym wybrano nowe władze na kolejną 4-letnią kadencję w następującym składzie:

c.d. na s. 150

NEUROPAT. POL., 1982, 20, 1—2
PL ISSN 0028—3894

HALINA WEINRAUDER, STANISŁAW KRAJEWSKI

LOCATION OF SPECIFIC ANTIGENS IN BRAIN BY IMMUNOFLUORESCENCE IN HOMO- AND HETEROGENEOUS SYSTEMS

Department of Neuropathology, Medical Research Centre, Polish Academy of Sciences

The isolation of specific antigens of the nervous system and description of their properties (Moore, 1965; Weinrauder, 1969; Warecka, 1970; Eng et al., 1971; Weinrauder, Lach, 1975; 1977) opens perspectives of their utilisation in investigations on the development, differentiation and interrelations between glial and nerve cells both *in vivo* and *in vitro*. Most of the known antigens do not show any species specificity; there are, however, some indications of existence in the nervous system of some organ-species specific antigens.

It was found in earlier studies that there are in the rat brain specific antigens localized in the glia, immunologically identical with the brain antigens of other species (Weinrauder, Lach, 1977; 1978). One of these antigens also exhibited features of species specificity (Weinrauder, Lach, 1979).

The present study was undertaken to establish the cellular localization of antigens with different specificity by means of immune sera against the rat and baboon brains.

MATERIAL AND METHODS

Sera obtained by repeated immunisation of rabbits with baboon brain homogenate and extract from rat brain were used for the investigations. Immune sera were absorbed by normal sera, homogenates of body organs and by lyophilized human brain extract, respectively. In the immunofluorescence reaction (IF) sera containing specific brain antibodies were used after checking them in the immunodiffusion (ID) reaction and in the IF test on sections of the organs previously applied for absorption.

The IF reaction was performed by the indirect method on cryostat sections of human and rat brain and on cell cultures from the cerebellum of newborn rats, run according to the method described by Kraśnicka and Mossakowski (1965). As first layer immune sera were used, followed by anti rabbit gamma-globulin goat serum labeled with fluorescein isothiocyanate, and absorbed with acetone powder from mouse livers and polymer of human serum gammaglobulin. The specificity of reaction was checked by substituting for the first layer normal serum or PBS, inhibition of the reaction on sections of the organs used for absorption and inhibition after absorption of immune serum with brain antigen. Details of the methods used are given elsewhere (Weinrauder 1969; Weinrauder, Krajewski 1975).

RESULTS

The IF reaction with anti rat brain serum on sections of rat brain is shown in Figs 1—4. In the cerebral cortex and basal nuclei intensive fluorescence of neuropil was observed, most pronounced in the form of rings around the dark nuclei of cells which according to their localization may be considered as oligodendrocytes (Fig. 1). The cortical neurones were always negative. The intensive reaction of neuropil and the negative one in the neurons were most distinct in brain stem (Fig. 2) and cerebellar sections (Figs 3, 4). A negative reaction in nerve cell processes of the white matter was visible both on cross and longitudinal sections of the fibres (Figs 2, 3). The IF reaction with this serum on human brain sections (basal nuclei, cerebellum, brain stem) was localized similarly and did not show differences in intensity and fluorescence character. After absorption with human brain the anti rat brain serum gave a positive IF reaction on brain, localized similarly but of somewhat lower intensity. In the basal ganglia (Fig. 5) and the cerebellum distinct fluorescence of neuropil was observed. The reaction on human brain sections was inhibited.

Serum against baboon brain reacted specifically both on rat brain (Fig. 6) and human brain sections. The character of fluorescence, its localization in the neuropil with distinctly negative neurones were very similar to the fluorescence pattern observed in reactions in which anti rat brain serum was applied. After absorption with human brain antigen the reaction was completely inhibited on both the tested brains (Figs 7, 8). All control reactions were quite negative.

In in vitro culture of newborn rat cerebellum intensive fluorescence was observed in the reaction with both the tested sera in the cytoplasm and glial cell processes and was particularly intensive in the oligodendrocytes. The positive reaction appeared already in one-week cultures

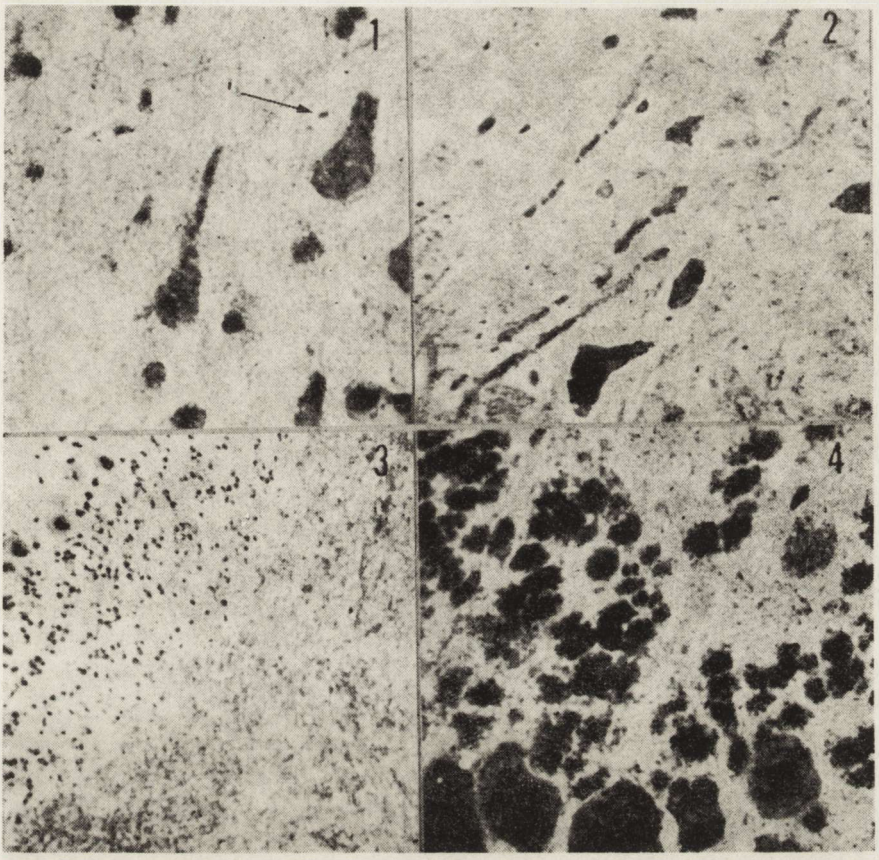

Fig. 1. Serum against rat brain. Rat cerebral cortex. Strong positive reaction in neuropil and cytoplasm of oligodendrocytes (arrow). Neurons and nuclei of glial cells negative. × 250

Fig. 2. Serum as in Fig 1. Reticular formation of the pons in rat. Strong positive reaction of neuropil in the basal portion of the pons. Large neurons and longitudinal sections of processes negative. × 250

Fig. 3. Serum as in Fig. 1. Intensive IF reaction in rat cerebellar hemispheres. The perikarya and longitudinally sectioned neuronal processes in white matter are negative. × 60

Fig. 4. Serum as in Fig. 1. Rat cerebellum in higher magnification. Negative Purkinje cells and neurons of the granular layer surrounded by strongly fluorescent neuropil. × 250

and became more intensive with ageing of the culture. In the growth zone intensive fluorescence was observed in single cells or their agglomerations surrounded by much weaker reacting cells or completely negative ones.

Anti rat brain sera, both unabsorbed and absorbed with human brain (Fig. 9), reacted strongly and positively with antigens localized in the

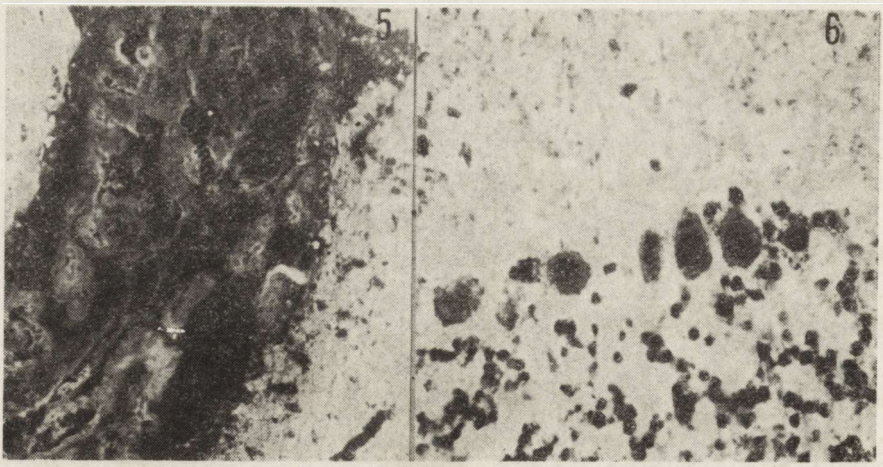

Fig. 5. Rat brain antiserum absorbed by human brain. Rat brain. Positive reaction in nerve tissue surrounding lateral ventricle. Choroid plexus and ependymal cells negative. × 60

Fig. 6. Baboon brain antiserum. Rat cerebellum. IF reaction very similar to the pattern observed with rat brain antiserum. Purkinje cells and granular layer cells negative, neuropil strongly positive. × 130

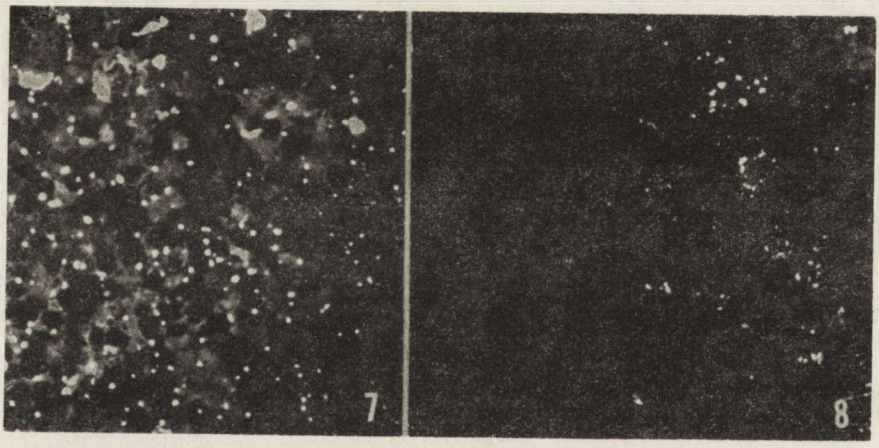

Fig. 7. Baboon brain antiserum absorbed by human brain. Human cerebellum. Inhibition of specific IF reaction. Weak unspecific autofluorescence of tissue and of lipofuscin grains. × 130

Fig. 8. Serum as in Fig. 7. Rat cerebellum. Inhibition of specific IF reaction. Unspecific fluorescence of scarse lipofuscin grains in Purkinje cells. × 130

cytoplasm of glial cells. Anti baboon brain serum containing antibodies against an antiorgan antigen gave a very strong positive reaction, mainly in the oligodendrocytes, although fluorescence of some astrocytes was also noted (Fig. 10).

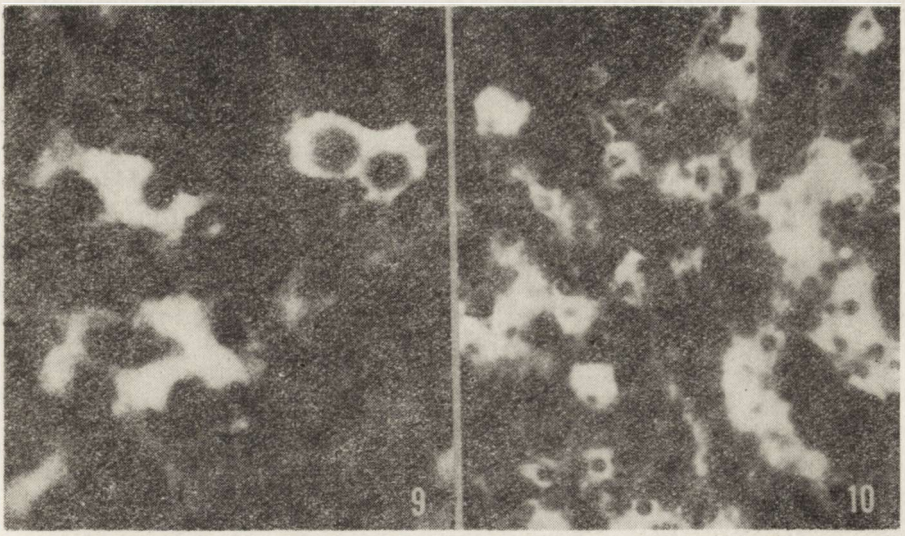

Fig. 9. Rat brain antiserum absorbed by human brain. Culture of newborn rat cerebellum. Specific fluorescence in cytoplasm and processes of glial cells. × 400

Fig. 10. Baboon brain antiserum. Culture of newborn rat cerebellum. Intensive specific fluorescence in glial cells, particularly strong in oligodendrocytes. × 250

DISCUSSION

The sera obtained by rabbit immunization with rat and baboon brain contain antibodies reacting in the IF reaction with specific antigens localized in the neuropil from various regions of rat and human brain and in glial cells — mainly oligodendrocytes — cultured in vitro. The localization and character of fluorescence as well as its intensity are in both cases very similar. The glial antigen recognised by these antibodies is of an organ-specific antigen character and occurs in the brains of a number of species.

In earlier investigations (Weinrauder, 1978) the serum against baboon brain reacted equally with the homologous antigen and the antigen from human brain in the ID reaction, whereas the reaction with the rat brain antigen is very weak or negative. Some data indicate that the concentration of the organ-specific antigen is low in the rat brain (MacPherson, Liakopoulou, 1966). This would explain the failure in obtaining positive ID reactions. The antibodies contained in anti baboon brain serum react, however, intensively in the IF reaction with glial antigens localized in tissue or cell culture in vitro. Similar observations are reported by Delpech et al. (1976) suggesting oligodendroglial localization of these antigens.

After absorption of both the tested sera with human brain antigen the reaction on sections of this brain is completely inhibited. The IF reaction with baboon brain antiserum on rat brain is also negative, thus

indicating absorption of organspecific antibodies. On the other hand, the IF reaction of anti rat brain serum on rat brain and in rat glial cell culture continues to be positive. This seems to confirm the occurrence in the rat brain of glial antigen with a double organ-species specificity. The presence in the brain of this kind of antigens has been described earlier (Hatcher, MacPherson 1970; Liakopoulou, MacPherson, 1970), their character, however, is but little known and the scarse data do not allow any suggestions as to their function in the nervous system. Their cell localization is not known; the data gained by us, although strongly supporting localization in the oligodendroglia, do not rule out the occurrence of this antigen in the astrocytes as well.

PIŚMIENNICTWO

1. Delpech B., Vidard M. N., Delpech A.: Caractérisation immunochimique et immunologique d'une glycoprotéine associée au système nerveux. Immunochemistry, 1976, 13, 113—116.
2. Eng L. F., Vanderhaeghen J. J., Bignami A., Gerstl B.: An acidic protein isolated from fibrous astrocytes. Brain Res., 1971, 28, 351—354.
3. Hatcher V. B., MacPherson C. F. C.: Studies on brain antigens. III. Purification and characterization of a water soluble bovine antigen specific for nervous tissue (α-BASNT). J. Immunol., 1970, 104, 633—640.
4. Kraśnicka Z., Mossakowski M. J.: Zagadnienie zmienności morfologicznej tkanki glejowej hodowanej in vitro. Neuropat. Pol., 1965, 3, 397—408.
5. Liakopoulou A., MacPherson C. F. C.: Studies on brain antigens. IV. Isolation and partial characterization of a rat species-restricted antigen of nervous tissue (SRANT). J. Immunol., 1970, 105, 512—520.
6. MacPherson C. F. C., Liakopoulou A.: Studies on brain antigens. I. Water soluble antigenic proteins of rat brain. J. Immunol., 1966, 97, 450—457.
7. Moore B. W.: A soluble protein characteristic of the nervous system. Biochem. Biophys. Res. Commun., 1965, 19, 739—744.
8. Warecka K.: Isolation of brain-specific glycoprotein. J. Neurochem., 1970, 17, 829—830.
9. Weinrauder H.: Studies on cat brain antigens. I. Soluble precipitation protein antigens. Bull. Acad. Pol. Sci. Cl. VI, 1969, 17, 423—426.
10. Weinrauder H., Lach B.: Immunofluorescence studies on the localization of the brain specific antigens in the central nervous system of the rat. Proc. VIIth Intern. Congress Neuropath., Budapest 1974. Ed. St. Környey, St. Tariska, G. Gosztonyi, Excerpta Med. Amsterdam 1975, 115—118.
11. Weinrauder H., Lach B.: Localization of organ-specific antigens in the nervous system of the rat. Acta neuropath. (Berl.), 1977, 39, 109—114.
12. Weinrauder H.: Antibodies against organ-specific brain antigens in heterologous antisera. Bull. Acad. Pol. Sci. Cl. VI, 1978, 26, 221—224.
13. Weinrauder H., Lach B.: Studies on glia-specific antigen of rat brain. Proc. Intern. Symp. "Functions of Neuroglia" Tbilisi 1976, Ed. A. Roitbak, Metsniereba, Tbilisi 1979, 281—286.
14. Weinrauder H., Krajewski S.: Immunofluorescencyjna lokalizacja narządowo-swoistych antygenów w mózgu przy użyciu surowic homo- i heterologicznych. Neuropat. Pol., 1979, 17, 273—285.

Adres autorów: Zespół Neuropatologii Centrum Medycyny Doświadczalnej i Klinicznej PAN, ul. Dworkowa 3, 00—784 Warszawa

NEUROPAT. POL., 1982, 20, 1—2
PL ISSN 0028—3894

JOLANTA JURANIEC, RON E. STEINER, EDWARD G. JONES

SOME CONNECTIONS OF THE BASAL NUCLEUS OF MEYNERT IN THE SQUIRREL MONKEY (SAIMIRI SCIUREUS)

Department of Anatomy, Institute of Medical Biology, School of Medicine, Gdańsk
Department of Anatomy and Neurobiology, Washington University, School of Medicine, St. Louis

The present paper is a continuation of studies on the basal nucleus of Meynert in the squirrel monkey (Saimiri sciureus). Observations referring to the ultrastructure of this nucleus are the subject of another paper (Juraniec, 1979). As we know the basal nucleus belongs to the magnocellular nuclei of the basal forebrain (Divac, 1975) and has numerous afferent connections arising from different regions of brain (Kodama, 1929; Akert, Pilleri, quoted by Gorry, 1963; Norgren, 1974; Leich-

Fig. 1. Dark field photomicrograph of a section from an experimental injection of horseradish peroxidase into the frontal cortex. Note the island of large cells of the basal nucleus (arrow). Several cells in this island are labeled by retrograde axonal transport of enzyme. BM — basal nucleus. Thionin counterstain. × 110

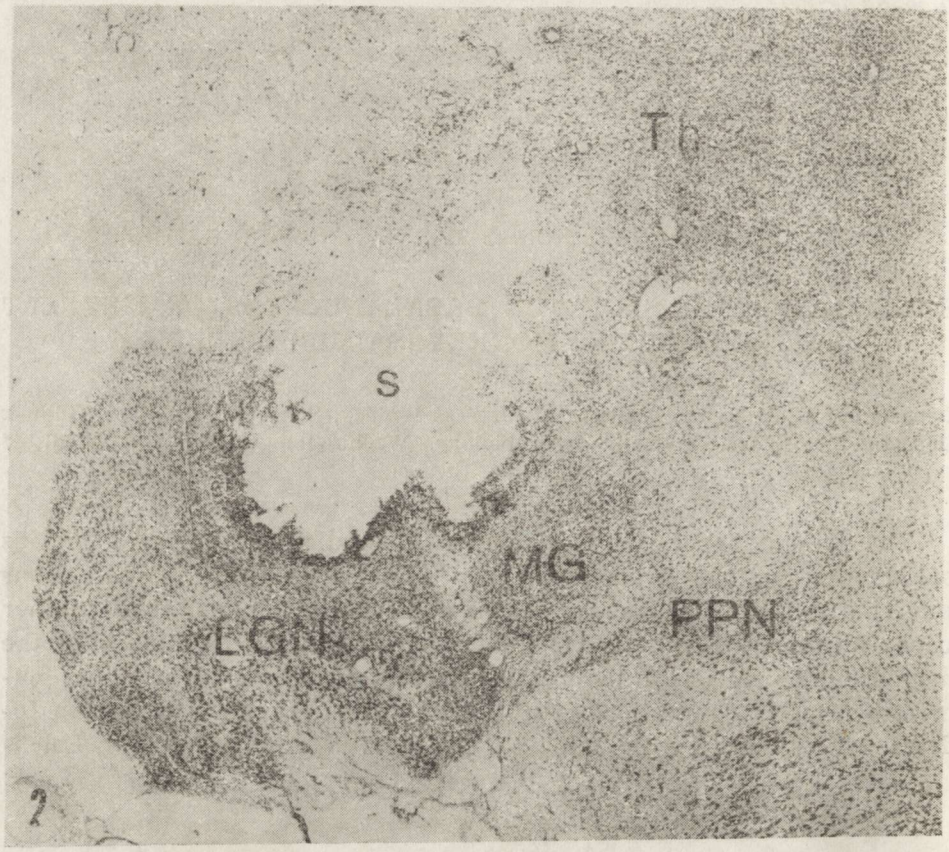

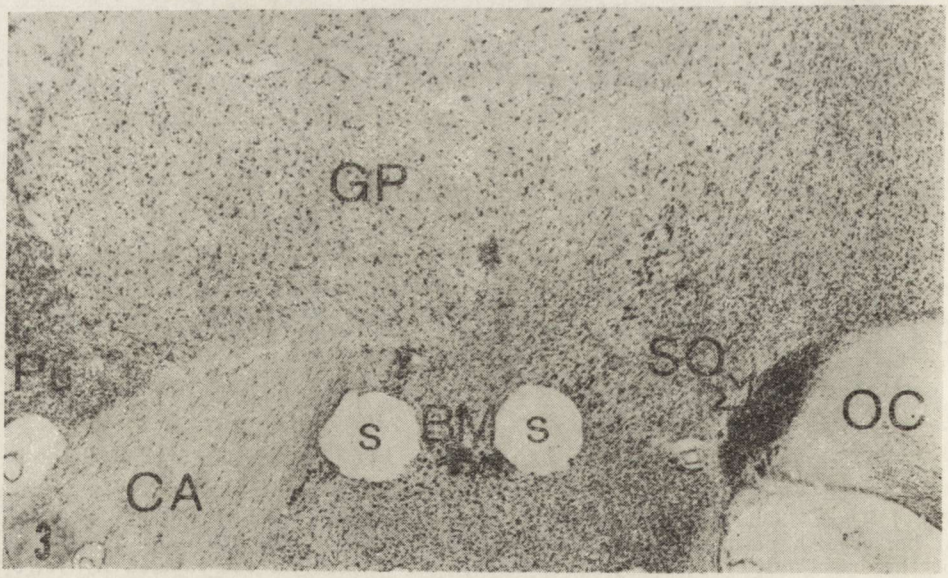

netz, Astruc, 1977). Efferent connections of this nucleus are also described (Nauta, Mehler, 1966; Kievit, Kuypers, 1975 a, b; Ogren, Hendrickson, 1976). The paper of Jones et al. (1976) is particularly worth noting. In experiments using the retrograde axonal flow it was shown that cells of the basal nucleus were labeled after injections of horseradish peroxidase into the neocortex (Fig. 1). In addition, the studies of the above mentioned authors based on the anterograde autoradiographic method showed that the basal nucleus receives connections from the peripeduncular nucleus of the midbrain.

The purpose of the present paper is to confirm the existence of afferent connections of the basal nucleus with the peripeduncular nucleus by means of the degenerative electron microscopic method. Efferent connections of this nucleus with other parts of brain were investigated simultaneously by means of the autoradiographic method.

MATERIAL AND METHODS

The brains of 4 adult squirrel monkeys (Saimiri sciureus) were used for these investigations. Surgery was performed on all animals with Nembutal anesthesia and aseptic precautions.

In 2 squirrel monkeys unilateral or bilateral multiple electrolytic lesions aimed at the peripeduncular nucleus itself or fibers leaving the nucleus (Fig. 2) were interrupted in the stereotaxic apparatus by using alternating current of 1.5—2 mA at each point, applied for about 20—30 seconds. The survival period was 4 and 5 days. Brains were fixed by intracardiac perfusion through the ascending aorta; first with a solution of White's saline and then with a mixture of 1% glutaraldehyde and 4% paraformaldehyde. A detailed description of the method is given in a previous paper (Juraniec, 1979). Bilaterally, about 20 cores were taken from different regions of the basal nucleus (Fig. 3) for electron microscopic studies.

The remaining 2 brains were prepared for autoradiographic tracing of efferent connections of the basal nucleus. Tritium labeled amino acids, proline and leucine (New England Nuclear), were injected stereotaxically at multiple sites into the basal nucleus. One brain was injected on one

Fig. 2. Location of lesion made by an inserted electrode. The lesion includes the lateral geniculate nucleus and other neighbouring nuclei of the thalamus and axons arising from the peripeduncular nucleus. Frontal section. PPN — peripeduncular nucleus, MG — medial geniculate complex, LGN — lateral geniculate nucleus, Th — thalamus, s — site of lesion. Thionin counterstain. × 17

Fig. 3. Frontal section of the basal nucleus. BM — basal nucleus of Meynert, Pu — putamen, GP —globus pallidus, CA — anterior commissure, OC — optic chiasm, SO — supraoptic nucleus, s — sites from which cores were taken for electron microscopic studies. Thionin counterstain. × 17

side, the other on both sides. The stereotaxic coordinates were used from Emmers' and Akert's atlas (1963). The proline and leucine were evaporated and reconstituted in normal saline to give a solution with an activity of 50 μCi/μl. The injections were made with a o.1μl Hamilton syringe. Usually 0.1—0.2 μl was injected at each location. The Injections lasted for 15—20 minutes. After a survival time of one week, the animals were perfused with 10% formol-saline at room temperature. The brains were embedded in Paraplast and sectioned at 20 μm. Every tenth section was coated with Kodak NTB2 emulsion and exposed at 4°C for a period of two weeks. Then they were developed in Kodak developer D-19 and fixed in Kodak rapid fixer. Subsequently they were stained through the emulsion with thionin (Cowan et al., 1972).

RESULTS

In order to study afferent connections of the basal nucleus, which arise from the peripeduncular nucleus, lesions were made within the latter. As a result degenerations in the basal nucleus occured. Terminal degenerations were also found in the basal nucleus after lesions which included the lateral geniculate nucleus, nucleus reticularis thalami, nucleus lateralis posterior thalami, nucleus ventralis posterior basalis lateralis thalami and nuclei of the pulvinar. From these experiments we may suppose that fibers arising from the peripeduncular nucleus pass through some of these nuclei. Following lesions a small number of degenerating axon terminals were seen in the basal nucleus. Four days after lesion, the degenerating terminals were dark but not very shrunken. Synaptic vesicles and mitochondria were swollen and could still be seen within the terminals with astrocytic processes often surrounding them. All the degenerating axon terminals usually formed synapses with asymmetrical membrane thickening and probably had spherical synaptic vesicles. They were in contact with dendritic spines, which were not numerous and with some larger dendrites (Fig. 4). In some cases degenerating axon terminals were observed in contact with the perikarya of large cells of the basal nucleus (Fig. 5). At more advanced stage of degeneration most of the degenerating terminals were almost surrounded by glia as was clearly seen after 5 days survival. Altered terminals contained very dark cytoplasm, their profiles grossly distorted and shrunken; the vesicles were not clearly visible. Most of them were engulfed by astrocytic processes. Some degenerating terminals were seen in contact with dendritic spines or shafts or even with perikarya.

From the above experimental material we see that some axon terminals filled with spherical vesicles are endings of connections arising from the peripeduncular nucleus.

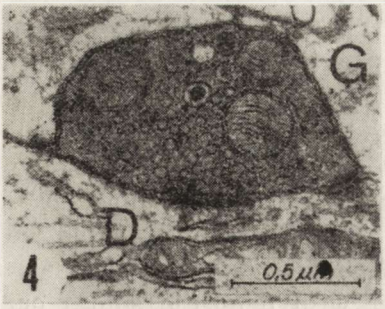

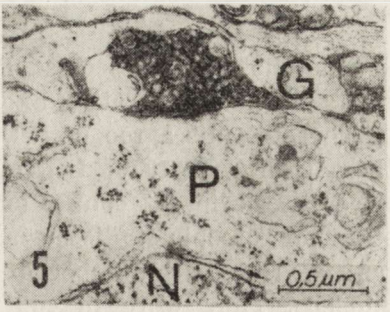

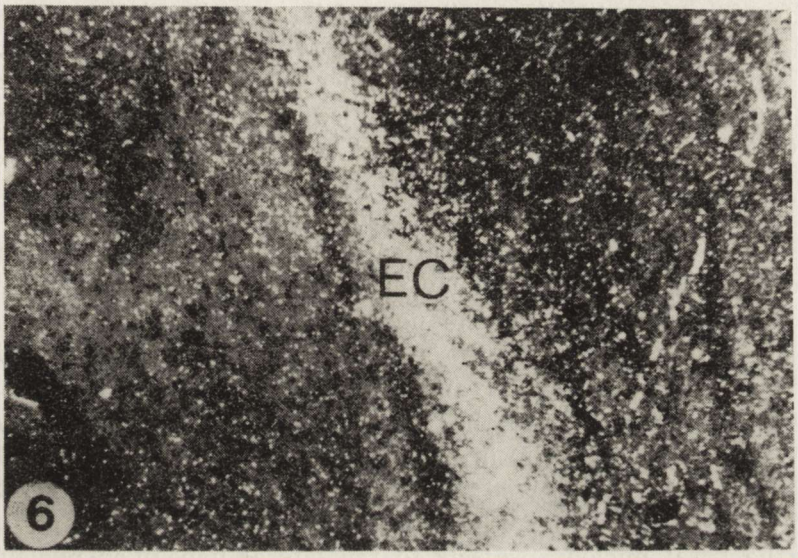

Fig. 4. A typical degenerating axon terminal 4 days after damage to the axons of the peripeduncular nucleus, forms an asymmetrical synapse with a dendritic shaft. Bouton surrounded by glia. D — dendrite, G — glia

Fig. 5. Axosomatic degenerating synapse 4 days after damage to the axons of the peripeduncular nucleus. P — perikarya, N — nucleus, G — glia

Fig. 6. Dark field photomicrograph of an autoradiograph showing the intense concentration of silver grains in the external capsule after an injection of the basal nucleus with tritiated amino acids. — EC — external capsule. Thionin counterstain. × 150

Tritiated amino acids were injected into the basal nucleus for the purpose of studying its efferent connections. As a result labeled axons could be seen leaving the basal nucleus and entering the external capsule (Fig. 6), passing through all the layers of large areas of the neocortex. They were also visible in several parts of the midbrain reticular formation. A detailed description by means of the autoradiographic method and the results obtained will be a subject of a separate report (Jones, Juraniec).

DISCUSSION

Following the above described lesions of the peripeduncular nucleus itself or its fibers degenerating axon terminals were found in the basal nucleus. These results agree with the observations of Jones et al. (1976) and others (Norgren, 1976; Leichnetz,. Astruc, 1977), that the basal nucleus receives afferent connections from the peripeduncular nucleus. In electron microscopic studies using the degenerative method we found that there was a small number of degenerating axon terminals in the basal nucleus. They were in contact with dendritic spines or larger dendrites or even with the perikarya of large cells. The appearance of the degeneration corresponds to the dark type of degeneration and does not seem to differ from that seen in other parts of brain (Grofová, Rinvik, 1970; Jones, Powell, 1970; Juraniec et al., 1974). Such endings usually contain spherical vesicles and make synaptic contacts of an asymmetrical type (Gray, 1959; Colonnier, 1968). They are probably excitatory in nature (Uchizono, 1965; Walberg, 1968; Gray, 1969).

Our autoradiographic studies after injections of tritiated proline and leucine into the basal nucleus showed that this nucleus has a widespread projection to large areas of the neocortex. Our studies confirmed the results obtained by other authors. Labeled cells were revealed in the basal nucleus after Kievit's and Kuypers' (1975a, b) injections of horseradish peroxidase into the frontal and parietal cortex as well as after Winfield's et al. (1975) injections into the occipital cortex. Whereas Jones et al., (1976) received similar results after injections into the postcentral gyrus. On the other hand, according to Nauta and Mehler (1966) the basal nucleus projects to the lateral habenular nucleus.

The results of our investigations presented and discussed above confirm the existence of afferent connections of the basal nucleus with the peripeduncular nucleus and efferent connections of this nucleus with large areas of neocortex.

REFERENCES

1. Colonnier M.: Synaptic patterns on different cell types in the different laminae of the visual cortex. An electron microscope study. Brain Res., 1968, 9, 268—287.
2. Cowan W. M., Gottlieb D. I., Hendrickson A. E., Price J. L., Woolsey T. A.: The autoradiographic demonstration of axonal connections in the central nervous system. Brain Res., 1972, 37, 21—52.
3. Divac I.: Magnocellular nuclei of the basal forebrain project to neocortex, brain stem, and olfactory bull. Review of some functional correlates. Brain Res., 1975, 93, 385—398.
4. Emmers R., Akert K.: A stereotaxic atlas of the brain of the squirrel monkey (Saimiri Sciureus). University of Wisconsin Press, Madisson, Wisconsin 1963.

5. Gorry J. D.: Studies on the comparative anatomy of the ganglion basale of Meynert. Acta Anat., 1963, 53, 268—275.
6. Gray E. G.: Axo-somatic and axo-dendritic synapses in the cerebral cortex: an electron microscopic study. J. Anat. (Lond.), 1959, 93, 420—433.
7. Gray E. G.: Electron microscopy of excitatory and inhibitory synapses: a brief review. Progr. Brain Res., 1969, 31, 141—155.
8. Grofová I., Rinvik E.: An experimental electron microscopic study on the striatonigral projection in the cat. Exp. Brain Res., 1970, 11, 249—262.
9. Jones E. G., Burton H., Saper C. B., Swanson L. W.: Midbrain, diencephalon and cortical relationships of the basal nucleus of Meynert and associated structures in primates. J. Comp. Neurol., 1976, 167, 385—420.
10. Jones E. G., Powell T. P. S.: An electron microscopic study of terminal degeneration in the neocortex of the cat. Phil. Trans. Roy. Soc. Lond., 1970, 257, 29—43.
11. Juraniec J.: Basal nucleus of Meynert. Folia Morphol., 1979, 38, 217—225.
12. Juraniec J., Narkiewicz O., Wrzołkowa T.: Changes in axon terminals of the claustrum following cortical lesions — electron microscopic investigations. Neuropat. Pol., 1974, 12, 1—11.
13 Kievit J., Kuypers H. G. J. M.: Basal forebrain and hypothalamic connections to the frontal and parietal cortex in the rhesus monkey. Science, 1975 a, 187, 660—662.
14. Kievit J., Kuypers H. G. J. M.: Subcortical afferents to the frontal lobe in the rhesus monkey studied by means of retrograde horseradish peroxidase transport. Brain Res., 1975 b, 85, 261—266.
15. Kodama S.: Pathologisch-anatomische Untersuchungen mit Bezug auf die sogenannten Basalganglien und ihre Adnexe. Neurol. Psychar. Abh. (Schweiz. Arch. Neurol. Psychiol.), 1929, 8, 1—206.
16. Leichnetz G. R., Astruc J.: The course of some prefrontal corticofugals to the pallidum, substantia innominata, and amygdaloid complex in monkeys. Exp. Neurol., 1977, 54, 104—109.
17. Nauta W. J. H., Mehler W. R.: Projections from the lentiform nuclei in the monkey. Brain Res., 1966, 1, 1—38.
18. Norgren R.: Gustatory afferents to ventral forebrain. Brain Res., 1974, 81, 285—295.
19. Ogren M., Hendrickson A.: Pathways between striate cortex and subcortical regions in Macaca mulatta and Saimiri sciureus: evidence for a reciprocal pulvinar connection. Exp. Neurol., 1976, 53, 780—800.
20. Uchizono K.: Characteristics of excitatory and inhibitory synapses in the central nervous system of the cat. Nature (Lond.), 1965, 207, 642—643.
21. Walberg F.: Axoaxonic contacts in the cuneate nucleus, probable basis for presynaptic depolarization. Exp. Neurol., 1965, 13, 218—231.

Author's address: Dr. med. Jolanta Juraniec, Department of Anatomy, Institute of Medical Biology, School of Medicine, 1 Dębinki Str., 80—211 Gdańsk, Poland

c.d. ze s. 136

Prezydent:	— Dr T. Yonezawa
Wiceprezydénci:	— Dr K. Jellinger
	Dr H. de F. Webster
	Dr Y. Olsson
	Dr R. Terry
Sekretarz Generalny:	— Dr J. H. Adams
Skarbnik:	— Dr J. Ulrich
Członkowie:	— Dr S. Aronson
	Dr E. Reske-Nielsen
	Dr S. Brion
	Dr. J. Escalona
	Dr G. Kreutzberg
	Dr S. Ludwin

Na członków honorowych wybrano następujące osoby:
— Dr J. Gruner (Francja)
— Dr I. Környey (Węgry)
— Dr W. Krücke (RFN)
— Dr H. M. Zimmerman (USA)

*

W 1981 r. tematyka kolejnych posiedzeń Stowarzyszenia Neuropatologów Polskich była następująca:

Posiedzenie Nr 1 — 30 stycznia 1981 r.
B. Zgorzalewicz, V. Neuhoff (Klinika Neurologii AM, Poznań i Forschungstelle für Neurochemie, Max Planck Institut, Getynga) — Białka i glikoproteiny nerwu wzrokowego w rozwoju ontogenetycznym królika.
L. Dydyk, J. Borowicz (Pracownia Ultrastruktury Układu Nerwowego CMD i K PAN, Warszawa) — Ultrastructura rdzeniaka u dzieci.

Posiedzenie Nr 2 — 27 lutego 1981 r.
D. Wierzbicka, L. Szemis, M. Koziak, J. Kulczycki (Zakład Neuropatologii i I Klinika Neurologii Instytutu Psychoneurologicznego, Warszawa) — Przypadek raka tarczycy (guz Hürtlera) z przerzutami do układu nerwowego.
A. Goncerzewicz, R. Madrid, H. Wiśniewski (Klinika Neurologii AM, Poznań i Institute for Basic Research in Mental Retardation, Staten Island, USA) — Aktywność biologiczna makrofagów jako czynnik patogenetyczny w nawracającym doświadczalnym alergicznym zapaleniu mózgu i rdzenia.

Posiedzenie Nr 3 — 28 marca 1981 r.
M. Dąmbska, D. Maślińska (Pracownia Neuropatologii Rozwojowej CMD i K PAN, Warszawa) — Wpływ dichlorfosu na mózg królika w różnych okresach rozwoju.
J. Dąbrowska, P. Olejniczak (Klinika Neurologii AM, Wrocław) — Naczyniopochodne uszkodzenie pnia mózgu pod postacią „ocular bobbing, locked in syndrome".

Posiedzenie Nr 4 — 14—16 kwietnia 1981 r. — V Krajowa Konferencja Neuropatologiczna, Szczecin.

c.d. na s. 174

NEUROPAT. POL., 1982, 20, 1—2
PL ISSN 0028—3894

ROLF WARZOK, HILTRUD WARZOK

THE INFLUENCE OF HYPOXIA ON THE INDUCTION OF EXPERIMENTAL BRAIN TUMORS IN RATS

Institute of General Pathology and Pathological Anatomy of the Medical Academy, Erfurt

In recent years, by means of animal experimentation it has been demonstrated that brain tumors can be induced by application of resorptive chemical carcinogens. These results proved to be of major importance and led to a completely new understanding of possible external influences in the development of CNS neoplasms (Jänisch, Schreiber, 1969; Warzok, 1973; Jänisch et al., 1976). However, our knowledge concerning factors which could play a role in the etiology of brain tumors in man is still rather more incomplete than in many other types of tumors.

In connection with this, we performed a number of experiments to find out whether the induction of brain tumors in rats can be influenced by such factors as hormonal imbalance (Schreiber et al., 1973; Batka et al., 1977) and hypoxia. In the present experiments, we investigated the effect of hypoxia on the development of brain tumors induced by N-methyl-N-nitrosourea (MNU) in rats.

MATERIAL AND METHODS

Hundred hooded rats of the inbred strain E were used. MNU was dissolved in phosphate-buffered saline (pH 4.3) and injected intravenously. In the first group, 50 rats received 18 injections of 10 mg/kg b.w. MNU in intervals of two weeks. In the second one, the left carotid artery was ligated twice and dissected in between. As a result a left-sided permanent Horner's syndrome occurred. In an exsiccator of 10 litres these rats were exposed to an oxygen concentration of 9.5% and immediately afterwards received the carcinogen application. The animals died naturally or were killed when moribund. A complete autopsy was performed including the preparation of major nerve roots and spinal cord. Three to five frontal sections of the brain, 10 slices of the spinal

cord as well as specimens of all tumor bearing organs were embedded in paraffin and stained with hematoxylin and eosin. In the second group the brain was dissected and each half was cut separately. Confidence intervals were determined for the statistical investigation (Weber, 1967).

RESULTS

Five animals died before the 97th day of the experiment and were excluded from the analysis. Out of 95 rats 80 animals developed 138 tumors of different organs. In 73 cases (76.7%) the neoplasms were located in the central nervous system. Tables 1 and 2 show the frequency of neurogenic tumors and their localization in both groups. Differences found in both groups are statistically not significant. In the second group 14 CNS tumors were found in the right and 15 in the left half of the brain. In 6 cases tumors occurred in midline structures or infiltrated both hemispheres. Tumors were classified as glioblastomas (11),

Table 1. Number of rats with tumors of the central nervous system

Group	Number of rats with CNS tumors		
	absolute	in %	multiple tumors
I	41	85.4	12
II	32	68.1	15
Total	73	76.7	27

Table 2. Localization of 109 neurogenic tumors

Group	Localization of tumors		
	brain	spinal cord	nerve roots and peripheral nerves
I	43	6	9
II	35	6	10
Total	78	12	19

astrocytomas (22), oligodendrogliomas (21), sarcomas (25), gliosarcomas (5), mixed gliomas (1) and neurinomas (19). Five neoplasms remained unclassified. The mean latency period of neurogenic tumors showed no significant differences, neither between both experimental groups as a whole (group I — 248 days, group II — 256 days) nor between single histological tumor types.

DISCUSSION

It is a well established fact that in man the tumor spectrum of the central nervous system depends largely on the age. Ependymomas and medulloblastomas, for instance, are typical childhood tumors, whereas meningiomas and glioblastomas occur mostly in older patients. In connection with this, it seems possible that vascular disturbances frequently observed in older age could influence the incidence of one or other types of growths.

In rats, after a ligation of one carotid artery the blood supply of the corresponding site goes predominantly via the anterior cerebral artery (Colmant, 1965). With the aid of light microscopy, Colmant (1965) could not find hypoxic brain damage after a simple ligation of the carotid artery. Such changes occurred only after an additional reduction of the oxygen concentration and were always limited to the side of ligation. Spataro (1966) used the combined effect of diminution of oxygen concentration in the breathing air and ligation of the carotid artery for investigation of the hypoxic brain damage and found necroses of the nerve and microglial cells, edema, and reduction of lysosomes. The activities of acid phosphatase, succinic dehydrogenase and DPNH diaphorase were also diminished.

In our experiments, which were planned as a pilot study we observed no hints favouring the idea that under experimental conditions the development of brain tumors is influenced by hypoxia. Therefore, it seems to be likely that vascular disturbances do not influence the spectrum of brain tumors in man.

Meanwhile, we were able to demonstrate that there are substantial differences concerning the incidence as well as the spectrum of brain tumors after transplacental and postnatal application of certain chemical carcinogens (Warzok et al., 1977; 1978). At various stages of the development of brain in rats there appeared a typical sensitivity to chemical carcinogens and a specific spectrum of tumors developed. In this connection it seemed to be possible that the different sensitivity of brain structures in prenatal and postnatal life might also be responsible for the typical spectrum of tumors at different ages in man.

REFERENCES

1. Batka H., Warzok R., Scholtze P.: Der Einfluss von Prednisolut auf die Induktion neurogener Tumoren mit N-Methyl-N-nitrosoharnstoff bai Ratten. Zbl. allg. Path., 1977, 121, 76—81.
2. Colmant H. J.: Zerebrale Hypoxie. G. Thieme, Stuttgart, 1965.
3. Jänisch W., Güthert H., Schreiber D.: Pathologie der Tumoren des Zentralnervensystems. VEB, G. Fischer, Jena 1976.
4. Jänisch W., Schreiber D.: Experimentelle Geschwülste des Zentralnervensystems. VEB, G. Fischer, Jena 1969.

5. Schreiber D., Batka H., Lageman A.: Hormonelle Störungen und Geschwulstentwicklung im Zentralnervensystem. Experimentelle Untersuchungen an Ratten. Zbl. allg. Path., 1973, 117, 180—184.
6. Spataro J.: Anoxic ischemic encephalopathy of the rat brain. Exp. Neurol., 1966, 16, 238—246.
7. Warzok R.: Experimentelle Geschwülste des Zentralnervensystems der Ratte — Morphologie, biologische Wertigkeit und präventivonkologische Bedeutung. Promotion B (Habil.-Schrift), Erfurt 1973.
8. Warzok R., Thust R., Schneider J.: Transplazentare kanzerogene Wirkung von Äthylnitrosoharnstoff bei verschiedenen Tierarten. Zbl. allg. Path., 1977, 121, 273.
9. Warzok R., Schreiber D., Schneider J., Batka H., Scholtze P.: Transplazentare Erzeugung experimenteller Hirntumoren und ihre Relevanz für die Genese der ZNS Geschwülste des Menschen. Erg. exp. Med., 1978.
10. Weber E.: Grundriss der biologischen Statistik. 6. Aufl. VEB, G. Fischer, Jena 1967.

Authors' address: Doz. Dr. sc. med. R. Warzok, Pathologisches Institut, Medizinische Akademie Erfurt, DDR 50 Erfurt.

NEUROPAT. POL., 1982, 20, 1—2
PL ISSN 0028—3894

JANUSZ SZYMAŚ, WIESŁAWA BICZYSKO, PRZEMYSŁAW GABRYEL, HRISTO PROKOPANOW

HISTOLOGICAL FEATURES OF MENINGIOMAS WITH THEIR ULTRASTRUCTURAL ASPECTS

Department of Pathological Anatomy, School of Medicine, Poznań

The study of histogenesis of meningiomas permits to form an opinion about congenerous derivation of these tumors from arachnoid cells, particularly those covering arachnoid villi (Rubinstein, 1972). The identity of meningioma cells and arachnoid cells was determined on the basis of biochemical studies of fatty acids (Stein et al., 1963) and gangliosides (Sunder-Plassmann, Bernheimer, 1974). The quality and quantity of these substances are identical in both the cell types but different in dura mater. The comparative electron microscopic studies of meningiomas and arachnoid cells also confirmed the identity of both these cell types (Guseck, 1962; Ishida et al., 1964). Histological features of arachnoid inflammatory tumors are similar in both human (Jänisch et al., 1976) and experimental meningiomas (Naumenko, 1967).

Derivation of meninges in the embriogenesis is regarded as neuroectodermal (Napolitano et al., 1964; Jänisch et al., 1976). The neuroectodermal origin of meningiomas is postulated on the basis of the similarity between meningothelial cells in tumors and arachnoid cells (Guseck, 1962; Ishida et al., 1964).

Mesodermal origin of these tumors has been postulated on the basis of the similarity between fibroblasts and tumor cells (Kepes, 1961; 1962; Nyström, 1962); both of them synthetizing collagen fibers. Another group of authors (Chominskij, 1958) stressed the multipotential capacity of meningothelial cells and tried to connect both hypotheses in one.

On the basis of the histological examination four subtypes of meningiomas are distinguished: meningotheliomatous, fibrous, transitional (or mixed) and angioblastic (WHO, 1976). Angioblastic meningioma is now under discussion (Müller, Mealey, 1971; Popoff et al., 1974) and will not be presented in this paper. Ultrastructural study of meningotheliomatous and fibrous meningioma were essential for hypothesis on the morphogenesis of those tumors.

Having a large collection of meningiomas in our Institute we decided to discuss some aspects of the histogenesis of these tumors.

MATERIAL AND METHODS

The material obtained during surgical procedure carried out in 13 patients was used for electron microscopy studies. The tissue samples were taken from different areas of each tumor immediately after its removal from the cranial cavity. They were fixed in Karnovsky solution (1965) and postfixed in osmium tetroxide, then dehydrated and embedded in Epon resin. Semithin and ultrathin sections were cut with ultramicrotom OmU_3. Semithin sections were stained with toluidine blue, ultrathin ones were counter stained with uranyl acetate and lead citrate. Electron microscopic pictures were made in JEM 7A microscope.

For light microscopy the material was fixed in 4% calcium formalin and after dehydration, embedded in paraffin. Paraffin sections were stained with hematoxylin and eosin, PTAH method and impregnated according to Tibor-Pap's and Cajal's methods. The basing data concerning the material used for study are summarized in Table 1.

Table 1. Localization and subtypes of meningiomas

Case number	Age (in years)	Sex	Site	Subtype of meningioma
1	24	F	parasagittal, parietal (bilateral)	meningotheliomatous
2	50	M	frontal left	meningotheliomatous
3	49	F	frontal left	meningotheliomatous
4	45	F	temporo-parietal left	meningotheliomatous
5	52	F	frontal left	meningotheliomatous
6	59	M	frontal left	meningotheliomatous
7	40	F	frontobasal	meningotheliomatous
8	52	F	temporal left	meningotheliomatous
9	27	M	frontobasal	transitional
10	30	M	frontal right	transitional
11	64	M	temporal left	transitional
12	18	F	lateral ventricle	fibrous
13	50	F	sphenoid, en plaque	fibrous

RESULTS

The light microscopic study allowed the classification of the material into typical groups according to the predominance of meningotheliomatous or fibrous components. Only three cases were classified as transitional meningioma (Table 1). One of the fibrous subtype of meningiomas with intraventrical location had heavy fibroblastic components, but in all tumors islands of meningothelial cells were observed (Fig. 1a, b).

In the electron microscopic study in all tumors, groups of cells with

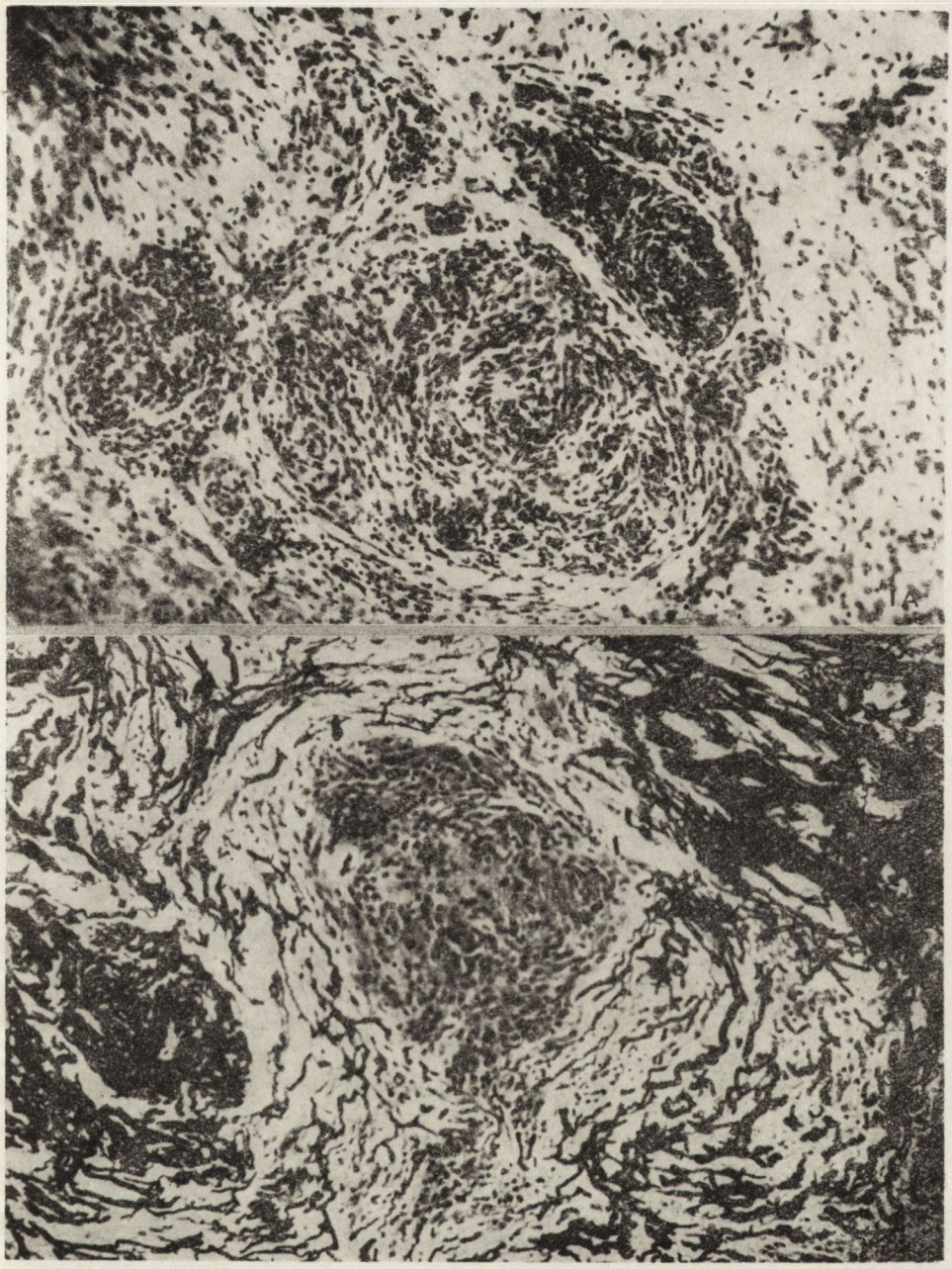

Fig. 1. Meningothelial cell groups between heavy fibroblastic components. a) H—E. × 100; b) Gomori. × 100

meningotheliomatous and fibroblastic features were mixed together. A high consistence between light and electron microscopic observations with regard to the classification and predominance of each cell population is worthy of noting.

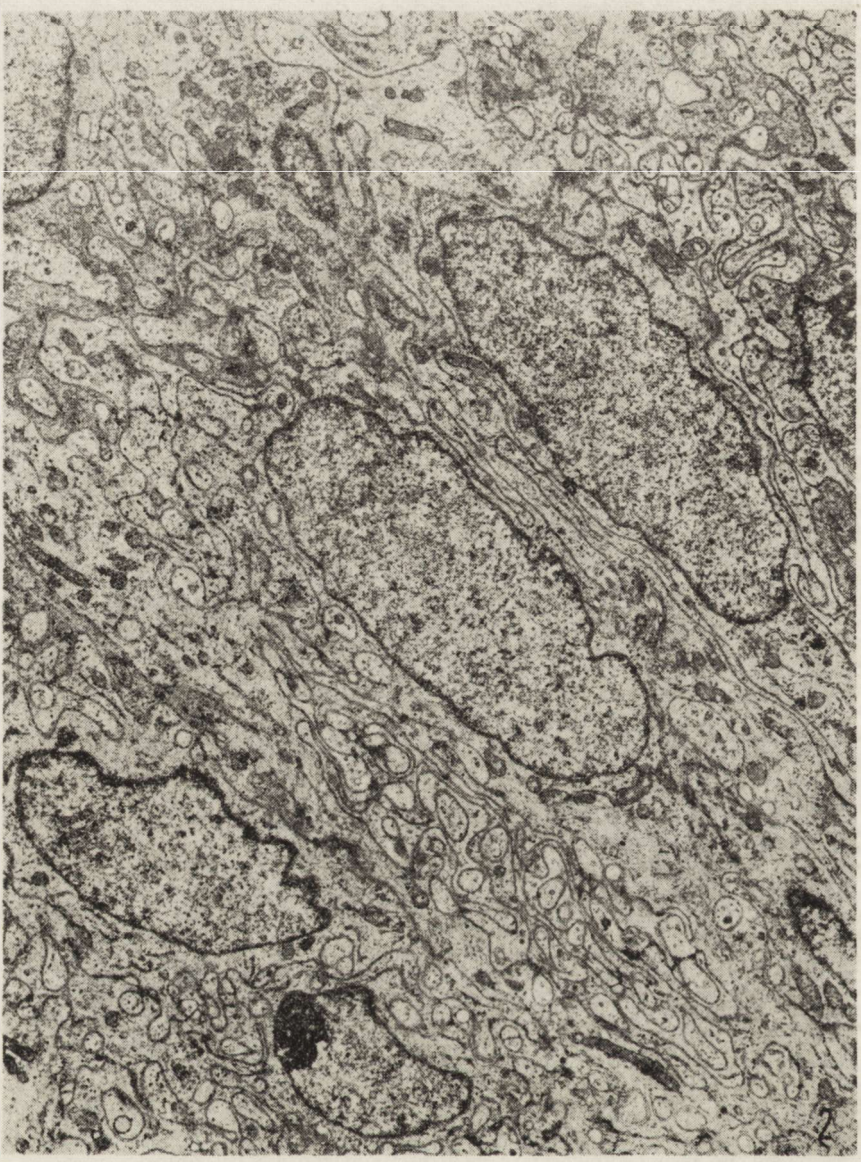

Fig. 2. Typical electron microscope picture of meningothelial cells area. × 6 000

Meningotheliomatous areas were composed of cells with large cytoplasm, loosely arranged (Fig. 2). Oval or round nuclei were rich in euchromatin; heterochromatin formed only a narrow rim beneath nuclear envelope. Perichromatin granules were spread in euchromatin territory and on the border line of hetero- and euchromatin. Nucleoli had four typical components. Nuclei envelope formed few invaginations in the cytoplasm territory. The space between the leaflets of the nuclear envelope was narrow. Regular nuclear pores were seen. The cytoplasm

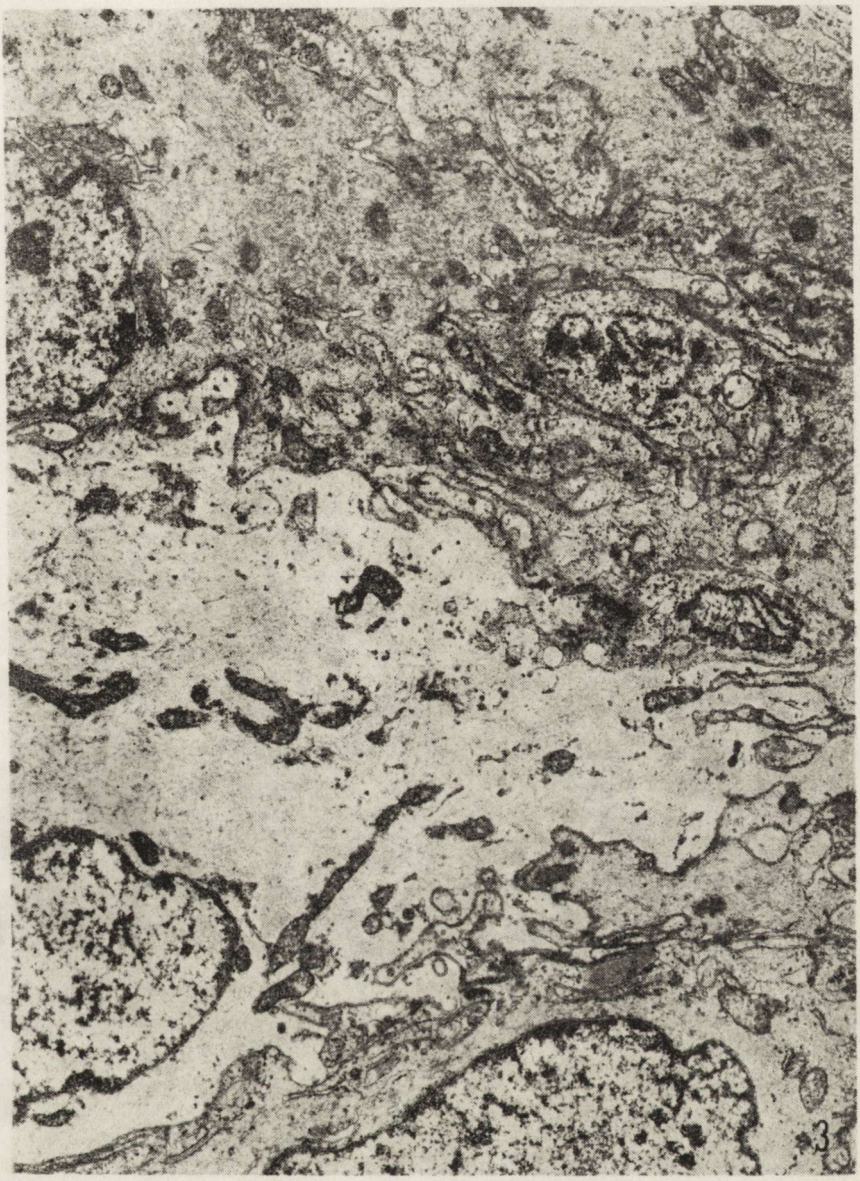

Fig. 3. Area of meningothelial cells. Different number of filaments in neighbouring cells. × 7 500

contained few rough reticulum channels and Golgi areas in perinuclear space and polirybosomes and mitochondria spread through the cytoplasm. Mitochondria contained dark matrix and short cristae. Occasionally a few lipid droplets in the cytoplasm were present. Typical of these cells were delicate filaments in the cytoplasm. The amount of filaments in meningothelial cells varied (Fig. 3). Cell membrane formed numerous processes. Desmosome-like structures between cell processes

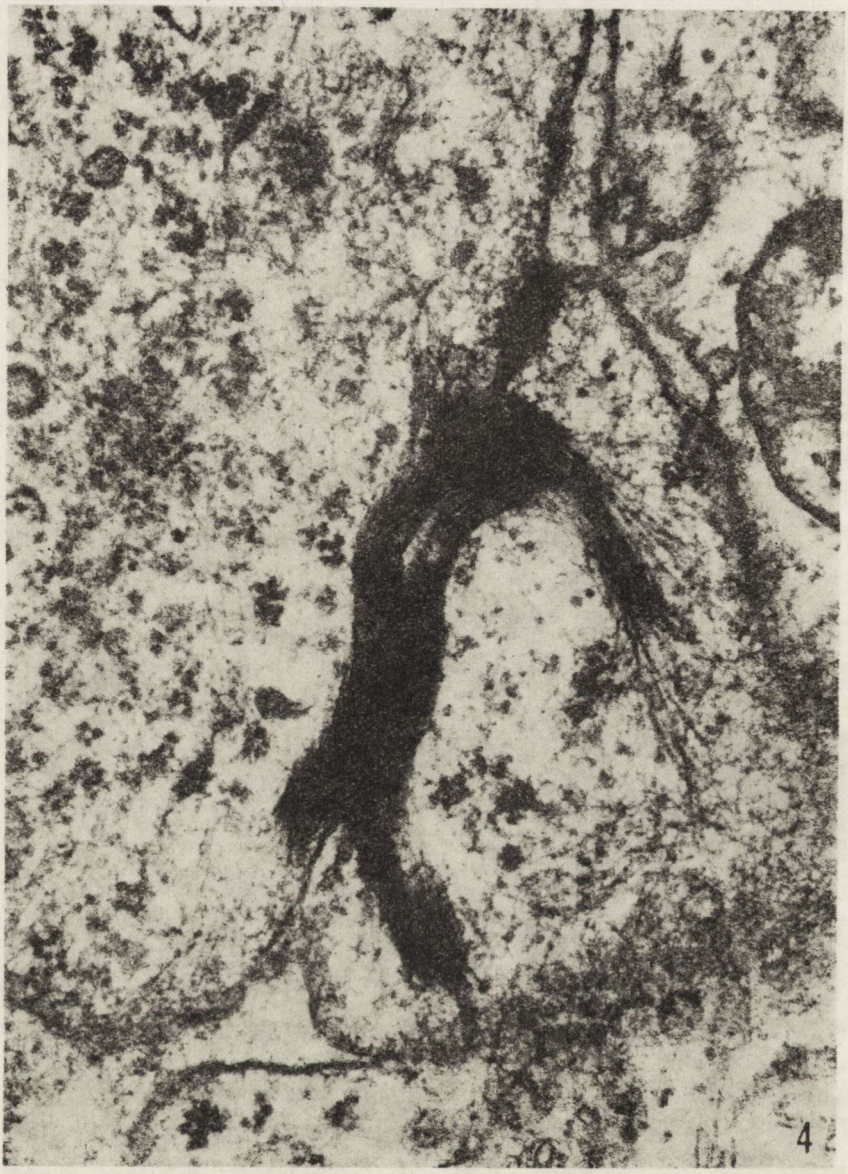

Fig. 4. Area of meningothelial cells. Desmosome like structure between cell processes. × 78 700

were present (Fig. 4). Occasionally cilia in the intracellular space were visible. Intercellular space between meningothelial-like cells was narrow. There were cytoplasmic organelles lying in the enlarged intercellular spaces in the areas of tumor cells disintegration.

Between meningotheliomatous cells a few astrocyte-like cells were present. Electron microscopic feature was characteristic of this cell line (Fig. 5). These criteria were: regular nuclei with heterochromatin

Fig. 5. Astrocyte-like cell in an area of meningothelial cells. × 17 500

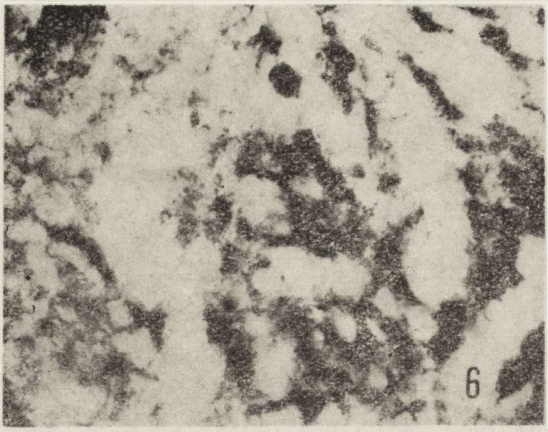

Fig. 6. Focus of astrocyte-like cells in meningioma. Cajal. × 400.

Fig. 7. Area of fibroblast-like cells. Broad intercellular spaces. × 6 100.

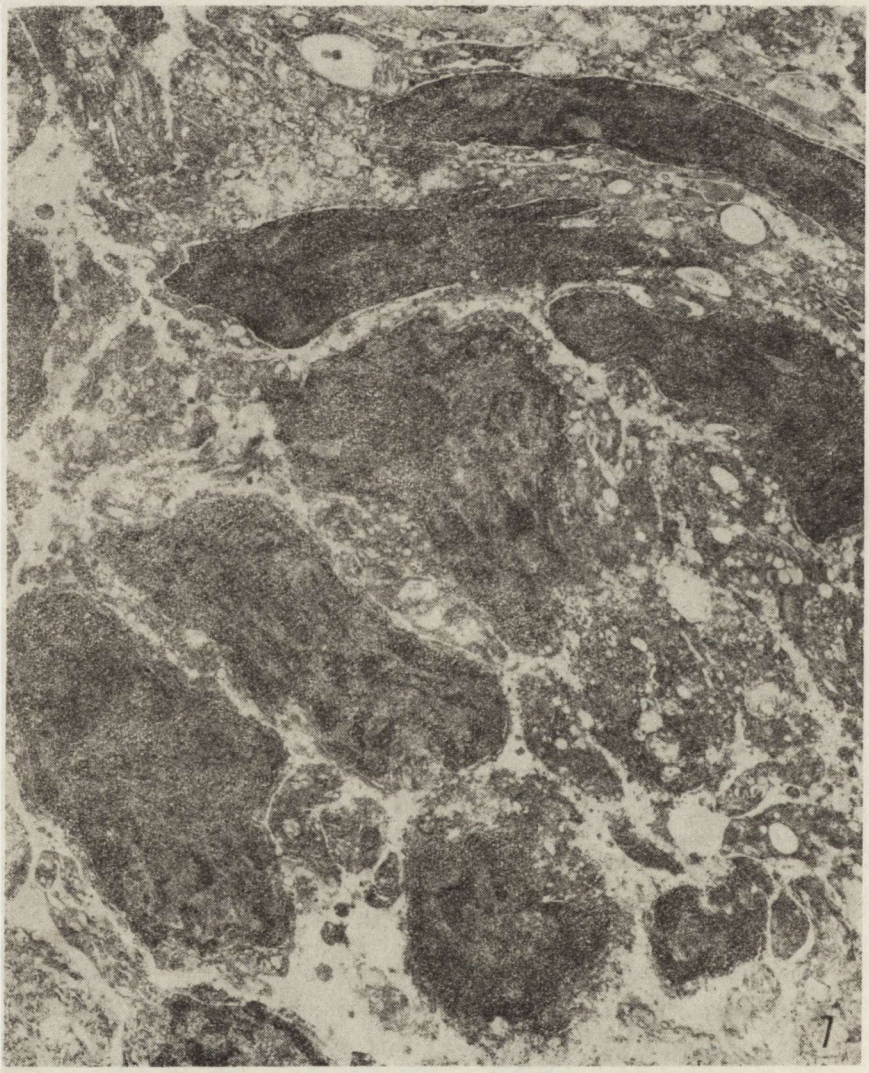

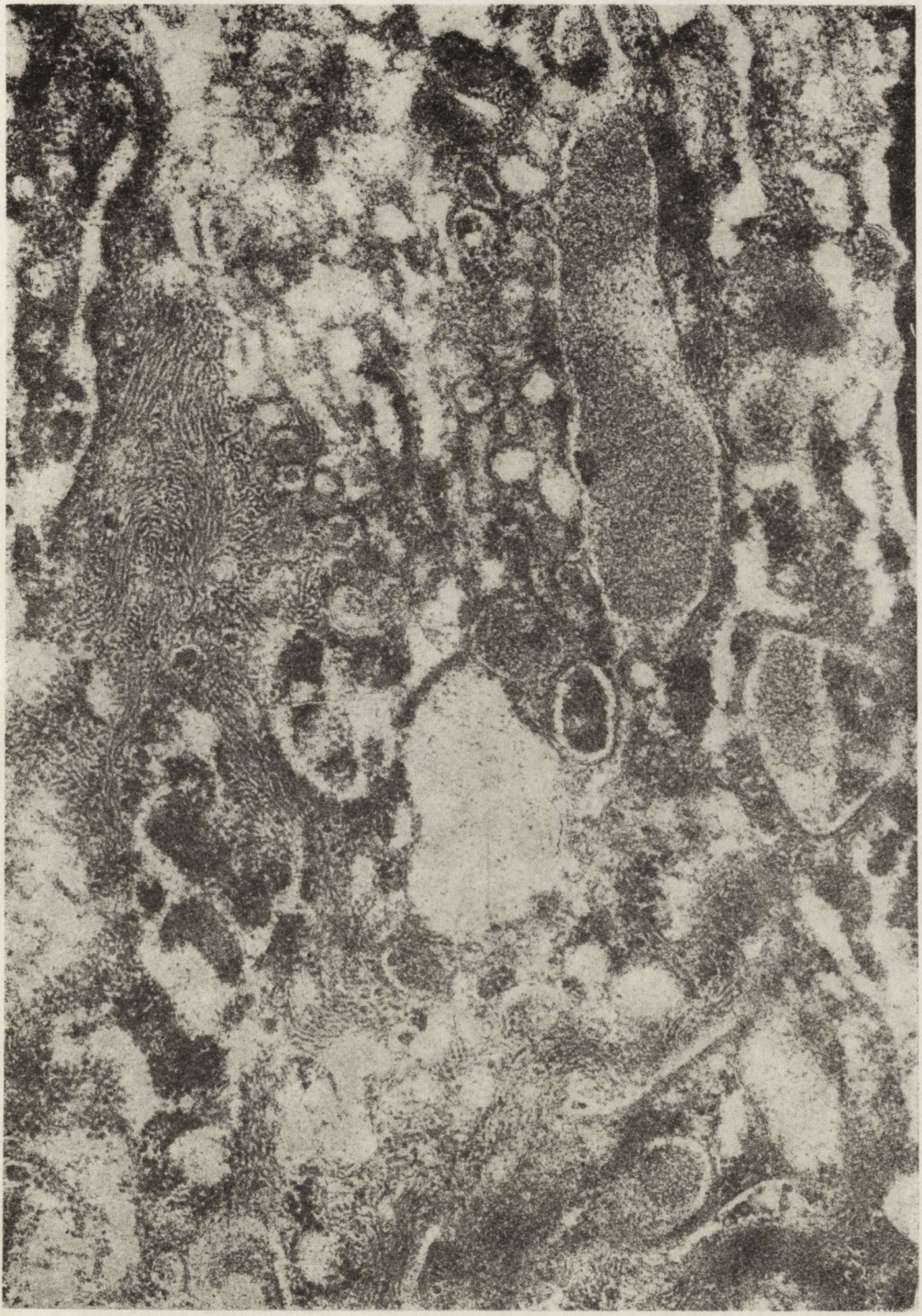

Fig. 8. Area of fibroblast-like cells. Cytoplasm of cells contains large amount of rough endoplasmic reticulum channels, synthetizing fibrillary material. × 61 500

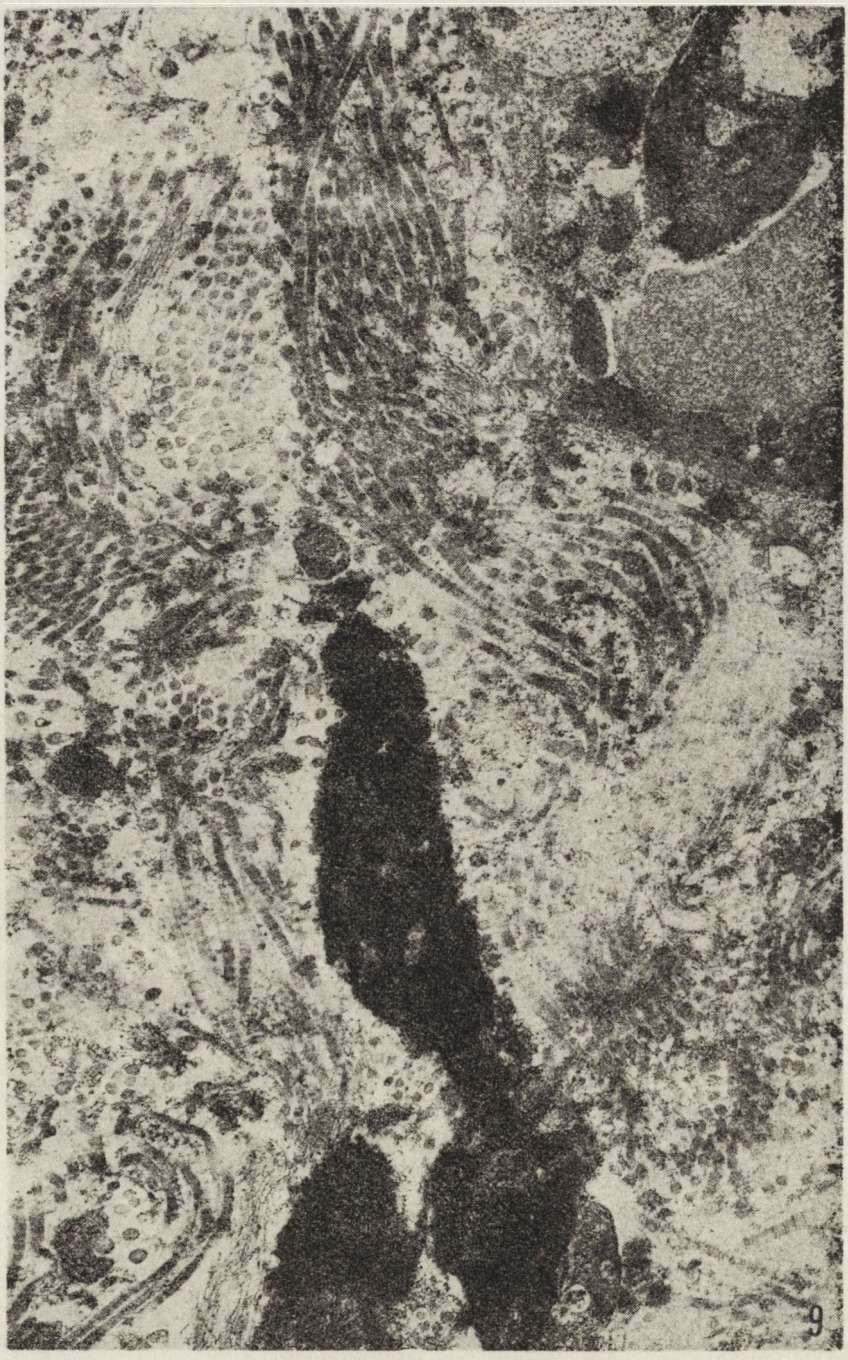

Fig. 9. Area of fibroblast-like cells. Disintegration of cell cytoplasm is visible. Remnants of fibroblast nuclei are surrounded by collagen fibers. × 26 250

Fig. 10. A few meningothelial cell processes lying in broad areas built with fibroblast. Basement membrane-like structures are not present. × 5 750

marginated under nuclear envelope in the typical amount; the regular nuclear envelope with a narrow space between its two leaflets; the channels of rough endoplasmic reticulum and polyribosomes aggregated mainly in perinuclear areas and a few in processes; Golgi areas and smooth endoplasmic reticulum in perinuclear areas; glial filaments regularly distributed through the cytoplasm as well as the processes of

cells. Confirmation of these findings were made by light microscopy with Cajal methods (Fig. 6).

Areas of fibroblast-like cells contained large amount of precollagen and collagen fibers and proteoglicans lying in the broad intracellular spaces (Fig. 7). Cytoplasm of fibroblast cells contained a large amount of rough endoplasmic reticulum channels, all of them synthetizing fibrillar material, probably of precollagen nature. This fibrillar material crossed through partialy disintegrated cell membrane (Fig. 8). A highly suggestive picture was obtained in the areas where fibers lying in cytoplasm were smooth and their parts lying in the intercellular space had characteristic stratations. Disintegration of fibroblasts during the production of fibers was also visible. On some electron microscopic pictures, remnants of fibroblast nuclei were surrounded by collagen fibers (Fig. 9).

Some meningothelial cells lay in broad areas built by fibroblasts in fibrous meningiomas (Fig. 10). In these areas basement membrane-like structures between meningothelial and fibrous cells were not present.

In the perivascular space, basement membrane was frequently disrupted. Beyond the examined areas blood capillaries had no continuous endothelial layers. Gap junctions, fenestrations and lack of endothelial cells as well as sinusoid-like capillaries were visible. Perivascular spaces were broad and contained collagen fibers and pericytes.

DISCUSSION

In the meningotheliomatous areas of meningiomas we observed similarly to other authors, a typical feature of this neoplasm (Luse, 1960; Napolitano et al., 1964; Cervós-Navarro, 1967; Cervos-Navarro, Vazquez, 1969; Woyke et al., 1971; Jänisch et al., 1976).

The existence of astrocyte-like cells among meningotheliomatous cells of meningioma was surprising. A similar observation was made by Zülch (1956), with the impregnation technique according to Cajal, in a meningioma-like tumor of dura mater. Heterotopic glial foci in dura mater were found in brain of fetuses with developmental disturbances (Hrabowska, Kozłowski, 1975). This may also be a point for discussion for the still controversial subject of a mixed tumor such as meningioma and glioma (Henry, Leestma, 1973). On the other hand the existence of a mixed tumor can be explained on the basis of common derivation from neuroectodermal tube of glial as well as arachnoid cells.

The most interesting among microscopic features of meningiomas was the coexistence of meningotheliomatous and fibrous components occurring in all cases investigated by electron microscopy. The fibrous component consisted of fibroblasts and wide areas of collagenosis. These fibroblasts had a prominent rough endoplasmic reticulum and only

a few polyribosomes. All cells were filled with precollagen fibers, which crossed through the cell membrane and caused its disintegration. There were only few young fibroblasts. This morphological feature seems to suggest, that the fibrous component is only a form of reaction, like that for example in chronic inflammation (Wierzbicka, Biczysko, 1977; Łukaszewski, 1977). This may suggest the stimulation of fibroblastic component growth by a not yet identified factor, similar to that which stimulates the growth of capillaries in neoplasm and is called "tumor angiogenesis factor" (Folkman, Klagsbrun, 1975).

In recapitulating one can say, that all meningiomas, except the angioblastic subtype, are meningotheliomatous meningiomas and derive from arachnoid cells. Differences in histological features result from a different reaction of connective tissue on the presence of meningothelial neoplastic cells.

Meningotheliomatous meningioma has only scanty fibrous stroma, which is confined to trabecule that divides the tumor into distinct lobules. The transitional subtype has steady growth of meningothelial cells and connective tissue elements. The most distinctive feature of the fibroblastic meningioma is the presence of a prominent part of stroma, that separates the individual meningotheliomatous cells.

REFERENCES

1. Cervós-Navarro J.: Zur Feinstruktur endotheliomatöser Meningeome des Menschen. Acta neuropath. (Berl.), 1967, 8, 141—148.
2. Cervós-Navarro J., Vazquez J. J.: A microscopic study of meningiomas. Acta neuropath. (Berl.), 1969, 13, 301—323.
3. Chominskij B. S.: Patomorfołogija i klassifikacija. Meningeoma (arachnoidethelioma). Arch. Patol., 1958, 20, 3—20.
4. Folkman J., Klagsbrun M.: Tumor angiogenesis: Effect on tumor growth and immunity. In: Fundamental Aspects of Neoplasia. Eds. A. A. Gottlieb, O. J. Plescia, D. H. L. Bioshop. Springer. Berlin—Heidelberg—New York 1975.
5. Guseck W.: Submikroskopische Untersuchungen als Beitrag zur Struktur und Onkologie der Meningiome. Beitr. Path. Anat., 1962, 127, 274—326.
6. Henry J. M., Leestma J. E.: Astrocytoma arising in meningeal fibrosarcoma. Acta neuropath. (Berl.), 1973, 23, 334—337.
7. Hrabowska M., Kozłowski H.: Das histologische Bild der heterotopischen Gliaherde in Hirnmissbildungsfällen. Zbl. allg. Path., 1975, 119, 163—169.
8. Ishida Y., Kawai S., Sato S., Takayanagi T., Kawafuchi J. I.: Electron microscopy of meningothelial meningioma. Gunma J. Med. Sci., 1964, 13, 181—197.
9. Jänisch W., Güthert H., Schreiber D.: Pathologie der Tumoren des Zentralnervensystems. VEB, G. Fischer. Jena, 1976.
10. Karnovsky M.: A formaldehyde — glutaraldehyde fixative of high osmolality for use in electron microscopy. J. Cell Biology, 1965, 27, 137 A.
11. Kepes J.: Electron microscopic studies of meningiomas. Am. J. Path., 1961 39, 499—510.

12. Kepes J.: Observation on the formation of psammoma bodies and pseudopsammoma bodies in meningiomas. J. Neuropath. exp. Neurol., 1961, 20, 255—262.
13. Luse S. A.: Electron microscopic studies of brain tumors. Neurology, 1960, 10, 881—905.
14. Łukaszewski B.: Tenosynovitis nodularis jako problem kliniczny i anatomopatologiczny. Sprawozdanie z realizacji programu rządowego PR-6-0401.2-1976 (pierwszy etap).
15. Müller J., Mealey J. Jr.: The use of tissue culture in differentiation between angioblastic meningiomas and hemangiopericytoma. J. Neurosurg., 1971, 34, 341—348.
16. Napolitano L., Kyle R., Fischer F. R.: Ultrastructure of meningiomas and the derivation and nature of their cellular components. Cancer, 1964, 17, 233—241.
17. Naumenko V. I.: Arachnoidalnyje skoplenija w twardoj obołoczki mozga (eksperimentalnoje issljedowanie). Vopr. Neurochir., 1967, 31, 46—51.
18. Nyström S. H. M.: Fine structure of tumor stroma and blood vessel stroma in human supratentorial meningiomas. Nature, 1962, 194, 587—588.
19. Popoff N. A., Malinin T. I., Rosomoff H. L.: Fine structure of intracranial hemangiopericytoma and angiomatous meningioma. Cancer, 1974, 34, 1187—1197.
20. Rubinstein L. J.: Tumors of the central nervous system. Atlas of tumor pathology. Fascicle 6. Arm. Forces Institute of Pathology. Washington, 1972.
21. Stein A. A., Opalka E., Schilp A. O.: Fatty-acid analysis of meningiomas by gasphase chromatography. J. Neurosurg., 1963, 20, 435—438.
22. Sunder-Plassmann M., Bernheimer H.: Ganglioside in Meningioma und Hirnhäuten. Acta neuropath. (Berl.), 1974, 27, 289—297.
23. W. H. O.: Classification of the tumors of the central nervous system. Material of the Meeting of Investigators. WHO, Genewa 1976.
24. Woyke S., Domagała W., Olszewski W.: Some peculiar ultrastructural features of meningiomas. Pol. Med. J., 1971, 10, 975—1005.
25. Zülch K. J.: Biologie und Pathologie der Hirngeschwülste. Handbuch der Neurochirurgie. Vol. III. Springer. Berlin—Göttingen—Heidelberg 1956.

Authors' address: Department of Pathological Anatomy, School of Medicine, 49 Przybyszewski Str., 60—355 Poznań, Poland

NEUROPAT. POL., 1982, 20, 1—2
PL ISSN 0028—3894

JANUSZ ALWASIAK, GABRIELA HAJDUKIEWICZ, MICHAŁ KARASEK, KRYSTYNA MAREK, MARIAN MAJAK, WIELISŁAW PAPIERZ

SOME ASPECTS OF THE ULTRASTRUCTURE OF GLIOMAS *

Department of Oncology and Department of Pathological Anatomy, School of Medicine, Łódź

The aim of our study was to compare the ultrastructural pattern of glioblastomas with the pattern of anaplastic gliomas. Eight glioblastomas and 10 anaplastic gliomas were examined.

METHODS

Tissue for light microscopy was processed in the routine manner following fixation in formalin. Sections were stained with hematoxylin and eosin, phosphotungstic acid hematoxylin (PTAH) and according to Cajal's impregnation method. For electron microscopy within few minutes of tumor resection, small pieces of specimen were fixed in 5% glutaraldehyde. Tissue was kept in the fixative for 2 h, washed in 0.1 M sodium cacodylate buffer, pH 7.4, postfixed for 2 h in 1% OsO_4, washed again in buffer, dehydrated in a series of graded ethanols and embedded in Epon 812. Semithin sections were stained with toluidine blue. Ultrathin sections were cut from selected areas of the blocks, using an LKB ultrotome III, counterstained with uranyl acetate and lead citrate and examined in a JEM 100 B electron microscope.

RESULTS

Within the group of glioblastomas more or less distinct features of astrocytic differentiation were found in 4 cases. Both astrocytic and oligodendrocytic differentiation was presented in 3 cases. In only 1 case there was no tendency to any type of differentiation. As characteristic for astrocytic differentiation the occurrence of delicate intracytoplasmic fibrils (Fig. 1) collecting themselves into bundles as they pass into the

* The work was supported by Polish National Cancer Programme PR 6-04-01.

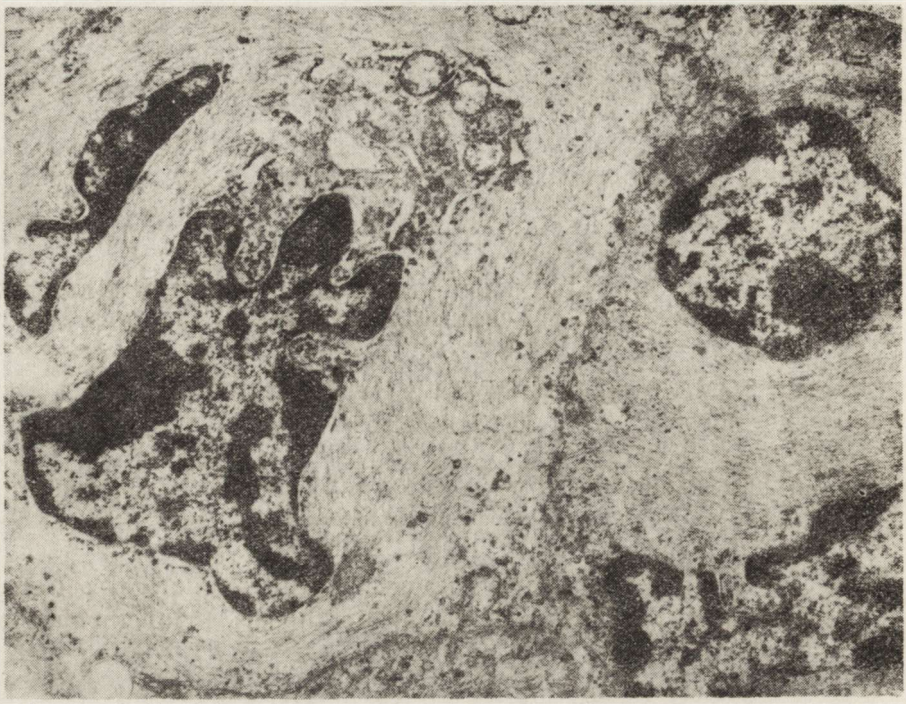

Fig. 1. Anaplastic astrocytoma (A-63). Abundant fibrils within the cytoplasm of cells. × 12 000

Fig. 2. Glioblastoma multiforme (A-58). The cell with features of oligodendroglial differentiation: numerous microtubules within the cytoplasm and membranous expansions of cell membrane. × 16 000

cellular processes was taken into consideration (Luse, 1960; 1961; Raimondi et al., 1962; Duffell et al., 1963). The differentiation toward oligodendroglia was based on the presence of numerous fine processes or membranous expansions of cell membranes (Fig. 2), large quantities of free ribosomes or ribosomal rosettes, numerous nuclear pores and light patches of otherwise dense chromatin adjacent to the pores and extensive cytoplasmic microtubules (Fig. 3) (Raimondi et al., 1962; Mori, Leblond, 1970).

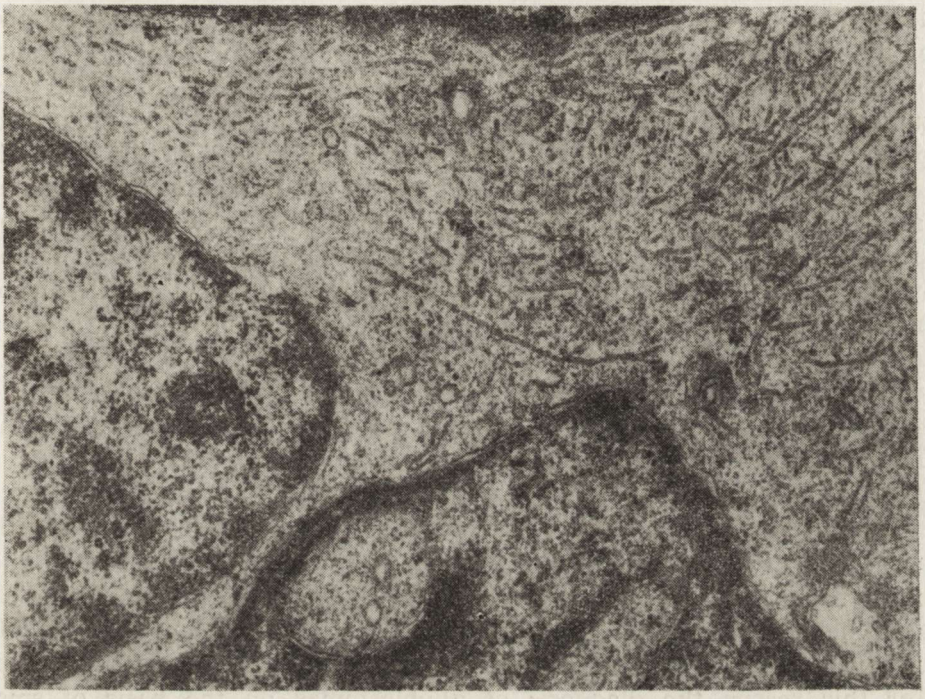

Fig. 3. Glioblastoma multiforme (A-58). Numerous microtubules within the cell cytoplasm. × 30 000

All examined anaplastic gliomas revealed morphological signs of differentiation toward either astroglia (5 cases), or oligodendroglia (1 case), or both (4 cases). It is worth noting that in this group of gliomas the amount of cells with astroglial differentiation was higher than in the group of glioblastoma similarly as the amount of gliofibrils within the cytoplasm of tumor cells.

DISCUSSION

Glioblastomas are the most common glial tumors and the most common primary intracranial neoplasms. Rubinstein (1972) feels that the majority of glioblastomas arise from anaplasia of smaller pre-existing astrocytomas. The elder pathologists were of similar opinion and these

neoplasms were placed in the old classification into the group of astrocytic tumors as the most malignant ones. Majority of patients with glioblastomas survive less than nine months and virtually all die within two years (Schochet, McCormick, 1976). However, aside from the typical glioblastoma there exists a form of astrocytoma that shows evident anaplastic features *de novo,* for which the term of malignant astrocytoma seems more appropriate. Microscopically these features fall short of the classic histologic picture of glioblastoma multiforme. They consist in increased cellularity, nuclear irregularity and hyperchromasia, occasional giant cells, vascular endothelial proliferation, and a variable number of mitotic figures (Rubinstein, 1972). In the "Classification of Tumours of the Central Nervous System", accepted by W.H.O. in 1976 these tumors are comprised to anaplastic (malignant) astrocytomas group. The prognosis in these neoplasms is not as invariably unfavorable as in the usual glioblastoma, which was placed to the group of "poorly differentiated and embryonal tumors". But only some of the tumor cells resemble small, poorly differentiated cells — glioblasts. "Others are predominantly glioblastomas with focal areas of recognizable astrocytoma, less commonly oligodendroglioma or, exceptionally, ependymoma. Any of these gliomas may in fact terminate as a glioblastoma" (W.H.O., 1976).

In our material the tumor cells of 7 glioblastomas (from total of 8 examined cases) were recognizable as the cells of astroglial line. These findings are in agreement with the opinion, that most cases of glioblastomas result probably from anaplasia of the pre-existing astrocytomas (Rubinstein, 1972). It seems, that the differences between the neoplastic astrocytic cells of anaplastic astrocytomas and those of glioblastomas are of the quantitative nature: the former contains more cells with signs of astroglial differentiation and the higher amount of gliofibrils. The peripheral parts of glioblastomas often appears less malignant. For this reason the diagnosis of glioblastomas on the basis of small biopsy specimen is often misleading (Schochet, McCormick, 1976). Similar aspects should be taken into consideration for minute specimens used for electron microscopical examination. So in routine diagnostic work light microscopy surpasses electron microscopy. However, the latter is sometimes necessary to explain the real nature of low differentiated tumors (Hirano, 1978) and answers very important question (for example primary or metastatic tumor). From time to time each of us is facing such difficult diagnostic problems. Therefore in modern neurooncological laboratory fixation of small pieces of each tumor tissue for ultrastructural studies seems to be necessary.

REFERENCES

1. Duffell D., Farber L., Chou S., Hartmann J., Nelson E.: Electron microscopic observations on astrocytomas. Am. J. Path., 1963, 43, 539—554.
2. Hirano A.: Some contributions of electron microscopy to the diagnosis of brain tumors. Acta Neuropath. (Berl.), 1978, 43, 119—128.
3. Luse S.: Electron microscopic studies of brain tumors. Neurology, 1960, 10, 881—905.
4. Luse S.: Ultrastructural characteristics of normal and neoplastic cells. Progr. exp. Tumor Res., 1961, 2, 1—35.
5. Mori S., Leblond C.: Electron microscopic identification of three classes of oligodendrocytes and a preliminary study of their proliferative activity in the corpus callosum of young rats. J. comp. Neurol., 1970, 139, 1—30.
6. Raimondi A., Mullan S., Evans J.: Human brain tumors: An electron microscopic study. J. Neurosurg., 1962, 19, 906—908.
7. Rubinstein L.: Tumors of the central nervous system. Atlas of tumor pathology. Second series. Fascicle 6. Armed Forces Institute of Pathology. Washington, 1972.
8. Schochet S., McCormick W.: Neuropathology. Case studies. Medical Examination Publishing. Flushing, N. Y. 1976.
9. W. H. O.: Histological Classification of Tumors of the CNS. Definitions and Explanatory Notes. Geneve 1976.

Authors' address: Department of Oncology, School of Medicine, 4, Gagarin Str., 93—508 Łódź

c.d. ze s. 150

Posiedzenie Nr 5 — 26 czerwca 1981 r.

M. Kozik, M. Znamierowska-Kozik (Zakład Neuropatologii AM i Oddział Neurologii Szpitala im. Strusia, Poznań) — Patomorfologia kryptokokowego zapalenia opon mózgowych o wieloletnim przebiegu.

B. Schmidt-Sidor, M. Eibl, K. Rusiecka (Zakład Neuropatologii Instytutu Psychoneurologicznego i Oddział Neurochirurgii Szpitala Chirurgii Urazowej Dziecięcej, Warszawa) — Dwa przypadki brodawczaka splotu naczyniastego u dzieci.

Posiedzenie Nr 6 — 17 października 1981 r.

J. Kałuża, J. Stachura, R. Kijak (Samodzielna Pracownia Neuropatologii Instytutu Neurologii AM i Pracownia Mikroskopii Elektronowej i Histochemii Instytutu Patologii AM, Kraków) — Cytoprotekcyjne działanie prostaglandyn w stosunku do komórek pochodzenia neuroektodermalnego w warunkach *in vitro*.

P. P. Liberski (Klinika Neurologii AM, Łódź) — Niektóre zagadnienia z patologii scrapie.

Posiedzenie Nr 7 — 14 listopada 1981 r.

A. Jędrzejewska (Zakład Diagnostyki Patomorfologicznej CMKP, Warszawa) — Przypadek choroby Picka ze stanem gąbczastym.

J. Kałuża (Samodzielna Pracownia Neuropatologii Instytutu Neurologii AM, Kraków) — Ocena morfologiczna nowotworów glejopochodnych po kobalto- i chemioterapii.

Posiedzenie Nr 8 — 12 grudnia 1981 r.

M. Górny, J. Szymaś (Zakład Anatomii Patologicznej AM, Poznań) — Odporność humoralna przeciwnowotworowa u chorych z glejakami mózgu. J. Szymaś, W. Biczysko, Z. Pawlak (Zakład Anatomii Patologicznej AM, Poznań) — Granulomatyczne zapalenie mózgu typu Cervos-Navarro.

Jerzy Dymecki

NEUROPAT. POL., 1982, 20, 1—2
PL ISSN 0028—3894

MARIAN MAJAK, JANUSZ ALWASIAK, WIELISŁAW PAPIERZ, MACIEJ PRUSZCZYŃSKI

TYPES OF GROWTH AND SPREAD OF BRAIN LYMPHOMAS *

Department of Pathological Anatomy and Department of Oncology, School of Medicine, Łódź

Malignant lymphomas of the central nervous system (CNS) are recently becoming more common (Zimmerman, 1971; 1974; Henry et al., 1974; Jellinger et al., 1974; Jellinger, Radaszkiewicz, 1976; Alwasiak et al., 1979). According to some of the above authors primary intracranial lymphomas range from 0.3% to 1.5% of all tumors in the CNS. In the material of our Laboratory they composed 1.3% of all tumors of the central nervous system.

The subject of this paper is the clinico-morphological study of primary malignant lymphomas of the human CNS as well as the comparison of their morphological picture with the pattern of transplantable lymphoma (NK/Ly — Nemeth—Kellner lymphoma) of the brains of mice. Special attention was paid to the mode of spreading of neoplastic cells within human and animal brains.

The ascites tumor NK/Ly developed after inoculating of splenic extracts from mice suffering of lymphatic leukemia into the peritoneal cavity (Nemeth, Kellner, 1960; 1961).

MATERIAL AND METHODS

The human material comprised 11 cases of primary CNS malignant lymphomas. They were diagnosed from the biopsy specimens and confirmed in 9 cases in the autopsy material. The tumors were grouped according to the Lennert classification (Lennert, 1974). In the experimental part of the study, 50 male Swiss mice were used. The animals were anesthetized with ether. After desinfection of the skin over the skull the cells of 10-day old NK/Ly tumor (0.02 ml) were injected by a needle into the left hemisphere of the brain at a constant depth.

* This investigation was supported by the Polish National Cancer Programme — PR 6-04.-01.

Twelve days after inoculation the animals were killed by cervical dislocation (Majak, 1977; Majak, Pruszczyński, 1978). Human and animal brains were fixed in 10% buffered formalin. Paraffin sections were stained with hematoxylin and eosin, PAS, pyronine and by Klüver-Barrera's, Gomori's and May-Grünwald-Giemsa's methods.

RESULTS

Human material

The age of patients ranged from 8 to 64 years (47 in average). There was no sex-dependence in the tumor occurrence. Brain tumor was diagnosed in the most cases on the clinical ground. The duration of neurological symptoms oscillated from 5 days to 2 years and survival time from a few weeks to a few months. Only in one case 3.5 years survival time was observed (Table 1).

Table 1. Clinical data

No.	Age (years)	Sex	Clinical diagnosis	Duration of clinical symptoms	Basic clinical symptoms	Survival
1	50	M	Brain tumor	2 years	Hemianopsia L. hemiparesis	3,5 years
2	64	M	Organic damage of the brain	2 years	Diplopia L. hemiparesis	2 months
3	26	M	Brain tumor	1 month	Increase of intracranial pressure	3 months
4	8	M	Leptomeningitis	5 days	Meningeal symptoms	3 weeks
5	64	F	Brain tumor	5 weeks	L. hemiparesis	1 week
6	56	F	Brain tumor	1 month	Headache L. hemiparesis	4 months
7	57	F	Brain tumor	2 weeks	Aphasia	4 months
		F	Brain tumor		L. hemiparesis	
8	51	F	Brain tumor	1 month	L. hemiparesis	3 weeks
9	46	M	Brain tumor	2,5 months	Psychopathy L. hemiparesis	3,5 months
10	46	M	Brain tumor	2 months	R. hemiparesis	2 weeks
11	58	F	Brain tumor	2 months	R. hemiparesis	2 months

In 9 cases the neoplasm grew as a localized, grey-pink, poorly demarcated mass occupying most often the temporal and occipital lobes (tumor-like type of growth) (Figs. 1, 2). In two other cases neoplasm infiltrated the leptomeninges and to a lesser degree cortex and white matter (inflammatory-like type of growth: Fig. 3).

Microscopically, several patterns of lymphoma cells spreading within the brains could be distinguished. The most common was the peri-

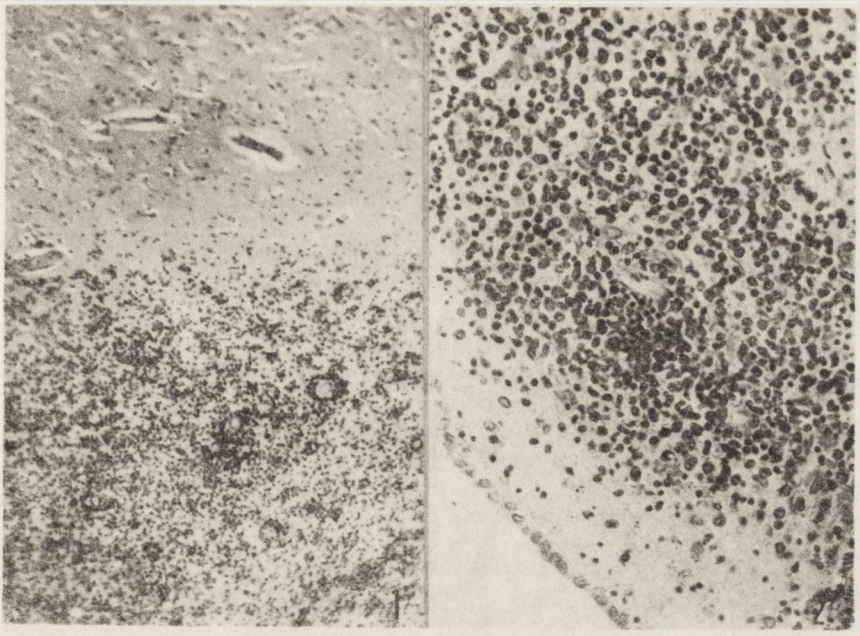

Fig. 1. Intrahemispheric growth of human lymphoma in the CNS. The relatively distinct border between the neoplastic masses and the grey matter is seen. H—E. × 50

Fig. 2. Subependymal spread of centroblastic lymphoma. H—E. × 180

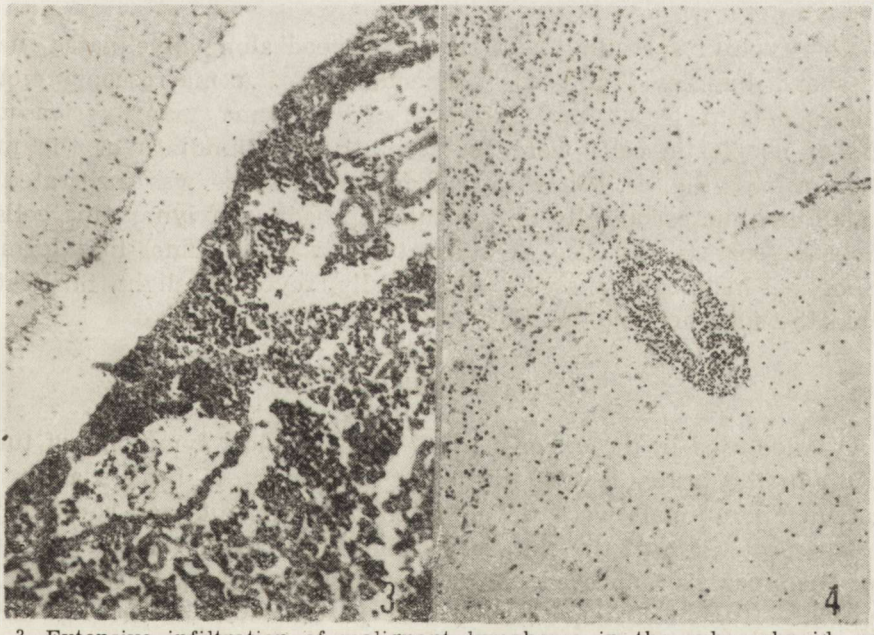

Fig. 3. Extensive infiltration of malignant lymphoma in the subarachnoid space. H—E. × 90

Fig. 4. Human lymphoma. Perivascular infiltration in the Virchows-Robin space is seen. In the upper right corner lymphoblastic cells resemble an inflammatory infiltration. H—E. × 50

Table 2. Morphological data

No.	Cellular type (Lennert)	Localization	Type of growth	Mode of spreading			
				P	S	My	Ss
1	Lympho-plasmocytic	R. temporal, parietal and occipital lobes	Tumor masses	+	+	−	+
2	Centrocytic	Leptomeninges, superficial gray matter	Diffuse	+	+	+	+
3	Centroblastic-centrocytic	R. occipital lobe	Tumor masses	+	−	+	−
4	Lymphoblastic	Leptomeninges, superficial gray matter	Diffuse	+	−	−	+
5	Centroblastic	R. temporal, parietal lobes, basal ganglia	Tumor masses	+	−	+	+
6	Centroblastic	R. frontal lobe	Tumor masses	+	−	+	−
7	Centroblastic – immunoblastic	R. frontal, temporal lobes	Tumor masses	+	−	+	−
8	Lymphoblastic	R. temporal, parietal, occipital lobes	Tumor masses	+	+	−	−
9	Unclassified	R. frontal lobe	Tumor masses	+	−	+	−
10	Unclassified	L. basal ganglia	Tumor masses	+	−	+	−
11	Unclassified	L. temporal, occipital lobes	Tumor masses	+	+	+	−

P – perivascular; S – subependymal; My – along myelinated nerve fibres; Ss – subarachnoid space

vascular type of spreading as well as a spread along myelinated, nerve fibres and bundles (Table 2) independently of a macroscopic picture of the neoplasm. In a tumor-like form of lymphoma, many perivascular cuffs of neoplastic cells were found in the surroundings of the main tumor masses (Fig. 4). When the subarachnoid space was infiltrated by tumor cells, microscopically perivascular spreading of lymphoma cells in the brain cortex was also seen. In two cases of tumor-like form of lymphoma, histologic analysis additionally revealed slight infiltration wtihin the subarachnoid space.

Experimental material

All mice used in the experiment revealed clinical symptoms of tumor growth in the brain. It was first seen as soon as 4—5 days after inoculation. The animals were slower in their movements and showed progressive protrusion of the skin on the head. On about the 6th day right sided hemiparesis appeared. Microscopically it was seen as soft and grey-white tumor tissue, about 3 mm in diameter in the left hemisphere.

Light microscopy revealed 3 forms of tumor growth i.e.: intrahemispheric, subarachnoid and intraventricular. Occasionally all three forms

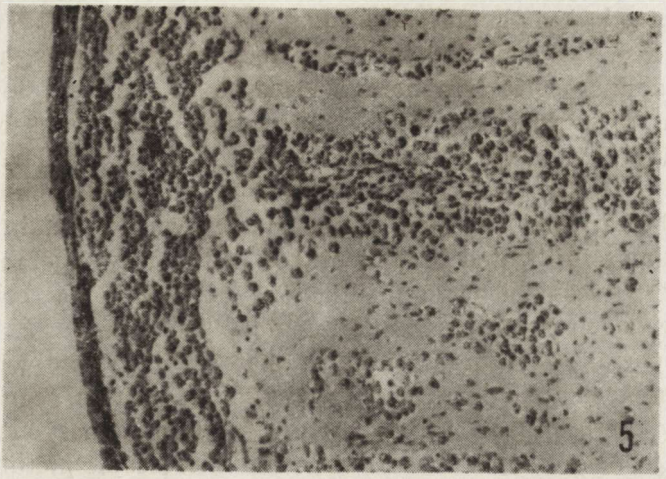

Fig. 5. Subarachnoid growth and the invasion of the mice brain cortex by tumor cells in the experimental ascites lymphoma. H—E. × 90

together could be identified. Predominantly intrahemispheric and subarachnoid types of growth were observed (Fig. 5). Most frequently the tumor cells were grouped in the perivascular spaces. Additional foci of such a spread in the surroundings of each type of tumor growth were present. Interfascicular pattern of spreading was also common, especially in cases when the corpus callosum was infiltrated. In mice with intraventricular tumor growth NK/Ly cells were seen in all portions of the ventricular system.

DISCUSSION

Primary neoplastic growth of lymphatic cells in the human brain is diagnosed in most cases only during the autopsy, after exclusion of similar changes in other body organs. In our material autopsies in 9 cases have been performed. In 2 other cases diagnosis of primary CNS lymphoma was determined with a high degree of probability, on the ground of clinical examination and microscopic pictures of the biopsy material.

The origin of lymphomas in the human brain is not certain. Many authors link their genesis with undifferentiated mesenchymal cells or with primitive reticulum cells (Blackbourne et al., 1967; Williams, Peters, 1967; Meyer-Lindenberg, Gullota, 1970; Zimmerman, 1971; Rubinstein, 1972; Henry et al., 1974; Zimmerman, 1974). In this way the maternal cells of these tumors in the CNS could be meningeal or perivascular histiocytes, reticuloendothelial cells or microglia. Lennert (1974) considered that lymphomas in the CNS derive rather from the immunologic system than from reticulum cells or histiocytes. The most of examined tumors belonged to the high malignancy group (lympho-

and centroblastic lymphomas) according to the Lennert (1974) classification. One case was included intro centrocytic lymphomas, another one into lymphoplasmocytic lymphomas. Because of the very low cell differentiation we could not more exactly classify three cases but we suspected their relation with the reticulum cell line. Similarly to other authors we observed two types of growth of human lymphomas in the brain. In 9 cases well defined tumor masses were seen, in two other cases the tumor infiltrated leptomeninges in the way resembling an inflammatory process (disperse infiltrations of lymphoma cells in the white matter also resembled an inflammatory process).

It is important for further studies that all mice into whose brains NK/Ly was inoculated developed rapid growth of this neoplasm. Morphologically, both human and experimental lymphomas showed many similarities in macroscopic as well as in the microscopic picture. It seems that NK/Ly can be useful in further studies as an experimental.

CONCLUSIONS

1. Histopathological diagnosis of the primary lymphomas in the CNS can be based on cytodiagnostic criteria generally accepted for the classification of extracranially localized tumors.

2. There are similarities between human lymphomas and experimental NK-lymphoma in their pattern of growth and type of spread in the brain.

3. NK/lymphoma grows easily in the brain of the mice and can be used as an experimental model in further investigations of malignant lymphocytic proliferations in the CNS.

REFERENCES

1. Alwasiak J., Papierz W., Szulc-Kuberska J., Zawadzki Z.: Pierwotny chłoniak złośliwy ośrodkowego układu nerwowego. Neurol. Neurochir. Pol., 1979, 13, 209—213.
2. Blackbourne B. D., Waggener J. D.: Ultrastructure of primary cerebral reticulo-endothelial sarcoma (microgliomatosis). J. Neuropath. exp. Neurol., 1967, 26, 141.
3. Henry J. M., Heffner R. R., Dillard May S. H., Earle K. M., David R. L.: Primary malignant lymphomas of the central nervous system. Cancer, 1974, 34, 1293—1302.
4. Jellinger K.: Primary malignant lymphomas of the central nervous system in man. Symp. "Malignant Lymphomas of the Nervous System", Vienna, 29—30. 08.1974. Abstracts.
5. Jellinger K., Radaszkiewicz T.: Involvement of the CNS in malignant lymphomas. Virchows Arch. Abt. A. Path. Anat., 1976, 370, 345—362.
6. Lennert K.: Morphology and classification of malignant lymphomas and so-called reticuloses. Symp. "Malignant Lymphomas of the Nervous System". Vienna, 29—30.08.1974. Abstracts.

7. Majak M.: Ascites tumour NK/Ly as a model of the growth of malignant lymphoma in the brain of mice. Acta Neuropath. (Berl.), 1977, 39, 169—171.
8. Majak M., Pruszczyński M.: An autoradiographic study of the ascites tumour NK/Ly transplantated into the brain of the mouse. Neoplasmy, 1978, 24, 461—463.
9. Meyer-Lindenberg J., Gullota F.: Das "Mikrogiom" als ortsspecifische mesenchymale Hirn Geschwülst. Arch. Psychiat. Nervenkrank., 1970, 213, 66—77.
10. Nemeth L., Keller B.: In Form von Ascites transplantierbare leukämische Lymphadenose bei Mäuse. Die Naturwissenschaften, 1960, 47, 544—545.
11. Nemeth L., Keller B.: New mouse ascites tumour to be used as a creening tool. Neoplasma (Wien), 1961, 8, 337—343.
12. Rubinstein L.: Tumours of the lymphoreticular system. In: Atlas of Tumour Pathology. Fascicle 6, "Tumours of the central nervous system". Arm. Forc. Inst. of Path., Washington 1972.
13. Williams J. L., Peters H. J.: Malignant reticulosis limited to the central nervous system. J. Neurosurg., 1967, 26, 532—535.
14. Zimmerman H. M.: Malignant lymphomas. In: "Pathology of the nervous system". Ed. J. Mincler. Mc Graw-Hill Book Comp., New York 1971, 2165—2177.
15. Zimmerman H. M.: Malignant lymphomas of the nervous system. Brain Nerve (Tokyo), 1974, 26, 1153—1160.

Authors' address: Department of Pathological Anatomy, School of Medicine, 96, Narutowicz Str., 90—141 Łódź.

NEUROPAT. POL., 1982, 20, 1—2
PL ISSN 0028—3894

II-nd POLISH-SCANDINAVIAN NEUROPATHOLOGICAL SYMPOSIUM

Szczecin, May 15th 1981

CEREBRAL ISCHEMIA
BRAIN EDEMA
VASCULAR PERMEABILITY
FREE COMMUNICATIONS

Diemer N. H., E. Siemkowicz
(*Copenhagen, Denmark*)

LOSS OF HIPPOCAMPAL CA-1 NEURONS AFTER CEREBRAL ISCHEMIA IN RATS WITH DIFFERENT GLUCOSE LEVELS

The selective vulnerability of certain brain regions to complete ischemia of shorter duration is not due to impaired recirculation and the possibility of influencing the tissue by pharmacotherapy therefore exists.

Both in human and experimental ischemia the most sensitive neurons are the Purkinje cells and the hippocampal CA-1 neurons. Up to 1 hour after 10 min ischemia in the rat, hippocampus CA-1, substantia nigra, globus pallidus and cerebellar molecular layer had higher flow deoxyglucose uptake than all other regions.

Rats given glucose i.p. before the 10 min.'s of ischemia did not survive longer than 24 hours. If insulin was administered during ischemia, the survival rate was similar to that of normoglycemic rats subjected to the same period of cerebral ischemia.

These findings indicate that treatment in the postischemic period is effective and that lactate production during ischemia cannot be the only factor responsible for the tissue damage.

Ekström von Lubitz D. K. J., H. H. Diemer
(*Copenhagen, Denmark*)

ULTRASTRUCTURAL MORPHOMETRY OF HIPPOCAMPAL CA-1 IN RATS WITH CEREBRAL ISCHEMIA

A period of cerebral ischemia evokes several changes in the affected neurons and both subtle volume changes and modifications of normal

infraneuronal structure might be readily observed. Our investigation consists of a qualitative and quantitative survey of such changes observed in the hippocampal striatum radiatum (CA-1).

Male Wistar rats were anesthetised with Halothane^R, N_2O and curarised. Siemkowicz and Hansen methods was used to induce a 10 min long ischemic period. 15 and 60 min after restitution of the cerebral blood flow, the animals were perfused for 20 min. with 3-aldehyde fixative introduced through the heart ventricle. The brains were removed, cut into 1 mm thick slices and immersion fixed for the following 3 h. OsO_4, postfixation and subsequent processing for TEM followed standard procedures. Survey micrographs were taken at 9000× and the micrographs of the synaptic regions at 27000×. Final print magnification was 32000× and 97000× respectively. Morphometric analysis was performed by means of a test-point array with 6 × 7 points. The neurons and their organelles were assigned specific numerical code designations and the designators were stored in a 6 × 7 matrix in the memory of a desk top computer for future analysis.

Qualitative study showed that 10 min. after ischemic period there were very limited changes at the level of somas, consisting mainly of sporadic dilatations of endoplasmic reticulum (ER) and of a few slightly swollen mitochondria. There were no changes in either dendrites or axons at their non-synapting levels. On the other hand, the synaptic regions showed initial stages of synapse degeneration consisting of changes in the curvature of the synaptic membranes, slight reduction in the number of synaptic vesicles and various extent of the vesicle pool-presynaptic membrane separation. Reduction of neurotubules entering the synaptic region was also noteworthy. Astrocytes were typified by their slightly swollen end-feet but no changes at the level of the nucleus.

60 min. after the ischemic period the changes were very pronounced. In the neuronal somas there was loss of ribosomes along considerable stretches of RER, vacuolisation of the ER and disruption of several mitochondria. Dendrites had intensely dilated mitochondria and showed disruption, branching and occasionally, "bubbling-up" of the neurotubule. Similar changes were found in the axons. Synaptic regions were characterised by drastic modifications of the synaptic membrane shape, reduction in area (loss of presynaptic densities), frequent dissociation of the postsynaptic densities and often a complete disruption and disappearance of the vesicle pool. Astrocytes had strongly swollen end-feet and contained aggregations of an osmiophilic substance. Although slightly swollen mitochondria were observed, there were no pronounced changes at the level of the astrocyte nucleus.

In several instances we have found in both normal and postischemic material slightly disrupted myelin sheaths. Such observations are at-

tributed to the poor fixing capabilities of aldehydes with respect to myelinated structures, reported by several authors in their studies of non-pathological nervous system.

The quantitative analysis of the ischemic changes is being performed at the time of writing and its results will be presented later.

Kalimo H., C-D. Agardh, M. Gardiner, Y. Olsson, B. K. Siesjö
(Turku, Finland; Uppsala, Sweden)

EFFECT OF PHENOBARBITONE ON HYPOGLYCEMIC BRAIN INJURY

Severe hypoglycemia with isoelectric EEG for 30 to 60 min causes cerebral cortical nerve cell injury, which evidently related to the energy failure, though clearly different from the hypoxic-ischemic injury. Morphologically it results in two types of neuronal alterations: Type I is characterized by condensation of cyto- and karyoplasm with perineuronal vacuolization and type II by clearing of peripheral cytoplasm (Agardh et al., Acta Neuropath. 50, 31—41, 1980; Kalimo et al., Acta Neuropath. 50, 43—52, 1980).

Since barbiturates have been shown to alleviate hypoxic brain injury, we decided to test the possible beneficial effect of barbiturates on hypoglycemic brain injury in rats, which were given phenobarbitone 57 mg/kg 1.5—2.5 hrs prior to the hypoglycemic insult.

After 30 min of hypoglycemia cerebral cortical concentrations of labile energy rich phosphates were reduced to the same extent as previously described during hypoglycemia without phenobarbitone. In microscopy the number of type II injured neurons did not change in the phenobarbitone-treated group compared to non-treated rats, whereas the number of type I injured neurons decreased suggesting slight protective effect.

The mechanism of the protective effect of barbiturates in hypoxia--ischemia is not known, but e.g. depression of active function, free radical scavenging vasoconstrictory action and lowering of ICP have been suggested. Since the hypoglycemic rats were isoelectric further depression of electric function is an unlikely explanation. More likely the protection in hypoglycemia may be related to the lesser degree of edema with which the type I injured neurons are often associated, or to free radical damage in the presence of ample oxygen in the energy deprived tissue.

Olejniczak P., J. Dąbrowska
(Wrocław, Poland)

PARTICIPATION OF CEREBRAL EDEMA IN THE DEVELOPMENT OF STROKES IN ALCOHOLICS

The materials consist of 10 "gamma"-alcoholics who died at the age ranging from 44 to 65 years at the Neurologic Clinic in Wrocław in the years 1971—1980. The reasons for their admission to the Clinic were stroke-like cerebral diseases which occurred following several days of an excessive drinking. In the studied group there were no cerebral hemorrhages, either traumatic or spontaneous.

In all cases the brains were subject to postmortem examination. Macroscopic abnormalities consisted of: 1) marked brain edema located, as a rule, in the cerebral middle-line white substance, 2) relatively small hemorrhagic reaction and congestion of cerebral tissue, 3) foci or encephalomalacia, predominantly pale (in brain stem — 5 cases, in both frontal lobes — 2 cases, in the corpus callosum — 2 cases). In one case marked cortical atrophy concomitant with brain stem edema were the only findings.

From the clinical and neuropathological point of view 5 cases with malacia in the brain stem are worth to be mentioned. In 3 cases in which foci of malacia were located in the ventral portion of the brain stem, clinically the disease manifested as tetraparesis, symptoms of decerebration, disturbances of eye-ball movements (ocular bobbing — 2 cases, "floating" and deviation — 1). In 3 further cases edema and malacia in the brain stem were also found. Two cases with malacia in corpus callosum require additional comment. In the first case at the time of intoxication coma bilateral pyramidal signs and decerebration rigidity appeared. The patient died on 70th day of coma. On naked eye examination the brain abnormalities were similar to those typical for Marchiafava-Bignami syndrome. Detailed neuropathological examination revealed destruction of corpus callosum by pale malacia. In the vicinity of the main lesion disseminated small hemorrhagic changes were found. In the second case in which clinical symptomatology consisted of left sided hemiparesis, changes in corpus callosum took the form of severe edema with small foci of disseminated pale malacia.

In all 9 cases with macroscopic features of malacia the diagnosis was confirmed microscopically. In the whole materials brain edema, involving mostly cerebral white matter, corpus callosum and brain stem was present. The edema accompanied primarily the foci of encephalomalacias.

In 3 cases only atherosclerosis of the components of the cerebral arterial circle was severe. In 7 remaining cases it was slight.

Stroke in alcoholics is probably due to cerebral edema. Cerebral vasomotor paralysis, which takes place during alcoholic intoxication (Pentschew, 1956), is with all probability the most significant factor, contributing in the development of brain edema and hypoxia of the central nervous system. The cerebral middle-line structures are rather rarely involved in vasogenic pathological processes, due to their good bilateral blood supply. Edema and necrosis in the middle-line structures must then result from bilateral lesions. Alcoholic vasomotor paralysis explains well the symmetry of both edema and necrosis in alcoholics.

Besides the development of alcoholic edema and encephalomalacia toxic influences, nutritional (including vitamin) deficiencies, and disorders in electrolyte and water metabolism have also to be taken into account. Burcar et al. (1977) have recently pointed out to the possible role of hyponatremia in the pathogenesis of central pontine myelinolysis. Messert and Orrison (1979) believe that in acute alcoholic intoxication after original decrease of ADH-secretion, it comes to this hormone's overproduction in the course of alcohol's withdrawal and easy development of cerebral edema. The edema of basal portion of the pons is of particular danger due to the fact that swelling of its grid structure can produce compression of blood vessels resulting in tissue necrosis or focal demyelination.

Paljärvi L., B. Söderfeldt, H. Kalimo, Y. Olsson, B. K. Siesjö
(*Turku, Finland*)

BRAIN ULTRASTRUCTURE IN HYPERCAPNIA

Lactic acidosis has been shown both biochemically and structurally to exaggerate ischemic brain injury (Rehncrona, Thesis, Lund 1980). In contrast to lactic acidosis, during severe hypercapnic acidosis the energy state of the brain is remarkably well upheld (Folbergrova et al., J. Neurochem. 22, 1115—1125, 1974). Very little attention has hitherto been paid to brain morphology in hypercapnia.

Respiratory acidosis was induced in paralysed and artificially respirated rats by exposing them to CO_2 concentrations yielding arterial pCO_2 or 150 or 300 mmHg. Arterial pH was reduced to about 6.8 and 6.6, respectively. After 50 min the animals were perfusion fixed with buffered glutaraldehyde. Samples from two cortical areas, hippocampus and cerebellum were examined with light and electron microscopy. Astrocytes, particularly those with perivascular location in the hippocampus, displayed slight to moderate edema. Neuronal changes were scanty. Nuclei showed early chromatin clumping. The mitochondria started to swell and ribosomes tended to detach from the RER in cere-

bellar Purkinje cells in the more acidotic group of animals. The results show that neurons tolerate this degree of acidosis well, if it is not accompanied by energy failure as in lactic acidosis of incomplete ischemia. Astrocytic edema may be due to the manyfold increase of cerebral blood flow and subsequent blood-brain barrier dysfunction induced by hypercapnia.

Stelmasiak Z.
(*Lublin, Poland*)

MONOAMINES IN ISCHEMIA AND EDEMA OF THE BRAIN

Monoamines are known as neurotransmitters in the specific neurons. The role of catecholamines and serotonin in the pathogenesis of stroke and brain edema is still an open problem.

During ischemia decrease of DA (Chikvaidze, Melitauri, 1974; Lust et al., 1975; Gadamski et al., 1976) * decrease of 5-HT (Chikvaidze, Melitauri, 1974), decrease of MAO (Davies, Carlsson, 1973) and increase of cAMP (Schweitz et al., 1976) were found in different brain ischemic areas. The results obtained during postischemic period are not as univocal and exact but generally they are indicating for a gradual levelling of the content of monoamines and their metabolites in ischemic area of brain (Harrison et al., 1978; Kogure et al., 1975; Mrsulja et al., 1976; Stelmasiak, 1976; Welch et al., 1977; Zervas et al., 1974).

In perifocal edema increase of 5-HT and 5-HIAA but no differences in DA content were found inpatients who died because of stroke (Jellinger et al., 1978). In nonischemic areas some changes in the distribution of monoamines and their metabolites were also found.

In CSF of patients with recent cerebral infarction increase of 5-HT and NA (Southern, Christoff, 1962; Misra et al., 1967; Berzin, 1969; Meyer et al., 1974), increase of TP, a gradual increase of 5-HIAA and decrease of HVA concentration were observed. In blood of patients with stroke increase of free TP, decrease of 5-HT concentration (Sikorski, 1973) and increase of DBH activity (Kanda et al., 1979) were found. In urine of patients with stroke increase of excretion of A and NA (Markiewiczowa, 1964; Ilinsky, Astrakhantseva, 1967), increase of VMA (Kawiak, Stelmasiak, 1967) and decrease of 5-HIAA (Kawiak, 1967) were noted.

In experimental cerebral infarction in animals changes in the distribution of monoamines and their metabolites in some internal organs were also stated.

---

* References in author's possesion.

These indicate that experimental brain ischemia or stroke leads to intracerebral and extracerebral consequences, including monoamines metabolism.

Intracerebral consequences seems to be mostly dependent of the disturbances in oxygen-glucose and energy supply and leads to decrease of synthesis, degradation and increase of monoamines release, especially serotonin, when reuptake and oxidative deamination are disturbed (Wurtman, Zervas, 1974).

Extracerebral consequences of stroke seems to be dependent of stress reaction connected with hypothalamo-hypophyseo-suprarenal axis disturbances.

Monoamines, probably in interaction with other vasoactive substances seem to play some role in pathogenesis of experimental brain ischemia and in stroke in patients. They may influence progression of cerebral infarction, development of postischemic brain damage and brain edema.

Torvik A.
(Oslo, Norway)

CHANGES IN THE FREQUENCY OF STROKES IN OSLO, NORWAY, FROM 1958 TO 1977

The frequency of lethal strokes was examined over a 20-year period in a large autopsy material and compared with the official death statistics for the same period. The frequency of lethal strokes in the autopsy material was calculated as percentage of the total number of autopsied cases in the corresponding age groups. Similarly, the frequency of strokes in the death statistics was calculated as percentage of all deaths in the corresponding age groups.

In the autopsy material the overall stroke frequency fell by 14 per cent during the period. For cases between 40 and 69 years the decline was 25 per cent while cases over 70 years showed only a minor fall. The heaviest decline was found for intracerebral hemorrhages which decreased by 70 per cent in cases between 40 and 69 years and by 33 per cent for cases over 70. For brain infarcts the decline was 32 per cent in the youngest age group while cases over 70 showed no decrease at all.

Also the death statistics showed a steady decline in the frequency of stroke deaths and the overall figures in the two materials were not much different. However, the figures for the stroke subgroups (brain infarcts and intracranial hemorrhages) were markedly different from those of the autopsy material. For instance, the frequency of hemorrhages was several times higher than that of infarcts in the death statistics

while the reverse was true in the autopsy material. The sources of error are discussed for both types of material. It is concluded that the overall figures for stroke deaths are largely reliable for both materials. In the death statistics the separate figures for hemorrhages and infarcts were obviously wrong and long term changes in these figures should therefore be interpreted with caution. The figures in the autopsy material are considered more reliable and it is concluded that the decline in hemorrhages and infarcts described above was real.

Simon E.
(Poznań, Poland)

VASCULAR LESIONS AND BRAIN EDEMA AFTER ANGIOGRAPHY

Brain edema resulting from lesions of the vessels caused by angiography is one of the side-effects of contrast media action. Clinical symptoms of these changes have been usually described as complications but in experimental investigations they are constant phenomena. Computer tomography has reduced angiographic examinations, but has not eliminated contrast media utilization which are given nowaday intravenously in much larger doses.

The changes found in patients after brain angiography were compared with those observed in experimental animals. Several contrasts (Triuropan, Uromiro, Angiografin, Conray) were used in doses of 0.3—1.0 ml/kg. For evaluation of the changes, the following procedures were applied: a) histological staining, b) histochemical reactions, c) phase-contrast techniques, d) electron microscopy, e) autoradiography (contrast media marked with iodine isotope). 250 brains and biopsy material from 200 patients after cerebral angiography, 27 rats, 8 dogs and 55 cats were examined. The material for investigations was taken from 30 seconds to 5 month after the injections of contrast media.

A contrast medium that may give an embolic effect in the vessels, damages elements of the vascular walls, the cerebral parenchyma and that of other organs, first of all kidneys. Passage of the PAS-positive substance from the vessels to the nerve tissue can be evaluated. This was also found in phase-contrast microscopy. Cerebral macro-radiography carried out after application of contrast medium labelled with iodine isotope, gave evidence of an increased activity of the respective hemisphere which did not decrease even, though there was a decrease of the total blood activity. In specimens taken for electron-microscopic examinations globular concrements deposited in the vascular walls were found. In addition swelling of astrocytic processes adjacent to the vessel walls was present. Changes in blood vessels, particularly in the capillari-

es, were dependent on the time which elapsed after the contrast medium injection.

After 15 minutes endothelial cells of some capillaries became swollen while the endoplasmic reticulum canals were widened and the number of micropinocytic vesicles increased. After 60 minutes in the neighbourhood of the changed vessels swollen astrocytic processes with features of their injury were found. The basement membrane of the vessels surrounded by swollen astrocytic processes showed presence of granular concretions probably permealing throughout the membrane. Investigations carried out seven days after the contrast injection revealed necrosis and desquamation of the endothelial cells. There appeared macrophages in the surroundings of changed vessels. The above described abnormalities were accompanied by decreased activity of alcaline phosphatase, magnesium dependent ATP-ase and increased activity of acid phosphatase. In the cytoplasm of some swollen astrocytes PAS-positive substance was found, as well as granular concretions resembling those seen in vascular walls. In the neurons widened channels of the endoplasmic reticulum were observed. Their cytoplasm contained PAS-positive substance.

Conclusions: 1) Complex pathomorphological investigations permit a detailed evaluation of the damages caused by contrast media; 2) Brain edema involving the hemisphere on the side of injection and same localization of the contrast extravasation, point out to the specificity of the changes observed and to the permanent brain damage; 3) Pathomorphological changes following angiography show that contrast media that are at our disposal are by no means harmless; 4) The irreversible character of the changes and their sequelae should limit indications to cerebral angiography.

Tengvar Ch., M. Forssen, D. Hultström, Y. Olsson, H. Pertoft, A. Pettersson (*Uppsala, Sweden*)

USE OF NEW SPECIFIC GRAVITY TECHNIQUE FOR MEASUREMENT OF CEREBRAL EDEMA

For studies on the pathogenesis and effects of brain edema quantitative methods are needed by which one can determine the magnitude and extent of edema in the cerebral grey and white matter. One such technique relies on specific gravity measurements to reveal changes in brain water contents (Nelson et al., J. appl. Physiol. 1971, 30, 268—271). Samples are then dropped into a calibrated cylinder containing a density gradient composed of bromobenzene and kerosene (B—K). Since these compounds due to their toxicity might create problems in

laboratory work we have started to use polyvinyl pyrrolidone coated colloidal silica particles instead of B—K.

As compared with B—K the new gradient was remarkably stable and could be used for repeated experiments over a long period of time. Linear density gradients in the interval 1.0200—1.0600 g/ml could easily be prepared and the osmotic condition in the cylinder could be varied by the addition of sodium chloride (Pertoft et al., Annal. Biochem. 1978, 88, 271—282).

Samples were removed from mouse cerebral cortex and white matter under a plexiglass hood at 90 per cent relative humidity to minimize loss of water during dissection. The values obtained in the 300 mOsm Percoll gradient were somewhat lower than those measured in the organic B—K medium; the differences being 0.0032 for cerebral cortex and 0.0049 for frontal white matter.

Preliminary experiments with triethyltin (TET) induced brain edema have also shown that the values obtained in 300 mOsm Percoll are lower than those measured in B—K. However, the time course for the developing edema as indicated by changes in tissue density at various intervals after a single i.p. injection of TET was similar when measured in Percoll as compared to B—K (Laurent et al., J. Colloid. Interf. Sci. 1980, 76, 124—132). Therefore, Percoll may well be used as an alternative to bromobenzene-kerosene in some studies on brain edema.

Arvidson B.
(Uppsala, Sweden)

VASCULAR PERMEABILITY CHANGES IN THE PERIPHERAL NERVOUS SYSTEM AFTER ACUTE CADMIUM INTOXICATION

The industrial use of cadmium has increased during recent years and cadmium has become recognized as a toxicologically important environmental contaminant. Among toxic effects of cadmium salts are nephropathy, arteriosclerosis, liver damage and pulmonary disorders. In 1966, Gabbiani accidentally discovered that parenteral administration of cadmium salts produces selective hemorrhagic lesions of sensory ganglia in several animal species. These lesions have later been shown to be due to a primary damage to endothelial cells in ganglia. The present investigation was undertaken to find out to what extent cadmium may cause vascular damage also in a peripheral nerve like the sciatic.

Adult mice of the NMRI strain were injected with a single subcutaneous doses of cadmium chloride at a dose of 5 mg/kg body weight (b.w.) and the animals were divided into three experimental groups. In group 1, the frequency of hemorrhages in the sciatic nerve was deter-

mined by light microscopy 24 h after the cadmium injection. In group 2, the method of vascular labelling with carbon was used in order to detect injurious effects on blood vessels. Mice were injected with colloidal carbon (0.1 ml/100 g b.w.) 23.5 h after the administration of cadmium and were killed after another 30 min. In group 3, the animals were given an intravenous injection of horseradish peroxidase (HRP) type II, Sigma, 30 min. before being killed and were taken at a total time of 1, 2, 4 and 8 h after the cadmium injection.

Interstitial hemorrhages with edema and vascular labelling with carbon were observed in the sciatic nerve of about 50% of the animals taken 24 h after cadmium administration. In control nerves from animals injected with (HRP), the tracer remained restricted to the lumina of endoneurial blood vessels and the cytoplasm of interstitial macrophages. In animals injected with cadmium and HRP, the peroxidase spread diffusely outside endoneurial blood vessels. This increase in vascular permeability started as early as 1 h after the administration of cadmium. Electron microscopy of the sciatic nerve from mice killed 24 h after treatment with cadmium showed distension of some blood vessels with accumulation of erythrocytes and platelets. The endothelial cells of such vessels were degenerated with condensation and thinning of the cytoplasm and large gaps were seen in the endothelial lining.

In conclusion the present study shows that acute cadmium intoxication may produce endothelial cell damage not only in sensory ganglia, but also in a peripheral nerve like the sciatic. The endothelial lesions are accompanied by an increased vascular permeability to the tracer horseradish peroxidase.

Dąmbska M., L. Iwanowski, D. Maślińska, M. Ostenda
(Warszawa, Poland)

CHANGES IN PERIVASCULAR AREA OF YOUNG RABBIT BRAIN FOLLOWING DICHLORVOS INTOXICATION

Chronic intoxication with dichlorvos (DDVP) — organophosphorus pesticide and strong inhibitor of acetylcholinesterase (AChE) leads to the morphological, biochemical and functional disorders in the central nervous system. Some authors speculate that the location of AChE in capillary walls of some brain regions is connected with their innervation and/or permeability. Therefore the present work was undertaken to study the effect of DDVP on postnatal development of the morphological structures of the perivascular area in rabbit brain and subsequent features of the blood-brain barrier.

Experiments were performed on rabbits of both sexes, treated *per os* with DDVP (9 mg/kg/body weight/day) during 10 days starting from the 6th day after birth; 16-day old rabbits were perfused with buffered glutaraldehyde and some of them were injected before perfusion with horseradish peroxidase, then ultrastructural study was performed. Activity of AChE was estimated histochemically according to Karnovsky and Roots. Ultrastructural appearance of the perivascular area in the cerebral and cerebellar hemispheres and corpus calosum were examined in 16 and 32-day old rabbits. The strong inhibition of acetylcholinesterase activity in brain tissue and in blood vessel walls was found. In endothelial cells of 16-day old animals the features indicating stimulation of cytoplasmic organelles were observed (proliferation of rough and smooth endoplasmic reticulum, increased amount of free ribosomes). They were more pronounced comparing with the control animals of the same age and persisted to the 32nd day of life. The increase of the permeability for horseradish peroxidase reaction products was not observed. In perivascular tissue rarefaction of cytoplasm, mitochondrial lessions and swelling of astrocytes adjacent to the vessel walls were found in 16-day old rabbits. The tissue abnormalities persisted 10 days after last treatment with dichlorvos. The changes in perivascular tissue allows to presume the active transport of DDVP through the capillary wall. It could be admitted that dichlorvos intoxication is responsible for observed morphological alterations.

Renkawek K.
(Warszawa, Poland)

MORPHOLOGICAL AND ENZYMATIC PROPERTIES OF CEREBELLAR CAPILLARIES AS A DETERMINATIVE FACTORS OF BARRIER FUNCTION

In vitro study

In the cerebellar cultures originally explanted as well as newly formed capillaries are present. Both in the explant and in the outgrowth capillaries maturation and following stages of vasculogenesis are observed. Morphological structures such as tight junctions, basement membrane and perivascular glial endfeet are formed. Some hydrolytic enzymes such as butyrylcholine esterase (BuChE), alkaline phosphatase (AlpH), (CTP-ase), γ-glutamyltranspeptidase (γ-GGTP) and nucleotide phosphatases (CTP-ase, IDP-ase, GTP-ase and ATP-ase) can determine the "barrier" function of brain capillaries.

Westergaard E.
(Copenhagen, Denmark)

VESICULAR TRANSPORT OF MICROPEROXIDASE AND HORSERADISH PEROXIDASE ACROSS ARTERIOLES IN THE MOUSE BRAIN

Horseradish peroxidase (HRP) has previously been demonstrated to be able to cross the blood-brain barrier in short segments of small arterioles on the surface of the brain and in the underlying neuropil. HRP is an enzyme (MW: 40000) obtained from the plant, horseradish. For comparison, microperoxidase (MP, MW: 2000) was used as tracer. MP is a peptide, with similar enzymatic properties, obtained from horse spleen by enzymatic digestion of cytochrome c.

The investigations revealed that both tracers crossed short arteriolar segments in the mouse brain. The endothelial cells were not injured. No sign of interendothelial passage was demonstrated since reaction product never formed a continuous column from the first luminal to the first abluminal tight junctions. The tight junctions thus seem to have functioned as a barrier to both tracers. HRP does not bind to proteins. Some of the injected MP was bound to plasma proteins, but a minor part of the MP circulated freely in the blood stream. It is concluded for MP as well as for HRP, that the tracers might have been transferred in vesicles across the endothelium. However, it was not possible to determine whether the MP, that crossed the endothelium in vesicles was bound to albumin or it remained unaltered during the permeation.

Dymecki J., E. Medyńska, M. Walski
(Warszawa, Poland)

INFLUENCE OF THE METHOD OF SACRIFICING THE EXPERIMENTAL MICE ON THE CHOLINERGIC SYNAPSES PATTERN

(Morphometric evaluation)

In electron microscope investigations on the dynamics of changes in the synapses in the course of experimentally evoked epileptic seizures it is necessary to use such a method of sacrificing the animals which

would reveal the current functional state of the synapses at any chosen moment of the seizure. The number of synaptic vesicles in the axon terminal is a morphological manifestation of the intensity of neuron excitation; this decreases considerably under the influence of excitation.

The study was undertaken to compare various ways of sacrificing the animals in order to evaluate their usefulness in investigations on the dynamics of changes in the synapses of the mouse central nervous system. Two basic routine methods were applied: perfusion and decapitation; the latter consisting of three variants. Ten mice divided into groups were used for the experiments: 1) subjected to perfusion under nembutal anesthesia, 2) decapitated under nembutal anesthesia, 3) decapitated after two weeks earlier taming and familiarisation with the laboratory room, instruments and personel, 4) decapitated without anesthesia or taming.

The last group consisted of animals killed by throwing into liquid nitrogen, however, in view of the severe destruction of the tissue due to freezing, the material was not suitable for morphometric analysis.

Material for the ME examination was taken from the motor cortex and impregnated by the zinc-iodide-osmium tetroxide method. For each group about 60 electronograms of synapses in a final magnification of 123 000 were prepared.

Morphometric analysis comprised calculation of the number of synaptic vesicles per 1 μm^2 of synaptic bouton cross section surface area measured planimetrically, taking into account the number of synaptic vesicles containing transmitter substance (ZIO-positive) and those deprived of it (ZIO-negative).

The values obtained reveal that the number of synaptic vesicles in the axon terminals in all groups of animals (after perfusion under nembutal anesthesia, decapitation under nembutal anesthesia and decapitation after familiarisation with the surroundings) is high and does not show significant differences, this indicating that the degree of excitation of the neurons was low. The number of synaptic vesicles in the group of animals decapitated without previous anesthesia or taming was significantly lower as compared with the remaining three groups, indicating a high excitation of the neurons.

The results obtained evidence that not as much the decapitation procedure itself but the stress and accompanying psychomotor reaction of the animals are the cause of high neuronal excitation in the group of animals decapitated without anesthesia or taming.

Familiarisation of the animals with the surroundings before decapitation eliminated the stress of the animals, which made difficult the differentiation between changes evoked by epileptic seizures from those due to psychomotor reaction. This method seems to be most suitable in studies on the dynamics of changes in the brain axon terminals.

Haltia M., H. Somer, S. Rehunen
Helsinki, Finland

ADVANCES CONGENITAL FIBER TYPE DISPROPORTION

Congenital fiber type disproportion is a rare condition, usually associated with the floppy infant syndrome. Muscle biopsy reports of congenital fiber type disproportion have almost exclusively concerned infants or young children. We describe the association of advanced fiber type disproportion with a marfanoid habitus in a 22-year-old man with negative family history. He showed generalized muscular hypotonia and weakness since birth. His psychomotor development was retarded and he could not walk without assistance before the age of 3 years. The symptoms did not progress. At the age of 20 years his body height was 195 cm. He was hypognathic and had a high palate, a very long and slender neck, and long fingers and toes. His thorax was flattened and elongated with thoraciscoliosis to the left. The span/height ratio and the upper/lower segment ratio were pathological. There was moderate muscular hypotrophy in the scapulo-humeral region and slight proximal muscle weakness in the extremities. The tendon reflexes were symmetrically depressed. Electromyography showed polyphasic potentials of long duration. Neuroophthalmological and cardiological special investigations and computerized tomography of the skull did not reveal anything abnormal, and extensive laboratory investigations were unrewarding. The results of morphometric, histochemical and microchemical analyses of muscle biopsies are presented.

Kristensson K., T. Olsson
Huddinge, Sweden

RETROGRADE AXONAL TRANSPORT OF CATIONIZED AND NATIVE FERRITIN

The present study was undertaken with the aims to compare retrograde axonal transport of materials after fluid-phase pinocytosis versus adsorptive pinocytosis, and to examine the longterm effect of iron on nervous tissue. Native ferritin (NF) and cationized ferritin (CF) were injected into the muscle of the vibrissae in mice. CF adsorbed onto the surface of axonal terminal at the neuromuscular junction, while NF did not. Both CF and NF were incorporated into vesicles and vacuoles at the synapse, but CF uptake was detected after injections at much lower concentrations than NF. In contrast to NF, CF was also found histochemically in cell bodies of facial neurones after a single i.m. injection. In spite of a marked iron load of Schwann cells and nerve cell bodies no signs of toxicity appeared.

Markiewicz D.
Warszawa, Poland

ON THE PATHOGENESIS OF POSTICTAL DAMAGE OF THE BRAIN IN MICE WITH AUDIOGENIC EPILEPSY

The influence of generalized epileptic seizures on the permeability of the blood-brain barrier, the water content and microcirculation in the brain were investigated in mice with genetically conditioned audiogenic epilepsy in reference to the number of seizures and the time of survival after them.

The following experimental groups were singled out: group A — one epileptic seizure, group B — a series of 6—10 seizures during one day, C — a series of 6—10 seizures daily for 6 days. The animals were decapitated immediately after cessation of the convulsions and 1—48 h after the last seizure.

The following results were obtained: 1) The permeability of the blood-brain barrier increased in all three experimental groups (A, B, C) in the mice decapitated immediately after the seizures. The intensity of changes increased with the number of seizures suffered; 2) A statistically significant increase of water content was noted in group C in the brain of mice which survived 24 h after the last seizure; 3) Disturbances of the cerebral microcirculation, observed in groups A and B, receded almost at once after cessation of the convulsions, whereas in group C these disturbances increased reaching highest intensity after 24 h and they were of the character of anemisation and stasis with prevalence of anemisation changes.

Analysis of the results of the investigations point to the significance of microcirculation disturbances, occurring in the postictal period for the morphological pattern of postictal brain lesions, which are connected with the development of brain edema.

Nordborg C., N. Conradi, P. Sourander, B. Westerberg
(Göteborg, Sweden)

NON-PROGRESSIVE SENSORY NEUROPATHY WITH DYSAUTONOMIA. A REPORT OF THREE CASES

Three cases of non-progressive, sensory neuropathy with dysautonomia are presented. Light- and electron microscopy on whole nerve sural biopsies revealed an almost total lack of myelinated nerve fibers. The total fiber count was also reduced as was the total number of Schwann cell nuclei. No degenerative phenomena were seen within nerve fibers.

The aberrations are probably caused by a maldevelopment of the neural crest, implying a stunted proliferation and growth of sensory and autonomous neurons as well as a reduced proliferation of Schwann cells. Since the morphology and clinics differ from that in other cases of sensory neuropathy with dysautonomia the three present cases are considered to represent a new type of this disease.

Oldfors A.
(Göteborg, Sweden)

NERVE FIBER DEGENERATION OF THE CENTRAL AND PERIPHERAL NERVOUS SYSTEMS IN SEVERE PROTEIN DEPRIVATION IN RATS

Knowledge from previous reports that kwashiorkor may lead to nerve fiber degeneration prompted this study on rats. The rats were subjected to severe protein deprivation from 6 weeks of age. Protein deprivation was achieved by feeding the rats *ad libitum* with a diet containing only 1.5 per cent protein. Control rats received an iso-caloric diet with 14 per cent protein. The vitamin content in both diets was well above normal requirements. In relation to body weight the protein-deprived rats did not consume less food than the control rats. Protein deprivation resulted in stunted body growth, markedly reduced values of serum albumin, and changes in the fur accompanied by areas of alopecia. Furthermore, the protein-deprived rats showed degeneration of nerve fibers in the medial parts of the posterior columns of the cervical but not the sacral part of the spinal cord and nerve fiber degeneration in the distal but not the proximal parts of the longitudinal tail nerves. Teased nerve fiber preparations of the tail nerves revealed changes consistent with the Wallerian type of degeneration. It is concluded that severe protein deprivation in young rats may lead to a "dying-back" type of neuropathy in the central and peripheral nervous systems.

Olsson Y., B. Söderfeldt, G. Blennow, H. Kalimo, B. K. Siesjö
(Uppsala, Sweden — Lund, Sweden — Turku, Finland)

INFLUENCE OF SYSTEMIC FACTORS ON EXPERIMENTAL EPILEPTIC BRAIN INJURY

Brain edema and ischemic nerve cell changes are generally considered to the major alterations that can be seen in patients dying of status epilepticus. However, these patients have suffered not only from epi-

lepsy, but also from various complicating systemic factors like hypoxia, hypotension and hypoglycemia. From studies on human neuropathological material it is difficult to evaluate the relative importance of primary (epileptic) and secondary (systemic) factors for the development of the associated brain damage. We have therefore studied status epilepticus induced by bicuculline (a GABA blocking agent) in a rat model under strict control of physiological parameters during and after periods of epilepsy for 1 or 2 h.

In our standard, normoxic and normotensive mocel light (LM) and electron microscopy (EM) of the cerebral cortex revealed status spongiosus and nerve cell injury of two types: one reversible with cytoplasmic vacuolation due to swelling of rough endoplasmic reticulum and the other irreversible with marked shrinkage of entire neuron (Söderfeldt et al., Acta neuropath. (Berl.) 1981, 54, 219—231).

In animals exposed to moderate hypotension (BP $\sim$ 70 mm Hg) during the seizure period the LM changes were of the same type as those observed in the standard model. In both the hypotensive and severely hypoxic (arterial $pO_2 \sim$ 50 mm Hg) rats the number of injured neurons was approximately the same (66%) as in the standard group. However, in the hypoxic rats the nuclear chromatin became clumped and EM showed that neuronal mitochondria were markedly damaged, whereas the latter change was absent or only rarely observed in the hypotensive group.

Persson L.
(Huddinge, Sweden)

CNS AND PNS MYELINATION IN MOUSE TRIGEMINAL ROOT

CNS and PNS myelination was studied in the trigeminal sensory root of mice ranging from newborn to 120 days of age. In the trigeminal root CNS white matter extrudes a little from the brain stem into the root and directly meets the PNS in a transitional zone. CNS and PNS myelination could thus be studied in the same population of axons. Myelination was quantitated on electron micrographs by conventional methods.

Myelinogenesis, in terms of established contacts between axons and myelinating cells (so-called promyelin fibers) started at the same time in CNS and PNS, and the transformation from "non-myelinated" to myelinated fibers occurred concomitant in the central and peripheral parts of the root. The later phase of myelination, i.e. growth in thickness of the myelin sheath, was however faster and more extended in PNS than in CNS. The gained findings suggest that neurons may initiate

both CNS and PNS myelination by a common mechanism. A different growth pattern of the later phase of myelination may reflect a difference in biological behavior of Schwann cells and oligodendrocytes, perhaps the phenomenon that a Schwann cell provides myelin only for one internode, while an oligodendrocyte myelinates several internodes in different axons. The trigeminal root may provide a useful model for studies of impaired myelin formation and the present results imply that disturbances occurring at the initiation of myelinogenesis may have a different effect on myelination than disturbances occurring at later phases of the process.

Reske-Nielsen E., U. Baandrup, P. Bjerregaard, I. Bruun
(*Aarhus, Denmark*)

PATHOLOGICAL CHANGES OF THE HEART IN SPIELMEYER-VOGT'S DISEASE

Juvenile amaurotic idiocy (JAI) is a rare disorder of autosomal recessive inheritance. It belongs to the so-called ceroid lipofuscinoses and the central system is the target organ. Only very few reports refer to the accumulation of lipopigment in the heart of JAI patients. This study describes the morphology of the heart from all 13 patients with JAI in Denmark who died within a seven year period; electrocardiographic findings are related to structural changes.

All compartments of the heart were involved, including the conduction system. Not only very substantial deposition of lipopigment in the myocytes was found, but we have also observed striking amounts of calcium and cholesterol compounds indicating a restrictive type of heart muscle disorder. These structural changes are uniform from case to case.

Because of the nature of the disease only rather poor information of the cardiac state is available in JAI patients. 11 patients showed some cardiac enlargement. In 6 patients abnormal P-waves were recorded in the ECG suggesting increased atrial and ventricular diastolic pressure. Two patients had bradycardia, probably due to sinus node involvement, and one patient developed complete right bundle branch block. However, in the 4 patients in whom the cardiac conduction system could be examined histologically no evidence of disturbance of cardiac impulse formation and conduction was seen in the few standard ECG strips available in spite of extensive deposition of abnormal material throughout the conduction system.

There seems to be a discrepancy between the relatively minor functional disturbances observed and the heavy morphological changes in the entire heart. This aspect, however, may well be altered by an intensified clinical observation and examination of JAI patients.

Schneider J., D. Schreiber
(*Erfurt, GDR*)

SELECTED PROBLEMS OF INTRACRANIAL AND INTRASPINAL MENINGIOMAS

Meningiomas occur in 0.55% of all autopsy cases of the Institute of Pathology of the Medical Academy of Erfurt in the years 1953 until 1976. Thus they form 20.5% of all CNS tumors observed and are next to astrocytomas (18.4%) the most frequent CNS tumor type. In 13.1% of the cases the meningiomas were associated with malignant extraneural tumors. In 2.5% there was a combination of this tumor type with other CNS neoplasms. In 8 among 305 cases we observed multiple maningiomas.

Analysing our biopsy material we found 431 meningiomas (25.7% of all CNS tumors). In this group the meningioma is the predominating CNS tumor type.

The mean age of autoptically diagnosed meningiomas was 60.6 years, in bioptic cases it was 50.1 years, respectively. The sex distribution revealed a preponderance of females over males (7 : 3). Only 109 of 175 patients, in which the meningioma represented the basic disease, were operated upon. This results from the old age of the majority of patients and from the late tumor diagnosis.

According to the new WHO classification of CNS tumors, the endotheliomatous type predominated.

In the spinal canal 78 meningiomas were found bioptically and 23 by autopsy being mainly localized in the thoracic region. The predominance of females among the spinal meningiomas (7 : 1 in biopsies, 5 : 1 in autopsies) corresponds to data of the literature.

Sourander P., O. Järvi, P. Hakola
(*Göteborg, Sweden — Turku, Finland — Kuopio, Finland*)

NEUROPATHOLOGICAL ASPECTS OF A NEW HEREDITARY DISEASE AFFECTING BONES AND CEREBRAL WHITE MATTER

Since 1961 some 70 cases of a previously unknown hereditary disease characterized by systemic cysts in the bones of the extremities and slowly progressive degeneration of the cerebral white matter have been

reported. The first reports on this new disease came from Japan (Terayama, 1961) and Finland (Järvi et al., 1964). An extensive neuropsychiatric and genetic study on nine Finnish cases was published by Hakola (1972). Recently the disease has been recognized also in northern Sweden (Adolfsson et al., 1978) and in USA (Wood, 1978). In Japan this new disease is known as "membranous lipodystrophy" or „Nasu disease", in Scandinavian as "hereditary polycystic osteodysplasia with sclerosing leucoencephalopathy".

The bone cysts or symptoms indicating their existence may appear at an early age, mostly, however, during adolescence. During the fourth decade of life, serious neuropsychiatric symptoms are associated with the disease: a prefrontal syndrome, progressive dementia, involvement of the upper motor neurons, motor aphasia, myoclonic twitches, and later, also epileptic seizures. The disease leads to death at the age of about 40 years. The diagnosis can be made by X-ray examination and biopsy of the affected bones. Until now 3 Japanese and 5 Finnish cases of the disease have been neuropathologically investigated.

The present report is a summary of the neuropathological findings in the cases from Finland. Moderate to severe atrophy affecting particularly the white matter of the frontal and temporal lobes was noticed in every case. There was marked loss of the myelin sheaths and irregular swellings and fragmentation of the remaining ones. In most cases sudanophilic break down products of myelin were absent thus excluding the relationship to "sudanophilic leucodystrophy". Marked vascular changes were observed particularly in the bone lesions. Light and electron microscopic changes were present also in the cerebral vessels.

As to the pathogenesis of the condition the following hypothesis has been advanced by Järvi and Sourander. A developmental deficiency of blood vessels particularly in the bones and nervous system. Secondary edema and nutritional disturbances leading to slowly developing fat necrosis in the bones. Proliferation of astrocytes and glial fibers with slight to moderate degree of degeneration of the cerebral white matter.

Schreiber D., Schneider J.
(*Erfurt, GDR*)

AGE-DEPENDENCE OF TUMORS IN HUMAN AND EXPERIMENTAL NEURO-ONCOLOGY

It is well-known that different age periods are preferred by special types of CNS tumors. Analysing our autopsy material we found about one third of all CNS tumors in humans beyond the age of 60. Among

these tumors 60% of meningiomas and 55% of pituitary adenomas occurred. Unfortunately, the neoplasms in old age have been more frequently misdiagnosed clinically than in younger patients.

During the first two decades of life 10% of all CNS tumors were registered. In this age group, however, 75% of all medulloblastomas, 70% of the germ cell tumors and 43% of the ependymomas were observed. Moreover, a large amount of angioblastomas, choroid plexus papillomas, and craniopharyngiomas (about 1/4 in each case) were found in young men. Other relationship are remarkable in infancy, since the choroid plexus papilloma is the predominating tumor type in this group. In stillborn children the intracranial teratomas rank first. Therefore, some age-dependent characteristics are concealed by CNS tumors statistics.

In experiments, the peculiarities of age distribution of CNS neoplasms may be imitated only to a limited extent. Astrocytomas, oligodendrogliomas, mixed gliomas, ependymomas, and choroid plexus papillomas induced by viruses or chemical substances have been found in various age groups in animals. On the other hand, dysontogenic tumors which are comparatively frequent tumor types in man have not been produced experimentally so far. There is no connection between brain malformation and brain tumors in ENU and/or MNU experiments of rats.

Further relations between the age group and tumor-bearing individuals in human and experimental neuro-oncology are discussed.

Wender M., M. Śniatała-Kamasa, A. Piechowski
(Poznań, Polska)

CONTRIBUTION TO THE PATHOMECHANISM OF LESIONS OF CENTRAL MYELIN IN CHRONIC TET INTOXICATION

The results of an ultrastructural study on central demyelination, as exemplified by events occurring in the rat optic nerve following chronic TET-intoxication, in which demyelination is believed to constitute most likely a primary effect, are presented.

Adult Wistar rats, chronically intoxicated by TET-sulfate intake (Eto et al., 1971) served as experimental animals, and their optic nerves were examined in electron microscope at various periods of intoxication.

The obtained observations seem to indicate that TET when applied chronically produces both intramyelin vesiculation and necrosis of nerve fibers followed by phagocytosis of the resulting myelin debris by reactive astroglial cells. Splitting of myelin lamellae occurring at the

intraperiod line is characteristic of TET intoxication, and that is why the similarity of spongious changes in TET intoxication and in human as well as experimental subacute spongious encephalopathy is only an apparent one.

During the third week of TET intake perivascular edematous fluid tended to accumulate, indicating some impairment of the permeability of the endothelium; this event coinciding with the most severe clinical symptoms of chronic poisoning.

ADDRESSES

Denmark

N. H. Diemer, Institute of Neuropathology, Frederik V's, Str. 2100 Copenhagen

D. K. J. Ekström von Lubitz, Institute of Neuropathology, 11, Frederik V's, Str. 2100 Copenhagen

E. Reske-Nielsen, Department of Neuropathology, Arhus Kommunehospital, DK-8000 Arhus C

E. Westergaard, Anatomy Department C., 1, Universitetsparken, Str. 2100 Copenhagen

Finland

M. Haltia, Department of Pathology, University of Helsinki 3, Haartmaninkatu Str., SF-00290 Helsinki 29

H. Kalimo, University of Turku, Department of Pathology, SF-20520 Turku 52

I., Paljärvo, University of Turku, Department of Pathology, SF-20520 Turku 52

GDR

J. Schneider, Pathological Institute, 5060 Erfurt, 74 Nordhäuser Str.

D. Schreiber, Pathological Institute, 5060 Erfurt, 74 Nordhäuser Str.

Norway

A. Torvik, Department of Pathology, Ulleval Hospital, Oslo 1

Poland

M. Dąmbska, Medical Research Centre, Division of Developmental Neuropathology, 3, Pasteur Str. 02—093 Warszawa

J. Dymecki, Psychoneurological Institute, Department of Neuropathology, 1/9 Sobieski Al., 02—957 Warszawa

D. Markiewicz, Psychoneurological Nnstitute, Department of Neuropathology, 1/9 Sobieski Al., 02—957 Warszawa

P. Olejniczak, Neurological Clinic, School of Medicine, 118, Traugutt Str., 50—420 Wrocław

K. Renkawek, Medical Research Centre, Department of Neuropathology 3 Dworkowa Str., 00—784 Warszawa

E. Simon, Institute of Pathology, Medical School 49 Przybyszewski Str., 60—355 Poznań

Z. Stelmasiak, Neurological Clinic, School of Medicine, 8 Jaczewski Str., 20—090 Lublin

M. Wender, Neurological Clinic, School of Medicine, 49 Przybyszewski Str., 60—355 Poznań

Sweden

E. Arvidson, Neuropathological Laboratory, Institute of Pathology P.O. Box 553, 751 22 Uppsala

K. Kristensson, Karolinska Institute, Department of Pathology, S-14186 Huddinge

C. Nordborg, Department of Pathology, Sahlgren Hospital, S—413 45 Göteborg

A. Oldfors, Department of Pathology, Sahlgren Hospital, S-413 45 Göteborg

Y. Olsson, Neuropathological Laboratory, Institute of Pathology P.O. Box 553, 751 22 Uppsala

L. Persson, Department of Pathology, Huddinge University Hospital, S-14186 Huddinge

P. Sourander, Division of Neuropathology, Institute of Pathology, Hospital Sahlgren, S-413 45 Göteborg

Ch. Tengvar, Neuropathological Laboratory, Department of Pathology, Dag Hammarskjolds väg 17, 75 122 Uppsala

NEUROPAT. POL., 1982, 20, 1—2
PL ISSN 0028—3894

HALINA WEINRAUDER, ZUZANNA KRAŚNICKA, BARBARA GAJKOWSKA

WPŁYW SUROWICY ANTYGLEJOWEJ NA POZAUSTROJOWĄ HODOWLĘ MÓŻDŻKU NOWORODKA SZCZURA

Zespół Neuropatologii Centrum Medycyny Doświadczalnej i Klinicznej PAN
Pracownia Ultrastruktury Układu Nerwowego Centrum Medycyny Doświadczalnej i Klinicznej PAN

Badania wpływu surowic o właściwościach demielinizujących na organotypowe hodowle tkanki nerwowej zostały zapoczątkowane przez Bornsteina i Appela w r. 1961. W dalszych pracach wykazano, że surowice królików uodpornianych całą substancją białą (Bornstein, Raine, 1970; Raine, Bornstein, 1970; Fry i wsp., 1972), mieliną (Bornstein, 1970) lub galaktocerebrozydami mózgu (Dubois-Dalcq i wsp., 1970; Fry i wsp., 1974) zawierają zależne od dopełniacza czynniki, które powodują demielinizację, zahamowanie różnicowania oligodendrocytów i zahamowanie mielinizacji w hodowli OUN. Efektu tego nie obserwowano przy stosowaniu surowic, pochodzących od zwierząt uodpornianych oczyszczonym białkiem zasadowym (Seil, 1977; Johnson, Bornstein, 1978) lub oczyszczonym proteolipidem mieliny (Mithen i wsp., 1980).

Poprzez połączenie technik immunologicznych i hodowli tkankowej uzyskano więc model do badania procesów tworzenia się mieliny, różnicowania oligodendrocytów i wzajemnych stosunków między różnymi typami komórek w hodowli. Reakcje hodowanej tkanki mogą dostarczyć informacji dotyczących swoistości przeciwciał zawartych w surowicach, roli jaką odgrywają one w procesach chorobowych, a także dają możliwość reprodukowania *in vitro* zmian morfologicznych i zaburzeń funkcji układu nerwowego przebiegających *in vivo*.

W poprzednich pracach (Weinrauder, Kraśnicka, 1980 a, b) wykazano, że surowice królików uodpornionych homogenatem lub wyciągiem z mózgu szczura zawierają przeciwciała, wiążące się na komórkach glejowych hodowanych *in vitro*. Celem obecnej pracy było stwierdzenie czy surowice te, podane do środowiska odżywczego hodowli, wywierają wpływ na ich obraz morfologiczny i ultrastrukturalny.

MATERIAŁ I METODY

Badania przeprowadzono na 1, 2, 3 i 4-tygodniowych hodowlach móżdżku noworodków szczurzych. Hodowle prowadzono wg metody opisanej poprzednio (Kraśnicka, Mossakowski, 1965).

Surowica odpornościowa. Posługiwano się surowicą przeciwko wyciągowi z mózgu szczura. Króliki uodporniano wyciągiem z mózgu w buforze fosforanowym o pH 7,3 z dodatkiem niepełnego adjuwantu Freunda (IFA, Difco). Surowicę o najwyższym poziomie przeciwciał precypitujących absorbowano w celu usunięcia przeciwciał o swoistości gatunkowej, zagęszczano do objętości wyjściowej i sączono przez sączki miliporowe. Jałową surowicę dodawano do medium odżywczego w objętości 20% i hodowle inkubowano przez 48 godzin. Po inkubacji z surowicą odpornościową siostrzane hodowle dokładnie przemywano i używano do barwień histologicznych oraz do badań w mikroskopie fluorescencyjnym i elektronowym.

Jako kontrolę stosowano normalną, jałową surowicę króliczą, dodawaną do medium w tej samej objętości.

Odczyn fluorescencji. Hodowle tkankowe inkubowane z surowicą odpornościową oraz hodowle kontrolne w tym samym wieku utrwalano w acetonie i inkubowano z tą samą surowicą odpornościową jaka była dodawana do medium. Preparaty inkubowano następnie z kozimi gammaglobulinami przeciwko gammaglobulinom króliczym, koniugowanymi z izotiocjanianem fluoresceiny i absorbowanymi pudrem z wątrób mysich oraz polimerem globulin surowicy ludzkiej. Kontrolę swoistości odczynu stanowiły preparaty inkubowane z normalną surowicą króliczą i PBS zamiast surowicy odpornościowej. Szczegóły przeprowadzania odczynu podano poprzednio (Weinrauder, Kraśnicka, 1980).

Barwienia histologiczne. Hodowle doświadczalne i kontrolne, oceniane w mikroskopie świetlnym, barwiono metodą Nissla i Bodiana.

Badania w mikroskopie elektronowym. Hodowle utrwalano w 4% glutaraldehydzie w buforze kakodylowym o pH 7,4 oraz w 2% czterotlenku osmu w tym samym buforze. Następnie materiał odwadniano w roztworach alkoholu o wzrastającym stężeniu i w tlenku propylenu oraz zatapiano w Eponie 812. Ultracienkie preparaty podbarwiano na siateczkach octanem uranylu i cytrynianem ołowiu. Zdjęcia wykonywano w mikroskopie elektronowym JEM 7A.

WYNIKI

Badania w mikroskopie świetlnym

W okresie wzrostu hodowli, od 1 do 4 tygodni, po podaniu do medium surowicy odpornościowej obserwowano dyskretne zmiany dotyczące oligodendrocytów, przeważnie w strefie wzrostu. W hodowlach 1-tygodniowych (ryc. 1) spotykano komórki z jądrami typowymi dla

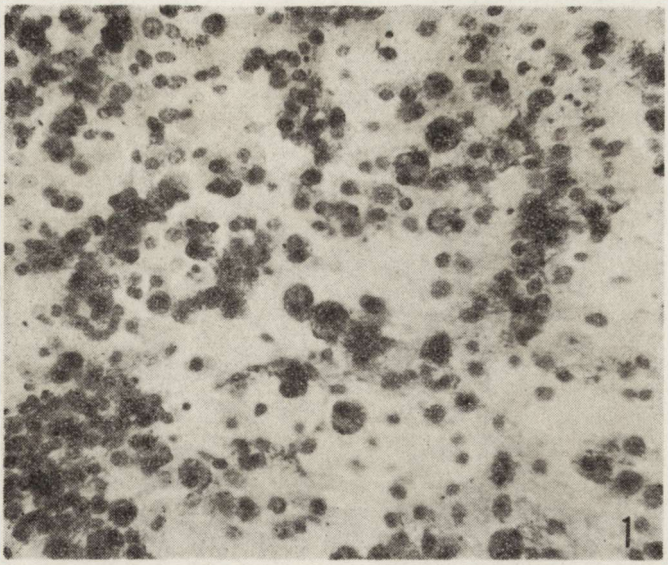

Ryc. 1. Hodowla 1-tyg. Widoczne zmienione komórki glejowe pozbawione wypustek. Nissl. Pow. 200 ×

Fig. 1. One-week culture. Altered glia cells depleted of processes. Nissl. × 200

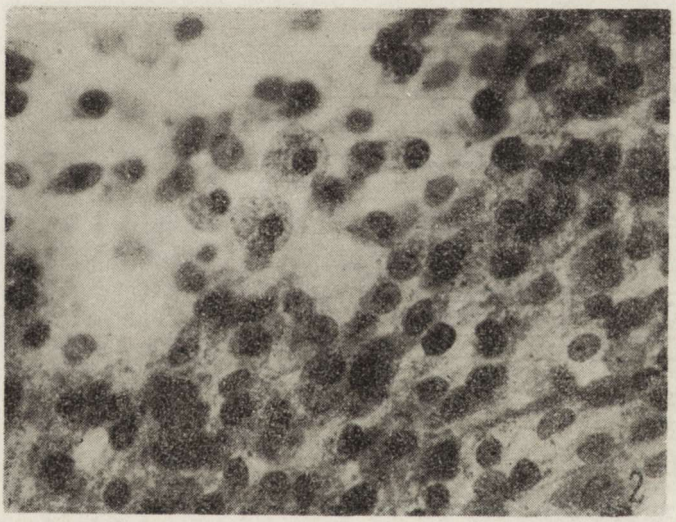

Ryc. 2. Hodowla 3-tyg. Obraz hodowli podobny jak w przypadku hodowli 1-tygodniowej. Nissl. Pow. 400 ×

Fig. 2. Three-week culture. Appearance similar to one-week culture. Nissl. × 400

oligodendrocytów, których perykariony przybierały kształty okrągłe. Komórki te pozbawione były wypustek, barwiły się intensywniej błękitem toluidyny, a w ich cytoplazmie spostrzegano drobne wodniczki. Astrocyty i neurocyty nie wykazywały widocznych zmian.

Hodowle starsze (2, 3 i 4-tygodniowe) poddane działaniu surowicy wykazywały zmiany o podobnym charakterze, dotyczące oligodendrocy-

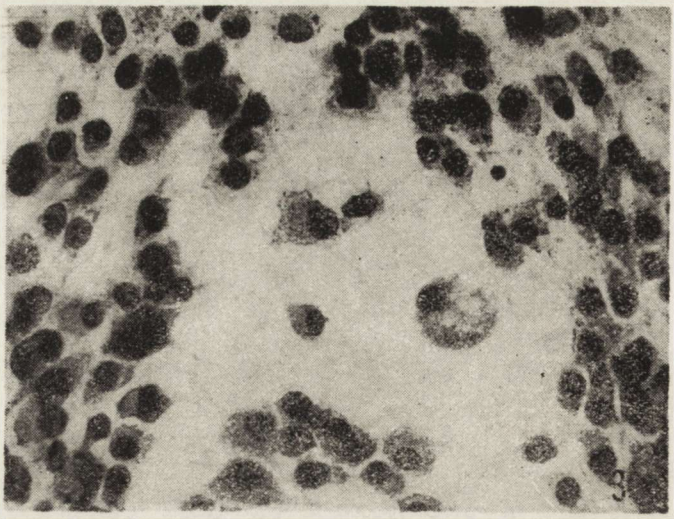

Ryc. 3. Hodowla 4-tyg. Część komórek o prawidłowym wyglądzie. Widoczne komórki o różnym stopniu uszkodzenia. Nissl. Pow. 400 ×

Fig. 3. Four-week culture. A part of the cells with normal appearance. Visible cells with a different degree of damage. Nissl. × 400

Ryc. 4. Hodowla 1-tyg. Odczyn immunofluorescencji (IF). Skupienie bezwypustkowych oligodendrocytów z bardzo silnym świeceniem cytoplazmy. Astrocyty ze znacznie słabszym odczynem. Pow. 200 ×

Fig. 4. One-week culture. Immunofluorescence reaction (IF). Accumulation of oligodendrocytes free of processes with very strong fluorescence of cytoplasm. Astrocytes with a much weaker reaction. × 200

tów (ryc. 2). Liczba zmienionych bezwypustkowych oligodendrocytów wydawała się największa w hodowlach 2 i 3-tygodniowych. W hodowlach 3 i 4-tygodniowych obserwowano liczne formy pośrednie — od komórek o prawidłowym wyglądzie i z wypustkami, aż do oligodendrocytów

obrzmiałych, całkowicie pozbawionych wypustek (ryc. 3). Pozostałe elementy komórkowe starszych hodowli nie wykazywały odchyleń od normy.

W barwieniu metodą Bodiana, hodowle we wszystkich badanych okresach wykazywały obecność komórek pozbawionych wypustek.

Hodowle inkubowane przez 48 godzin z 20% normalnej surowicy króliczej miały wygląd prawidłowy, nie odbiegający od obrazów obserwowanych w hodowlach kontrolnych.

Badania w mikroskopie fluorescencyjnym

W hodowlach kontrolnych (bez dodawania do medium surowicy odpornościowej) obserwowano świecenie dwóch typów komórek — silniejsze w oligodendrocytach i nieco słabsze w astrocytach. Obrazy fluorescencji w hodowlach 1—4-tygodniowych nie różniły się od poprzednio opisanych (Weinrauder, Kraśnicka, 1980).

W hodowlach poddanych działaniu surowicy odpornościowej obraz fluorescencji był nieco zmieniony. W hodowlach 1-tygodniowych obserwowano skupienia okrągłych komórek z silną fluorescencją, odpowiadające bezwypustkowym komórkom spotykanym w preparatach barwionych metodami histologicznymi. Spotykano także oligodendrocyty o prawidłowym wyglądzie, z silnym świeceniem skąpej cytoplazmy. Fluorescencja w astrocytach była słabsza niż w hodowlach kontrolnych (ryc. 4).

W hodowlach 2-tygodniowych obserwowano populacje zarówno zmienionych jak i niezmienionych oligodendrocytów. Obraz fluorescencji oligodendrogleju o prawidłowym wyglądzie nie odbiegał od obserwowanego w hodowlach kontrolnych. Bardzo silne, homogenne świecenie wykazywały okrągłe pozbawione wypustek oligodendrocyty. Silne świecenie stwierdzano także w eksplantacie. Astrocyty w strefie wzrostu przeważnie nie wykazywały dodatniej fluorescencji (ryc. 5).

W hodowlach 3 i 4-tygodniowych spotykano liczniejsze skupienia silnie świecących oligodendrocytów pozbawionych wypustek: liczba ich była różna w poszczególnych hodowlach. Pole tak zmienionych komórek w hodowli 4-tygodniowej przedstawia ryc. 6.

Wszystkie odczyny kontrolne przy użyciu normalnej surowicy króliczej i PBS były całkowicie ujemne, co wskazuje na swoistość obrazów immunofluorescencyjnych.

Badania w mikroskopie elektronowym

Hodowle 1-tygodniowe. Badania mikroskopowo-elektronowe wykazały nieznaczne zmiany w ultrastrukturze mało zróżnicowanych komórek glejowych. W niektórych komórkach obserwowano słaby obrzęk mitochondriów polegający na przejaśnieniu macierzy i skróceniu grze-

Ryc. 5. Hodowla 3-tyg. IF. Pole astrocytów z ujemnym odczynem immunofluorescencyjnym. Widoczne pojedyncze oligodendrocyty z dodatnim odczynem w cytoplazmie oraz bardzo silny odczyn w komórce bezwypustkowej. Pow. 200 ×
Fig. 5. Three-week culture. IF. Field of astrocytes with negative reaction. Single oligodendrocytes with a positive reaction in cytoplasm and very strong reaction in a cell free of processes. × 200

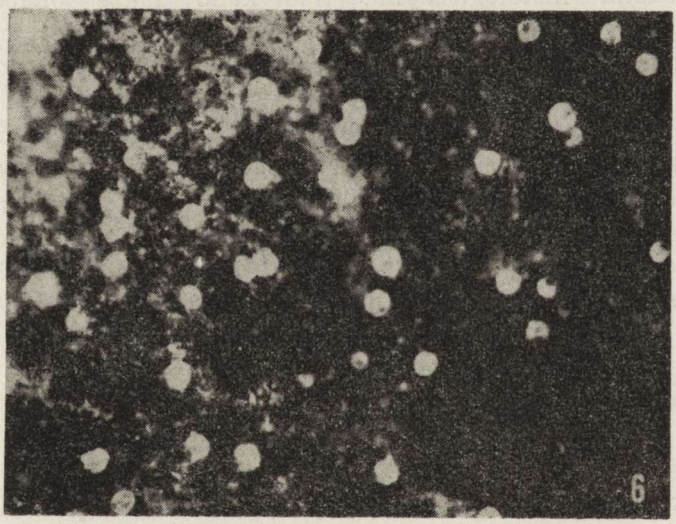

Ryc. 6. Hodowla 4-tyg. IF. W pobliżu silnie świecącego eksplantatu liczne pozbawione wypustek oligodendrocyty z bardzo intensywnym odczynem (widoczne jądro całkowicie ujemne). Pow. 200 ×
Fig. 6. Four-week culture. IF. In the vicinity of strongly fluorescent explantate, numerous oligodendrocytes free of processes with very strong reaction (totally negative nucleus). × 200

bieni mitochondrialnych (ryc. 7). Charakterystyczną cechą większości komórek glejowych była uboga szorstka siatka śródplazmatyczna; niektóre jej kanały były znacznie rozdęte i pokryte nielicznymi rybosoma-

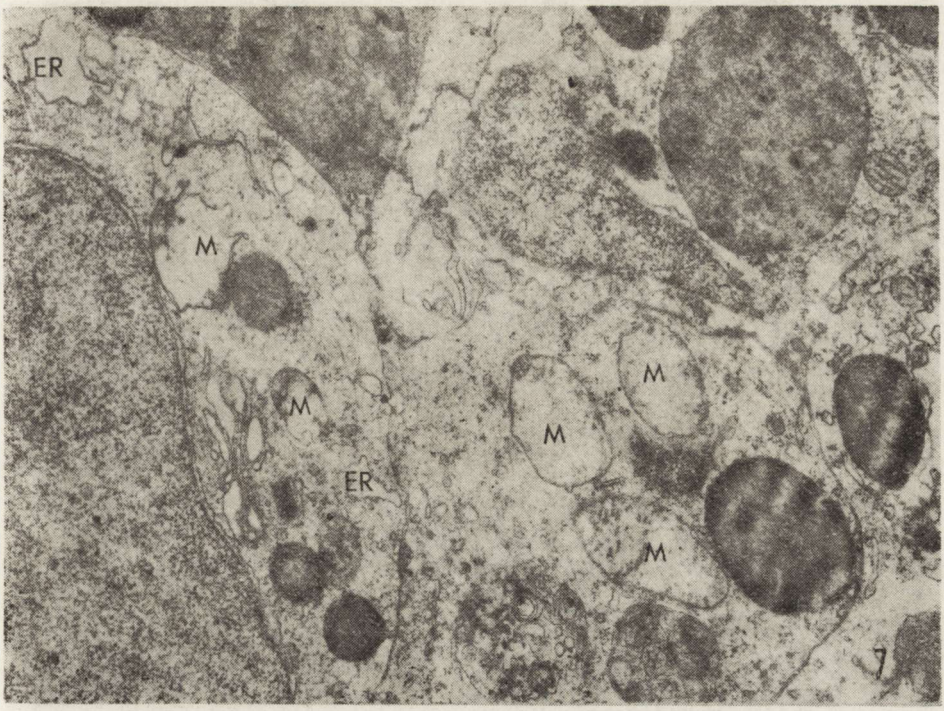

Ryc. 7. Hodowla 1-tyg. Fragmenty niezróżnicowanych komórek glejowych. W cytoplazmie widoczne obrzmiałe mitochondria (M), poszerzone kanały siatki śródplazmatycznej szorstkiej (ER) z małą ilością rybosomów, lizosomy i ciała lizosomopodobne. Pow. 9 300 ×

Fig. 7. One-week culture. Fragments of nondifferentiated glia cells. In cytoplasm swollen mitochondria (M), dilated rough endoplasmic reticulum channels (ER) with the small number of ribosomes, lysosomes and lysosome-like bodies. × 9 300

mi. W cytoplazmie komórek glejowych stwierdzono ciała gęste i kule tłuszczu. Sporadycznie obserwowano pojedyncze elementy włókniste (gliotubule). Aparat Golgiego nie wykazywał odchyleń od normy.

Hodowle 2-tygodniowe. Obserwacje mikroskopowo-elektronowe nie wykazały istotnych zmian w budowie ultrastrukturalnej komórek nerwowych. Natomiast zaobserwowano niewielkie zmiany w astrocytach polegające na zwiększonej ilości elementów włóknistych, przeważnie gliofibryli i ziarnistości glikogenowych. Niektóre astrocyty wykazywały również nieznaczne cechy obrzmienia cytoplazmy i mitochondriów. Najwyraźniejsze zmiany ultrastrukturalne obserwowano w cytoplazmie oligodendrocytów. Zmiany te wyrażały się przede wszystkim proliferacją siatki gładkiej, obecnością licznych, drobnych pęcherzyków i większych wakuoli, wypełniających prawie całą cytoplazmę. W obwodowej części perykarionów oligodendrocytów widoczne były krótkie i niekiedy rozdęte kanały siatki szorstkiej z nielicznymi rybosomami. W cytoplazmie niektórych oligodendrocytów stwierdzono obecność struktur mielinopodobnych (ryc. 8).

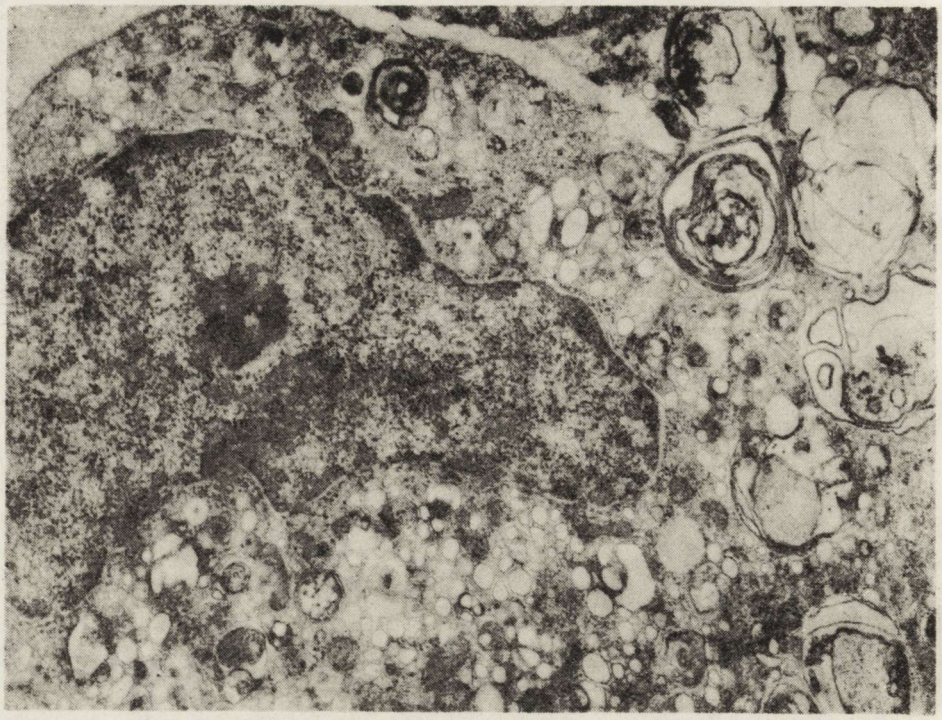

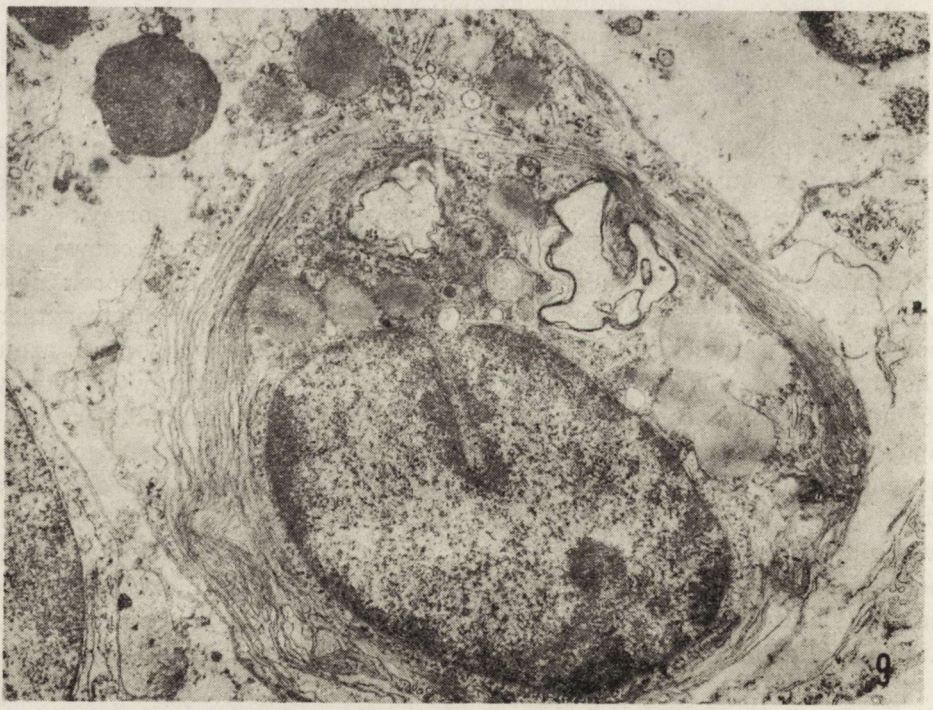

Większość włókien nerwowych wykazywała duży stopień uszkodzenia mieliny. Wyraźne było rozluźnienie blaszek mielinowych. Aksoplazma niektórych włókien zawierała ziarna glikogenu i wykazywała różnego stopnia zwyrodnienie.

Hodowle 3-tygodniowe. Zmiany ultrastrukturalne dotyczyły głównie komórek glejowych, natomiast neurony nie wykazywały odchyleń od stanu prawidłowego.

W większości oligodendrocytów obserwowano zmiany podobne do stwierdzonych w hodowlach 2-tygodniowych. Ich cytoplazma zawierała

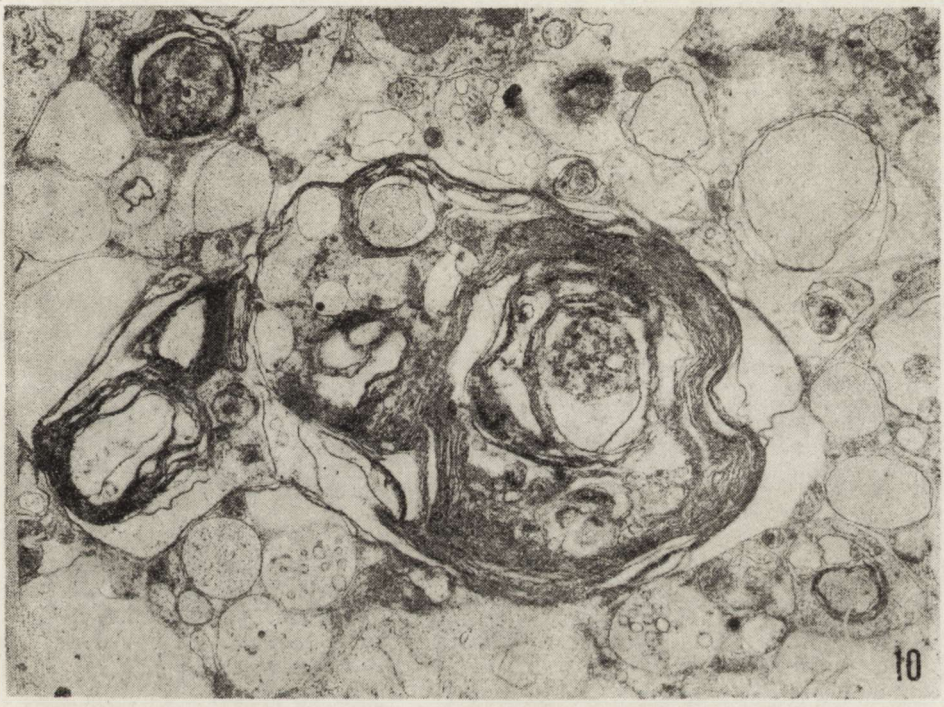

Ryc. 10. Hodowla 3-tyg. Widoczne liczne włókna nerwowe w różnych stadiach mielinizacji. Wyraźne uszkodzenie struktury blaszek mielinowych i aksoplazmy. Pow. 9 000 ×

Fig. 10. Three-week culture. Numerous nerve fibers at different stages of myelination. Marked impairment of the structure of myelin lamellae and axoplasm. × 9 000

Ryc. 8. Hodowla 2-tyg. Fragment oligodendrocyta. W cytoplazmie widoczne namnożenie siatki gładkiej, ciała lizosomopodobne i ciała mielinowe. Obok komórki włókna zmielinizowane z uszkodzoną strukturą mieliny. Pow. 9 300 ×

Fig. 8. Two-week culture. Oligodendrocyte fragment. In cytoplasm proliferation of smooth reticulum, lysosome-like bodies and myelin bodies. Close to the cell myelinated fibers with impaired myelin structure. × 9 300

Ryc. 9. Hodowla 3-tyg. Komórka oligodendrogleju oraz włókna z kilkoma warstwami mieliny otoczone wspólną osłonką mielinową. W skąpej cytoplazmie oligodendrocyta widoczne kule tłuszczowe. Pow. 9 000 ×

Fig. 9. Three-week culture. Oligodendrocyte and fibers with a few layers of myelin surrounded by a common myelin sheath. In poorcytoplasm of oligodendrocyte lipid balls. × 9 000

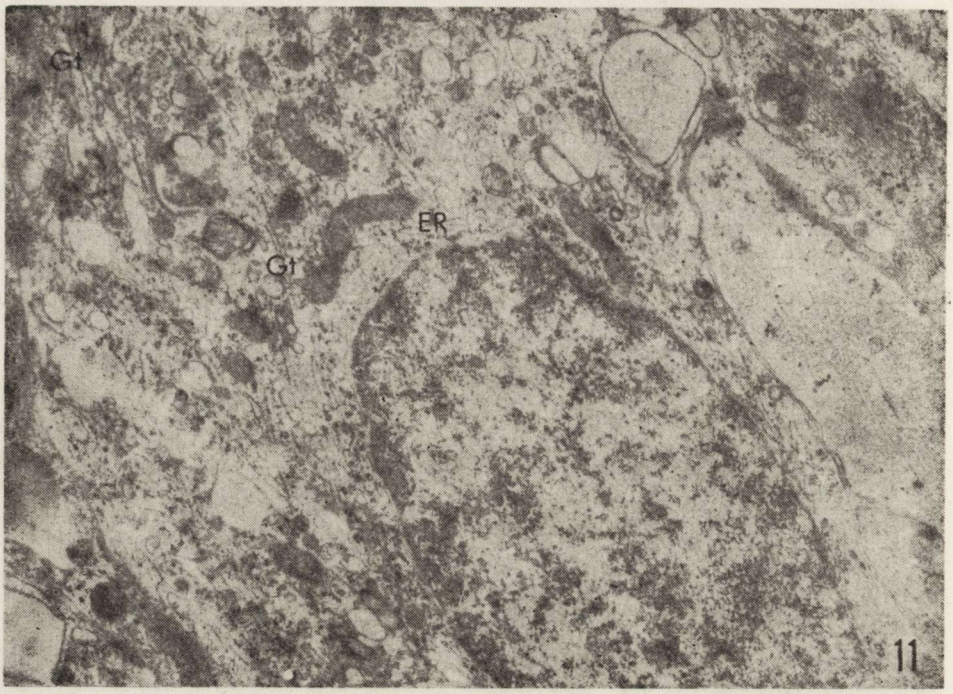

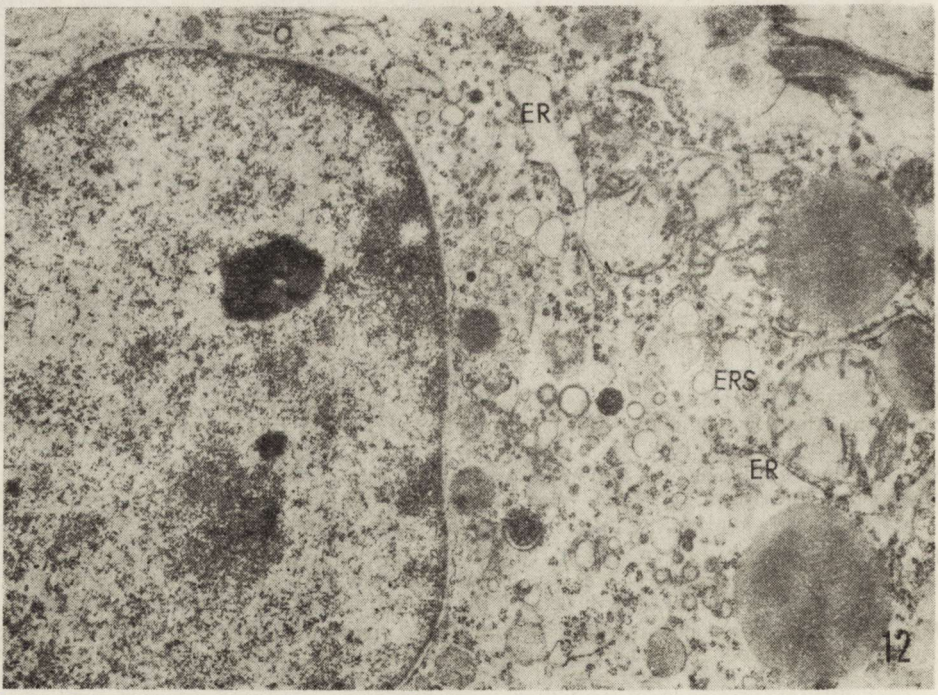

dużą ilość siatki gładkiej; w niektórych spotykano ponadto kule tłuszczu oraz struktury mielinopodobne. Siatka szorstka była bardzo skąpa, występowała w postaci krótkich kanałów z niewielką ilością rybosomów. W tej grupie doświadczalnej zaobserwowano wytwarzanie się wielowarstwowej błony komórkowej wokół nielicznych oligodendrocytów za-

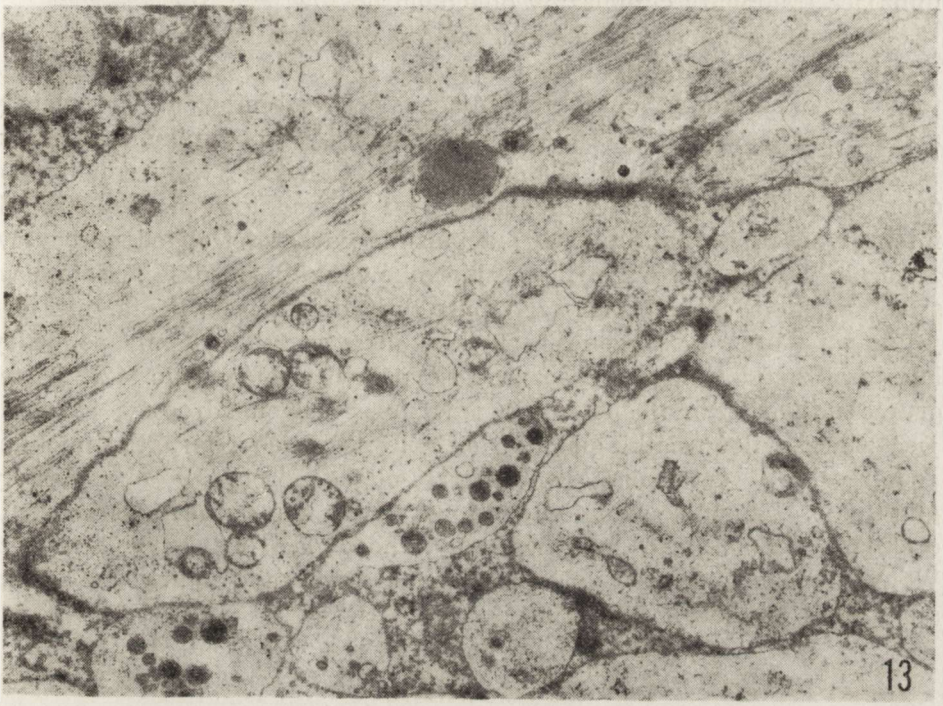

Ryc. 13. Hodowla 4-tyg. Widoczne obrzmiałe wypustki astrocytów z obecnością gliofilamentów. Pow. 9 300 ×

Fig. 13. Four-week culture. Swollen astrocyte processes with the presence of gliofilaments. × 9 300

Ryc. 11. Hodowla 2-tyg. Fragment astrocyta z niewielkimi zmianami ultrastrukturalnymi. W cytoplazmie widoczne krótkie kanały szorstkiej siatki śródplazmatycznej, (ER), niezmienione mitochondria, dość liczne gliotubule (Gt). Obok widoczny fragment nieznacznie obrzmiałej wypustki astrocyta. Pow. 9 000 ×

Fig. 11. Two-week culture. Fragment of astrocyte with slight ultrastructural changes. In cytoplasm short rough endoplasmic reticulum channels (ER), unchanged mitochondria, relatively numerous gliotubules (Gt). In the vicinity fragment of a slightly swollen astrocyte process. × 9 000

Ryc. 12. Hodowla 4-tyg. Fragment oligodendrocyta. W cytoplazmie widoczne poszerzone kanały szorstkiej siatki śródplazmatycznej (ER) oraz liczne polirybosomy. Ponadto nieliczne pęcherzykowate układy siatki gładkiej (ERS), obrzmiałe mitochondria i kule tłuszczowe. Pow. 9 300 ×

Fig. 12. Four-week culture. Oligodendrocyte fragment. In cytoplasm dilated rough endoplasmic reticulum channels (ER) and numerous polirybosomes. Beside a few vesicular structures made of smooth reticulum (ERS), swollen mitochondria and lipid balls. × 9 300

angażowanych w proces mielinizacji aksonów (ryc. 9). Większość obserwowanych aksonów, zwłaszcza w początkowych stadiach mielinizacji, wykazywała prawidłową budowę ultrastrukturalną aksoplazmy i mieliny. Jednak w porównaniu z hodowlami 2-tygodniowymi, nasilał się nieprawidłowy proces mielinizacji. Widoczne było rozluźnienie blaszek mielinowych i wypełnienie przestrzeni między nimi substancją przypominającą fragmenty cytoplazmy oligodendrocytów (ryc. 10).

Większość obserwowanych astrocytów nie wykazywała nieprawidłowości w budowie organelli komórkowych (ryc. 11), jednakże spotykano pojedyncze astrocyty charakteryzujące się przejaśnieniem cytoplazmy z małą ilością organelli. Zmiany te świadczyły o obrzmieniu komórek.

Hodowle 4-tygodniowe. Hodowane komórki wykazywały zmiany podobne do obserwowanych w hodowlach 2 i 3-tygodniowych, jednakże ich intensywność była mniejsza. W cytoplazmie większości oligodendrocytów zwracała uwagę mniejsza ilość zbiorników siatki gładkiej. Natomiast szorstka siatka śródplazmatyczna była dość dobrze rozwinięta, niektóre jej kanały były poszerzone i zwykle pokryte rybosomami; pomiędzy kanałami znajdowała się znaczna ilość polirybosomów (ryc. 12). W tej grupie doświadczalnej spotykano pojedyncze oligodendrocyty, zawierające znaczną ilość siatki gładkiej, ciał tłuszczowych i struktur mielinopodobnych. W cytoplazmie większości oligodendrocytów obecne były gliotubule. Zmielinizowane włókna nerwowe wykazywały uszkodzenia o stopniu podobnym do opisywanego w hodowlach 2 i 3-tygodniowych. W astrocytach obserwowano obrzmienie cytoplazmy, a niekiedy zwiększoną ilość gliofibryli (ryc. 13).

OMÓWIENIE

Inkubowanie hodowli móżdżku noworodków szczurzych w medium z dodatkiem 20% nieinaktywowanej surowicy antyglejowej przez 48 godz. wywoływało zmiany morfologiczne w komórkach glejowych. Zmiany obserwowane w mikroskopie świetlnym były dyskretne i dotyczyły oligodendrocytów, których część leżąca w strefie wzrostu traciła wypustki, przybierała kształt okrągły, a ich cytoplazmę wypełniały liczne wodniczki. Zmiany te były niezależne od wielu hodowli, jedynie w hodowlach starszych zmienione komórki były liczniejsze. Pozostałe elementy komórkowe hodowli nie wykazywały dostrzegalnych zmian. Dodanie do medium normalnej surowicy króliczej w tym samym stężeniu nie wpływało na morfologiczny obraz hodowli.

Podanie do medium surowicy antyglejowej miało nieznaczny wpływ na obraz immunofluorescencji we wszystkich grupach wiekowych hodowli. Obserwowano populacje prawidłowych komórek, w których świecenie było podobne jak w hodowlach kontrolnych. Spotykano jednak

również komórki znacznie zmienione, o bardzo intensywnym, homogennym świeceniu, które odpowiadały oligodendrocytom z utraconymi wypustkami. Liczba tych komórek wzrastała z wiekiem hodowli. Struktura fluorescencji niektórych oligodendrocytów uwidaczniała również wodniczki obserwowane w cytoplazmie w barwieniu histologicznym. Świecenie astrocytów było słabsze niż w hodowlach kontrolnych, w niektórych hodowlach obserwowano pola astrocytów całkowicie ujemnych.

Zmiany ultrastrukturalne były znacznie silniej zaznaczone, co szczególnie dotyczyło oligodendrocytów w 2 i 3 tygodniu wzrostu hodowli. Cytoplazma tych komórek wykazywała charakterystyczne uszkodzenia w postaci zwiększonej ilości zmienionej siatki gładkiej i zmniejszenia ilości szorstkiej siatki śródplazmatycznej. Równolegle z uszkodzeniem oligodendrocytów obserwowano duże zmiany w strukturze mieliny, świadczące o nieprawidłowym procesie mielinizacji.

Zmiany ultrastrukturalne w astrocytach były znacznie słabiej zaznaczone, polegały na nieznacznym obrzmieniu cytoplazmy oraz na niewielkim zwiększeniu ilości gliofilamentów i zmniejszeniu (w pojedynczych komórkach) ilości gładkiej siatki śródplazmatycznej.

Neurony we wszystkich okresach wzrostu hodowli nie wykazywały nieprawidłowości ultrastrukturalnych.

Obserwowane zmiany świadczą o swoistym oddziaływaniu surowicy odpornościowej na komórki glejowe. Surowica ta zawiera przeciwciała zarówno przeciwko oligo- jak i astrocytom. Jednak, jak wynika z poprzednich obserwacji (Weinrauder, Kraśnicka 1980), reakcja surowicy z oligodendrocytami jest znacznie silniejsza, świadcząc o większej zawartości swoistych antygenów w oligodendrogleju, bądź o niższym poziomie przeciwciał skierowanych przeciwko astrocytom. Wyraźnie nasilone zmiany w oligodendrocytach stanowią potwierdzenie tej obserwacji.

Obserwowane równolegle z uszkodzeniem oligodendrogleju zaburzenia procesu mielinizacji, rozpoczynające się od cytoplazmy oligodendrocytów i nieprawidłowości w strukturze mieliny, przemawiają za pierwotnym uszkodzeniem oligodendrocytów, a więc stanowią również potwierdzenie swoistego oddziaływania surowicy odpornościowej. Biorąc pod uwagę, że surowica pochodzi od królika uodpornionego wodnym wyciągiem z mózgu z dodatkiem niepełnego adjuwantu Freunda, u którego nie obserwowano objawów alergicznego zapalenia mózgu i rdzenia, nie należało się spodziewać obecności w niej przeciwciał przeciwko mielinie — zatem należy uznać, że zaburzenia mielinizacji są wtórne w stosunku do pierwotnego uszkodzenia i zaburzenia funkcji oligodendrocytów.

Wpływ na hodowlę surowicy odpornościowej zawierającej dopełniacz sugeruje immunologiczny charakter reakcji, jednak ostateczne jego po-

twierdzenie będzie można uzyskać po zastosowaniu do badań surowic pozbawionych dopełniacza i surowic z dodatkiem dopełniacza heterologicznego. Różnice w oddziaływaniu na hodowle surowic zawierających i nie zawierających dopełniacza były stwierdzane w badaniach nad demielinizacją i hamowaniem mielinizacji (Bornstein, Raine, 1977; Ulrich, Lardi, 1978; Raine i wsp., 1978; Johnson i wsp., 1979; Lapin i wsp., 1979). Obserwowano także różnice w obrazie demielinizacji lub uszkodzenia oligodendrocytów w zależności od stężenia surowicy i wieku hodowli (Ulrich, Lardi, 1978). To ostatnie stwierdzenie wykazuje pewną analogię z naszymi badaniami — nasilenie zmian w hodowlach 2- i 3-tygodniowych sugeruje większą wrażliwość aktywnych, różnicujących się oligodendrocytów na działanie surowicy. Być może pewną rolę odgrywa także większe stężenie swoistego antygenu w bardziej dojrzałych komórkach. Tego rodzaju sugestie wysunęli w swoich badaniach Johnson i wsp. (1979).

Charakter zmian ultrastrukturalnych oligodendrocytów, a szczególnie zwiększenie ilości siatki gładkiej, przy równoczesnym (niekiedy bardzo znacznym) zmniejszeniu ilości szorstkiej siatki śródplazmatycznej, może przemawiać za zmniejszoną syntezą białek. Osłabienie intensywności fluorescencji, świadczące o zmniejszonej w niektórych komórkach produkcji antygenów, może poprzeć ten pogląd. Trudno jest jednak na podstawie dotychczasowych badań wypowiedzieć się, czy jest to swoiste zahamowanie produkcji antygenów białkowych czy też efekt bardziej ogólny.

Zbliżone obrazy ultrastrukturalne obserwowano w hodowlach poddanych działaniu demielinizującej surowicy antycerebrozydowej (Dubois-Dalcq i wsp., 1970), ale dotyczyły one głównie neuronów, a także innych elementów komórkowych i zachodziły w znacznie krótszym czasie. Autorzy przypisują je nieswoistemu toksycznemu oddziaływaniu niektórych surowic na hodowlę. Nasilenie zmian w oligodendrocytach w określonym okresie rozwoju hodowli obserwowane przez nas pozwala wyłączyć możliwość takiego toksycznego działania surowicy.

Zmiany w astrocytach obserwowane w odczynie immunofluorescencji (osłabienie świecenia lub odczyn negatywny) mogą sugerować obniżenie syntezy swoistego antygenu. Zjawisko to nie znajduje jednak odbicia w ultrastrukturalnych obrazach tych komórek. Zmiany w tym typie neurogleju są mało swoiste i były już obserwowane w hodowlach prowadzonych w warunkach niedotlenienia (Kraśnicka, i wsp., 1973; 1976) lub w zatruciu tlenkiem węgla (Korthals i wsp., 1973).

Kontynuacją zapoczątkowanych badań będzie stwierdzenie, czy usunięcie z medium surowicy odpornościowej spowoduje powrót do normy uszkodzonych komórek, tak jak to ma miejsce w procesach demielinizacji hodowli, zdemielinizowanych działaniem surowic EAE.

EFFECT OF ANTIGLIA SERUM ON RAT CEREBELLAR TISSUE CULTURE

Summary

The effects of antiserum against rat brain extract on the morphological and ultrastructural picture of organotypic culture of the newborn rat cerebellum were investigated.

The studies were performed on 1-, 2-, 3- and 4-week cultures. The incubation medium was supplemented with 20% non inactivated immune rabbit serum and the cultures were incubated for 48 h. A part of them was stained after Nissl and Bodian and another part was routinely fixed and stained for electron microscopy.

Light microscopic observations revealed slight changes in oligodendrocytes, mostly in the outgrowth zone. The cells lost their processes and the cytoplasm contained small vacuoles. Most pronounced changes were observed in 2- and 3-week cultures. No changes were noticed in the other cellular elements.

Electron microscopic observations of 1-week cultures disclosed minute changes in the ultrastructure of poorly differentiated glial cells. Most marked changes, consisting in the proliferation of smooth endoplasmic reticulum and appearance of numerous small vesicles filling cytoplasm, were observed in oligodendrocytes in 2-week cultures. Myelin-like structures became apparent in some of the cells. In astrocytes, the changes were rather insignificant and consisted mainly in the increased number of gliofibrills and glycogen granules and slight swelling of cytoplasm. In 3-week cultures, the changes in most of the oligodendrocytes were similar; some of them were covered by a multilayer cell membrane. The features of irregular myelination became more pronounced. At all stages of the culture growth, degenerative changes of varying intensity were observed in neuronal processes but not in neuronal perikarya.

PIŚMIENNICTWO

1. Bornstein M. B., Appel S. H.: The application of tissue culture to the study of experimental "allergic" encephalomyelitis. I. Patterns of demyelination. J. Neuropath. exp. Neurol., 1961, 20, 141—157.
2. Bornstein M. B., Raine C. S.: Experimental allergic encephalomyelitis. Antiserum inhibition of myelination in vitro. Lab. Invest., 1970, 23, 536—542.
3. Bornstein M. B., Raine C. S.: Multiple sclerosis and experimental allergic encephalomyelitis: specific demyelination of CNS in culture. Neuropath. appl. Neurobiol., 1977, 3, 359—367.
4. Dubois-Dalcq M., Niedeck B., Buyse M.: Action of anti-cerebroside sera on myelinated nervous tissue culture. Path. Europ., 1970, 5, 331—347.
5. Fry J. M., Lehrer C. M., Bornstein M. B.: Sulfatide synthesis: inhibition by experimental allergic encephalomyelitis serum. Science, 1972, 175, 192—193.
6. Fry J. M., Weissbarth S., Lehrer G. M., Bornstein M. B.: Cerebroside antibody inhibits sulfatide synthesis and myelination and demyelinates in cord tissue cultures. Science, 1974, 183, 540—542.
7. Johnson A. B., Bornstein M. B.: Myelin-binding antibodies in vitro. Immunoperoxidase studies with experimental allergic encephalomyelitis, anti-galactocerebroside and multiple sclerosis sera. Brain Res., 1978, 159, 173—182.
8. Johnson A. B., Raine C. S., Bornstein M. B.: Experimental allergic encephalomyelitis: serum immunoglobulin binds to myelin and oligodendrocytes in cultured tissue: ultrastructure-immunoperoxidase observations. Lab. Invest., 1979, 40, 568—575.

9. Korthals J., Hoppe B., Karwacka H.: Badania mikroskopowo-elektronowe nad toksycznym wpływem tlenku węgla na tkankę glejową hodowaną in vitro. Neuropat. Pol., 1973, 11, 315—322.
10. Kraśnicka Z., Mossakowski M. J.: Zagadnienie zmienności morfologicznej tkanki glejowej hodowanej in vitro. Neuropat. Pol., 1965, 3, 397—408.
11. Kraśnicka Z., Renkawek K., Gajkowska B.: Wpływ krótkotrwałej anoksji na obraz ultrastrukturalny komórek glejowych hodowanych in vitro. Neuropat. Pol., 1973, 11, 399—404.
12. Kraśnicka Z., Gajkowska B., Mossakowski M. J.: Effect of short-lasting anoxia on in vitro culture of cerebellum. Neuropat. Pol., 1976, 14, 11—22.
13. Lapin E. P., Maker H. S., Lehrer G. M., Weissbarth S., Raine C. S., Johnson A. B., Bornstein M. B.: Effects of anti-white matter serum on myelin and lipid synthesis in brain prisms. Brain Res., 1979, 173, 513—526.
14. Mithen F., Bunge R., Aggrawal H.: Proteolipid protein antiserum does not affect CNS myelin in rat spinal cord culture. Brain Res., 1980, 197, 477—483.
15. Raine C. S., Bornstein M. B.: Experimental allergic encephalomyelitis: an ultrastructural study of experimental demyelination in vitro. J. Neuropath. exp. Neurol., 1970a, 29, 177—191.
16. Raine C. S., Bornstein M. B.: Experimental allergic encephalomyelitis: a light and electron microscope study of remyelination and "sclerosis" in vitro. J. Neuropath. exp. Neurol., 1970b, 29, 552—561.
17. Raine C. S., Diaz M., Pakingan M., Bornstein M. B.: Antiserum-induced dissociation of myelinogenesis in vitro. An ultrastructure study. Lab. Invest., 1978, 38, 397—403.
18. Seil F. J.: Tissue culture in demyelinating diseases: a critical review. Ann. Neurol., 1977, 2, 345—355.
19. Ulrich J., Lardi H.: Multiple sclerosis: demyelination and myelination inhibition of organotypic tissue cultures of the spinal cord by sera of patients with multiple sclerosis and other neurological diseases. J. Neurol., 218, 1978, 7—16.
20. Weinrauder H., Kraśnicka Z.: Antygeny glejowe w hodowli tkankowej móżdżku szczura. Neuropat. Pol., 1980, 18, 181—190.
21. Weinrauder H., Kraśnicka Z.: Lokalizacja antygenów glejowych o różnej swoistości w pozaustrojowej hodowli tkanki nerwowej. Neuropat. Pol., 1980, 18, 337—351.

Adres autorów: Centrum Medycyny Doświadczalnej i Klinicznej PAN, ul. Dworkowa 3, 00—784 Warszawa

NEUROPAT. POL., 1982, 20, 1—2
PL ISSN 0028—3894

MIECZYSŁAW WENDER, MARIA ŚNIATAŁA-KAMASA,
ALEKSANDER PIECHOWSKI

MYELIN OF THE OPTIC NERVE IN RATS CHRONICALLY INTOXICATED WITH TRIETHYL TIN SULFATE (TET) *

Department of Neurology, Academy of Medicine, Poznań

Myelin lesions occur in several human and experimental diseases and are most frequently the result of a pathological process known under the term of demyelination. However, the mechanisms underlying myelin destruction have not been resolved in detail so far.

In EAE demyelination may result from the action of macrophages. Nonetheless, interlamellar splitting and vesiculation of myelin lamellae may also occur without an apparent involvement of phagocytic stripping or exogenous cell invasion (Lampert, 1965; Raine et al., 1969). The mechanism of this type of myelin decomposition is not well understood, as are those observed in many toxic processes, in which demyelination occurs as an early most likely primary effect of intoxication.

Some other, very specific myelin changes — in the form of massive intramyelin vacuolisation have been found in either acute or chronic TET intoxication. The chronic form of TET intoxication, with its remitting clinical picture and persisting very severe myelin changes (Eto et al., 1971) presents a convenient experimental model for studying not only the mechanism of toxic demyelination but also for studies of the effects of myelin destruction on brain function.

The herewith presented results of our ultrastructural studies of changes occurring in the optic nerve myelin following chronic TET intoxication should contribute to a better understanding of these problems.

MATERIAL AND METHODS

Adult Wistar rats were chronically intoxicated with TET sulfate according to the technique of Eto et al. (1971). The poison was administered in their drinking water. The contaminated water was accessible ad

* Supported by the Research Grant J-05-092-N.

libitum. The concentration of the poison was: 5 mg/liter during the first 16 days, 10 mg/liter during the next 14 days. During the consecutive 10 day periods the concentration of TET was changed alternately from 5 to 10 mg/l.

The experimental rats were killed by decapitation after various periods of TET intake (10, 28, 60, and 74 days) and their brains dissected across the region of the optic chiasma. The material for ultrastructural examination was fixed routinely by immersion in a mixture of glutaraldehyde and paraformaldehyde followed by osmium tetroxide. The sections were then dehydrated by means of ethanol and acetone and next were embedded in Epon. Semithin sections were stained with toluidine blue. Ultrathin sections were poststained with uracyl acetate and lead citrate and examined in the JEM-7A electron microscope.

RESULTS

Clinical picture

Starting from the second day of TET intake, the animals grew gradually somnolent. In the fourth week of experimental poisoning paresis of the hind legs and sphincter paralysis became manifest. During the eighth week, considerable improvement with respect to paresis of extremities and sphincter paralysis and general reactivity was observed.

Morphological pattern

On toluidine blue stained semithin sections of the optic nerve taken during the subsequent days of intoxication increasing vacuolar changes were seen in the myelin (Fig. 1).

Myelin changes are the dominating electron microscopic features occurring in the optic nerve following TET intoxication, with intramyelin vacuolization — leading frequently to delamination of the individual myelin lamellae (Figs. 2—4) — as the most characteristic exponent. Vacuolization occurrs predominantly within the outer layers of the myelin sheath, i.e. within the so called loose myelin lamellae. The interior of the vacuoles is electron transparent. Myelin lamellae delineating the vacuoles dissociate within the intraperiodic line. Fragments of disrupted myelin lamellae reside inside large vacuoles — in the form of small vesicles or loose fragments.

Another type of pathological changes occurring in the optic nerve of animals intoxicated by TET was degeneration of whole bundles of myelinated fibers (Fig. 5). The myelin sheath of these fibers turned into amorphous masses or became split into short fragments. In some

Fig. 1. The 24th day of TET intoxication. Widespread spongious changes in the optic nerve. Toluidine blue. × 700

Ryc. 1. 24 dzień zatrucia TET. Rozległe zmiany gąbczaste nerwu wzrokowego. Błękit toluidyny. Pow. 700 ×

of these fragments the major dense lines were still conserved though occasionally of much lesser osmophility. The intraperiod lines were no longer detectable.

Most axons did not show considerable structural changes, although in some of them, the axoplasm showed partial or complete homogenization changes. Some axons looked more or less completely disintegrated (Fig. 6).

In animals that ingested the poison for 24 days there appeared considerable amounts of extravascular electron dense fluid (Fig. 7).

The oligodendroglial cytoplasm contained a very rich and widened rough endoplasmatic reticulum, numerous polyribosomes and an expanded Golgi system. Many processes of the astroglia contained numerous intracellular fibrils.

In the cytoplasm of some astrocytes whole axonal fibers with a conserved myelin and axon were demonstrable. Other ones contained multilayered short myelin fragments showing up as straight or curved system of parallel arranged membranes, closely resembling the major dense periodic lines. Intraperiod lines were not detected (Figs 8—11).

DISCUSSION

Injury to any part of the glia — myelin — axon entity may cause metabolic injury to the total system. Myelin seems to be directly affected in some toxic conditions. A single large dose of triethyl tin causes white matter edema with large intramyelin vesiculation caused by

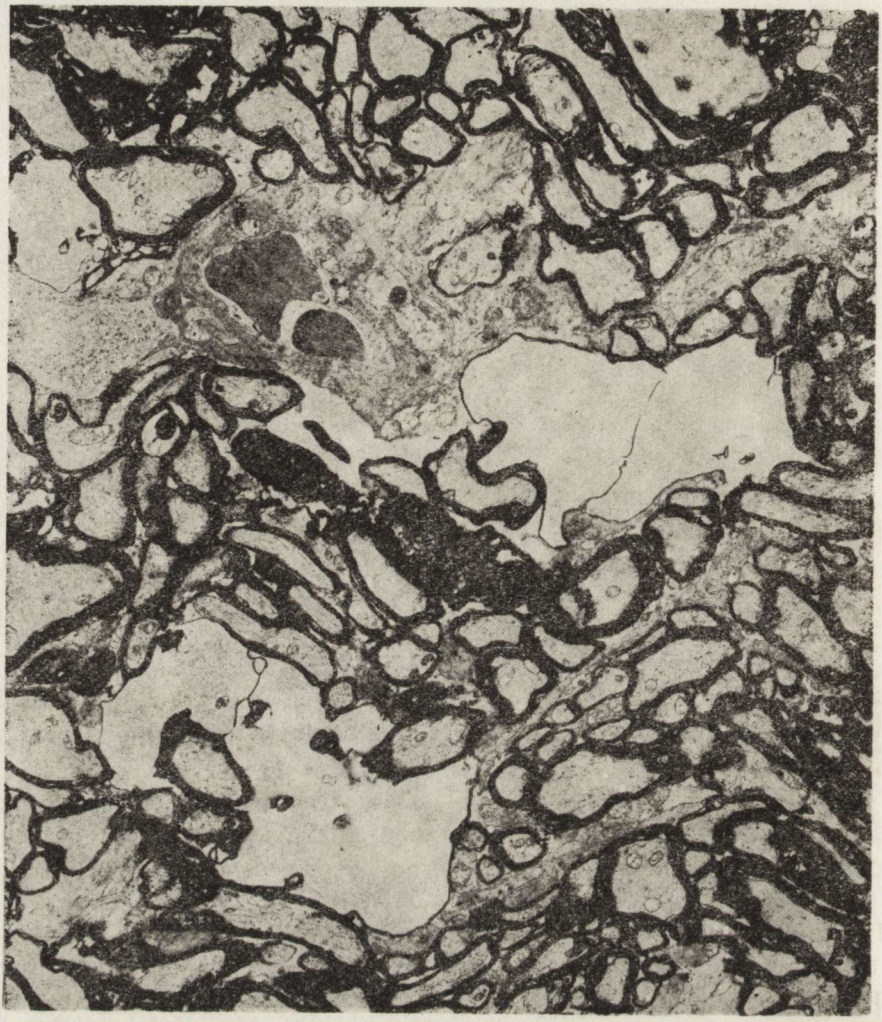

Fig. 2. Optic nerve. The 24th day of TET intoxication. Beside a number of intact axons with well preserved myelin, large intramyelin vacuoles of very low electron density. An electron dense angiogenic transsudate in the vicinity of one of these vacuoles. Osmiophilic deposits of degenerated myelin. × 8 400

Ryc. 2. Nerw wzrokowy. 24 dzień zatrucia TET. Widoczne, oprócz szeregu nie uszkodzonych aksonów z dobrze zachowaną mieliną, duże wakuole wewnątrzmielinowe o niskiej gęstości elektronowooptycznej. W sąsiedztwie jednej z wakuoli pozakomórkowy obrzęk naczyniopochodny, gęsty elektronowooptycznie. Widoczne również osmofilne złogi zwyrodniałej mieliny. Pow. 8 400 ×

splitting at the intraperiod lines with only slight demyelination (Aleu et al., 1963). Chronic administration of triethyl tin over a period of some weeks produces not only severe edema of the white matter in the central nervous system, but also a marked loss of myelin, as indicated by the diminished yield after cellular fractionation (Eto et al., 1971; Smith, 1973). The decreased yield of myelin indicates the disappearance of myelin with normal physical properties, but does not preclude the

Fig. 3. Optic nerve. The 74th day of TET intoxication. Giant intramyelin vacuoles containing small, disintegrating vesicles as well as loosely dispersed deposits of myelin debris. In the neighbourhood of most vacuoles many axons surrounded by unimpaired myelin. Oligodendroglial cell nuclei demonstrate structural homogenization. × 8 400

Ryc. 3. Nerw wzrokowy. 74 dzień zatrucia TET. Olbrzymie wakuole wewnątrzmielinowe, zawierające rozpadające się małe pęcherzyki oraz rozrzucone drobne złogi rozpadłej mieliny. W otoczeniu wakuoli szereg aksonów, łącznie z otaczającą mieliną nie wykazuje uszkodzeń. Homogenizacja jąder oligodendrocytów. Pow. 8.400 ×

presence of abnormal myelin with altered density (Smith, Benjamins. 1977). Since in acute TET intoxication the yield of myelin remains unaltered, the question arises as to the relation of TET effects on the myelin sheath to the mode of application of the poison.

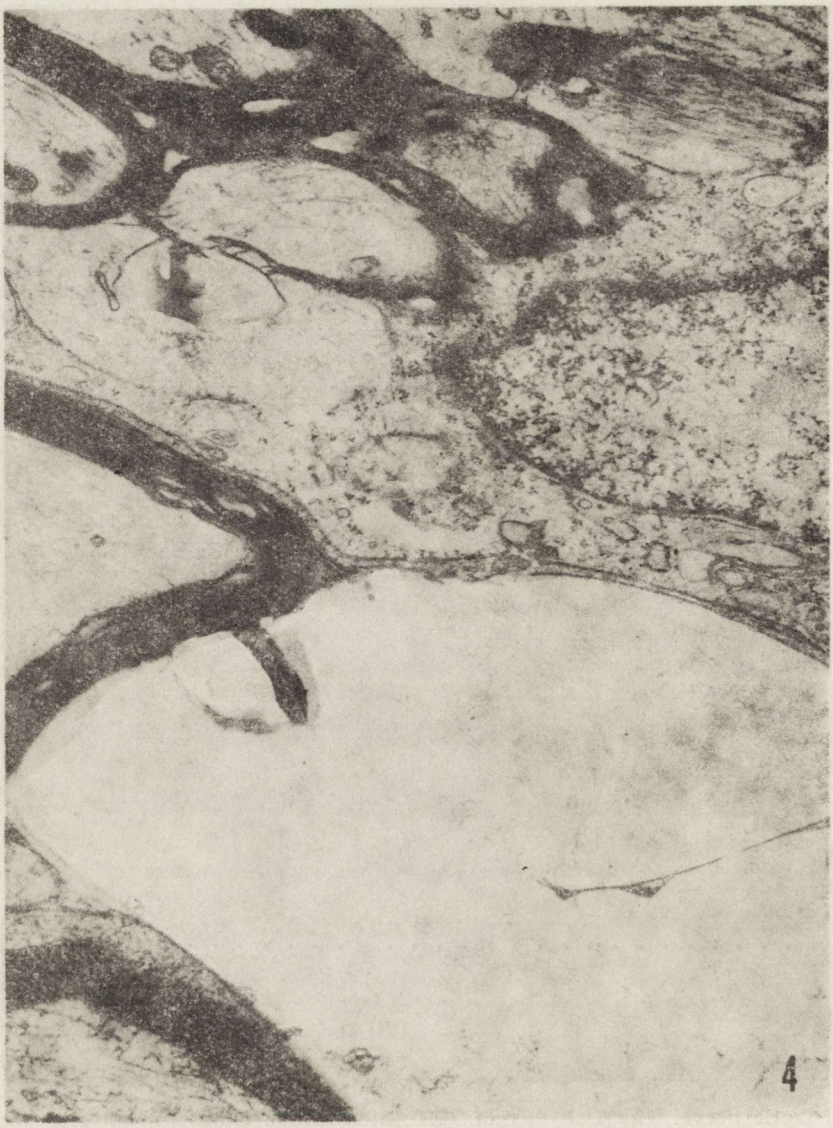

Fig. 4. Optic nerve. 10th day of TET intake. Large vacuoles surrounded by loose, external myelin lamellae. Relatively well preserved compact myelin layer. Astroglial processes contain numerous parallelly running fibrils. × 35 000

Ryc. 4. Nerw wzrokowy. 10 dzień zatrucia TET. Duże wakuole otoczone luźnymi, zewnętrznymi blaszkami mieliny. Warstwa zbita mieliny względnie dobrze zachowana. W wypustkach astrogleju liczne równolegle ułożone włókienka. Pow. 35.000 ×

The extent of intramyelin vesiculation in chronic TET poisoning is in fact larger than in the acute state, but the basic type of myelin injury, leading to splitting of myelin lamellae at the intraperiod lines is in either of these conditions identical.

On the other hand, the present study revealed that in the optic

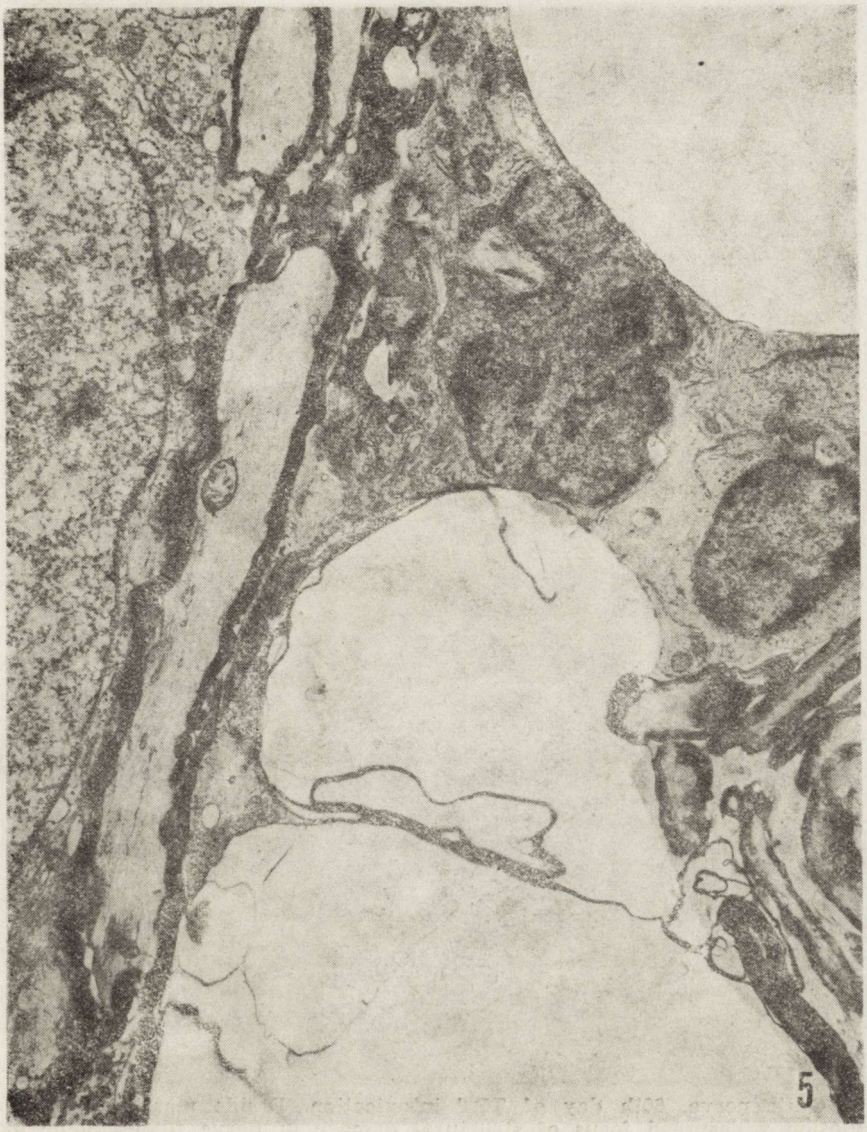

Fig. 5. Optic nerve. 10th day of TET intake. Fragments of inner myelin lamellae are bent towards the axoplasm. × 56 000

Ryc. 5. Nerw wzrokowy. 10 dzień zatrucia TET. Fragmenty blaszki wewnętrznej osłonki mielinowej zagięte do wnętrza aksonu. Pow. 56.000 ×

nerve of the chronically intoxicated rat, intramyelin vesiculation is not the only pathological change. Focal selective necrosis of nerve fibers accompanied by myelin decomposition and phagocytosis of the myelin debris was seen as well. From the morphological point of view this process was distinct from intramyelin vesiculation and its final outcome. In the latter case myelin disintegration pertains only to few peripheral layers of loose myelin, which form small vesicles without any apparent

Fig. 6. Optic nerve. 60th day of TET intoxication. Beside massive intramyelin vesiculation widespread focus of structural damage of nerve fibers. Some axons contain considerable amounts of granular electron dense material, others show focal clearing up. Some of them are collapsed. × 8 400

Ryc. 6. Nerw wzrokowy. 60 dzień zatrucia TET. Oprócz dużych wakuoli wewnątrzmielinowych widoczne jest rozległe ognisko zniszczenia struktury włókien nerwowych. Niektóre aksony zawierają znaczne ilości ziarnistego, elektronowooptycznie gęstego materiału, inne wykazują ogniskowe przejaśnienia, niektóre natomiast są zapadnięte. Pow. 8 400 ×

involvement of phagocytosis. The destruction of myelin occurring within the foci of selective necrosis of nerve fibers is entirely different in nature. Myelin undergoes either complete homogenization — forming amorphous lipid masses, closely resembling events observed in Wallerian degeneration or becomes fragmented into thick but short portions. The-

Fig. 7. Optic nerve. 60th day of TET intoxication. Giant electron transparent vacuoles contain portions of single and double myelin lamellae. Some axons are unchanged, but others demonstrate a homogeneous axoplasm or are almost completely collapsed. × 14 000

Ryc. 7. Nerw wzrokowy. 60 dzień zatrucia TET. W olbrzymich, przezroczystych elektronowooptycznie wakuolach widoczne są odsznurowane, pojedyncze i podwójne blaszki mielinowe. Aksony są częściowo niezmienione, inne wykazują homogenną aksoplazmę lub prawie całkowicie zapadnięte. Pow. 14 000 ×

se myelin fragments appear mainly in the cytoplasm of reactive glial cells. It should be noted that also in these fragments the intraperiod lines are not detectable, which means that molecules furnishing this very region of the myelin membrane, among others also high molecular weight proteins — are particularly susceptible to the poisonous effects of TET.

In general, our own observations seem to indicate that TET when applied chronically — produces both, intramyelin vesiculation and necrosis of nerve fibers followed by phagocytosis of the resulting myelin debris by reactive astroglial cells. The latter event may in fact explain

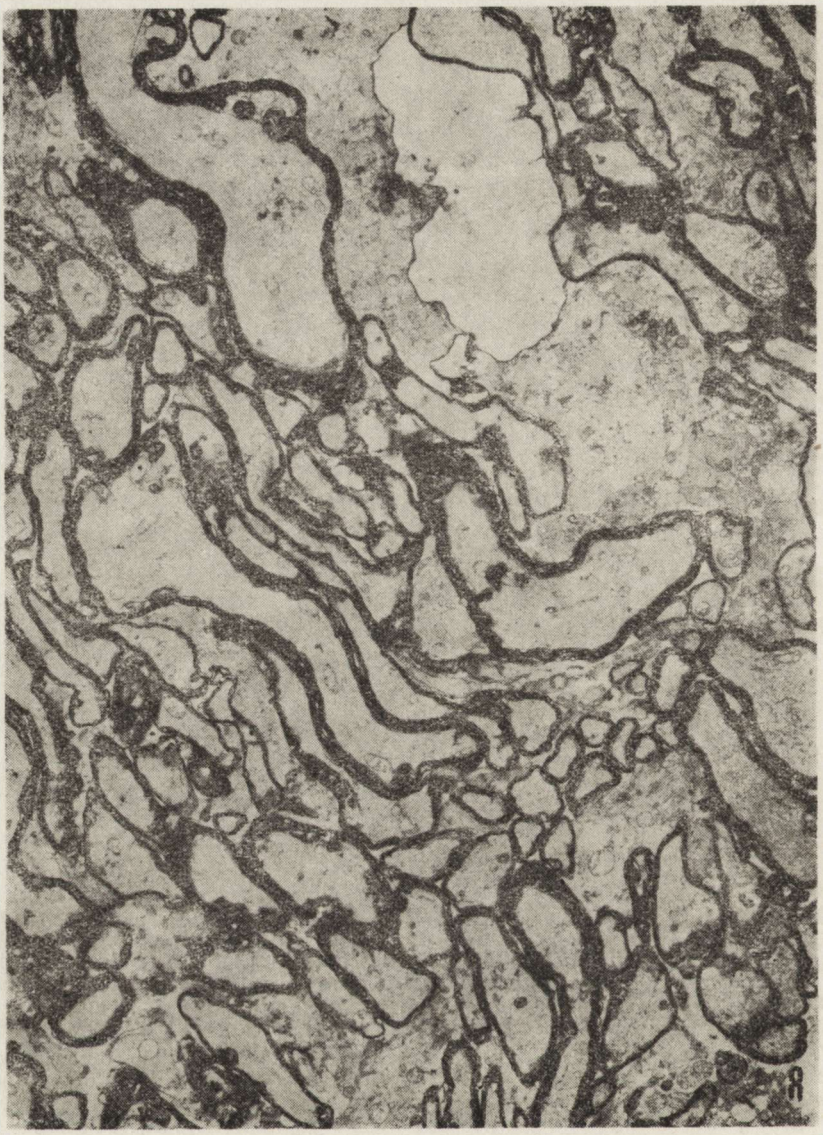

Fig. 8. Optic nerve. 24th day of TET intoxication. An electron dense angiogenic transsudate beside a large electron transparent intramyelin vacuole. × 8 400

Ryc. 8. Nerw wzrokowy. 24 dzień zatrucia TET. Obok dużej elektronowo przezroczystej wewnątrzmielinowej wakuoli elektronowooptycznie gęsty przesięk naczyniopochodny. Pow. 8.400 ×

the reduced myelin yield in chronic TET intoxication as described by Eto et al., (1971) and Smith (1973).

The splitting of myelin lamellae occurring at the intraperiod line — which is so specific for TET intoxication indicates that the similarity of spongious changes in TET intoxication and in human as well as experimental subacute spongious encephalopathy is only an apparent one.

Fig. 9. Optic nerve. 60th day of TET intoxication. A degenerated myelinated nerve fibre residues in the cytoplasm of a phagocyting cell of glial origin. Here and there the intraperiod lines are discernable within the masses of decomposing myelin. On the outer, loose surface, frayed ends of undermined myelin lamellae are seen situated along the nerve fiber in the form of elongated or round structures. In the neighborhood of degenerated axons bunches of rough endoplasmic channels, numerous lysosomes and mitochondria are gathered. On the periphery of the figure, there is a long portion of a myelin sheath that is only weakly osmiophilic, lacking entirely the intraperiod line. × 70 000

Ryc. 9. Nerw wzrokowy. 60 dzień zatrucia TET. Zwyrodniałe włókno mielinowe ułożone wewnątrz cytoplazmy komórki fagocytującej pochodzenia glejowego. Miejscami widoczne linie wewnątrzperiodyczne w zwartej masie rozpadającej się mieliny. Z zewnętrznej, luźnej warstwy blaszek mieliny oddzielone fragmenty, widoczne jako podłużne lub okrągłe twory leżące obok włókna. W okolicy zwyrodniałych włókien układy kanałów szorstkiej siatki endoplazmatycznej, liczne lizosomy i mitochondria. Na obwodzie ryciny widoczny długi fragment osłonki mielinowej o obniżonej osmofilności i całkowitym braku linii wewnątrzokresowej. Pow. 70 000 ×

Fig. 10. Optic nerve. 60th day of TET intoxication. Widespread degenerative changes of myelinated fibers. A fiber surrounded by the cytoplasm of a reactive astroglial cell, which already contains a whole degenerated fiber. × 35 000

Ryc. 10. Nerw wzrokowy. 60 dzień zatrucia TET. Daleko posunięte zmiany zwyrodnieniowe włókien mielinowych. Spostrzega się otaczanie włókna mielinowego przez cytoplazmę reaktywnego astrogleju, wewnątrz którego znajduje się również całe zwyrodniałe włókno. Pow. 35 000 ×

As shown by Sato et al. (1980), spongious changes evoked by transplantation of the human subacute spongious encephalopathy to experimental animals — are brought about by splitting of myelin lamellae within the main dense line as well as by intraaxonal vacuolization.

Fig. 11. Optic nerve. 74th day of TET intoxication. Large lysosomes in close contact with various fragments of myelin lamellae lacking the intraperiod line. × 70 000

Ryc. 11. Nerw wzrokowy. 74 dzień zatrucia TET. Duże lizosomy w bliskim kontakcie z różnorodnymi fragmentami blaszek mielinowych o niewidocznej linii wewnątrzokresowej. Pow. 70 000 ×

However, it is by no means clear, which of the molecular components of the intraperiod line including high molecular weight proteins constitute the target molecules for TET.

The hitherto published data on protein metabolism in TET intoxication, because of difference in the experimental approach, do not answer this question.

Wender et al. (1974) have reported a marked depression of the incorporation of radioactive leucine into the postmitochondrial fraction

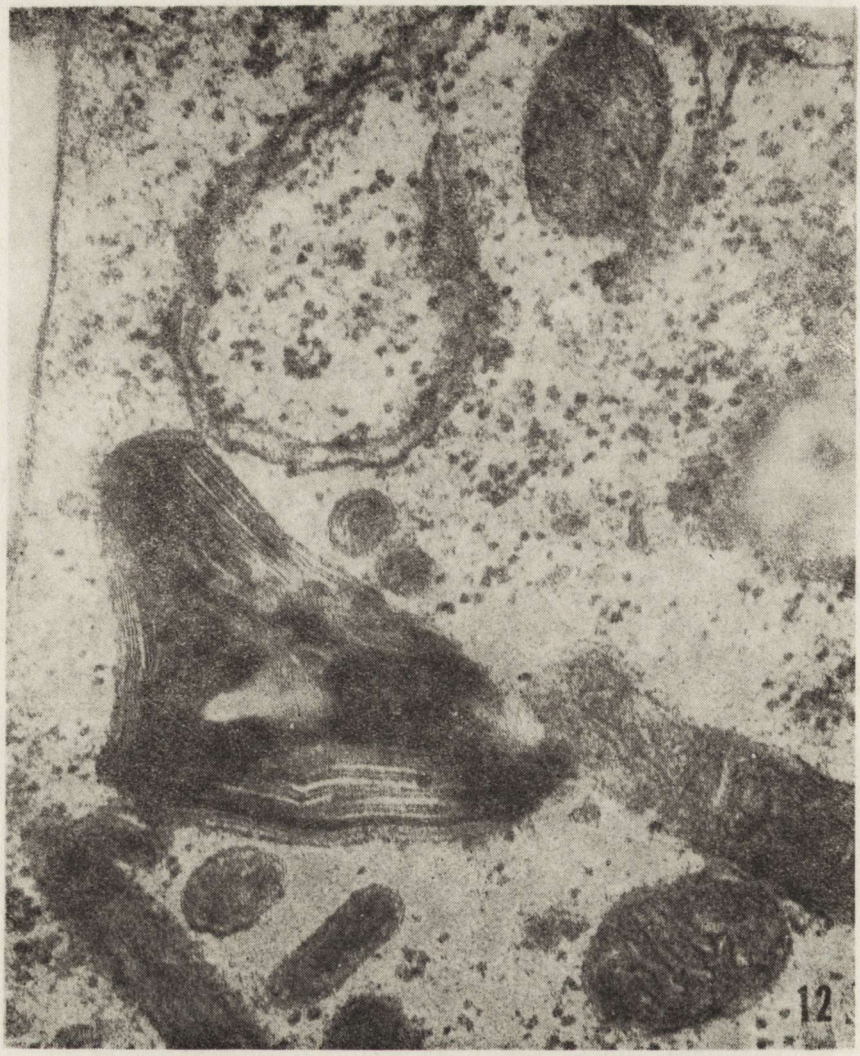

Fig. 12. Optic nerve. 74th day of TET intoxication. Decomposing myelin forming systems of parallel arranged membranes and smaller elements with a dark center and a partially preserved intraperiod line. Splitting intraperiod line in the vicinity of an endoplasmic reticulum channel. × 70 000

Ryc. 12. Nerw wzrokowy. 74 dzień zatrucia TET. Rozpadająca się mielina w postaci układów równoległych błon i mniejszych elementów z ciemnym rdzeniem. Częściowo dobrze zachowane linie wewnątrzokresowe. W sąsiedztwie widoczna linia wewnątrzokresowa ulegająca rozszczepieniu w pobliżu kanału szorstkiej siatki endoplazmatycznej. Pow. 70 000 ×

of the brain whereas Smith (1973) has shown a biphasic course of disturbances of incorporation of this amino acid into protein fraction, corresponding to myelin protein.

Hirano et al. (1968) who investigated the problem of the origin of the intravacuolar fluid in TET intoxication have found that the extracellular marker-peroxidase, when injected intracerebrally, does not

penetrate into the vacuoles, thus indicating that the intravacuolar fluid is located in different compartments separated by intact myelin lamellae.

However, TET could alter the permeability of myelin towards water thus causing the vacuoles to enlarge till eventually an equilibrium is reached. At this stage the hydrostatic pressure within the vacuole reaches the level adequate for balancing forces promoting the flow of water from extracellular space into vacuole.

Nevertheless, our own investigations on the effects of chronic TET poisoning performed after a 21 day period of TET intake have shown some accumulation of edematous fluid, and this observation indicates an increase of the endothelial permeability. This conclusion is consistent with the results obtained by Leow et al. (1979) who reported progressing cerebral edema in acute TET poisoning, following a single injection of this compound.

The above mentioned findings seem to explain the severe clinical symptoms of this poisoning occurring during the initial phase of the chronic experimental disease. The consecutive improvement thus could be rendered possible by the reabsorption of the edematous perivascular fluid in spite of the still progressing vesiculation of myelin.

CONCLUSIONS

The obtained observations seem to indicate that TET when applied chronically produces both, intramyelin vesiculations and necrosis of nerve fibers followed by phagocytosis of the resulting myelin debris by reactive astroglial cells. Splitting of myelin lamellae occurring at the intraperiod line is characteristic of TET intoxication, and that is why the similarity of spongious changes in TET intoxication and in human as well as experimental subacute spongious encephalopathy is only an apparent one.

The tendency of accumulation of perivascular edematous fluid during the third week of TET intake indicates some impairment of the permeability of the endothelium. This event coincides with the most severe clinical symptoms of chronic poisoning.

MIELINA NERWU WZROKOWEGO U SZCZURÓW PRZEWLEKLE ZATRUTYCH SIARCZANEM TRÓJETYLKU CYNY (TET)

Streszczenie

Przedstawiono wyniki badań ultrastrukturalnych ośrodkowej demielinizacji na przykładzie zjawisk występujących w nerwie wzrokowym szczura po przewlekłym zatruciu TETem, w którym demielinizacja jest prawdopodobnie zjawiskiem pierwotnym.

Doświadczenie przeprowadzono na szczurach Wistar zatrutych przewlekle siar-

czanem trójetylku cyny (Eto i wsp. 1971). Nerwy wzrokowe zwierząt doświadczalnych badano w mikroskopie elektronowym w różnych okresach zatrucia.

Uzyskane wyniki wskazują, że przewlekłe zatrucie TETem wywołuje zarówno wewnątrzmielinową wakuolizację, jak i martwicę włókien nerwowych z następowym fagocytowaniem pozostałych resztek mieliny przez reaktywne komórki astrogleju. Rozszczepienie blaszek mieliny występujące w obrębie linii wewnątrzokresowych jest charakterystyczne dla zatrucia TETem, co powoduje, że podobieństwo zmian gąbczastych w zatruciu TETem oraz w ludzkiej i doświadczalnej podostrej gąbczastej encefalopatii jest tylko pozorne.

Podczas trzeciego tygodnia zatruwania TETem następuje okołonaczyniowe gromadzenie się płynu obrzękowego, wskazując na uszkodzenie przepuszczalności śródbłonków, co przebiega łącznie z najcięższymi objawami klinicznymi przewlekłego zatrucia.

REFERENCES

1. Aleu F., Katzman R., Terry R.: Fine structure and electrolyte analyses of cerebral edema induced by alkyl tin intoxication. J. Neuropath. exp. Neurol., 1963, 22, 403—412.
2. Eto Y., Suzuki K., Suzuki K.: Lipid composition of rat brain myelin in triethyltin — induced edema. J. Lipid Res., 1971, 12, 570—579.
3. Hirano A., Zimmerman H., Levine S.: Intramyelinic and extracellular spaces in triethyltin intoxication. J. Neuropath. exp. Neurol., 1968, 27, 571—580.
4. Lampert P.: Demyelination and remyelination in experimental allergic encephalomyelitis. J. Neuropath. exp. Neurol., 1965, 24, 371—378.
5. Leow A., Anderson R., Little R., Leaver D.: A sequential study of changes in the brain and cerebrospinal fluid of the rat following triethyl poisoning. Acta neuropath. (Berl.), 1979, 47, 117—121.
6. Raine C., Wiśniewski H., Prineas J.: An ultrastructural study of experimental demyelination and remyelination. Lab. Invest., 1969, 21, 316—327.
7. Sato Y., Ohta M., Takeishi J.: Experimental transmission of human subacute spongiform encephalopathy. II. Ultrastructural study of spongy state in the grey and white matter. Acta neuropath. (Berl.), 1980, 51, 135—140.
8. Smith M.: Studies on the mechanism of demyelination. Triethyl tin — induced demyelination. J. Neurochem., 1973, 21, 357—364.
9. Smith M., Benjamins J.: Model system for study of perturbations of myelin metabolism. In: Myelin. Ed. P. Morell, Plenum Press, New York—London 1977, 447—488.
10. Wender M., Zgorzalewicz B., Piechowski A.: Cell free protein synthesis by rat brain in triethyl tin intoxication. Acta Neurol. Scand., 1974, 50, 103—107.

Authors address: Department of Neurology, Academy of Medicine, 49 Przybyszewskiego Str., 60—355 Poznań, Poland

NEUROPAT. POL., 1982, 20, 1—2
PL ISSN 0028—3894

JÓZEF SZCZECH, MARIAN KONTEK

ZMIANY MORFOLOGICZNE I HISTOENZYMATYCZNE W MÓZGU SZCZURA PO DOŚWIADCZALNYM ZATRUCIU BROMFENWINFOSEM (IPOFOS-IPO 62)

Zakład Neuropatologii Instytutu Chorób Układu Nerwowego i Narządów Zmysłów AM, Poznań
Klinika Chorób Zawodowych Instytutu Chorób Wewnętrznych AM, Poznań

Ipofos jest insektycydem dopuszczonym do stosowania w polskim rolnictwie od 1978 r. Składnikiem czynnym tego preparatu jest bromfenwinfos, który pod względem chemicznym jest fosforanem 0,0 dwuetylo 0-1(2,4-chlorofenylo)2-bromowinylowym. Chociaż połączenia estrowe kwasu fosforowego są związkami ulegającymi szybkiemu rozpadowi, to jednak możliwość zatruć przypadkowych jest duża. Jest to spowodowane łatwym wchłanianiem się przez drogi oddechowe, przewód pokarmowy i skórę.

Działanie toksyczne na organizmy zwierzęce polega na trwałym wiązaniu esterazy acetylocholinowej, co powoduje nagromadzenie acetylocholiny i endogenne zatrucie tym mediatorem (Modell i wsp., 1946; Rusiecki, 1973), zaś obserwacje kliniczne przebiegu zatruć potwierdzają czynnościowy charakter występujących zaburzeń (Kontek i wsp., 1974). Dokładniejsze opracowania neuropatologiczne ostrych zatruć są nieliczne (Maresch, 1957). Stosunkowo mało uwagi zwracano na możliwość powstania uszkodzeń strukturalnych w ośrodkowym układzie nerwowym, spowodowanych dłuższym podawaniem małych dawek związków fosforoorganicznych. Uzasadnia to podjęcie niżej przedstawionych badań.

MATERIAŁ I METODY

Badania przeprowadzono na 40 szczurach rasy Wistar, obu płci, o ciężarze ciała wynoszącym ok. 220 g. Ipofos rozpuszczano w oleju oliwkowym i podawano zwierzętom dożołądkowo za pomocą zgłębnika. Szczury doświadczalne podzielono na dwie grupy: I grupa, licząca 20

zwierząt, otrzymywała po 12 mg ipofosu na kg masy ciała przez 5 dni i po 18 mg przez następne 4 dni; II grupa, licząca również 20 zwierząt, otrzymywała ipofos przez 58 dni w dawkach wzrastających od 3 do 12 mg na kg masy ciała. Grupę kontrolną stanowiło 5 szczurów, które otrzymywały dożołądkowo wodę kranową.

Po przeprowadzeniu doświadczenia szczury uśmiercano w narkozie esterowej. Materiał do badań stanowiło mózgowie. Część materiału z każdej grupy doświadczalnej zatapiano w parafinie i skrawki barwiono H+E i met. Nissla. Pozostałą część materiału utrwalano w płynie Bakera w temp. 4°C przez 16 godzin, a następnie wykonywano skrawki na mikrotomie mrożeniowym i oznaczano aktywność następujących enzymów: pyrofosfatazy tiaminowej (TPP-aza — E.C. 2.5.1.3) * — wg metody Novikoffa i Goldfischera (1961), esterazy nieswoistej (NsE — E.C. 3.1.1.1) — wg metody Nachlasa i Seligmanna (1949), acetylocholinoesterazy (AChE — E.C. 3.1.1.7) — wg metody Koelle w modyfikacji Gerebtzoffa (1953), cholinoesterazy nieswoistej (ChE — E.C. 3.1.1.8) — wg metody Koelle w modyfikacji Gerebtzoffa (1953), fosfatazy zasadowej (FZ — E.C. 3.1.3.1) — wg metody Gomoriego (1953), fosfatazy kwaśnej (FK — E.C. 3.1.3.2.) — wg metody Gomoriego (1953), adenozynotrójfosfatazy (ATP-aza — E.C. 3.6.1.3) — wg metody Wachsteina i Meisela (1957). Mózgowia zwierząt grupy kontrolnej służyły jako punkt odniesienia w ocenie zmian enzymatycznych w grupach doświadczalnych.

WYNIKI

Dożołądkowe podawanie ipofosu nie wywoływało większych zmian somatycznych ani zmian zachowania. W szczególności nie obserwowano zaburzeń w pobieraniu pokarmu ani też spadku wagi ciała. Jedynie pod koniec doświadczenia zwierzęta grupy II były mniej ruchliwe, a u niektórych obserwowano biegunkę. W czasie trwania doświadczenia padły jednak 3 szczury z grupy I oraz 6 z grupy II.

Badania morfologiczne

Dożołądkowe wprowadzanie ipofosu przez 5 dni powodowało umiarkowane zmiany naczyniowe, neuronalne i glejowe w mózgu. Zmiany naczyniowe polegały głównie na poszerzeniu włośniczek i na obrzmieniu komórek śródbłonka. Najbardziej uszkodzone były włośniczki wzgórza, gdzie niejednokrotnie obserwowano erytrodiapedezę (ryc. 1). Mniejszego stopnia poszerzenie włośniczek z obrzmieniem komórek śródbłonka widoczne było w III i V warstwie kory ciemieniowej i skroniowej oraz w istocie białej i warstwie drobinowej móżdżku.

* Numer listy enzymów (Florkin, Stotz, 1973).

Zmiany neuronalne polegały najczęściej na pojawieniu się w cytoplazmie wodniczek, zmianach rozpływnych i zmianach typu schorzenia ischemicznego. Natomiast obkurczenie i cienie neurocytów obserwowano rzadziej. Topografia uszkodzeń neuronalnych była dość dobrze skorelowana z lokalizacją największych uszkodzeń naczyniowych. Zmiany rozpływne i wodniczkowe neurocytów dominowały w jądrze bocznym wzgórza (ryc. 2), w jądrze przedsionkowym i jądrze nerwu odwodzącego w moście oraz w warstwie komórek Purkinjego i w warstwie ziarnistej w móżdżku. Mniejsze nasilenie uszkodzeń tego typu widoczne było w korze zakrętu obręczy (ryc. 3). Opisanym uszkodzeniom neurocytów towarzyszył umiarkowany odczyn ze strony astrogleju, polegający na przeroście astrocytów i niekiedy obrzmieniu ich cytoplazmy.

W II grupie doświadczalnej uszkodzenie naczyń krwionośnych ograniczało się do umiarkowanego obrzmienia śródbłonków naczyniowych. W porównaniu do I grupy, w korze płaszcza mózgu i w warstwie komórek Purkinjego w móżdżku, narastała ilość neurocytów z oznakami schorzenia przewlekłego (ryc. 4). Długość okresu podawania ipofosu nie wpływała natomiast na charakter i intensywność zmian neuronalnych obserwowanych we wzgórzu i w części grzbietowej mostu. Również w tej grupie doświadczalnej, w wymienionych okolicach, przeważały rozległe zmiany rozpływne z umiarkowaną reakcją glejową.

Badania histoenzymatyczne

P y r o f o s f a t a z a t i a m i n o w a (TPP-aza). W grupie kontrolnej reakcja enzymatyczna na TPP-azę występuje w aparacie Golgiego neurocytów (ryc. 5 a), w wypustkach przynaczyniowych astrocytów protoplazmatycznych oraz w ścianie naczyń krwionośnych. Dożołądkowe podawanie ipofosu powoduje wzrost aktywności pyrofosfatazy tiaminowej w neurocytach, astrocytach oraz w ścianie naczyń krwionośnych. Ponadto pojawia się aktywność TPP-azy w oligodendrogleju. Szczególnie duży wzrost aktywności enzymu obserwuje się w komórkach piramidowych kory, mniejszy w komórkach piramidowych rogu Ammona, w neurocytach ciała migdałowatego i wzgórza. W pniu mózgu odczyn narasta w neurocytach jąder n. przedsionkowego i trójdzielnego. Dłuższe stosowanie ipofosu prowadzi do występowania bardzo silnej aktywności TPP-azy w całej cytoplazmie neurocytów (ryc. 5 b). Wzrost aktywności TPP-azy w komórkach glejowych zwierząt II grupy doświadczalnej (ryc. 5 b) jest słabszy w porównaniu z I grupą. Aktywność TPP-azy obserwowano głównie w oligodendrogleju spoidła wielkiego i pasma wzrokowego oraz w gleju przynaczyniowym mostu i warstwy zatokowo-drobinowej rogu Ammona.

E s t e r a z a n i e s w o i s t a (NsE). Odczyn na esterazę nieswoistą

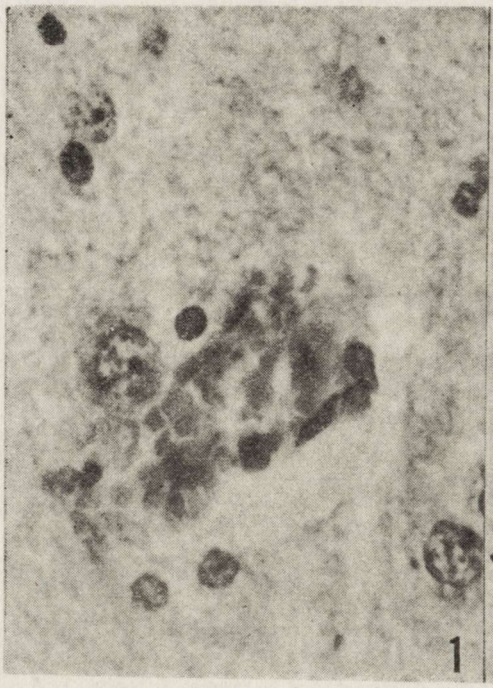

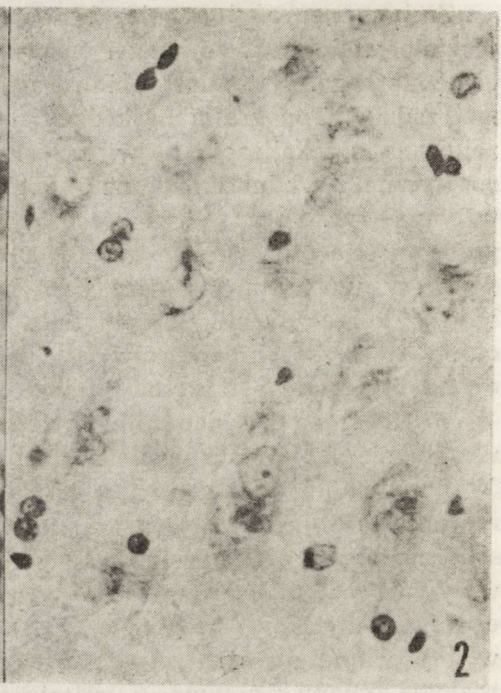

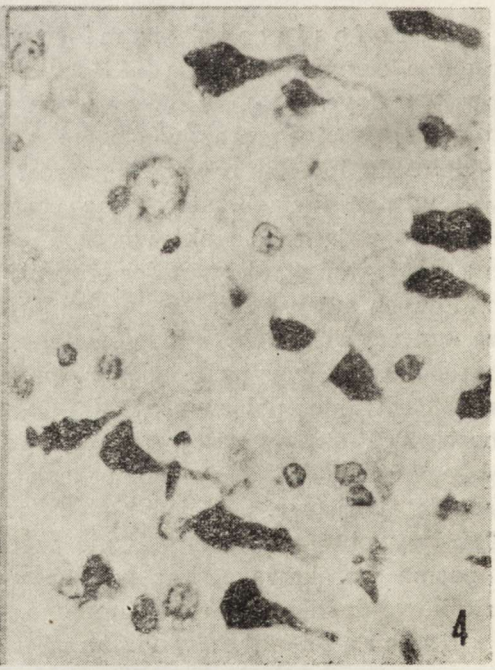

w mózgowiu zwierząt kontrolnych jest zlokalizowany w cytoplazmie niektórych neurocytów, w pericytach naczyń krwionośnych (ryc. 6 a), i w niektórych komórkach oligodendrogleju.

Podawanie ipofosu powoduje niewielki spadek aktywności enzymatycznej we wszystkich wymienionych elementach komórkowych (ryc. 6 b). Ponadto w korze śródwęchowej i w jądrze przyśrodkowym ciała migdałowatego obserwowano delikatną dyfuzję produktu reakcji enzymatycznej z cytoplazmy do najbliższego sąsiedztwa neurocytów. Przewlekłe podawanie ipofosu szczurom prowadzi do dalszego spadku aktywności NsE.

Acetylocholinoesteraza (AChE). Po podawaniu ipofosu u zwierząt doświadczalnych obserwuje się uogólniony spadek aktywności acetylocholinoesterazy. W okolicach mózgu, w których u zwierząt kontrolnych reakcja enzymatyczna jest najsilniejsza, u zwierząt doświadczalnych jest średnio nasilona lub słaba. Takie zmiany występują w neurocytach i neuropilu skorupy i gałki bladej (ryc. 7 a, b), w jądrze bocznym wzgórza i w jądrze podstawno-bocznym ciała migdałowatego. Odczyn na AChE słabnie także w neurocytach *striatum oriens* i *striatum radiatum* rogu Ammona, w neurocytach i neuropilu jądra przedsionkowego i jądra n. V w moście. W okolicach mózgu z fizjologicznie słabą reakcją na AChE, po zatruciu obserwuje się całkowity brak odczynu. Dotyczy to komórek piramidowych kory mózgu, neurocytów i neuropilu większości jąder ciała migdałowatego oraz neurocytów środkowej grupy jąder wzgórza. Opisane zmiany są bardziej nasilone w mózgowiach zwierząt I grupy doświadczalnej.

Cholinoesteraza nieswoista (ChE). U zwierząt kontrolnych reakcja na ChE jest widoczna w ścianach naczyń krwionośnych (ryc. 8 a) oraz w neurocytach jądra bocznego wzgórza. Bardzo słaby odczyn enzymatyczny obserwuje się w komórkach Purkinjego. Po po-

---

Ryc. 1. I grupa doświadczalna. Włośniczka w jądrze bocznym wzgórza. Obrzmienie komórek śródbłonka i erytrodiapedeza. HE. Pow. 510 ×

Fig. 1. Experimental group I. Capillary in the lateral thalamic nucleus. Swelling of endothelial cells and erythrodiapedesis. HE. × 510

Ryc. 2. I grupa doświadczalna. Zmiany ropływne w neurocytach jądra bocznego wzgórza. Nissl. Pow. 510 ×

Fig. 2. Experimental group I. Liquefaction in neurocytes of the lateral thalamic nucleus. Nissl. × 510

Ryc. 3. I grupa doświadczalna. Zmiany wodniczkowe w neurocytach III warstwy kory ciemieniowej. Nissl. Pow. 510 ×

Fig. 3. Experimental group I. Vacuolar changes in neurocytes of the IIIrd layer of parietal cortex. Nissl. × 510

Ryc. 4. II grupa doświadczalna. Większość neurocytów III warstwy kory ciemieniowej ze zmianami typu schorzenia przewlekłego. Nissl. Pow. 510 ×

Fig. 4. Experimental group II. Most of the neurocytes of the IIIrd layer of the parietal cortex with changes of a chronic type. Nissl. × 510

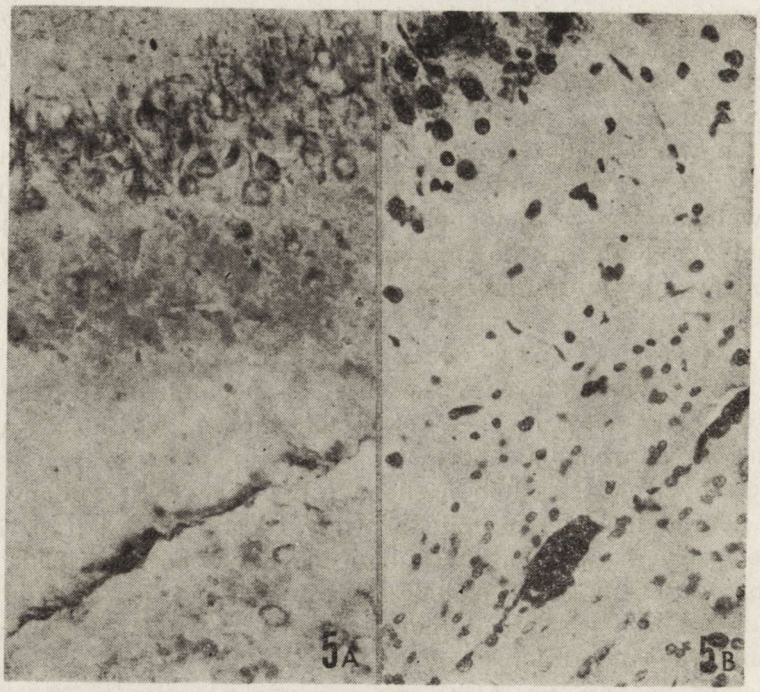

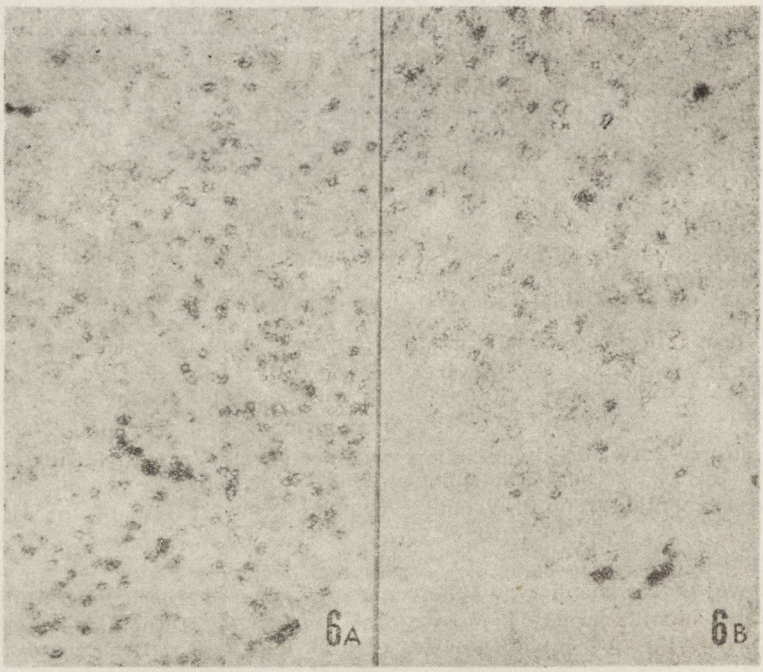

dawaniu ipofosu reakcja enzymatyczna znika w większości włośniczek i znacznie słabnie w tętniczkach i większych naczyniach krwionośnych. Zmiany te mają charakter uogólniony i są bardziej nasilone w mózgowiach zwierząt I grupy doświadczalnej (ryc. 8 b).

Fosfataza zasadowa (FZ). W porównaniu z mózgowiem zwierząt kontrolnych zatrucie ostre powoduje niewielki spadek odczynu enzymatycznego w ścianach naczyń krwionośnych oraz w komórkach nabłonka splotów naczyniastych komór mózgu. Słabnie także dyfuzyjny odczyn enzymatyczny obserwowany w niektórych neurocytach kory mózgu. Natomiast u zwierząt II grupy doświadczalnej obserwuje się niewielki wzrost aktywności FZ w neurocytach kory. W komórkach Purkinjego, neurocytach jądra zębatego i jąder oliw zarówno zatrucie ostre jak i przewlekłe powoduje niewielkie osłabienie reakcji enzymatycznej.

Fosfataza kwaśna (FK). W następstwie ostrego zatrucia ipofosem wzrasta aktywność FK w niektórych komórkach piramidowych kory mózgu, w płytce końcowej kory amonalnej, we wzgórzu, w neurocytach jąder oliw, nerwu trójdzielnego i przedsionkowego.

W porównaniu do zwierząt kontrolnych (ryc. 9 a) w móżdżku wzrasta aktywność FK w komórkach Purkinjego, w neurocytach warstwy drobinowej i w komórkach ziarnistych (ryc. 9 b).

W porównaniu z glejem mózgu zwierząt kontrolnych reakcja enzymatyczna jest intensywniejsza w oligodendrogleju spoidła wielkiego mózgu, strzępka hipokampa, pasma wzrokowego i w gleju przynaczyniowym warstwy zatokowo-drobinowej hipokampa.

W II grupie doświadczalnej obserwuje się tylko niewielki wzrost reakcji enzymatycznej w niektórych neurocytach kory i zwojów podstawy.

Adenozynotrójfosfataza (ATP-aza). W mózgu zwierząt kontrolnych dodatni odczyn na ATP-azę widoczny jest w naczyniach krwionośnych oraz w błonie jądrowej neurocytów niektórych struktur

---

Ryc. 5. A) Grupa kontrolna. Umiarkowana aktywność TPP-azy w neurocytach warstwy piramidowej rogu Amona i słabszy odczyn enzymatyczny w neurocytach wzgórza i pojedynczych komórkach glejowych. Pow. 200 × *B*) II grupa doświadczalna. Znaczny wzrost aktywności TPP-azy w neurocytach i mniejszy w gleju po długotrwałym podawaniu ipofosu. Pow. 200×

Fig. 5. A) Control group. Moderate TPPase activity in neurocytes of the pyramidal layer of the Ammons horn and a weaker reaction in thalamic neurocytes and in single glial cells. × 200 *B*) Experimental group II. Marked increase of TPPase activity in neurocytes and less pronounced increase in glia following long-term administration of Ipophos. × 200

Ryc. 6. A) Grupa kontrolna. Odczyn na NsE widoczny w neurocytach kory skroniowej i pericytach naczyń. Pow. 80 ×. *B*) I grupa doświadczalna. Widoczne zmniejszenie aktywności enzymu w neurocytach kory skroniowej. Pow. 80 ×

Fig. 6. A) Control group. Nonspecific esterase reaction in temporal cortex neurocytes and in pericytes of the blood vessels. × 80. *B*) Experimental group I. Decreased enzyme activity in temporal cortex neurocytes. × 80

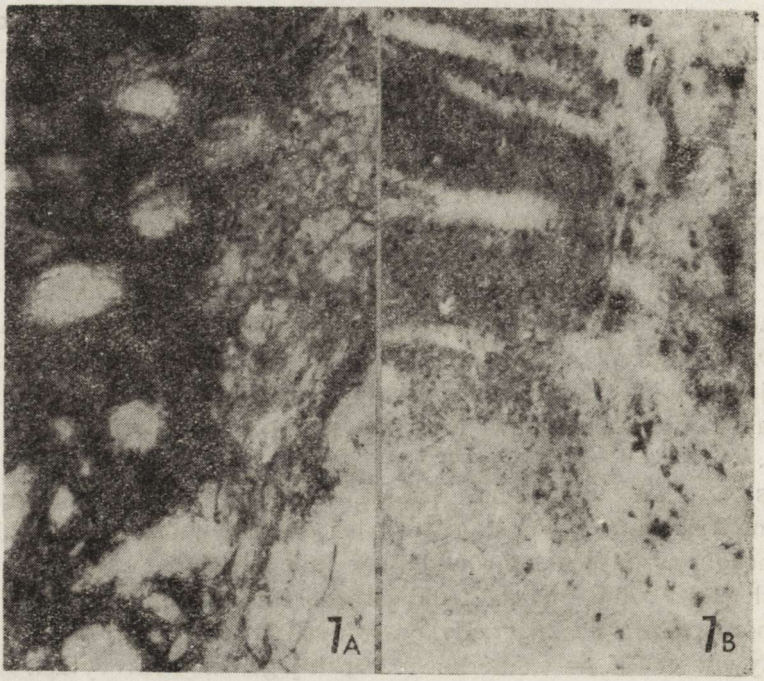

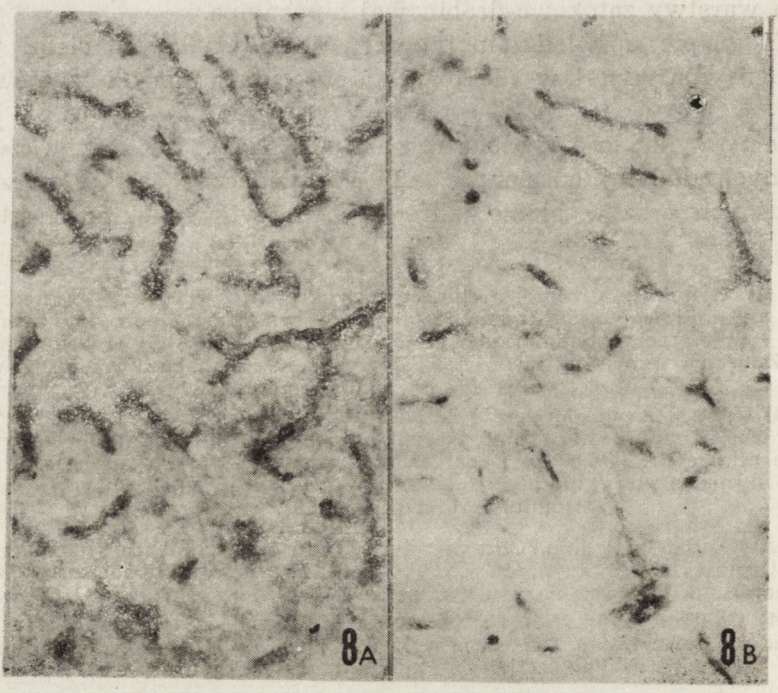

mózgowia (ryc. 10 a). U zwierząt I grupy doświadczalnej ipofos powoduje wzrost reakcji enzymatycznej w błonie jądrowej neurocytów. Zmiany obserwuje się w korze skroniowej, w jądrze bocznym wzgórza i w prążkowiu (ryc. 10 b). Narasta także reakcja enzymatyczna w komórkach Purkinjego i neurocytach warstwy drobinowej móżdżku.

W komórkach glejowych nieznaczny wzrost reakcji enzymatycznej obserwuje się w gleju przynaczyniowym warstwy zatokowo-drobinowej hipokampa oraz w oligodendrogleju strzępka hipokampa i spoidła wielkiego. Przewlekłe podawanie ipofosu powoduje wyraźny spadek intensywności odczynu w neurocytach kory, prążkowia (ryc. 10 c) i międzymózgowia, pnia mózgu i móżdżku. W naczyniach krwionośnych obserwowano spadek reakcji enzymatycznej przy niezmienionej aktywności enzymatycznej w tętniczkach.

OMÓWIENIE

Szerokie zainteresowanie grupą związków fosforoorganicznych wypływa z potrzeby znalezienia preparatów, które przy zachowanych właściwościach owadobójczych byłyby najmniej szkodliwe dla człowieka. Stąd właściwości chemiczne i farmakologiczne tych związków chemicznych są dość dobrze poznane (Mc Combie, Sounders, 1946; Holmstedt, 1959). Prawie wszystkie ze znanych związków fosforoorganicznych są inhibitorami esterazy cholinowej. Działanie ich polega na blokowaniu aktywnego centrum enzymu wskutek fosforylacji grup hydroksylowych seryny i grupy imidazolowej histydyny (Wilson, Bergman, 1950). Fosforylowany enzym hydrolizuje znacznie wolniej niż enzym acetylowany, który powstaje z naturalnego substratu, jakim jest acetylocholina. Wskutek tych zmian aktywność acetylocholinoesterazy znacznie spada poniżej normalnej wartości (Karczmar, 1967; Gadamski, Szumańska, 1977).

Obserwowany w przeprowadzonych badaniach znaczny spadek aktywności acetylocholinoesterazy jest prawdopodobnie spowodowany blokującym działaniem ipofosu na centrum aktywne enzymu. Spadek ak-

---

Ryc. 7. A) Grupa kontrolna. Silna aktywność AChE w neuropilu prążkowia. Pow. 80 ×. *B)* I grupa doświadczalna. Spadek aktywności AChE w neuropilu prążkowia po krótkotrwałym podawaniu dużych dawek ipofosu. Zachowana silna aktywność enzymu w neurocytach układu siateczkowatego międzymózgowia. Pow. 80 ×

Fig. 7. A) Control group. Strong AChE activity in the neuropil of striatum. × 80. *B)* Experimental group I. Decreased AChE activity in the neuropil of striatum after short-term administration of Ipophos in high doses. Preserved strong enzyme activity in neurocytes of the reticular formation of mesencephalon. × 80

Ryc. 8. A) Grupa kontrolna. Aktywność ChE w ścianie naczyń krwionośnych jądra bocznego wzgórza. Pow. 200 ×. *B)* I grupa doświadczalna. Znaczny spadek aktywności enzymu w ścianie naczyń. Pow. 200 ×

Fig. 8. A) Control group. Cholinesterase activity in blood vessel walls of lateral thalamic nuclei. × 200. *B)* Experimental group I. Marked decrease of enzyme activity in vessel walls. × 200

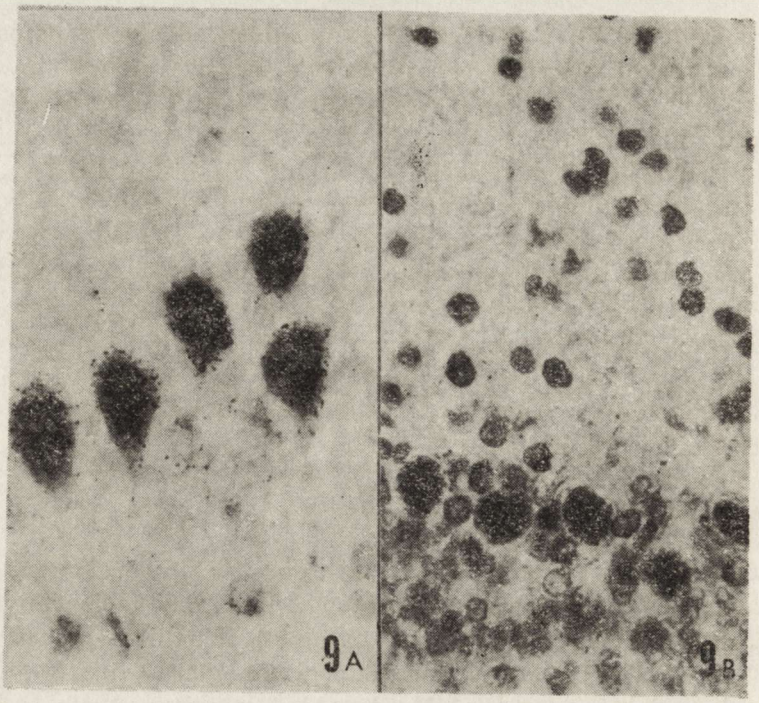

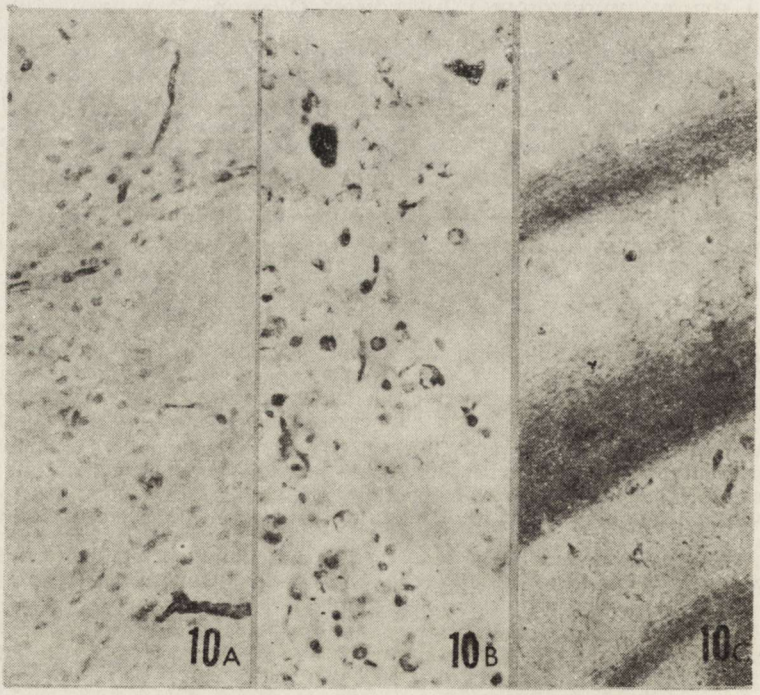

tywności enzymatycznej w przypadku AChE ma charakter uogólniony. W strukturach mózgu, wykazujących fizjologicznie silną aktywność AChE, dochodzi po intoksykacji ipofosem do wyraźnego obniżenia odczynu enzymatycznego, zaś w obszarach o niskiej aktywności AChE w stanach prawidłowych, odczyn ten po doświadczeniu zanika zupełnie. Spostrzeżenie to wydaje się wskazywać, że ipofos dobrze przenika przez barierę naczyniowo-mózgową w całym mózgowiu. Dłuższe podawanie ipofosu powoduje mniejsze zmiany aktywności AChE niż podawanie większych dawek w krótszym okresie. Zgodnie ze spostrzeżeniami Adamsa i wsp. (1976) zjawisko to może być spowodowane wzmożoną syntezą acetylocholinoesterazy u zatruwanych zwierząt. Zdaniem niektórych autorów (Alridge, 1957), organiczne połączenia kwasu fosforowego mają właściwości inhibicyjne nie tylko w odniesieniu do acetylocholinoesterazy, ale i do innych enzymów, zwłaszcza z grupy karboksyloesteraz. Obserwowany w przedstawionym materiale doświadczalnym spadek aktywności nieswoistych esteraz może być wynikiem inaktywującego wpływu ipofosu na tę grupę enzymów. Holmstaedt i wsp. (1957) oraz Zelman (1977) obserwowali u zwierząt po podawaniu związków fosforoorganicznych zmiany o cechach obrzęku mózgu. W przedstawionym materiale doświadczalnym obserwowano wykładniki zarówno naczyniopochodnego jak i cytotoksycznego obrzęku mózgu szczególnie nasilone w okolicy wzgórza. Wykładnikiem morfologicznym uszkodzenia funkcji naczyń krwionośnych jest również obserwowany we własnym materiale spadek aktywności cholinoesterazy i ATP-azy w ścianie naczyń powiązany z obrzmieniem śródbłonków naczyniowych i krwinkotokami okołonaczyniowymi.

Ryc. 9. A) Grupa kontrolna. Aktywność fosfatazy kwaśnej w komórkach Purkinjego móżdżku i w pojedynczych neurocytach warstwy ziarnistej. Pow. 510 ×. *B*) I grupa doświadczalna. Pojawienie się odczynu na FK w neurocytach warstwy drobinowej i w większości komórek ziarnistych. Komórki Purkinjego obkurczone. Pow. 510 ×

Fig. 9. A) Control group. Acid phosphatase activity in cerebellar Purkinje cells and in single neurocytes of the granular layer. × 510. *B*) Experimental group I. The appearance of acid phosphatase reaction in neurocytes of the molecular layer and in most granular cells. Shrunken Purkinje cells. × 510

Ryc. 10. A) Grupa kontrolna. Odczyn na ATP-azę widoczny w błonie jądrowej neurocytów i w ścianie naczyń prążkowia. Pow. 200 ×. *B*) I grupa doświadczalna. Wzrost aktywności enzymu w neurocytach, włośniczkach i arteriolach prążkowia. Pow. 200 ×. *C*) II grupa doświadczalna. W porównaniu do grupy kontrolnej spadek lub brak odczynu enzymatycznego w neurocytach i ścianie naczyń prążkowia. Pojawienie się odczynu enzymatycznego we włóknach nerwowych. Pow. 200 ×

Fig. 10. A) Control group. ATPase activity in nuclear membranes of neurocytes and in striatal vessel walls. × 200. *B*) Experimental group I. Increased enzyme activity in striatal neurocytes, capillaries and arterioles. × 200. *C*) Experimental group II. Decrease or absence of enzyme reaction in neurocytes and striatal vessel walls. The appearance of enzyme reaction in nerve fibers. × 200

WNIOSKI

1. Dożołądkowe podawanie ipofosu wywołuje u szczurów zmiany morfologiczne i histoenzymatyczne w ośrodkowym układzie nerwowym.
2. Zmiany morfologiczne polegają na występowaniu zmian zwyrodnieniowych i martwiczych neurocytów oraz komórek glejowych i uszkodzeniu ścian naczyń włosowatych z krwinkotokami.
3. Zmiany histoenzymatyczne polegają na spadku aktywności AChE, ChE i NsE oraz wzroście aktywności TPP-azy i FZ.
4. Duże dawki ipofosu prowadzą do wzrostu aktywności FK i ATP-azy.
5. Stopień nasilenia zmian morfologicznych zależy od czasu stosowania ipofosu, zaś stopień zmian aktywności enzymatycznej uzależniony jest od wysokości dawki badanego związku.

MORPHOLOGICAL AND HISTOENZYMATIC CHANGES IN THE RAT BRAIN FOLLOWING EXPERIMENTAL INTOXICATION WITH BROMOPHENVINPHOS (IPOPHOS-IPO 62)

Summary

Ipophos is a phosphoorganic insecticide introduced to Polish agriculture in 1978. The toxic effects of phosphoorganic compounds on animals consist in stable binding of acetylcholinesterase and endogenous intoxication with the mediator.

The effect of intragastric administration of Ipophos on the central nervous system was studied on adult rats. The animals received either 12 mg of Ipophos daily for 5 days and 18 mg daily for 4 days (group I), or 3—12 mg daily for 58 days (group II). The brains after the experiment were subjected to morphological and histoenzymatic examinations. Morphological changes consisted in degenerative and necrotic lesions in nerve cells and reactive hypertrophy in neuroglial cells. Histoenzymatic tests revealed a decrease of acetylcholinesterase and nonspecific esterase activity and an enhancement of the TPPase, alkaline phosphatase, acid phosphatase and ATPase reaction. The intensity of the morphological changes correlated with the duration of exposure, while that of the histoenzymatic reaction appeared dose-dependent.

PIŚMIENNICTWO

1. Adams G. K., Yamamura H. L., O'Leary J. F.: Recovery of central respiratory function following anticholinesterase intoxication. Europ. J. Pharmacol., 1976, 38, 101—112.
2. Alridge W. N.: Organophosphorus compounds and esterases. Ann. Rep. Chem. Sci., 1957, 53, 294—305.
3. Florkin M., Stotz E. H.: Enzyme nomenclature. W: Comprehensive biochemistry. Elsevier, Amsterdam 1973.
4. Gadamski E., Szumańska G.: Wpływ zatrucia fosforoorganicznym insektycydem — Dichlorfosem (DDVP) na aktywność acetylocholinoesterazy (AChE) w mózgu szczura. Neuropat. Pol., 1977, 15, 537—544.
5. Gerebtzoff M.: Recherches histochimiques sur les acetylocholine et choline esterases. Acta anat. 1953, 19, 336—339.

6. Gomori G.: Microscopic histochemistry. The University of Chicago Press, Chicago 1953.
7. Holmstedt B.: Pharmacology of organophosphorus cholinesterase inhibitors. Pharmacol. Rev., 1959, 11, 567—688.
8. Holmstedt B., Krook L., Rooney D. R.: The pathology of experimental cholinesterase-inhibitor poisoning. Acta Pharmacol., 1957, 13, 337—344.
9. Karczmar A. G.: Pharmacologic, toxicologic and therapeutic properties of anticholinesterase agents. W: Physiological pharmacology. Vol. III. Autonomic nervous system drugs. Academic Press, New York 1967, 163—250.
10. Kontek M., Pietraszek Z., Marcinkowska B.: Ocena odległych kontrolnych badań elektroencefalograficznych u pracowników rolnych intensywnie eksponowanych na związki fosforoorganiczne i karbaminiany. Pol. Tyg. Lek., 1974, 29, 1373—1374.
11. Maresch W.: Die Vergiftung durch Phosphorsäurester. Arch. Toxicol., 1957, 16, 285—319.
12. Mc Combie H., Saunders B. C.: Alkyl fluorophosphorates. Nature, 1946, 157, 287—289.
13. Modell W., Krop S., Hitchcoch P., Riker W. R.: General systematic actions of diisopropyl fluorophosphate in cats. J. Pharmacol. exp. Ther., 1946, 87, 410—412.
14. Nachlas M., Seligmann A.: The histochemical demonstration of esterases. J. nat. Cancer Inst., 1949, 9, 415—425.
15. Novikoff A., Goldfischer B. S.: Nucleoside diphosphatase activity in the Golgi apparatus and its usefulness for cytological studies. Proc. nat. Acad. Sci., 1961, 47, 802—810.
16. Rusiecki W.: Toksykologia środków ochrony roślin. Insektycydy fosforoorganiczne. PZWL, Warszawa 1973, 75—102.
17. Wachstein M., Meisel E.: Histochemistry of hepatic phosphatases of a physiologic pH with special reference to the demonstration of bile canaliculi. Amer. J. Clin. Path., 1957, 27, 13—23.
18. Wilson L. B., Bergmann F.: Acetylocholinesterase. VIII. Dissociation constants of the active groups. J. Biol. Chem., 1950, 186, 683—692.
19. Zelman I. B.: Patomorfologia mózgu szczura w doświadczalnym zatruciu fosforoorganicznym pestycydem Dichlorfosem (DDVP). Neuropat. Pol., 1977, 15, 515—222.

Adres autorów: Zakład Neuropatologii Instytutu Chorób Układu Nerwowego i Narządów Zmysłów AM, ul. Przybyszewskiego 49, 60—355 Poznań

NEUROPAT. POL., 1982, 20, 1—2
PL ISSN 0028—3894

ZUZANNA KRAŚNICKA, KRYSTYNA OLSZEWSKA

WPŁYW ETYLONITROZOMOCZNIKA (ENU) NA ORGANOTYPOWĄ HODOWLĘ TKANKI NERWOWEJ

(BADANIA W MIKROSKOPIE ŚWIETLNYM I ELEKTRONOWYM)

Zespół Neuropatologii Centrum Medycyny Klinicznej i Doświadczalnej PAN

Alkilowe pochodne nitrozomocznika: etylonitrozomocznik (ENU) i metylonitrozomocznik (MNU) znane są z onkogennego działania dla kilku gatunków zwierząt i dla różnych tkanek, a zwłaszcza dla tkanki nerwowej. Liczne badania wykonane na zwierzętach dowiodły, że właściwości neurotropowe tych związków nie zależą od sposobu i drogi podawania (Druckrey i wsp., 1965; Ivankovic, Druckrey, 1968; Wechsler i wsp., 1969). Badania Kroh (1973; 1976; 1978) wykazały ponadto, że ENU podany dożylnie ciężarnym myszom wywołuje u potomstwa, a również i u matek, ogniskowe uszkodzenia osłonki mielinowej. Obserwacje mikroskopowo-elektronowe potwierdziły zaburzenia w strukturze mieliny oraz wykazały towarzyszące im nieprawidłowości we włóknach osiowych (Kroh, Luciani, 1978). Działanie onkogenne i mielino-toksyczne pochodnych nitrozomocznika charakteryzuje się dość długim okresem utajenia. Procesy, które występują od momentu podania czynnika chemicznego aż do pojawienia się uchwytnych zmian, są nadal mało poznane (Laerum, Rajewsky, 1975; Schiffer i wsp., 1980). Zastosowanie modelu hodowli tkankowej okazało się przydatne do uchwycenia wczesnych zmian morfologicznych i ultrastrukturalnych w poszczególnych składnikach tkanki nerwowej, wywołanych bezpośrednim działaniem substancji onkogennych (Kraśnicka, Gajkowska, 1979; 1981). Poprzednie nasze badania dotyczyły wpływu MNU na hodowlę tkanki nerwowej, bezpośrednim zaś celem niżej przedstawionych doświadczeń jest prześledzenie zmian wywołanych działaniem ENU. W tej serii badań postanowiono wykonać doświadczenia z określoną dawką ENU (50 mg%) z dwóch powodów: 1 — wstępne badania wykazały, że ENU w dawce 100 mg% w środowisku odżywczym wywołuje ciężkie nieodwracalne zmiany doprowadzające do martwicy hodowanej tkanki; 2 —

w celu porównaniu działania obu związków pochodnych nitrozomocznika podanych w tej samej dawce i przy zachowaniu tego samego układu grup doświadczalnych.

MATERIAŁ I METODY

Badania wykonano na 3-tygodniowych organotypowych hodowlach móżdżku noworodków szczurzych, szczepu Wistar. Hodowle prowadzono według metody stosowanej rutynowo w naszej pracowni (Kraśnicka, Mossakowski, 1965). Doświadczenie obejmowało cztery grupy. Do środowiska odżywczego trzech grup hodowli dodawano jednorazowo ENU w dawce 50 mg% na okres 3 dni. Hodowle grupy I badano bezpośrednio po działaniu czynnika onkogennego. Hodowle grup II i III po 3-dniowym przetrzymaniu w środowisku z ENU przepłukiwano i przenoszono do normalnego środowiska odżywczego na 3 dni (grupa II) i 6 dni (grupa III). Grupę IV — kontrolną — stanowiły hodowle prowadzone w prawidłowych warunkach.

Obserwacje w mikroskopie świetlnym przeprowadzono na hodowlach utrwalonych i barwionych metodami histologicznymi (Nissl, Bodian, Sudan czarny B). Na hodowlach nieutrwalonych wykonano odczyny histochemiczne dla wykazania aktywności dehydrogenazy bursztynianowej (SDH), dehydrogenazy glutaminianowej (GDH) i dehydrogenazy glukozo-6-fosforanowej (G-6-PDH) według metod przedstawionych w poprzedniej pracy (Kraśnicka i wsp., 1971).

Badania mikroskopowo-elektronowe wykonano na siostrzanych hodowlach z każdej grupy doświadczalnej. Materiał przeprowadzano w sposób standardowy i zatapiano w eponie 812. Ultracienkie skrawki montowano na siatkach i kontrastowano octanem uranylu i cytrynianem ołowiu. Zdjęcia wykonano przy użyciu mikroskopu elektronowego JEM 7 A.

WYNIKI

Badania w mikroskopie świetlnym

Grupa I. Hodowle 3-tygodniowe, barwione metodą Nissla, obserwowane bezpośrednio po działaniu ENU, wykazują dyskretne zmiany w porównaniu z grupą kontrolną. Zwraca uwagę znaczny rozplem wszystkich komórek glejowych. Pomiędzy polami wypełnionymi przez oligodendrocyty, astrocyty i ich wypustki widoczne są skupienia jednorodnych, bezwypustkowych komórek wyściółki, tworzących dość często układy rozetowate (ryc. 1). Zbiory komórek wyściółki charakteryzuje znaczna monotypowość, dotycząca zarówno kształtu komórek jak i ich jąder. W strefie wzrostu komórek glejowych spostrzega się mitozy w ilości większej niż w hodowlach kontrolnych. Intensywność zabarwienia cy-

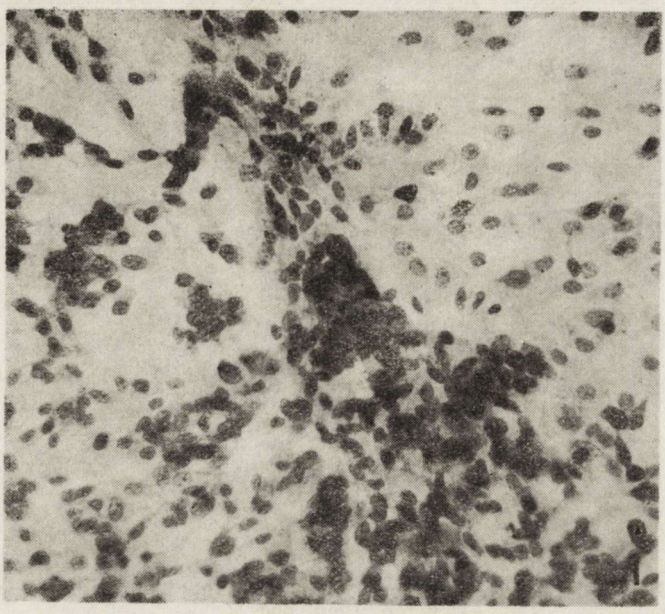

Ryc. 1. Grupa I. Hodowla 3-tyg. Obfity wzrost komórek glejowych. W prawym rogu widoczne komórki wyściółki z jaśniejszymi jądrami, tworzące układy rozetowate. Pow. 200 ×

Fig. 1. Group I. 3-week culture. Abundant growth of glial cells. In the right corner ependymal cells with brighter nuclei, forming rosette-like structures. × 200

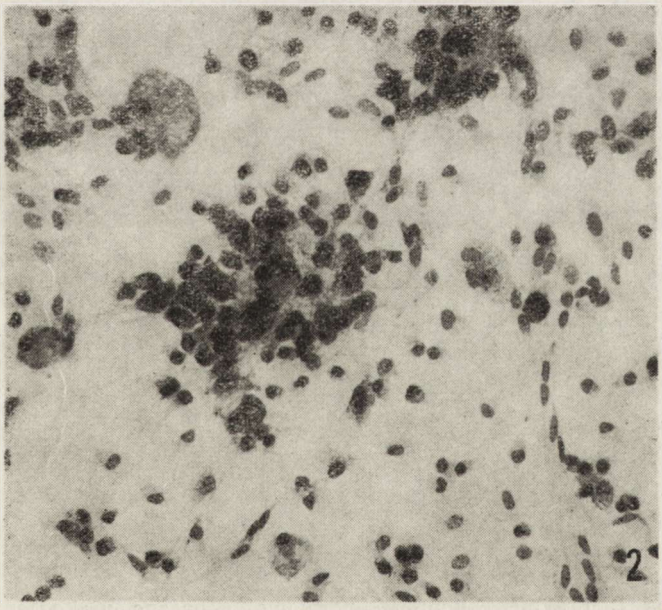

Ryc. 2. Grupa II. Hodowla 3-tyg. W polu wzrostu astrocytów i oligodendrocytów zaznaczony polimorfizm komórek. Pow. 200 ×

Fig. 2. Group II. 3-week culture. Cellular polymorphism in the growth zone of astrocytes and oligodendrocytes. × 200

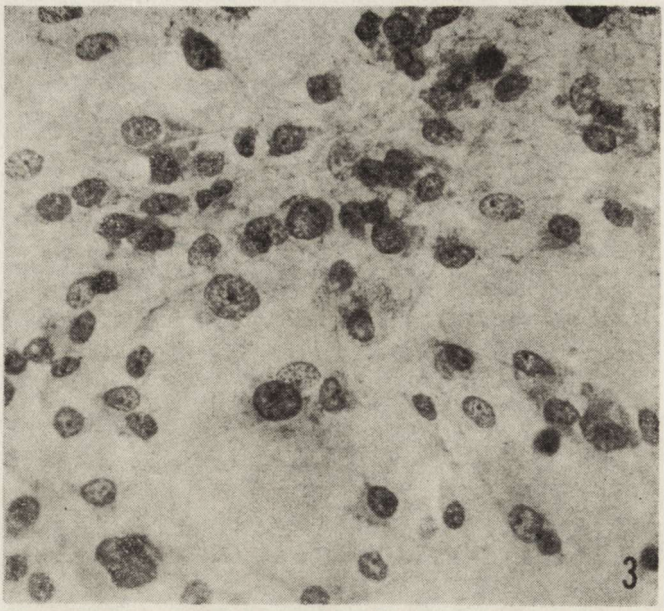

Ryc. 3. Grupa III. Hodowla 3-tyg. Wyraźny polimorfizm jąder komórek glejowych. Pow. 400 ×

Fig. 3. Group II. 3-week culture. Marked polymorphism of glial cell nuclei. × 400

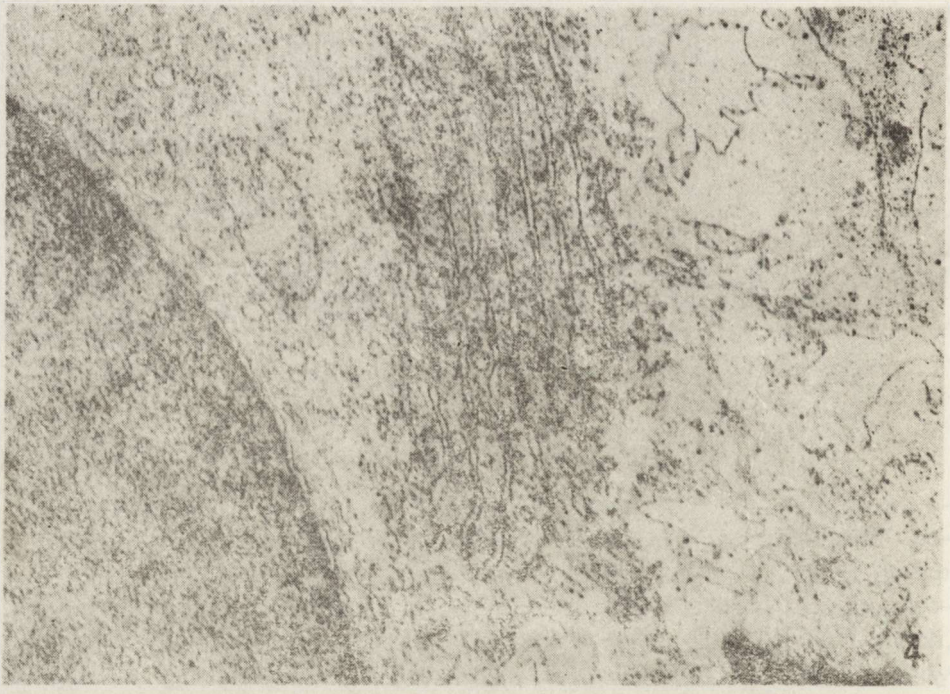

Ryc. 4. Grupa I. Fragment komórki nerwowej. Znaczne uszkodzenie szorstkiej siatki śródplazmatycznej, przeważnie w obwodowych częściach cytoplazmy. Obrzmiałe mitochondria. Pow. 10.500 ×

Fig. 4. Group I. Nerve cell fragment. Severe damage of rough endoplasmic reticulum, mostly in the peripheral parts of cytoplasm. Swollen mitochondria. × 10 500

toplazmy i jąder wszystkich typów komórek nie odbiega od normy. W niektórych eksplantatach spostrzega się neurocyty o prawidłowym wyglądzie. Jedynie niewielka liczba astrocytów leżących w obwodowych partiach strefy wzrostu wykazuje obecność drobnych wakuoli w cytoplazmie.

Hodowle barwione metodą Bodiana nie wykazują większych nieprawidłowości w porównaniu z hodowlami kontrolnymi. Natomiast w hodowlach barwionych Sudanem czarnym B ujawniają się odcinkowe obrzmienia osłonki mielinowej wzdłuż większości włókien nerwowych. Odczyny histochemiczne ujawniające aktywność 3 badanych dehydrogenaz wykazują takie samo umiejscowienie i intensywność reakcji jak hodowle grupy kontrolnej.

Grupy II i III. Hodowle z 3-dniowym i 6-dniowym przeżyciem po działaniu ENU wykazują niewielkie odrębności morfologiczne w stosunku do grupy I. Hodowle obu grup, podobnie jak i hodowle grupy I, cechuje obfita proliferacja wszystkich komórek pochodzenia glejowego. W preparatach barwionych metodą Nissla cechą wyróżniającą hodowle grupy II i III, w zestawieniu z hodowlami grupy I, jest znaczny polimorfizm astrocytów i oligodendrocytów. Ryc. 2, przedstawiająca pole wzrostu obu typów komórek glejowych, wykazuje obecność komórek dwujądrzastych oraz przerosłych komórek glejowych z obfitą cytoplazmą, zawierającą niekiedy drobne wakuole. Cechy polimorfizmu dotyczą również jąder komórkowych zarówno astrocytów, jak i oligodendrocytów (ryc. 3). W obszarach wzrostu komórek glejowych wszystkich typów obserwuje się liczne mitozy, niektóre z nich wykazują cechy patologiczne, np. podziały trójbiegunowe.

Komórki nerwowe zawarte w eksplantatach tkankowych wyróżniają się obecnością ziarnistości Nissla w cytoplazmie, a ich obrazy w mikroskopie świetlnym nie wykazują różnic w porównaniu z hodowlami kontrolnymi.

Hodowle grup II i III barwione metodą Bodiana i Sudanem czarnym B nie wykazują uchwytnych odchyleń od obrazów spostrzeganych w grupie I. Badania enzymatyczne hodowli z grup II i III wykazują nieznaczne osłabienie aktywności dehydrogenazy bursztynianowej tylko w komórkach glejowych, znajdujących się w strefie wzrostu hodowli. Odczyny pozostałych badanych enzymów (GDH i G-6-PDH) przedstawiają się prawidłowo, nie wykazując istotnych różnic w porównaniu z grupą kontrolną.

Badania mikroskopowo-elektronowe

Grupa I. Obserwacje mikroskopowo-elektronowe hodowli bezpośrednio po działaniu ENU wykazują zmiany we wszystkich składnikach tkanki nerwowej. Komórki nerwowe wykazują różny stopień uszkodzenia cytoplazmy. Największe zmiany dotyczą układu błon cytoplazma-

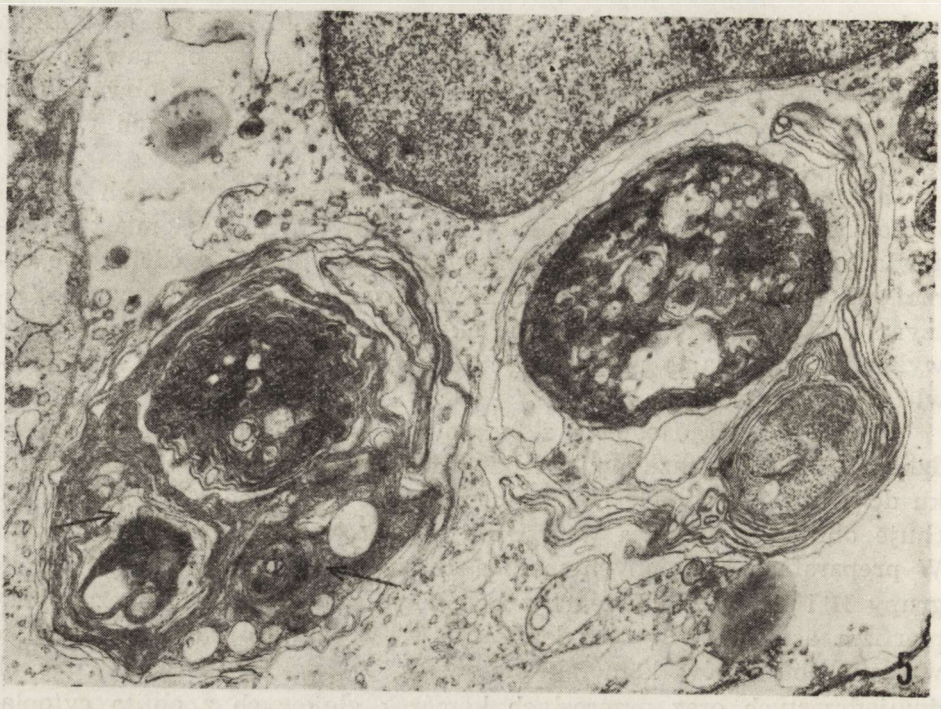

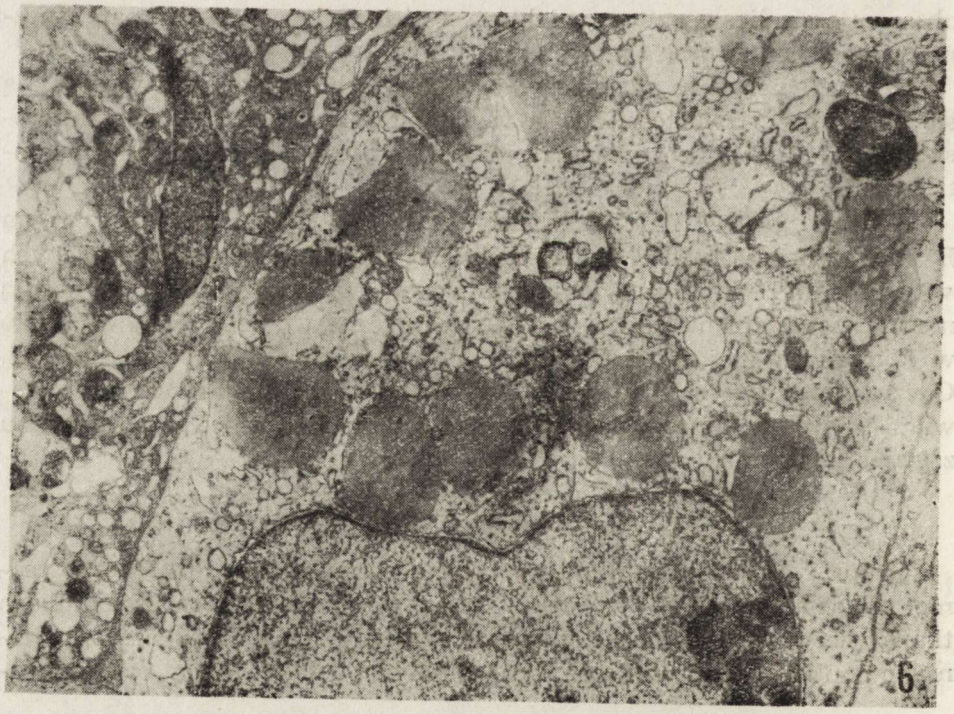

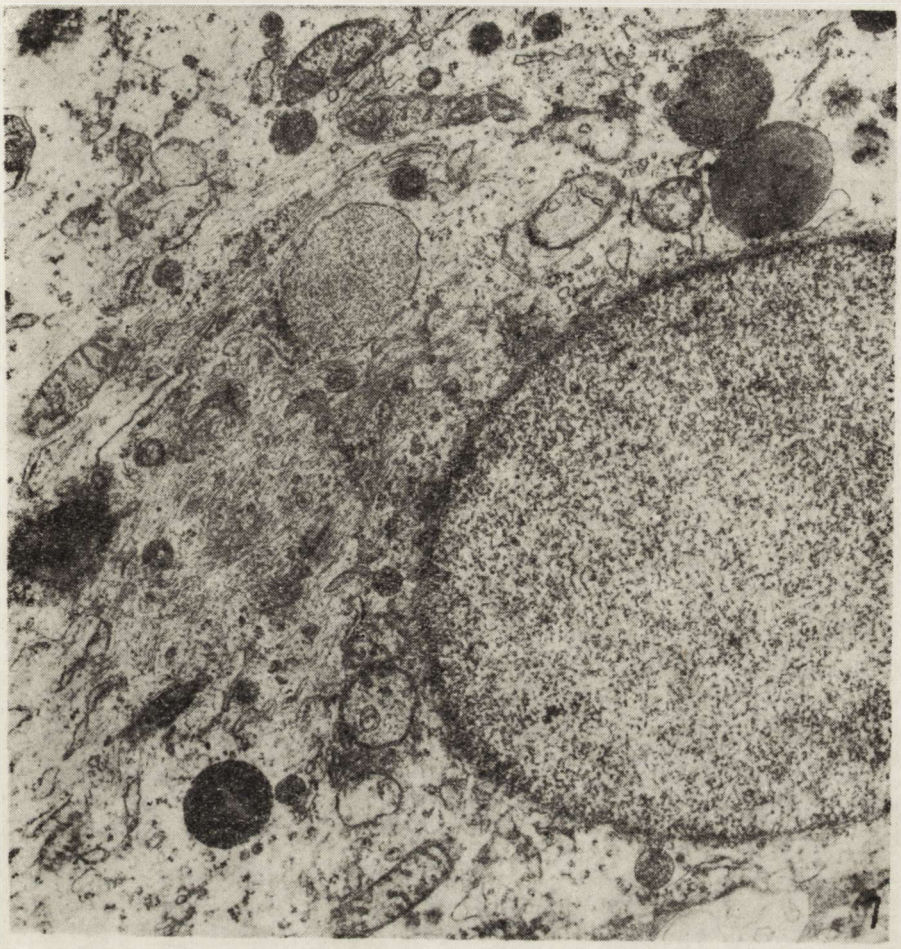

Ryc. 7. Grupa I. Fragment komórki astrogleju. Jądro z równomiernie rozłożoną chromatyną. W cytoplazmie dość liczne lizosomy, poszerzone kanały szorstkiej siatki śródplazmatycznej oraz nadmierna ilość gliofilamentów. Pow. 9 600 ×

Fig. 7. Group I. Astroglial cell fragment. Nucleus with uniformly distributed chromatin. In the cytoplasm relatively numerous lysosomes, dilated rough endoplasmic reticulum channels and abundance of glial filaments. × 9 600

Ryc. 5. Grupa I. Fragment hodowli tkanki nerwowej. Układy wypustek aksonalnych otoczonych blaszkami mielinowymi. Widoczne zlepienie blaszek mielinowych oraz ich rozwarstwienie. Pomiędzy niektórymi blaszkami widoczne resztki cytoplazmy komórki mielinizującej (strzałki). W prawym rogu akson wypełniony ziarnami glikogenu. Pow. 9.600 ×

Fig. 5. Group I. Nerve tissue culture fragment. Groups of axonal processes surrounded by myelin lamellae. Fusion and delamellation of myelin lamellae. Cytoplasmic residues of myelinating cells between some of the lamellae (arrows). In the right corner axon filled with glycogen granules. × 9 600

Ryc. 6. Grupa I. Fragment oligodendrocyta. W cytoplazmie liczne kule tłuszczowe oraz poszerzone kanały siatki gładkiej, obrzmiałe mitochondria, gliotubule i ciała lizosomopodobne. Pow. 9 300 ×

Fig. 6. Group I. Oligodendrocyte fragment. Numerous lipid balls, dilated smooth reticulum channels, swollen mitochondria, gliotubules and lysosome-like bodies in the cytoplasm. × 9 300

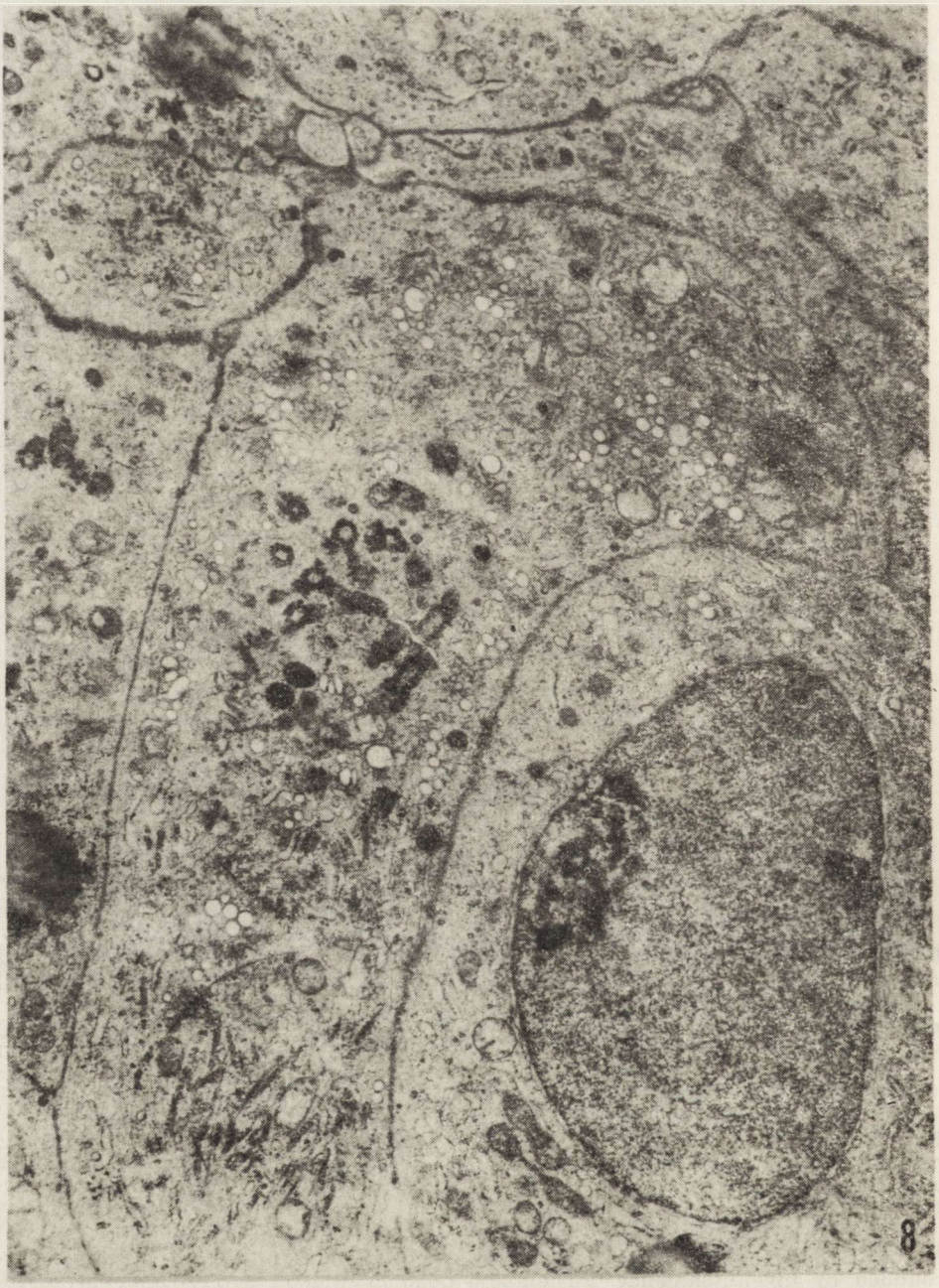

Ryc. 8. Grupa I. Fragment hodowli z komórkami wyściółki. W cytoplazmie widoczne przekroje rzęsek, poszerzone kanały szorstkiej siatki śródplazmatycznej oraz zwiększona ilość siatki gładkiej. Obserwuje się złącza komórkowe typu *zonulae adhaerentes* i *zonulae occludentes*. Pow. 9 600 ×

Fig. 8. Group I. Culture fragment with ependymal cells. In cytoplasm sections of cilliae, dilated rough endoplasmic reticulum channels and increased amount of smooth reticulum. Cellular junctions of the *zonulae adhaerentes* and *zonulae occludentes* type. × 9 600

tycznych. W większości neuronów obserwuje się uszkodzenie szorstkiej siatki śródplazmatycznej, polegające na poszerzeniu jej kanałów i zmniejszeniu ilości polirybosomów (ryc. 4). Niektóre neurony zawierają nadmiernie rozwiniętą siatkę gładką, tworząc poszerzone kanały i pęcherzyki przeważnie optycznie puste. Aparat Golgiego jest zwykle dobrze rozwinięty. Mitochondria są duże, o jasnej macierzy, często ze zmniejszoną ilością grzebieni.

Większość aksonów niezależnie od stopnia rozwoju osłonki mielinowej wykazuje cechy zwyrodnienia aksoplazmy, polegającego na zatarciu struktury i braku organelli. Niektóre aksony wypełnione są ziarnami glikogenu (ryc. 5). Mielina wokół aksonów wykazuje zaburzenia w układzie blaszek. Często obserwuje się ich zlepianie, zatarcie struktury oraz rozwarstwienie, przeważnie w powierzchownych warstwach osłonki. Niekiedy wśród rozwarstwień widoczne są resztki cytoplazmy komórki mielinizującej (ryc. 5).

Wśród komórek glejowych największe zmiany w obrazie ultrastrukturalnym występują w oligodendrocytach (ryc. 6). Cytoplazma tych komórek zawiera liczne kule tłuszczu i pojedyncze ciała mielinopodobne. Aparat Golgiego i gładka siatka śródplazmatyczna występują w postaci poszerzonych kanałów i różnej wielkości pęcherzyków. Szorstka siatka śródplazmatyczna tworzy krótkie kanały pokryte niewielką ilością rybosomów. W cytoplazmie oligodendrocytów spotyka się ponadto dość liczne gliotubule oraz obrzmiałe mitochondria ze zmniejszoną liczbą grzebieni. Jądra komórek są jasne, zaś ziarna chromatyny równomiernie rozłożone w całej nukleoplazmie.

Cytoplazma astrocytów jest przeważnie obrzmiała, miejscami przejaśniona, ze znaczną ilością mikrofilamentów (ryc. 7). Siatka śródplazmatyczna szorstka tworzy krótkie, nieregularne kanały ze zmniejszoną ilością rybosomów. Mitochondria wykazują różny stopień uszkodzenia struktury. Spotyka się zarówno mitochondria o prawidłowej budowie jak i obrzmiałe, pozbawione częściowo lub całkowicie grzebieni mitochondrialnych. Ilość ciał lizosomopodobnych i kul tłuszczowych jest różna w poszczególnych astrocytach. Jądra astrocytów o gładkich zarysach zawierają równomiernie rozproszoną chromatynę jądrową (ryc. 7).

Komórki wyściółki charakteryzują się obecnością rzęsek i złącz międzykomórkowych o typie *zonulae adhaerentes* i *zonulae occludentes* (ryc. 8). Budowa strukturalna rzęsek jest przeważnie prawidłowa. W cytoplazmie ependymocytów obserwuje się podłużne i poprzeczne przekroje przez ciałka podstawne i przez rzęski z typowym układem mikrotubul. Komórki wyściółki wykazują niewielkie zmiany w układzie błon cytoplazmatycznych. Siatka śródplazmatyczna szorstka tworzy długie kanały i tylko niektóre ich fragmenty ulegają poszerzeniu. W niektórych komórkach wzrasta ilość siatki gładkiej w postaci drobnych pęcherzyków przeważnie optycznie pustych. Drobne mitochondria ule-

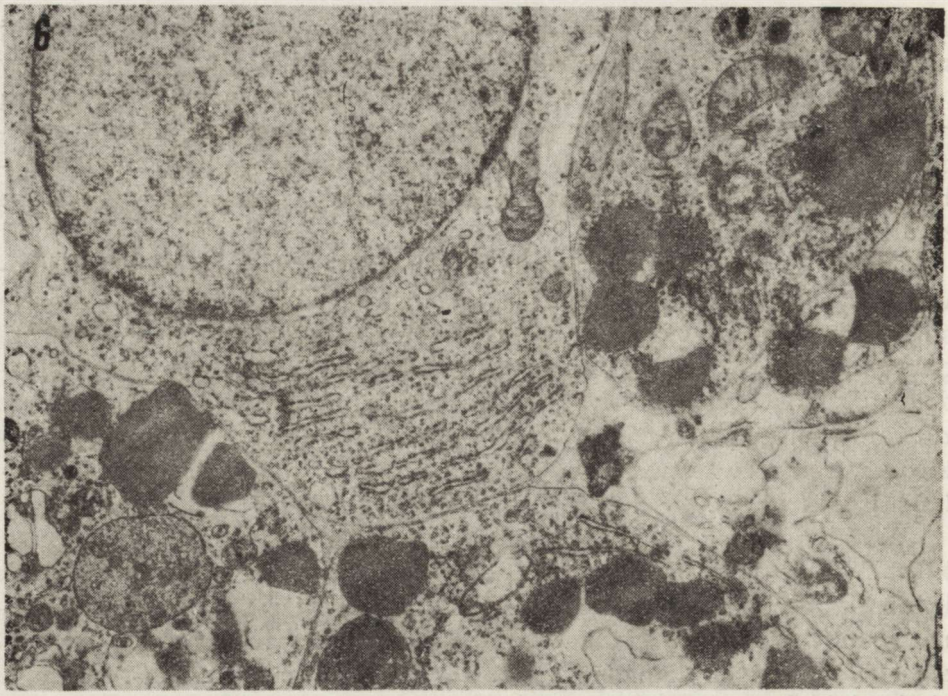

Ryc. 9. Grupa II. Fragment komórki nerwowej w otoczeniu komórek glejowych. W cytoplazmie komórki nerwowej widoczne kanały szorstkiej siatki, pokryte rybosomami oraz wolne polirybosomy. Znaczna ilość kul tłuszczowych w cytoplazmie oligodendrocytów. Pow. 9 600 ×

Fig. 9. Group II. Nerve cell fragment surrounded by glial cells. In the cytoplasm of nerve cell rough endoplasmic reticulum channels, covered by ribosomes and free polyribosomes. Numerous lipid balls in the cytoplasm of oligodendrocytes. × 9 600

Ryc. 10. Grupa II. Przekrój poprzeczny przez włókna nerwowe (A). Zmiany zwyrodnieniowe aksoplazmy i osłonki mielinowej. Pomiędzy blaszkami mielinowymi widoczna uszkodzona cytoplazma komórki mielinizującej (C). Pow. 9 600 ×

Fig. 10. Group II. Cross section of nerve fibre (A). Degenerative changes in axoplasm and myelin sheath. Damaged cytoplasm of myelinating cell (C) visible between myelin lamellae. × 9 600

Ryc. 11. Grupa II. Oligodendrocyt z dużą ilością kul tłuszczowych w cytoplazmie. Jądro z równomiernie rozłożoną chromatyną i z nielicznymi ziarnami perichromatynowymi (strzałki). Pow. 9 300 ×

Fig. 11. Group II. Oligodendrocyte with a great number of lipid balls in cytoplasm. Nucleus with uniformly distributed chromatin and few perichromatin granules (arrows). × 9 300

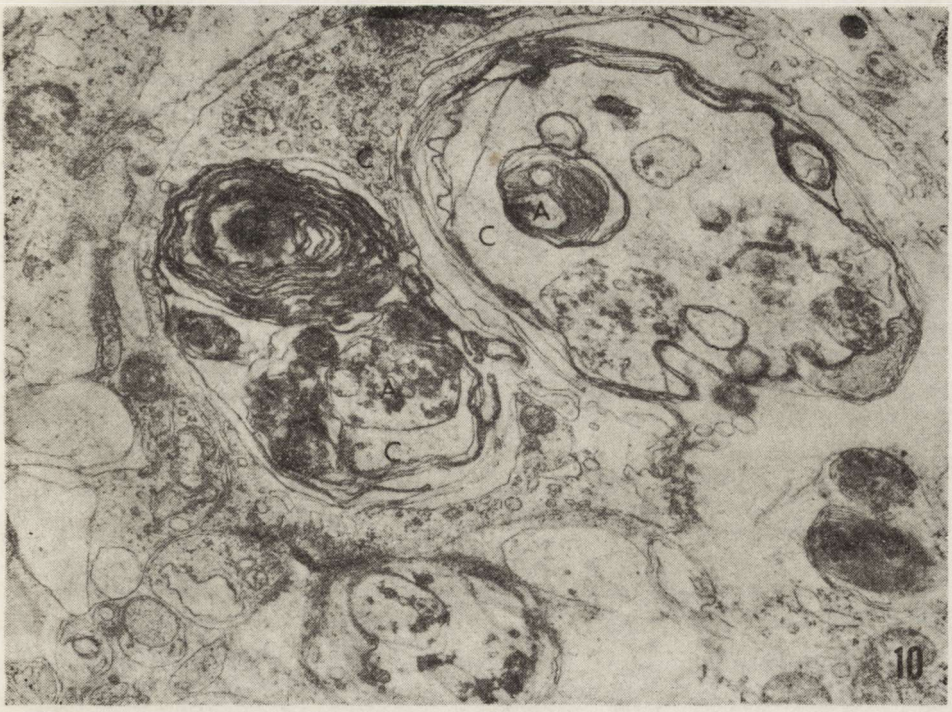

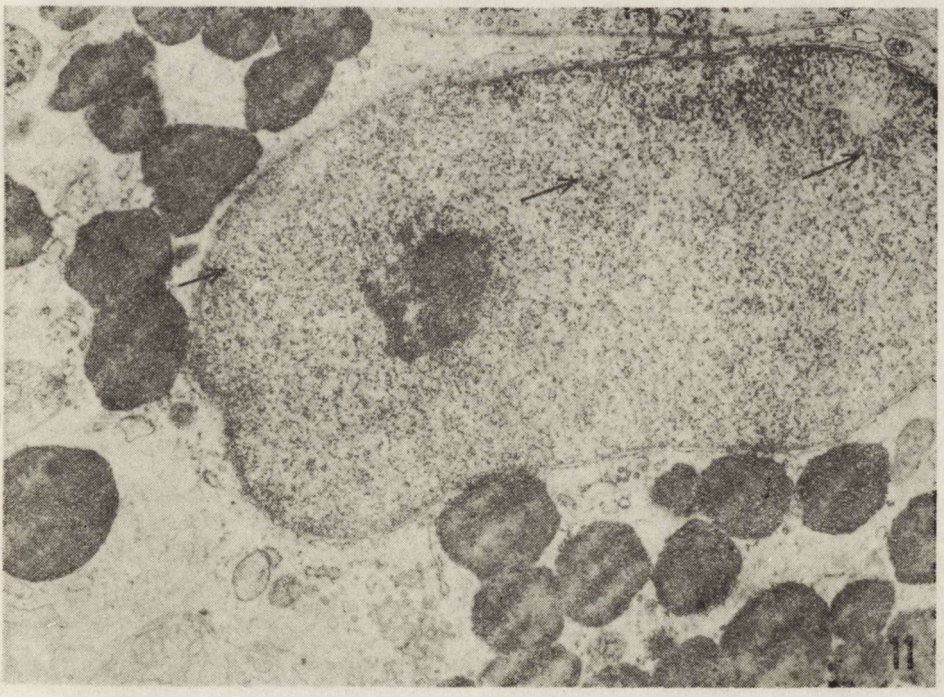

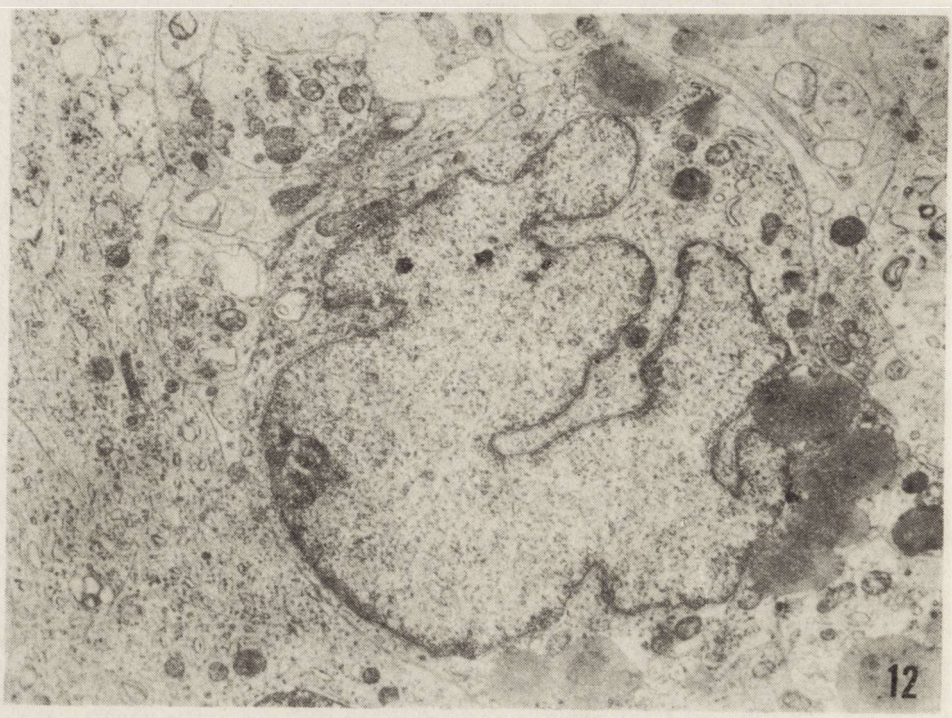

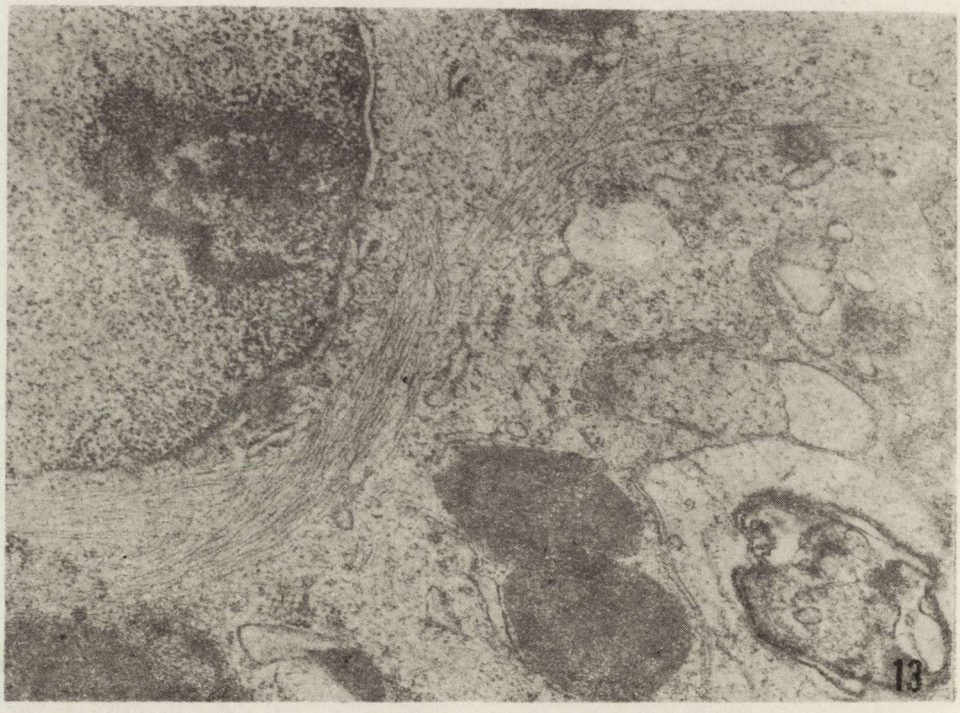

gają niekiedy obrzmieniu. W jądrach komórek wyściółki z jednolicie rozłożoną chromatyną widoczne są ziarna perichromatynowe.

Grupy II i III. Obserwacje hodowli po przeniesieniu do środowiska pozbawionego czynnika onkogennego wykazują różnice w obrazie ultrastrukturalnym komórek nerwowych i glejowych w porównaniu z grupą I.

Jądra komórek nerwowych wykazują zazwyczaj równomiernie rozłożoną chromatynę, a tylko w niektórych tworzą się niewielkie skupienia ziaren chromatynowych pod błoną jądrową. W chromatynie jądrowej występują ziarna perichromatynowe. Ilość ich jest największa w komórkach z grupy III. Cytoplazma komórek nerwowych wykazuje mniejsze nieprawidłowości w strukturze organelli w porównaniu z neuronami grupy I. Kanały szorstkiej siatki śródplazmatycznej tworzą typowe równoległe układy (ryc. 9, 10). Rybosomy pokrywające kanały siatki szorstkiej, oraz wolne polirybosomy występują w ilości prawidłowej. Aparat Golgiego składa się przeważnie z szorstkich kanałów i w większości komórek jest dobrze rozbudowany, natomiast układy gładkiej siatki śródplazmatycznej występują w mniejszej ilości i tylko w nielicznych neuronach. Mitochondria są przeważnie drobne, o prawidłowej strukturze.

Aksoplazma wypustek nerwowych w przeciwieństwie do dobrego stanu perikarionów wykazuje znaczne zmiany zwyrodnieniowe i wypełniona jest przeważnie kłaczkowatym materiałem. Struktura mieliny wykazuje zmiany podobne do spostrzeganych w I grupie doświadczalnej. Obserwuje się rozszczepienie poszczególnych blaszek lub ich zlepianie z zatarciem struktury warstwowej. Często pomiędzy blaszkami znajdują się resztki cytoplazmy komórki mielinizującej, zawierającej substancję kłaczkowatą, a niekiedy uorganizowane struktury o dużej gęstości elektronooptycznej (ryc. 10).

Cechą charakterystyczną oligodendrocytów z grupy II i III jest duża ilość kul tłuszczowych w cytoplazmie (ryc. 11). Komórki, zawierające mniej struktur tłuszczowych, wykazują prawidłową strukturę organelli cytoplazmatycznych. W niektórych oligodendrocytach zaobserwowano istotne zmiany w kształtach jąder, charakteryzujące się obecnością głę-

Ryc. 12. Grupa III. Oligodendrocyt. Nieregularne jądro z inwaginacjami. W cytoplazmie widoczne krótkie kanały szorstkiej siatki śródplazmatycznej oraz liczne kule tłuszczowe. Pow. 9 300 ×

Fig. 12. Group III. Oligodendrocyte. Irregular nucleus with invaginations. In cytoplasm short channels of rough endoplasmic reticulum and numerous lipid balls. 9 300 ×

Ryc. 13. Grupa III. Fragment astrocytu z obfitą ilością gliofibrylli w cytoplazmie. W pobliżu włókienek krótkie, poszerzone kanały szorstkiej siatki śródplazmatycznej. Pow. 10 000 ×

Fig. 13. Group III. Astrocyte fragment with abundance of glial fibrils in cytoplasm. Short, dilated channels of rough endoplasmic reticulum in the vicinity of fibrils. × 10 000

Ryc. 14. Grupa II. Fragment astrocyta. W cytoplazmie widoczne poszerzone kanały aparatu Golgiego, gliotubule, pofałdowany pęczek włókienek i obrzmiałe mitochondria. Pow. 10 000 ×

Fig. 14. Group II. Astrocyte fragment. In cytoplasm dilated channels of Golgi apparatus, gliotubules, folded bundle of fibrils and swollen mitochondria. × 10 000

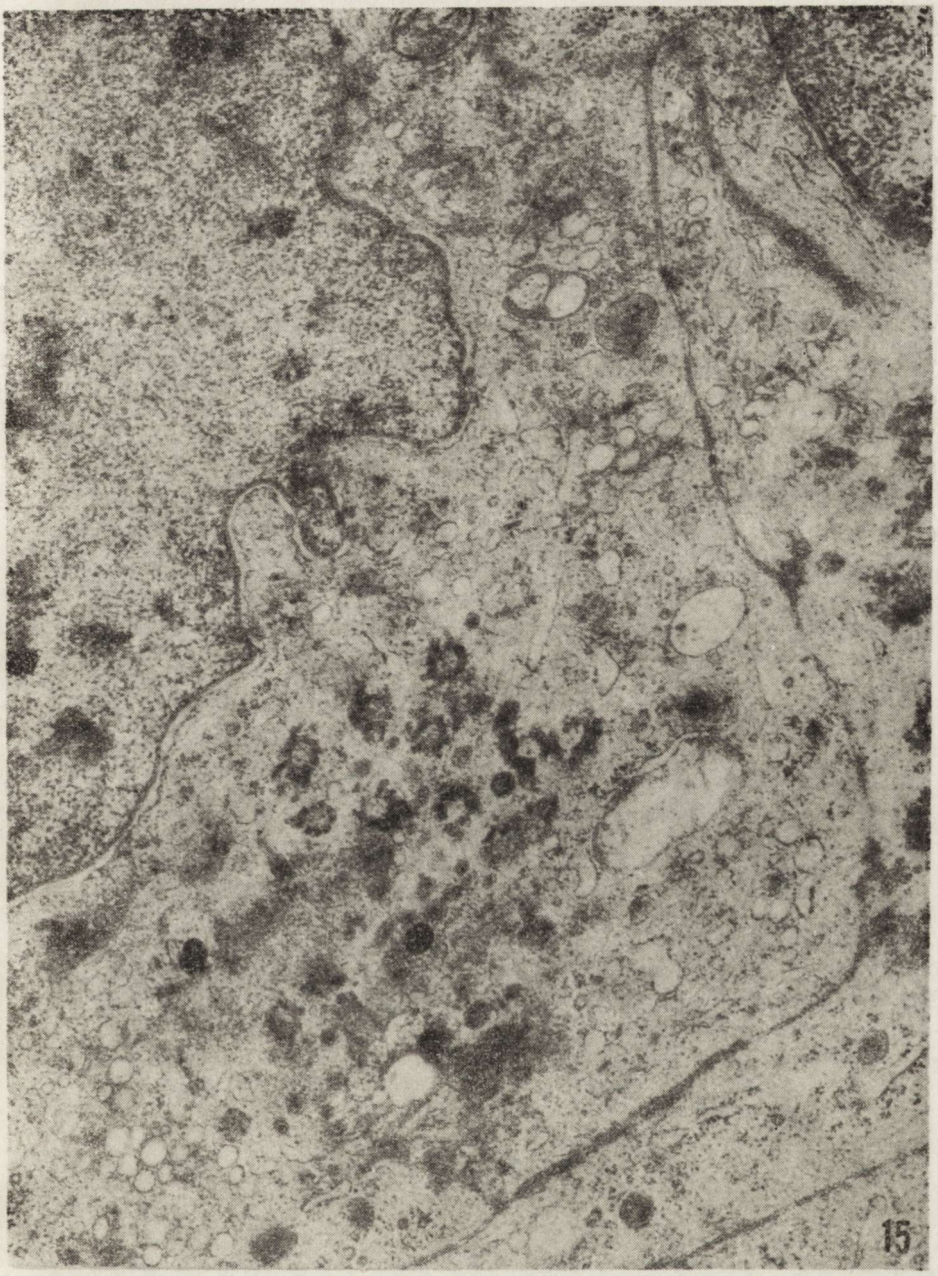

Ryc. 15. Grupa III. Fragment komórki wyściółki. W cytoplazmie widoczne przekroje rzęski, poszerzone kanały siatki gładkiej. W błonie komórkowej obecne liczne złącza typu *zonulae adhaerentes*. Pow. 12 600 ×

Fig. 15. Group III. Ependymal cell fragment. In cytoplasm sections of cilliae, dilated smooth reticulum channels. In cell membrane numerous junctions of the *zonulae adhaerentes* type. × 12 600

bokich inwaginacji otoczki, doprowadzających do powstawania nieregularnych, palczastych postaci jąder (ryc. 12).

W cytoplazmie większości astrocytów obserwuje się namnożenie struktur włókienkowych zarówno w perykarionach jak i w wypustkach. W niektórych astrocytach wiązki mikrofilamentów wypełniają całkowicie cytoplazmę (ryc. 13). W innych, obok mikrofilamentów, występują pojedyncze lub ułożone w pęczki mikrotubule. Układy pęczkowe gliotubul wykazują niekiedy charakterystyczne pofałdowanie (ryc. 14).

Komórki wyściółki cechuje najmniejsze nasilenie zmian i ich obraz ultrastrukturalny nie różni się zasadniczo od obrazów spostrzeganych w grupie I (ryc. 15). Niektóre jednak z komórek (z wyraźnymi złączami typowymi dla ich błon komórkowych) wykazują zmiany w kształcie jąder, podobne do spostrzeganych w jądrach oligodendrocytów. Głębokie wgłobienia błony jądrowej doprowadzają niekiedy do podziału zawartości jądra na kilka części, połączonych przez trójwarstwowe struktury powstające przez połączenie przeciwległych błon jądra komórkowego (ryc. 16).

Ryc. 16. Grupa II. Fragmenty dwóch komórek wyściółki z palczastymi jądrami. Głębokie inwaginacje błony jądrowej doprowadzają do powstawania trójwarstwowych błon (triple membrane). W błonie komórkowej obecne złącza komórkowe. Pow. 8 200 ×

Fig. 16. Group II. Fragments of two ependymal nuclei with finger-like nuclei. Deep invaginations of nuclear membrane lead to the formation of triple membrane. Cellular junctions in cell membrane. × 8 200

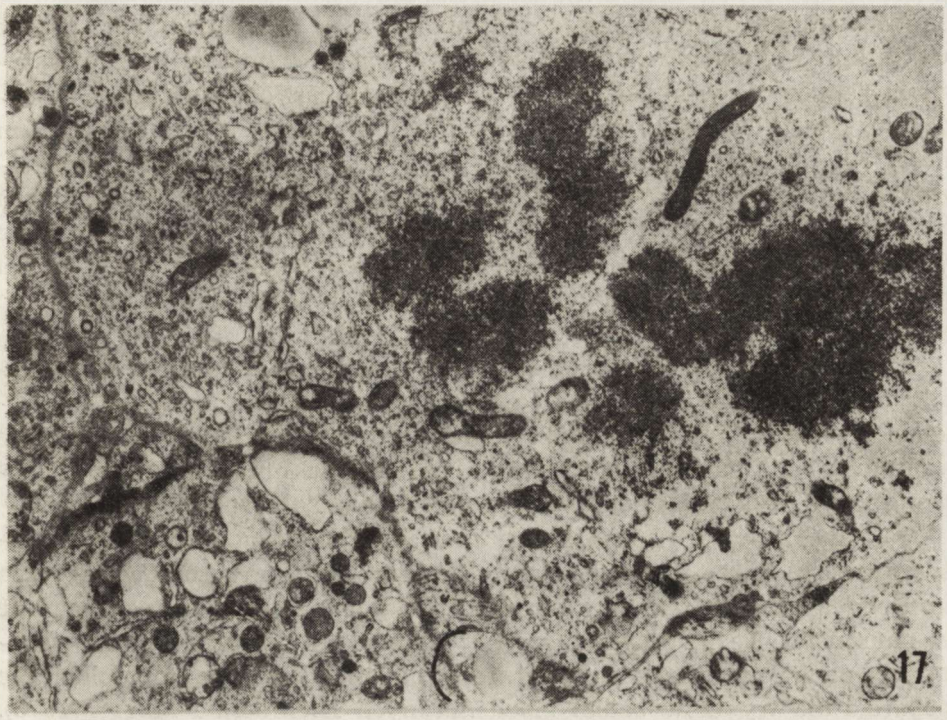

Ryc. 17. Grupa III. Komórka glejowa w stadium podziału mitotycznego. W cytoplazmie widoczne skupienia chromatyny tworzące chromosomy. Pow. 9 300 ×

Fig. 17. Group III. Glial cell in mitosis. Chromatin condensation and chromosome formation in cytoplasm. × 9 300

W materiale pochodzącym ze wszystkich grup doświadczalnych sporadycznie obserwowano komórki glejowe znajdujące się w różnych stadiach podziału mitotycznego. Rycina 17 przedstawia fragment komórki z obecnością chromosomów w cytoplazmie. Komórka nie zawiera żadnych fragmentów błony jądrowej.

OMÓWIENIE

Etylonitrozomocznik podany bezpośrednio do środowiska odżywczego hodowli w dawce 50 mg% wywołuje w niej dyskretne zmiany stwierdzane już w mikroskopie świetlnym, a znacznie wyraźniejsze w obrazach mikroskopowo-elektronowych.

Hodowle z grupy I w mikroskopie świetlnym charakteryzuje się jedynie ekspansywnym rozrostem komórek glejowych łącznie z wyściółką oraz niewielkim obrzmieniem osłonek mielinowych. Natomiast obserwacje w mikroskopie elektronowym ujawniają głębsze zmiany patologiczne stanowiące zapewne wykładnik cytotoksycznego działania ENU na wszystkie elementy komórkowe hodowanej tkanki.

Wykładniki cytotoksycznego działania ENU stwierdza się przede wszystkim w komórkach nerwowych. Należy tu wymienić przede wszystkim zaburzenia w układzie błon śródplazmatycznych. Występuje uszkodzenie szorstkiej siatki śródplazmatycznej ze znacznym zmniejszeniem ilości rybosomów i polirybosomów, proliferacja gładkiej siatki śródplazmatycznej oraz obrzmienie mitochondriów. Zmianom w perikarionach komórek nerwowych towarzyszą nieprawidłowości w ultrastrukturze włókien osiowych i ich osłonek mielinowych. Charakter tych zmian przypomina uszkodzenie układu nerwowego występujące u myszy po podaniu ENU (Kroh, 1976; Kroh, Luciani, 1978).

Objawy cytotoksycznego działania ENU występują również we wszystkich typach komórek glejowych, w najmniejszym stopniu w komórkach wyściółki. We wszystkich komórkach obserwuje się uszkodzenie szorstkiej siatki śródplazmatycznej i obrzmienie mitochondriów. Oligodendrocyty wykazują ponadto nagromadzenie substancji lipidowych.

Należy przy tym podkreślić, że zmiany w układzie błon śródplazmatycznych, z towarzyszącym zmniejszeniem ilości rybosomów, dotyczą wszystkich komórek tkanki nerwowej. Są one najbardziej zaznaczone w neuronach. Te nieprawidłowości w obrazie ultrastrukturalnym wskazywać mogą na upośledzoną syntezę białek, stanowiąc morfologiczne poparcie dla wyników badań biochemicznych Kleihuesa i Magge (1973).

Zestawienie wyników z grupy I z obserwacjami uzyskanymi z grup II i III pozwala na stwierdzenie cofania się zmian uznanych za wykładniki cytotoksycznego działania ENU na elementy komórkowe hodowli. Najistotniejsza poprawa w hodowlach grup II i III dotyczy perykarionów komórek nerwowych. Obraz mikroskopowo-elektronowy wskazuje na odnowę mitochondriów i szorstkiej siatki śródplazmatycznej ze zwiększeniem ilości rybosomów i wolnych polirybosomów. Jednocześnie w jądrach neurocytów pojawiają się ziarna perichromatynowe, które są uważane za morfologiczny odpowiednik przekaźnikowego kwasu rybonukleinowego (m-RNA) (Puvion i wsp., 1977; Gajkowska i wsp., 1977). Zmiany w obrazie mikroskopowo-elektronowym neuronów mogą przemawiać za wzmożoną aktywnością jądra i odhamowaniem syntezy białek. Należy jednak zwrócić uwagę na fakt, że pomimo odwracalności zmian stwierdzanych w perykarionach znacznej części komórek nerwowych nie stwierdza się poprawy w ultrastrukturze aksonów i mieliny.

Usunięcie ENU ze środowiska odżywczego hodowli prowadzi także do zmniejszenia się objawów cytotoksycznego uszkodzenia komórek glejowych, a zwłaszcza astrocytów. Obserwuje się odnowę szorstkiej siatki śródplazmatycznej oraz lepszy stan mitochondriów. Mniej wyraźna poprawa dotyczy oligodendrocytów, w których cytoplazmie gromadzą się nadal nagromadzone substancje tłuszczowe. Być może, nieodwracalne zmiany zwyrodnieniowe w oligodendrocytach są odpowiedzialne za utrzymujące się, po usunięciu ENU ze środowiska hodowli, uszkodzenie osłonek mielinowych.

W badanym materiale, zarówno w grupie I jak i w grupach II i III, występują pewne nieprawidłowości, które mogą przemawiać za transformacją blastomatyczną lub anaplastyczną komórek glejowych i komórek wyściółki. Zastosowany w naszych doświadczeniach ENU w dawce 50 mg% wyraźnie stymuluje proliferację komórek glejowych z obecnością licznych mitoz, w tym także sporadycznie występujących mitoz patologicznych. Przeniesienie hodowli do środowiska pozbawionego ENU nasila powyższe zmiany.

Pojawiają się także nowe nieprawidłowości, które mogą świadczyć na rzecz transformacji komórek. Należą do nich: polimorfizm komórek glejowych i ich jąder, wzmożone wytwarzanie włókienek glejowych w cytoplazmie astrocytów oraz pojawienie się dziwacznych, nieregularnych jąder glejowych. Identyczne cechy dotyczące jąder oraz fibryllogenezy opisywano w doświadczalnych guzach wzbudzonych przez pochodne nitrozomocznika (Benda i wsp., 1971; Koestner i wsp., 1971; Sipe i wsp., 1975). Analogiczne nieprawidłowości obserwowane były nie tylko w obrazie ultrastrukturalnym spontanicznych guzów, lecz także przekazywane były komórkom przeniesionym do hodowli *in vitro* (Vraa-Jensen i wsp., 1976; Goebel, Cravioto, 1972).

Zestawienie wyników przedstawionych w obecnej pracy z poprzednimi badaniami Kraśnickiej i Gajkowskiej (1979, 1981), dotyczącymi wpływu MNU na hodowaną tkankę nerwową wykazuje znaczne podobieństwo oraz pewne różnice w reakcji tej tkanki na dwie różne pochodne nitrozomocznika. Podobieństwa dotyczą przede wszystkim efektu cytotoksycznego, który wyrażony jest najsilniej bezpośrednio po działaniu zarówno MNU i ENU na hodowle. Transformacja komórkowa gleju w przypadku obu związków nasila się po przeniesieniu hodowli do środowiska prawidłowego. Różnice w reakcji na działanie obu związków wyrażają się tym, że MNU zaburza silniej aktywność enzymów oddechowych oraz prowadzi do pojawienia się większej ilości mitoz z przewagą mitoz patologicznych. Ponadto występują istotne różnice w strukturze jąder komórek glejowych po działaniu obu związków. W doświadczeniach z MNU jądra gleju oraz wyściółki są bogatochromatynowe z dużą ilością ziaren perichromatynowych. W hodowlach poddanych działaniu ENU wszystkie jądra komórek gleju i wyściółki są jasne z równomiernie rozłożoną chromatyną, bez skupień heterochromatyny.

Działanie nitrozopochodnych mocznika polega na alkilacji zasad kwasów nukleinowych. Najnowsze badania biochemiczne wykazują różnice w reagowaniu poszczególnych substancji onkogennych w zależności od ich grup alkilowych (Goth, Rajewsky, 1974; Sun, Singer, 1975; Hemminki, Savolainen, 1979). Etylonitrozomocznik charakteryzuje się wybiórczym powinowactwem do guaniny etylując jej pierścień w pozycji 6. Natomiast działanie metylonitrozomocznika nie jest tak specyficzne i może powodować metylację guaniny w różnych miejscach jej struktu-

ry chemicznej. Wydaje się przeto, że odmienności morfologiczne wykazane w naszych badaniach mogą być uzależnione od rodzaju grupy alkilowej nitrozomocznika.

EFFECT OF ETHYLNITROSOUREA (ENU) ON THE ORGANOTYPIC NERVE TISSUE CULTURE. LIGHT AND ELECTRON MICROSCOPIC STUDIES

Summary

The studies have dealt with the effect of ethylnitrosourea (ENU) on the morphology of 3-week organotypic cultures from newborn rat cerebellum. ENU was added to the culture medium in a 50 mg% dose for a period of 3 days. The cultures were examined directly after exposure to the carcinogen (group I) and following the transfer to a standard medium for 3 (group II) and 6 days (group III). Sister cultures grown in routine conditions served as control (group IV).

Light microscopic observations were performed on cultures fixed and stained after Nissl and Bodian and with Sudan black B. Unfixed cultures were assayed histochemically for the activity of respiratory enzymes. Electron microscopic studies were done with routine methods. The most pronounced structural changes in neurons and glia were observed in group I. The cultures of groups II and III after transient exposure to the toxic agent showed cytotoxic changes in neurons and glia of lower intensity than in group I. On the other hand, the persistence of changes in the glial cell nuclei and proliferation of glial fibrilles are indicative of anaplastic transformation of the cells.

PIŚMIENNICTWO

1. Benda P., Someda K., Sweet W. H.: Morphological and immunochemical studies of rat glial tumors and clonal strains propagated in culture. J. Neurosurg., 1971, 34, 310—323.
2. Druckrey H., Ivankovic S., Preussmann R.: Selektive Erzeungung maligner Tumoren im Gehirn und Rückenmark von Ratten durch N-Methyl-N-nitrosoharnstoff. Z. Krebsforsch., 1965, 66, 389—408.
3. Gajkowska B., Puvion E., Bernhard W.: Unusual perinucleolar accumulation of ribonucleoprotein granules induced by camptothecin in isolated liver cells. J. Ultrastruct. Res., 1977, 60, 335—347.
4. Goebel H. H., Cravioto H.: Ultrastructure of human and experimental ependyomas. J. Neuropath. exp. Neurol., 1972, 31, 54—71.
5. Goth R., Rajewsky M. F.: Persistance of 0^6-ethylguanine in rat brain DNA: correlation with nervous tissue system-specific carcinogenesis by ethylnitrosourea. Proc. Nat. Acad. Sci. USA, 1974, 71, 639—643.
6. Hemminki K., Savolainen H.: Methylation of neuronal and glial macromolecules by methylnitrosourea and dimethylnitrosamine in vivo. Toxical. Lett., 1979, 4, 287—293.
7. Ivankovic S., Druckrey H.: Transplacentare Erzeugung maligner Tumoren des Nervensystems. I.Äthyl-nitroso-harnstoff (ÄNH) an BD IX-Ratten. Z. Krebsforsch., 1968, 71, 320—360.
8. Kleihues P., Magee P.: Inhibition of protein synthesis by n-methyl-n-nitrosourea in vivo. Biochem. J., 1973, 126, 303—309.
9. Koestner A., Swenberg J. A., Wechsler W.: Transplancental production with

ethylnitrosourea of neoplasms of the nervous system in Sprague-Dawley rats. Am. J. Path., 1971, 63, 37—56.
10. Kraśnicka Z., Mossakowski M. J.: Zagadnienie zmienności morfologicznej tkanki glejowej hodowanej in vitro. Neuropat. Pol., 1965, 3, 397—408.
11. Kraśnicka Z., Mossakowski M. J., Renkawek K.: Morphologie et histochimie de neurones de ganglions spinaux cultives in vitro dans le conditions d'anoxie. Neuropat. Pol., 1971, 9, 93—101.
12. Kraśnicka Z., Gajkowska B.: Wpływ metylonitrozomocznika (MNU) na organotypową hodowlę tkanki nerwowej. Neuropat. Pol., 1979, 17, 557—570.
13. Kraśnicka Z., Gajkowska B.: Obraz histologiczny i ultrastrukturalny organotypowej hodowli tkanki nerwowej po działaniu metylonitrozomocznika. Neuropat. Pol., 1981, 19, 75—89.
14. Kroh H.: Ethylnitrosourea-induced microcephaly in brains of Swiss mice and Wistar rats. W: Donau Symposium für Neuropathologie. Aktuelle Probleme der Neuropathologie. Red. K. Jellinger, Facultas Verlag, Wien 1973, 29—35.
15. Kroh H.: Demyelination in the mouse brain after transplacental administration of N-ethyl-N-nitrosourea (ENU). Neuropat. Pol., 1976, 14, 115—119.
16. Kroh H.: Multiple demyelinating foci induced with ethylnitrosourea (ENU) in mouse brain. Proc. Intern. Neuropath. Symp. "Brain tumors and chemical injuries to the central nervous system", Warszawa 1976. Red. M. J. Mossakowski, PZWL, Warszawa 1978, 30—36.
17. Kroh H., Luciani A.: The effect of transplacental ethylnitrosourea on the fine structure of the adult mouse brain. I. Nerve cell. Neuropat. Pol., 1978, 16, 449—460.
18. Laerum O. D., Rajewsky M. F.: Neoplastic transformation of fetal rat brain cell in culture after exposure to ethylnitrosourea in vivo. J. Nat. Canc. Inst., 1975, 55, 1177—1187.
19. Puvion E., Viron A., Bernhard W.: Unusual accumulation of ribonucleoprotein constituents in the nucleus of cultured rat liver cells after hypothermal shock. Biol. Cel., 1977, 29, 81—88.
20. Sipe J. C., Rubinstein L. J., Herman W. M., Bignami A.: Ethylnitrosourea-induced astrocytomas. Morphologic observations on rat tumors maintained in tissue and organ culture systems. Lab. Invest., 1975, 31, 571—579.
21. Schiffer D., Giordana M. T., Mauro A., Racagni G., Bruno F., Pezzotta S., Paoletti P.: Experimental brain tumors by transplacental ENU. Acta neuropath. (Berl.), 1980, 49, 117—122.
22. Sun L., Singer B.: The specificity of different classes of ethylating agents toward various sites of HeLa cell DNA in vitro and in vivo. Biochemistry, 1975, 14, 1795—1802.
23. Vraa-Jensen J., Herman M. M., Rubinstain L. J., Bignami A.: In vitro characteristics of a fourth ventricle ependymoma maintained in organ culture systems: light and electron microscopy observations. Neuropath. appl. Neurobiol., 1976, 2, 349—364.
24. Wechsler W., Kleihues P., Matsumoto S., Zülch K. J., Ivankovic S., Preussmann R., Druckrey H.: Pathology of experimental neurogenic tumours chemically induced during prenatal and postnatal life. W: Research in the experimental and clinical aspects of brain tumours. Ann. N. Y. Acad. Sci., 1969, 159, 361—408.

Adres autorek: Zespół Neuropatologii Centrum Medycyny Doświadczalnej i Klinicznej PAN, ul. Dworkowa 3, 00—784 Warszawa

NEUROPAT. POL., 1982, 20, 1—2
PL ISSN 0028—3894

BARBARA GAJKOWSKA

ULTRASTRUKTURA UKŁADU PRZYSADKOWO-NADNERCZOWEGO SZCZURA W STRESIE WYWOŁANYM UNIERUCHOMIENIEM

Pracownia Ultrastruktury Układu Nerwowego, Centrum Medycyny Doświadczalnej i Klinicznej PAN

Unieruchomienie zwierząt wywołuje reakcję stresową manifestującą się aktywacją układu przysadkowo-nadnerczowego. Płat gruczołowy przysadki odpowiada na stres wydzielaniem nie tylko ACTH (Chowers i wsp., 1966), lecz również hormonu somatotropowego (Krulich, Mc Cann, 1966; Vernikos-Danellis, Trigg, 1967), prolaktyny (Grosvenor i wsp., 1965; Neill, 1970) oraz gonadotropin (Ajika i wsp., 1972). Stwierdza się jednocześnie zwiększenie poziomu kortykosterydów w nadnerczach i we krwi (Kvetnansky i wsp., 1970). Już w 30 min po unieruchomieniu zwierzęcia znacznie wzrasta poziom cyklicznego AMP w nadnerczach (Paul i wsp., 1971). Nieliczne są prace dotyczące morfologii układu przysadkowo-nadnerczowego w stresie wywołanym unieruchomieniem. W naszych badaniach ograniczyliśmy się do obserwacji w mikroskopie elektronowym płata gruczołowego przysadki i kory nadnerczy zwierząt unieruchomionych przez 2 dni, tzn. w okresie stresu, przed rozpoczęciem procesów adaptacyjnych (Mikulaj, Mitro, 1973). Badania mikroskopowo-elektronowe jąder podwzgórza i płata nerwowego przysadki w warunkach unieruchomienia były przedmiotem naszej wcześniejszej publikacji (Gajkowska i wsp., 1979).

MATERIAŁ I METODY

Szczury, samice szczepu Wistar, o wadze ok. 200 g umieszczano na okres 2 dni w klatkach wykonanych z metalowej siatki. W klatkach tych zwierzęta były całkowicie unieruchomione, mogły wykonywać tylko minimalne ruchy głową, umożliwiające im jedzenie i picie. Materiał do badań w mikroskopie elektronowym pobrano z płata gruczołowego przysadki i kory nadnerczy natychmiast po wyjęciu zwierząt z klatek. Wycinki utrwalano w 2,5% aldehydzie glutarowym w buforze

fosforanowym o pH 7,4 oraz w 2% czterotlenku osmu w tym samym buforze. Po odwodnieniu materiał zatapiano w Eponie 812 i ultracienkie skrawki barwiono octanem uranylu oraz cytrynianem ołowiu. Zdjęcia wykonano w mikroskopie elektronowym JEM 7A.

WYNIKI

Płat gruczołowy przysadki

W komórkach wydzielających ACTH nagromadzenie ziarnistości sekrecyjnych jest zbliżone do normy. Zwraca uwagę bardzo rozbudowany aparat Golgiego, składający się przeważnie z wąskich kanałów i bardzo licznych pęcherzyków różnej wielkości, wypełnionych niekiedy materiałem o małej gęstości elektronowej. Siatka śródplazmatyczna szorstka jest miernie rozwinięta, o kanałach nieznacznie poszerzonych. Lizosomy występują w ilości większej niż w normie (ryc. 1).

W większości komórek wydzielających hormon somatotropowy nagromadzenie ziarnistości sekrecyjnych jest mniejsze niż w normie. Apa-

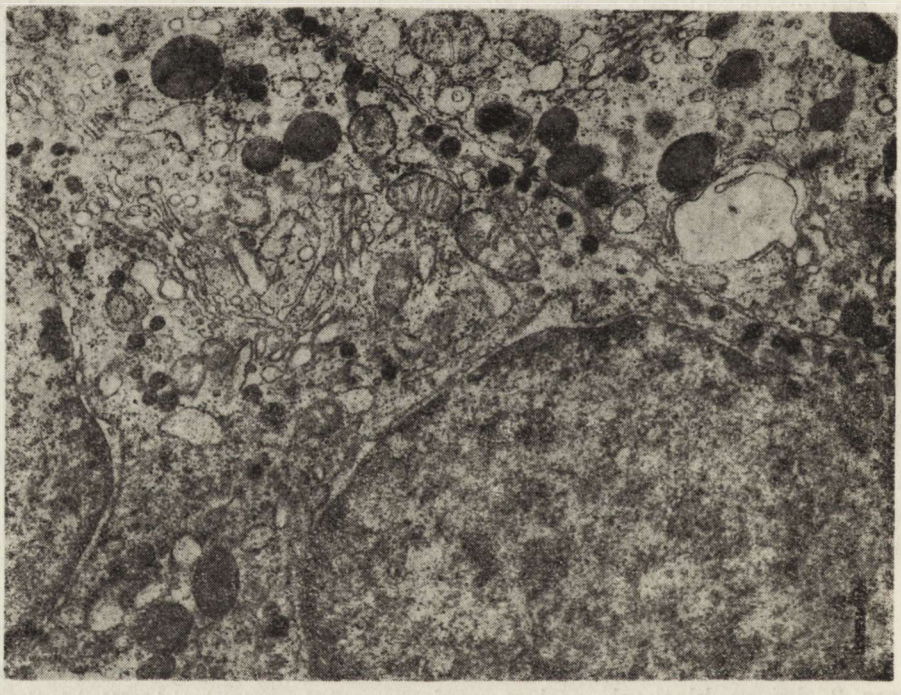

Ryc. 1. Komórka wydzielająca ACTH. Rozbudowany aparat Golgiego z licznymi drobnymi pęcherzykami wypełnionymi materiałem o różnej gęstości elektronowej. Kanały siatki śródplazmatycznej szorstkiej nieznacznie poszerzone, ułożone nierównomiernie. Dość liczne lizosomy. Pow. 13 950 ×

Fig. 1. ACTH-secreting cell. Well developed Golgi apparatus with numerous small vesicles filled with a material of different electron density. Rough endoplasmic reticulum channels slightly dilated and unevenly distributed. Numerous lysosomes. × 13 950

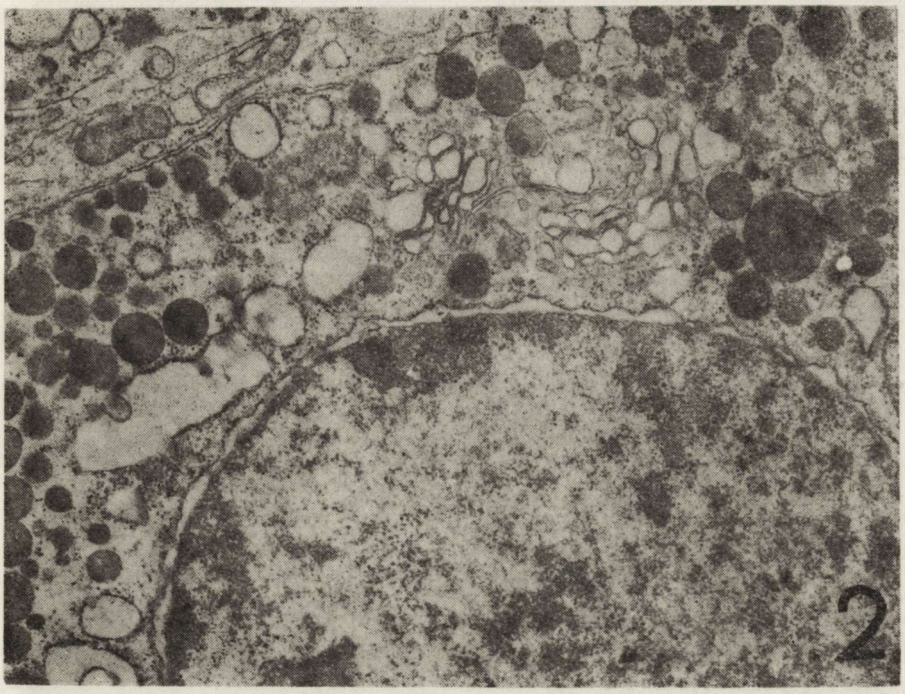

Ryc. 2. Komórka wydzielająca hormon somatotropowy. Aparat Golgiego rozbudowany, w jego pobliżu liczne ziarnistości sekrecyjne i lizosom. Kanały siatki śródplazmatycznej szorstkiej wyraźnie poszerzone. Jądro komórkowe o bogatej chromatynie. Pow. 13 950 ×

Fig. 2. STH-secreting cell. Well developed Golgi apparatus, in its vicinity numerous secretory granules and a lysosome. Rough endoplasmic reticulum channels strongly dilated. Chromatin-rich cell nucleus. × 13 950

rat Golgiego jest mocno rozbudowany, o szerokich kanałach i licznych pęcherzykach. Kanały siatki śródplazmatycznej szorstkiej są poszerzone balonowato. Dość licznie występują lizosomy (ryc. 2).

Komórki wydzielające prolaktynę zawierają niewiele ziarnistości sekrecyjnych. Silnie rozbudowany aparat Golgiego widoczny jest w wielu obszarach cytoplazmy. W jego otoczeniu występują liczne, drobne pęcherzyki, niektóre zawierające materiał o dużej gęstości elektronowej. Niektóre pęcherzyki zlewają się ze sobą, tworząc różnokształtne struktury. Siatka śródplazmatyczna szorstka, o licznych wąskich kanałach, ułożona jest na obwodzie komórki. W cytoplazmie znajdują się struktury błoniaste różnej wielkości, które wydają się mieć bezpośrednią łączność z kanałami siatki śródplazmatycznej i błonami aparatu Golgiego (ryc. 3).

Komórki wydzielające gonadotropiny charakteryzują się obecnością dużego, nieregularnego jądra, wypełnionego równomiernie chromatyną z dużą ilością ziarnistości perichromatynowych i interchromatynowych. Zwracają uwagę olbrzymie poszerzenia pomiędzy wewnętrzną i ze-

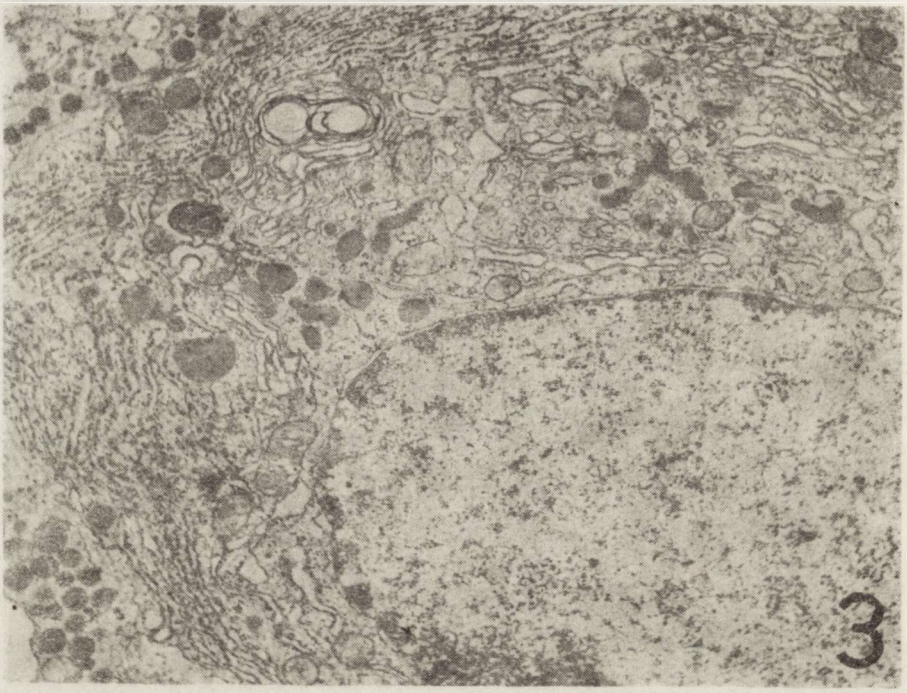

Ryc. 3. Komórka wydzielająca prolaktynę. Aparat Golgiego znacznie rozbudowany, drobne pęcherzyki z elektronowogęstym materiałem, niektóre łączące się ze sobą. Siatka śródplazmatyczna szorstka ułożona równomiernie na obwodzie komórki, obok struktury błoniaste. Liczne ziarnistości sekrecyjne. Pow. 10 200 ×

Fig. 3. Prolactin-secreting cell. Well developed Golgi apparatus, small vesicles with electron-dense material, some of them fused. Rough endoplasmic reticulum situated evenly on the cell periphery, in the vicinity membraneous structures. Numerous secretory granules. × 10 200

wnętrzną blaszką otoczki jądrowej. Podobnie balonowato poszerzone są kanały siatki śródplazmatycznej szorstkiej. Zarówno w przestrzeni pomiędzy blaszkami otoczki jądrowej, jak i w poszerzonych kanałach siatki szorstkiej, znajduje się niewielka ilość kłaczkowatego materiału. W cytoplazmie znajduje się duża ilość polirybosomów i okrągłe obrzmiałe mitochondria. Ilość ziarnistości sekrecyjnych jest wyraźnie mniejsza niż w normie (ryc. 4).

Ryc. 4. Komórka wydzielająca gonadotropiny. Duże nieregularne jądro. Przestrzeń pomiędzy blaszkami błony jądrowej miejscami bardzo poszerzona. Kanały siatki śródplazmatycznej szorstkiej balonowato rozdęte. W cytoplazmie ziarnistości sekrecyjne. Pow. 13 950 ×

Fig. 4. Gonadotropine-secreting cell. Large irregular nucleus. In some segments the space between the nuclear membrane lamellae markedly dilated. Rough endoplasmic reticulum channels dilated in a baloon-like fashion. In cytoplasm secretory granules. × 13 950

Ryc. 5. Komórka wydzielająca TSH. Nieco zmniejszone nagromadzenie ziarnistości sekrecyjnych, poza tym budowa nie odbiega od normy. Pow. 10 200 ×

Fig. 5. TSH-secreting cell. Somewhat decreased accumulation of secretory granules, otherwise no deviation from norm. × 10 200

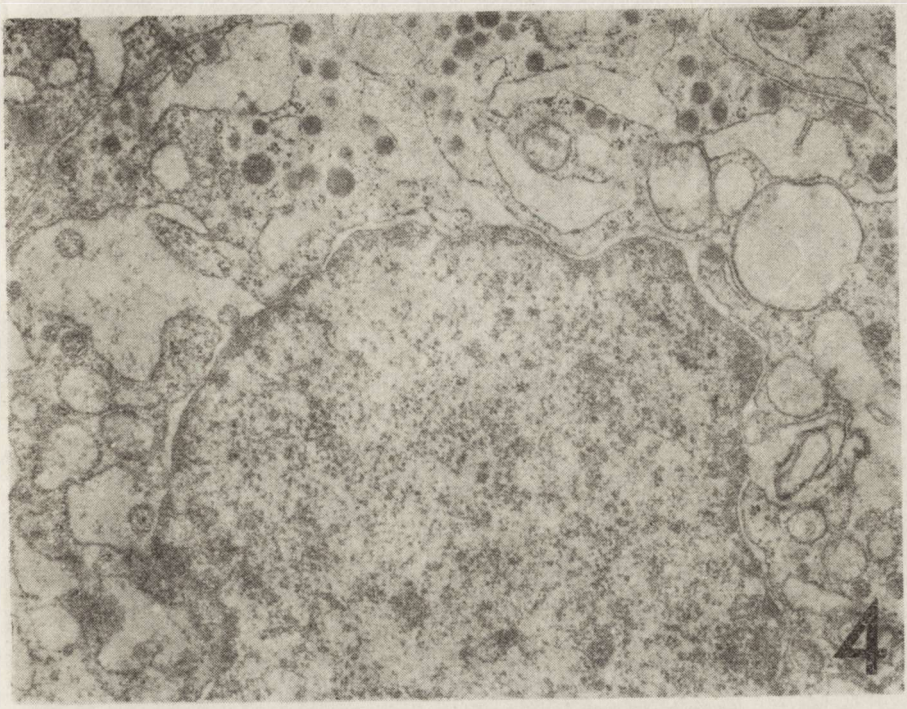

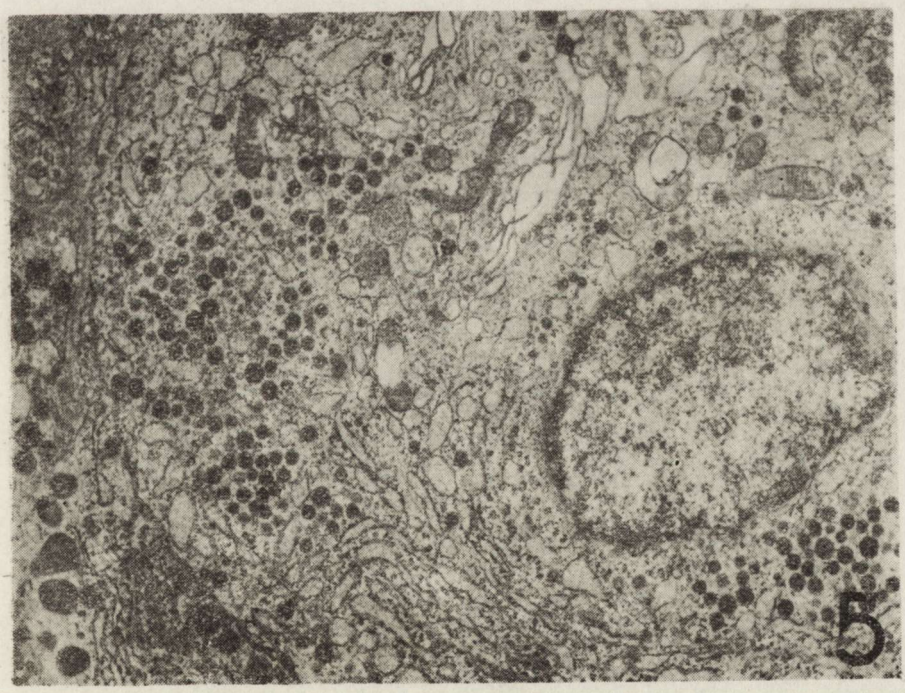

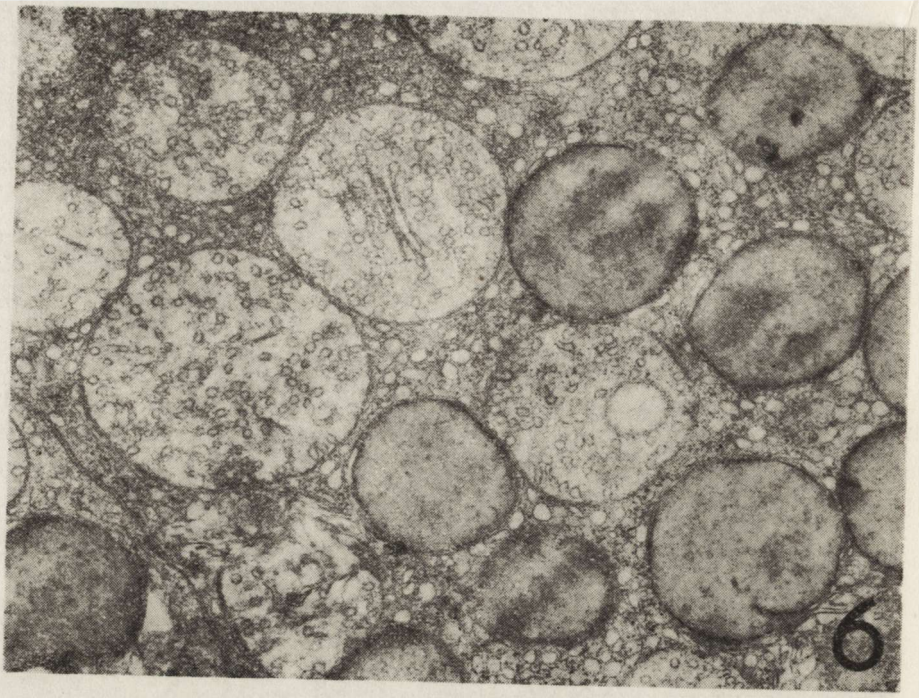

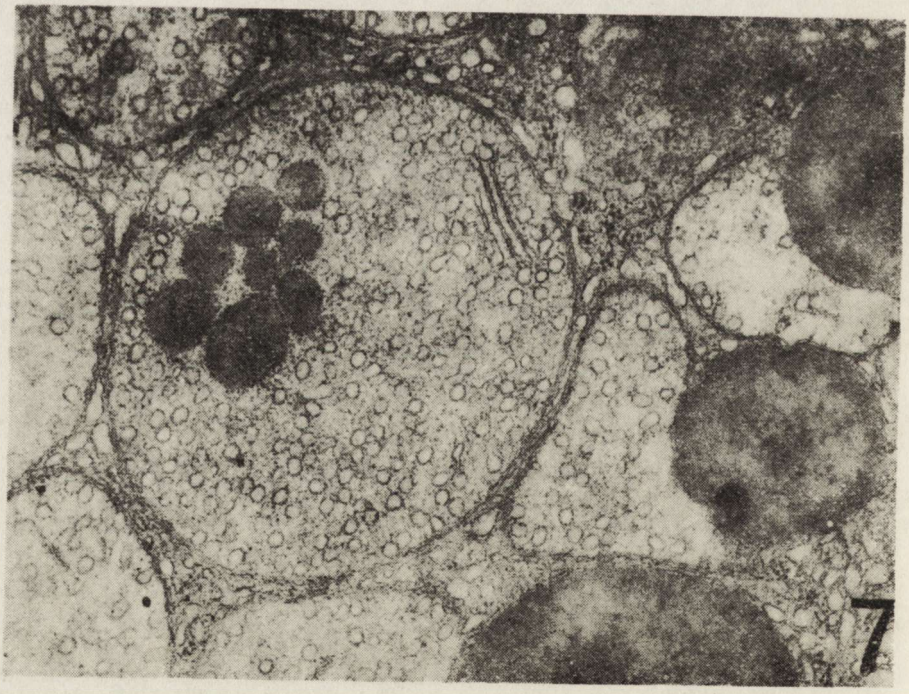

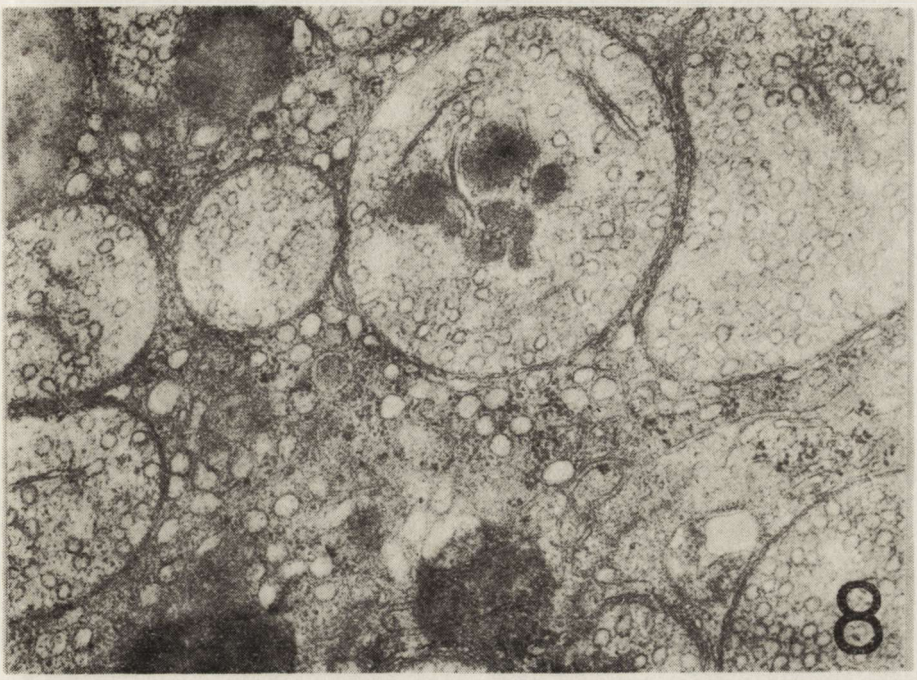

Ryc. 8. Fragment komórki warstwy pasmowatej. Mitochondria z licznymi grzebieniami pęcherzykowatymi, jedno z nich zawiera ciałka gęste. Siatka śródplazmatyczna pęcherzykowata. Struktury lipidowe. Pow. 33 600 ×

Fig. 8. Band layer cell fragment. Mitochondria with numerous vesicular cristae, one of them containing dense bodies. Vesicular endoplasmic reticulum. Lipid structures. × 33 600

W komórkach wydzielających TSH, oprócz nieznacznie zmniejszonej ilości ziarnistości sekrecyjnych, nie stwierdza się odchyleń od normy. Aparat Golgiego jest normalnie rozbudowany, a kanały siatki śródplazmatycznej szorstkiej są dość wąskie i ułożone równolegle (ryc. 5).

Ryc. 6. Fragment komórki warstwy pasmowatej kory nadnerczy. Duże mitochondria z licznymi pęcherzykowatymi grzebieniami, pojedyncze grzebienie w formie tubularnej. Siatka śródplazmatyczna gładka pęcherzykowata. Liczne struktury lipidowe. Pow. 20 400 ×

Fig. 6. Cell fragment of the band layer of the adrenal cortex. Large mitochondria with numerous vesicular cristae, single cristae in a tubular form. Vesicle-like smooth endoplasmic reticulum. Numerous lipid structures. × 20 400

Ryc. 7. Fragment komórki warstwy pasmowatej nadnerczy. Duże mitochondria z grzebieniami pęcherzykowatymi i pojedynczymi, zawierające ciałka gęste. Obok małe mitochondrium o jasnej macierzy z grzebieniami ułożonymi na obwodzie. Struktury lipidowe. Pow. 33 600 ×

Fig. 7. Adrenal band layer cell fragment. Large mitochondria with vesicular and single tubular cristae containing dense bodies. In the vicinity small mitochondria with bright matrix and cristae situated on the periphery. Lipid structures. × 33 600

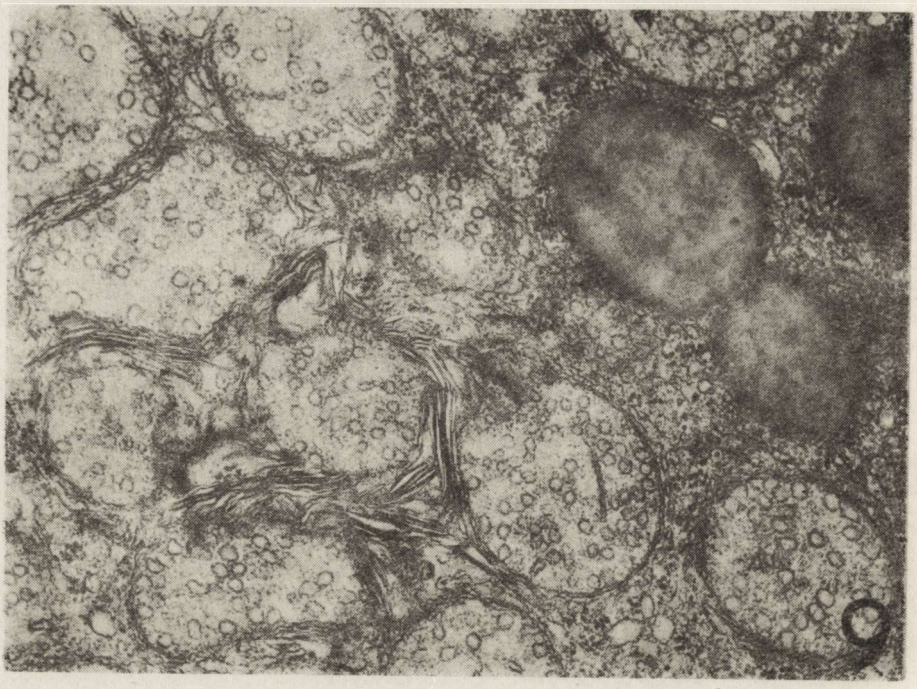

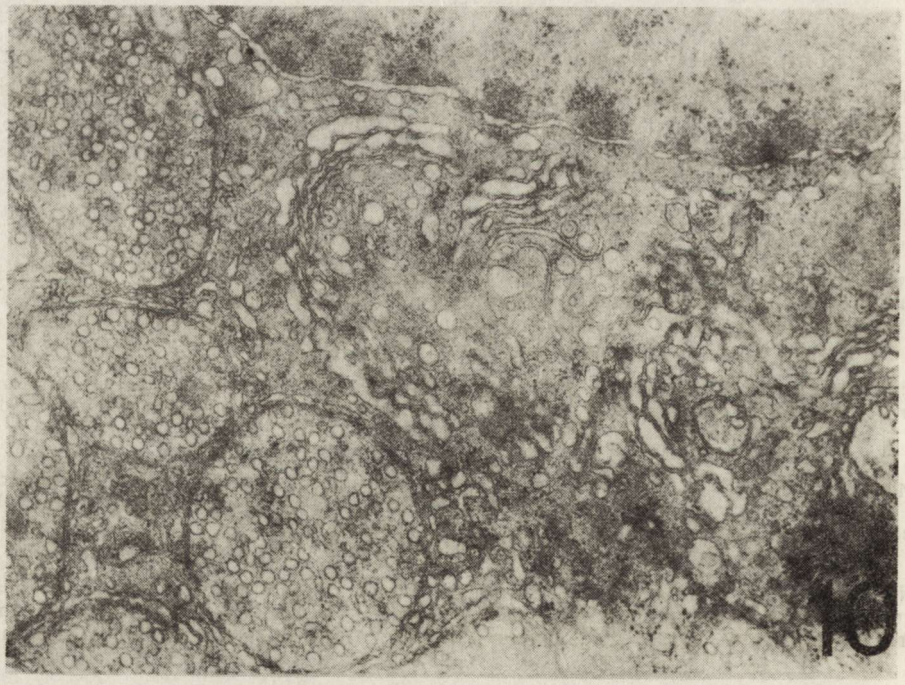

Warstwa pasmowata kory nadnerczy

W komórkach warstwy pasmowatej nadnerczy stwierdza się zmiany mikroskopowo-elektronowe głównie w budowie mitochondriów i siatki śródplazmatycznej. Większość mitochondriów jest powiększona; mają one kształt okrągły o gęstej macierzy i licznych grzebieniach przybierających formę pęcherzyków. W niektórych mitochondriach obserwuje się dodatkowo nieliczne układy tubularne wykazujące łączność z pęcherzykami (ryc. 6). Spotyka się także mitochondria, które zawierają w swojej macierzy różną ilość ciałek gęstych (ryc. 7). W nielicznych i przeważnie małych mitochondriach ilość grzebieni jest zmniejszona, układają się one na obwodzie, macierz mitochondrialna jest jasna. Siatka śródplazmatyczna występuje przede wszystkim w postaci błon gładkich tworzących układ pęcherzykowy typowy dla komórek warstwy pasmowatej. Jednakże w wielu komórkach siatka gładka tworzy dość liczne, wydłużone i częściowo spłaszczone kanały (ryc. 9). Aparat Golgiego, we wszystkich komórkach silnie rozbudowany, składa się z bardzo licznych kanałów i pęcherzyków (ryc. 10). W cytoplazmie występują bardzo liczne struktury lipidowe (ryc. 6, 7, 8, 9).

W komórkach warstwy kłębkowatej i siatkowatej nie obserwuje się wyraźnych zmian.

OMÓWIENIE

Stres wywołany unieruchomieniem powoduje wystąpienie zmian mikroskopowo-elektronowych w płacie gruczołowym przysadki, w komórkach wydzielających ACTH, hormon somatotropowy, prolaktynę i gonadotropiny, oraz w komórkach warstwy pasmowatej kory nadnerczy. Jedynie w komórkach odpowiedzialnych za wydzielanie hormonu tyreotropowego nie stwierdzono żadnych zmian.

W komórkach gruczołowych przysadki zmiany dotyczą budowy aparatu Golgiego oraz siatki śródplazmatycznej szorstkiej. Powiększony aparat Golgiego z licznymi pęcherzykami, zawierającymi materiał o różnej gęstości elektronowej, jest morfologicznym objawem syntezy sekretu (Caro, Palade, 1964; Borowicz i wsp., 1977). Również poszerzenie kanałów siatki szorstkiej i obecność w jej kanałach kłaczkowatego ma-

Ryc. 9. Komórka warstwy pasmowatej. Siatka śródplazmatyczna w postaci długich spłaszczonych kanałów, mitochondria z licznymi grzebieniami. Struktury lipidowe. Pow. 20 800 ×

Fig. 9. Band layer cell. Endoplasmic reticulum in the form of long flattened channels, mitochondria with numerous cristae. Lipid structures. × 20 800

Ryc. 10. Komórka warstwy pasmowatej. Bardzo rozbudowany aparat Golgiego, o poszerzonych kanałach i licznych pęcherzykach. Pow. 23 000 ×

Fig. 10. Band layer cell. Very well developed Golgi apparatus with dilated channels and numerous vesicles. × 23 000

teriału wskazuje na wzmożoną aktywność sekrecyjną (Pelletier i wsp., 1972; Danielewicz-Kotowicz, 1974; Zambrano i wsp., 1974). Poszerzenie przestrzeni pomiędzy blaszkami błony jądrowej może świadczyć o przedostawaniu się materiału jądrowego do cytoplazmy (Hindelang-Gertner i wsp., 1974). W komórkach wydzielających hormon somatotropowy, prolaktynę i gonadotropiny obserwuje się zmniejszone nagromadzenie ziarnistości sekrecyjnych, co przy objawach wzmożonej syntezy sekretu świadczy o jego wydzielaniu z komórek. W komórkach wydzielających ACTH, mimo zwiększonego wydzielania hormonu po unieruchomieniu (Kawakami i wsp., 1971), ilość ziarnistości sekrecyjnych jest zbliżona do normy, co jest zgodne z wynikami badań Pelletier i wsp. (1972) oraz Danielewicz-Kotowicz (1974).

Zmiany w komórkach warstwy pasmowatej kory nadnerczy dotyczą przede wszystkim mitochondriów. Uważa się, że pęcherzykowata forma grzebieni jest typowa dla aktywnego stadium komórki (Fujita, 1972). Zmniejszenie ilości grzebieni, ułożenie ich na obwodzie oraz jasna macierz mitochondrialna — są to zmiany występujące w komórkach regenerujących (Brownie, Skelton, 1968). Hipotezy lokalizujące syntezę liposomów w mitochondriach nie zostały dostatecznie udowodnione. Wtręty osmofilne, widoczne wewnątrz mitochondriów, wskazują na ich degenerację lub „przeciążenie" po bardzo intensywnej stymulacji hormonów sterydowych (Idelman, 1970). Zmienioną budowę siatki śródplazmatycznej, tzn. przekształcanie się formy pęcherzykowatej w wydłużone, spłaszczone kanały leżące w bliskim sąsiedztwie mitochondriów, opisano w komórkach warstwy pasmowatej nadnerczy po podaniu metyloandrostenediolu (Brownie, Skelton, 1968). Wydaje się, że są to zmiany typu regeneracyjnego.

Wiadomo, że w komórkach aktywnie syntetyzujących hormony sterydowe występuje obfita ilość silnie osmofilnych kropli lipidowych (Borowicz 1965), co obserwowaliśmy również w naszym materiale. Cechy morfologiczne komórek warstwy pasmowatej kory nadnerczy wskazują na wzmożoną aktywność sekrecyjną tych komórek.

Na podstawie badań przeprowadzonych w mikroskopie elektronowym można sądzić, że krótkotrwały i ostry stres wywołany całkowitym unieruchomieniem zwierzęcia powoduje aktywację układu przysadkowo-nadnerczowego.

PODSUMOWANIE

1. Stres wywołany całkowitym unieruchomieniem wywołuje w układzie przysadkowo-nadnerczowym szczura zmiany ultrastrukturalne, przemawiające za wzmożoną aktywnością sekrecyjną.

2. Zmiany te obserwowane są w komórkach wydzielających ACTH,

w komórkach wydzielających hormon somatotropowy, TSH, prolaktynę oraz w komórkach wydzielających gonadotropiny.

3. Cechy morfologiczne komórek warstwy pasmowatej kory nadnerczy wskazują również na wzmożoną aktywność sekrecyjną tych komórek, natomiast nie obserwuje się wyraźnych zmian w komórkach warstwy kłębkowatej i siatkowatej.

ULTRASTRUCTURE OF HYPOTHALAMO-ADRENAL SYSTEM OF THE RAT FOLLOWING STRESS PRODUCED BY IMMOBILIZATION

Summary

The hypophyseo-adrenal system was studied following stress produced by total immobilization for two days. In ACTH-, STH- prolactine- and gonadotrophins releasing cells as well as in the cells of fascicular zone morphological indices of increased secretory activity were observed, whereas no such changes occurred in the cells of the glomerular and reticular zone. The results indicate that the hypophyseo-adrenal system undergoes activation after total immobilization.

PIŚMIENNICTWO

1. Ajika K., Kalra S. P., Fawcet O. P., Krulich L., Mc Cann S. M.: The effect of stress and nembutal on plasma levels of gonadotropins and prolactin in ovariectomized rats. Endocrinology, 1972, 90, 707—715.
2. Borowicz J. W.: Some ultrastructural changes in adrenal cortical cells of rat after hypophysectomy and following ACTH administration. Beitr. Path. Anat., 1965, 132, 441—468.
3. Borowicz J. W., Danielewicz-Kotowicz A., Maryniak R.: Electronmicroscopic changes in rat hypophysis induced by morphine. I. Adenohypophysis. Neuropat. Pol., 1977, 15, 33—45.
4. Brownie A. C., Skelton F. R.: Adrenocortical function and structure in adrenal-regeneration and methylandrostenediol hypertension. W: Functions of the adrenal cortex. Red. K. W. Mc Kerns, North Holland, Amsterdam 1968, 691—718.
5. Caro L. G., Palade G. E.: Protein synthesis, storage and discharge in the pancreatic exocrine cell. An autoradiographic study. J. Cell Biol., 1964, 3, 473—496.
6. Chowers J., Hammel H. T., Eisenman J., Abrams R. M., Mc Cann B. M.: Comparison of effect of environmental and preoptic heating and pyrogen on plasma corticol. Am. J. Physiol., 1966, 210, 606—610.
7. Danielewicz-Kotowicz A.: Zmiany mikroskopowo-elektronowe w przysadce szczura po adrenalektomii oraz po podaniu ACTH. I. Płat gruczołowy przysadki. Neuropat. Pol., 1974, 12, 345—358.
8. Fujita H.: On the fine structure of alteration of the adrenal cortex in hypophysectomized rats. Z. Zellforsch., 1972, 125, 480—496.
9. Grosvenor C. E., Nallar R., Mc Cann S. M.: Inhibition of nursing-induced and stress-induced fall in pituitary prolactin concentration in lactating rats by injection of acid extracts bovine hypothalamus. Endocrinology, 1965, 76, 883—896.

10. Gajkowska B., Luciani A., Borowicz J.: Reakcja układu podwzgórzowo-przysadkowego szczura na stres wywołany unieruchomieniem. Neuropat. Pol., 1979, 17, 421—441.
11. Hindelang-Gertner C., Stöeckel M. E., Porte A., Dellmann H. D., Madarasz B.: Nematosomes or nucleolus-like bodies in hypothalamic neurons, the subfornical organ and adenohypophysial cells in the rat. Cell Tiss. Res., 1974, 155, 211—220.
12. Idelman S.: Ultrastructure of the mammalian adrenal cortex. Int. Rev. Cytol. 1970, 27, 181—281.
13. Kawakani M., Seloi K., Kimura F., Yanase R.: Difference in the butter action between the limbic structures and the hypothalamus to the immobilization stress in rabbits. W: Influence of hormones on the nervous system. Proc. Int. Soc. Psychoneuroendocrinol. Karger, Basel 1971, 107—120.
14. Krulich L., Mc Cann S. M.: Influence of stress on the growth hormone content of the pituitary of the rat. Proc. Soc. Exp. Biol. Med., 1966, 121, 1114—1119.
15. Kvetnansky R., Weise V. K., Kopin I. J.: Elevation of adrenal tyrosine hydroxylase and phenylethanolamine-N-methyl transferase by repeated immobilization of rats. Endocrinology, 1970, 87, 744—749.
16. Mikulaj L., Mitro A.: Endocrine functions during adaptation to stress. Neurohumoral and methabolic aspects of injury. Advances Exp. Med. Biol., Plenum Press, New York, London 1973, 631—638.
17. Neill J. D.: Effect of "stress" on serum prolactin and luteinizing hormone levels during the estrous cycle of the rat. Endocrinology, 1970, 87, 1192—1197.
18. Paul M. I., Kvetnansky R., Cramer H., Silbergelu S., Kopin I. J.: Immobilization stress induced changes in adrenocortical and medullary cyclic AMP content in the rat. Endocrinology, 1971, 88, 338—344.
19. Pelletier G., Lamay A., Borand G., Labrie F.: Ultrastructural changes accompanying the stimulatory effect of N^6 monobutyryl adenosine 3′5′ monophosphate on the release of growth hormone (GH), prolactin (PRL) and adrenocorticotropic hormone (ACTH) in rat pituitary gland in vitro. Endocrinology, 1972, 91, 1355—1371.
20. Vernikos-Danellis J., Trigg L. N.: Feed-back mechanism regulating pituitary ACTH secretion in rats bearing transplantable pituitary tumors. Endocrinology, 1967, 80, 345—350.
21. Zambrano D., Cuerdo-Rocha S., Bargmonn I.: Ultrastructure of rat pituitary gonodotrophs following incubation of the gland with synthetic LH-RH. Cell Tiss. Res., 1974, 150, 179—192.

Adres autorki: Pracownia Ultrastruktury Układu Nerwowego CMDiK PAN, ul. Dworkowa 3, 00—784 Warszawa

NEUROPAT. POL., 1982, 20, 1—2
PL ISSN 0028—3894

R. GADAMSKI, D. G. BARAMIDZE, G. I. MCHEDLISHVILI,
Z. T. GORDELADZE

UNERWIENIE WEGETATYWNE ORAZ AKTYWNOŚĆ NIEKTÓRYCH ENZYMÓW W NACZYNIACH OPONY MIĘKKIEJ KRÓLIKÓW Z JEDNO- I OBUSTRONNIE USUNIĘTYM ZWOJEM SZYJNYM GÓRNYM

Zespół Neuropatologii Centrum Medycyny Doświadczalnej i Klinicznej PAN

Zespół Patofizjologii Instytutu Fizjologii Gruzińskiej Akademii Nauk
Tbilisi

Jednym z czynników, który zdecydował o stanie współczesnej wiedzy dotyczącej unerwienia naczyń krwionośnych, było opracowanie przez Falcka i Owmana (1965) fluorescencyjnej techniki wykrywania tkankowych monoamin. Fakt ten łącznie z wcześniej opracowaną metodą wykrywania acetylocholiny za pomocą histochemicznej techniki na acetylocholinoesterazę (Holmstedt, 1957) ożywił znacznie zainteresowanie licznych ośrodków badawczych anatomią wegetatywnych struktur nerwowych znajdujących się w ścianach naczyń krwionośnych, a zwłaszcza czynnościową rolą, jaką struktury te odgrywają w mechanizmach naczynioruchowych. Ewolucja, którą te techniki przeszły w następnych latach, doprowadziła ostatecznie do ułatwienia ich laboratoryjnego stosowania, dzięki użyciu kwasu glioksalowego do wykrywania struktur adrenergicznych (Lindwall, Björklund, 1974), a przede wszystkim do podniesienia swoistości metod na acetylocholinoesterazę przez wprowadzenie wybiórczych i nieodwracalnych inhibitorów pseudocholinoesterazy (Karnovsky, Roots, 1964; El Badawi, Schenk, 1967).

Wyniki uzyskiwane w oparciu o te metody wskazują jednoznacznie na istnienie bogatego unerwienia naczyń opony miękkiej, w których włókna cholinergiczne wraz z aksonami adrenergicznymi tworzą gęste, zawarte w przydance sploty nerwowe (Edvinsson i wsp., 1972). Spostrzeżenia z mikroskopu świetlnego zostały uzupełnione badaniami w mikroskopie elektronowym, w których ujawniono, że zakończenie aksonów obu komponentów układu wegetatywnego są oddalone od siebie

przestrzenią nie wivkszą od 25 μm oraz że aksony te wchodzą w kontakt z komórkami mięśni gładkich ściany naczyniowej. Fakty te wskazują na bezpośredni funkcjonalny udział unerwienia wegetatywnego w mechanizmach naczynioruchowych (Nelson, Rennels, 1969; Iwayama i wsp., 1970; Nielsen i wsp., 1971), a także sugerują możliwość modyfikowania, poprzez uwolnione neurotransmitery, napięcia jednego komponentu przez drugi. Pogląd ten jest powszechnie przyjmowany w odniesieniu do układu cholinergicznego, którego aksony mogą hamować wydzielanie noradrenaliny przez leżące w ich bezpośrednim sąsiedztwie noradrenergiczne zakończenia nerwowe. Czy mechanizm ten działa również w odwrotnym kierunku, jest do chwili obecnej kwestią sporną.

W związku z powyższym w niniejszej serii badań zwrócono szczególną uwagę na ewentualne zmiany w obrazie anatomicznym unerwienia cholinergicznego naczyń opony miękkiej, zachodzące w wyniku jedno- i obustronnego usunięcia zwoju szyjnego górnego, a także w niedokrwieniu OUN, oraz w krótkich okresach poniedokrwiennych.

MATERIAŁ I METODY

Badania przeprowadzono na 21 królikach o ciężarze ciała od 2,5 do 3,5 kg. W ogólnej liczbie zwierząt użytych w doświadczeniu 3 króliki, u których nie wykonywano żadnych zabiegów, stanowiły grupę kontrolną, natomiast u pozostałych usuwano jedno- lub obustronnie zwój szyjny górny. Operację przeprowadzano aseptycznie w ogólnej narkozie nembutalowej oraz w dodatkowym, miejscowym znieczuleniu odsłoniętych naczyń i nerwów. Ranę operacyjną zaopatrywano zasypką penicyliny krystalicznej i zaszywano katgutem. Zwierzęta, po przeżyciu 3—4 tygodni w standardowych warunkach zwierzętarnianych, dzielono na dwie grupy po 9 królików (tj. na grupy z jedno- i obustronnie usuniętym zwojem szyjnym górnym). Materiał do badań, stanowiący wycinki opony miękkiej zdejmowanej z półkuli mózgu (z wyjątkiem obszaru obejmującego wyniosłość pośrodkową) pobierano w następujący sposób: od 3 królików z jednostronnym i od 3 z obustronnym usunięciem zwoju bezpośrednio po przeżyciu i w 3—4 tyg. po operacji, od następnych 6 zwierząt (podzielonych na dwie podgrupy w zależności od liczby usuniętych zwojów) po poddaniu ich 15-minutowemu niedokrwieniu OUN według metody opisanej przez Mchedlishvili (1973) i od pozostałych 6 (również zoperowanych i identycznie podzielonych), u których po 15-minutowym niedokrwieniu wykonywano retransfuzję krwi, a materiał do badań pobierano po upływie 20—25 min po retransfuzji.

W wycinkach opony miękkiej uzyskanych od wszystkich użytych w doświadczeniu zwierząt ujawniano: 1. Cholinergiczne włókna nerwowe za pomocą histochemicznej metody na acetylocholinoesterazę (hydrolaza acetylocholiny E. C. 3.1.1.7) opisanej przez El Badawi i Schenka

(1967) z użyciem jodku acetylotiocholiny (BDH) jako substratu oraz iso-OMPA (amid kwasu czteroizopropylofosforowego, Koch-Light) jako inhibitora butyrylocholinoesterazy. 2. Adrenergiczne włókna nerwowe według nieznacznie zmodyfikowanej metody Torre i Surgeona (1976). Celem oznaczenia swoistej, zielonej fluorescencji amin katecholowych, wycinki opony miękkiej inkubowano 30 min w temp. pokojowej w 2% roztworze kwasu glioksalowego w 0,1 M buforze fosforanowym o pH 7,4. Roztwór ten o wybitnie kwaśnym odczynie zobojętniano 10% NaOH do pH 7,0. Następnie wycinki opony naciągano na szkiełka podstawowe i suszono w strumieniu ciepłego powietrza z suszarki przez 15 min. Wysuszone preparaty przenoszono na 6—8 min do pieca utrzymującego stałą temperaturę 100°C, a następnie zamykano w polistyrenie rozpuszczonym w ksylenie. Tak przygotowane preparaty oglądano w mikroskopie fluorescencyjnym „Ljuman" U-1 wyposażonym w lampę rtęciową NBO-200 oraz filtry: SZS-21.2, SZS-24.4, SS-15 (wzbudzające) i ZS-8, ZS-9 (barierowe).

Ponadto oznaczano aktywność następujących enzymów: dehydrogenazy bursztynianowej (SDH) wg metody Novikoffa (1963), dehydrogenazy mleczanowej (LDH) wg Hessa i wsp. (1958) oraz adenozynotrójfosfatazy (ATP-azy) wg Wachsteina i Meisela (1957) z uwzględnieniem modyfikacji Toracka i Barnetta (1964).

Badania morfologiczne, pozwalające na ocenę stosunku powierzchni zajętej przez adrenergiczne lub cholinergiczne włókna nerwowe do powierzchni obwodu naczyń, przeprowadzono za pomocą siatki morfometrycznej umieszczonej w okularze mikroskopu świetlnego lub fluorescencyjnego. Dane liczbowe z odczytów poszczególnych siatek poddano analizie statystycznej przy pomocy testu t-Studenta.

W celu właściwej oceny otrzymanych wyników, poszczególne odczyny wykonywano na wycinkach opony zdejmowanej zawsze z tych samych okolic mózgu.

WYNIKI

Unerwienie cholinergiczne. U zwierząt, które przeżyły 3—4 tygodnie po jednostronnym usunięciu zwoju szyjnego górnego, obraz unerwienia tętnic opony miękkiej nad obiema półkulami mózgu był podobny do spotykanego w kontroli (ryc. 1). Gęsto utkane sploty włókien przywspółczulnych obserwowano w naczyniach o średnicy ponad 100 μm. Składały się one z pojedynczych włókien grubych o przebiegu podłużnym oraz znacznie liczniejszych aksonów średniej grubości i aksonów cienkich ułożonych często ukośnie lub poprzecznie w stosunku do osi naczynia. W miarę zmniejszania się średnicy tętnic, liczba włókien nerwowych ulegała zubożeniu z jednoczesnym zanikaniem w ich sieci włókien grubych. Odmienny i często zróżnicowany obraz unerwienia obser-

wowano w miejscach odgałęzień naczyń o średnicy 25—50 μm oraz w tętniczkach przedkorowych, wykazujących zazwyczaj znaczne zagęszczenie sieci włókien cholinergicznych. W ścianach anastomoz tętniczych, łączących naczynia oddające liczne tętniczki przedkorowe spotykano z reguły kilka aksonów w odróżnieniu od skąpego unerwienia, reprezentowanego często przez pojedyncze włókno przywspółczulne wyznaczające przebieg anastomozy łączącej naczynia średniej grubości.

Opisany obraz anatomiczny splotów nerwowych ulegał zmianie w materiale pobranym w 20—25 min po przebytym 15-minutowym niedokrwieniu OUN. Obserwowany w tym czasie wzrost aktywności acetylocholinoesterazy po stronie nieusuniętego zwoju prowadził do ujawnienia się w sieci włókien cholinergicznych większej liczby aksonów cienkich i średniej grubości, co w rezultacie dawało wrażenie gęstszego utkania splotów (ryc. 2). Po stronie usuniętego zwoju, utkanie sieci włókien przywspółczulnych w ścianach tętnic opony miękkiej było luźniejsze w porównaniu do strony nieoperowanej. Obserwowano tutaj również osłabienie intensywności odczynu histochemicznego na AChE.

Najwyraźniejszy spadek aktywności acetylocholinoesterazy, połączony ze znacznym rozluźnieniem splotów nerwowych utworzonych prawie wyłącznie z grubych włókien przywspółczulnych, był widoczny u zwierząt z obustronną sympatektomią (ryc. 3). Poddanie tej grupy zwierząt 15-minutowemu niedokrwieniu i pozostawienie ich na 20—25-minutowe przeżycie po przebytym niedokrwieniu, prowadziło do wzmożenia aktywności badanego enzymu, a jednocześnie do ujawnienia się w odczynie histochemicznym większej liczby włókien cholinergicznych (ryc. 4). Gęstość utkania splotów nerwowych oraz aktywność AChE były tutaj znacznie niższe w porównaniu do strony operowanej zwierząt nie poddanych niedokrwieniu OUN.

Unerwienie adrenergiczne. Nie podajemy tutaj opisu unerwienia adrenergicznego tętnic opony miękkiej w warunkach normy, ponieważ został on podany w poprzedniej pracy (Gadamski, Baramidze, 1979). Grupa zwierząt kontrolnych, użytych w przeprowadzonych badaniach, dostarczyła natomiast niezbędnego materiału do przeprowadzenia analizy morfometrycznej, a także dla anatomicznej oceny współczulnych splotów nerwowych w oponie nad kontralateralną półkulą u zwierząt z jednostronnie usuniętym zwojem szyjnym górnym.

U królików z jednostronną sympatektomią nie poddanych niedokrwieniu OUN, intensywność fluorescencji w przebiegu aksonów adrenergicznych po stronie kontralateralnej była podobna do spotykanej w kontroli (ryc. 5). Dawało się jednocześnie zauważyć nieznaczne rozluźnienie gęstości utkania splotów nerwowych. Po stronie ipsilateralnej zdecydowana większość naczyń nie wykazywała obecności aksonów współczulnych. W niektórych natomiast tętnicach, bez względu na ich grubość, spotykano pojedyncze włókna adrenergiczne z prawidłowo roz-

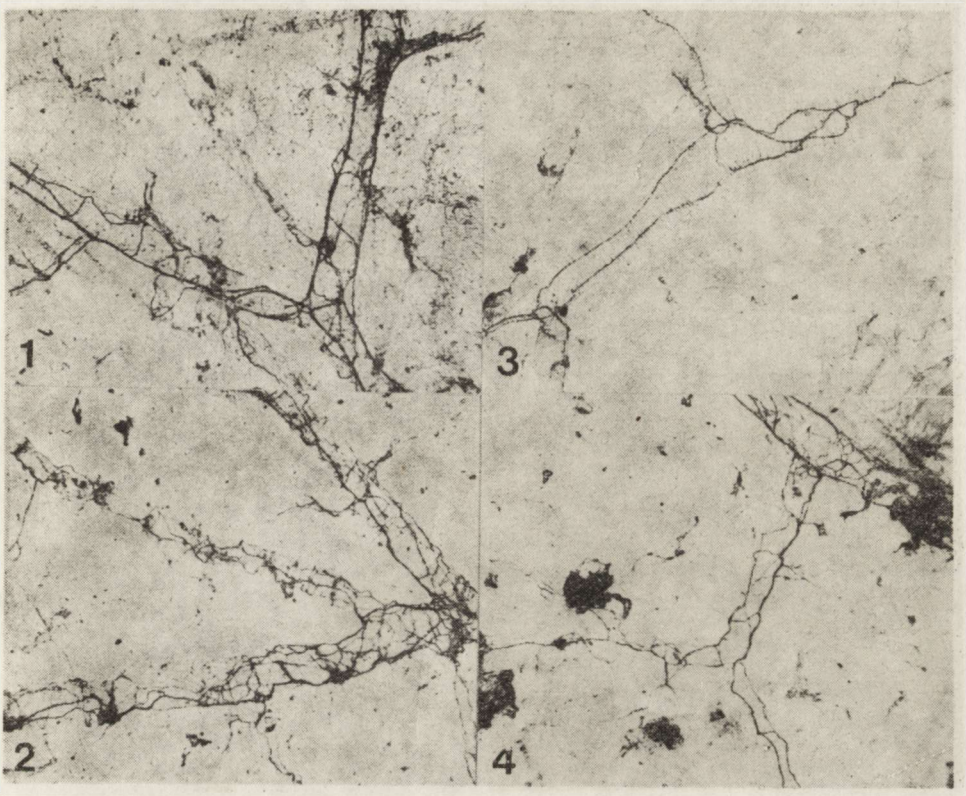

Ryc. 1. Jednostronna sympatektomia (strona operowana). Bogate unerwienie cholinergiczne ścian naczyń opony miękkiej podobne do występującego w kontroli. Pow. 60 ×

Fig. 1. Unilateral sympathectomy (operated side). Rich cholinergic innervation of pial arterial walls, similar to that in control. × 60

Ryc. 2. Jednostronna sympatektomia i stan poischemiczny (strona nie operowana). W splotach cholinergicznych widoczna gęsta sieć aksonów cienkich i średniej grubości. Pow. 60 ×

Fig. 2. Unilateral sympathectomy and postischemic state (nonoperated side). Dense net of thin and medium thick axons in cholinergic plexi. × 60

Ryc. 3. Obustronna sympatektomia (bez niedokrwienia). Cholinergiczny splot nerwowy utworzony z włókien grubych. Pow. 60 ×

Fig. 3. Bilateral sympathectomy (without ischemia). Cholinergic plexus made of thick fibers. × 60

Ryc. 4. Obustronna sympatektomia i stan poischemiczny. W splocie nerwowym pojawiają się obok włókien grubych aksony cienkie i średniej grubości wykazujące umiarkowaną aktywność AChE. Pow. 60 ×

Fig. 4. Bilateral sympathectomy and postischemic state. In nerve plexus beside thick fibers, thin and medium thick axons with moderate AChE activity. × 60

mieszczonymi w ich przebiegu ziarnistościami wykazującymi typową dla kontroli intensywność fluorescencji.

Opisany obraz unerwienia współczulnego ulegał zmianie u zwierząt pozostawionych na 20—25-minutowe przeżycie po przebytym niedokrwieniu OUN. Aksony adrenergiczne zawarte w ścianach tętnic opony

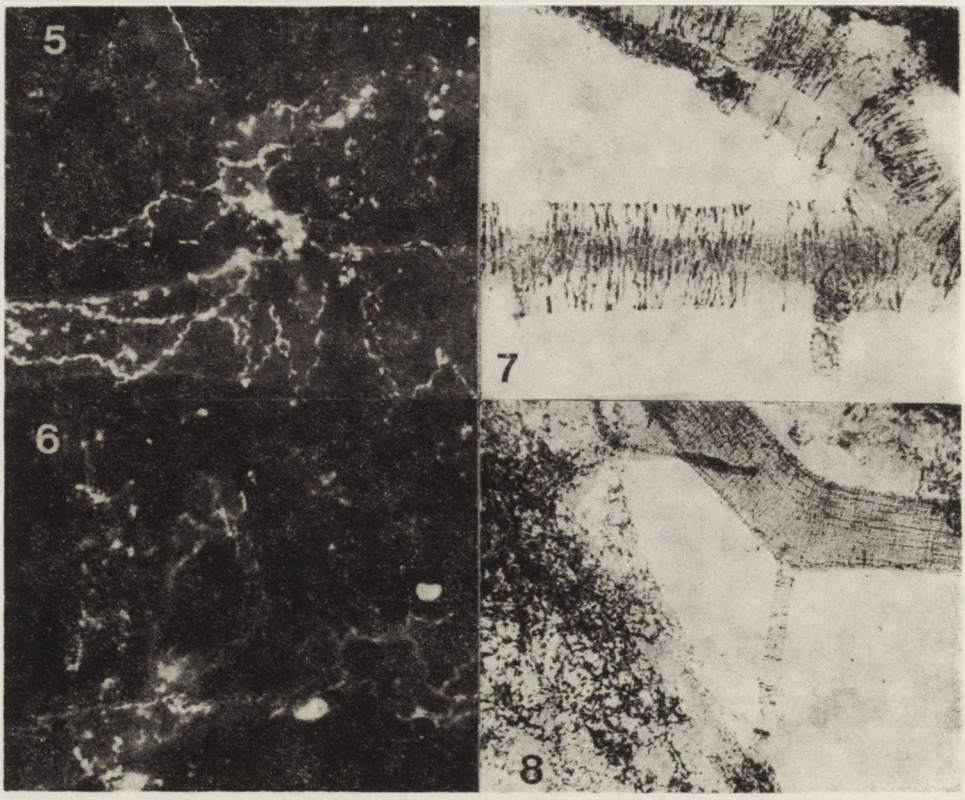

Ryc. 5. Jednostronna sympatektomia bez ischemii (strona nie operowana). Intensywna fluorescencja amin katecholowych w przebiegu włókien adrenergicznych podobna do spotykanej w kontroli. Pow. 200 ×

Fig. 5. Unilateral sympathectomy without ischemia (nonoperated side). Intense fluorescence of catecholamines covering adrenergic fibers, pattern similar to control. × 200

Ryc. 6. Jednostronna sympatektomia i stan poischemiczny (strona nie operowana). Widoczny spadek intensywności fluorescencji amin katecholowych w przebiegu włókien nerwowych. Pow. 200 ×

Fig. 6. Unilateral sympathectomy and postischemic state (nonoperated side). Decreased intensity of catecholamine fluorescence along nerve fibers. × 200

Ryc. 7. Obustronna sympatektomia. Wyraźnie widoczny układ włókien mięśniowych wykazujących silną aktywność SDH w 8 min niedokrwienia oun. Pow. 200 ×

Fig. 7. Bilateral sympathectomy. Distinct arrangement of muscle fibers with strong SDH activity. 8 min ischemia. × 200

Ryc. 8. Jednostronna sympatektomia (strona operowana). Wyraźne osłabienie odczynu histochemicznego na SDH w 15 min niedokrwienia. Pow. 200 ×

Fig. 8. Unilateral sympathectomy (operated side). Marked decrease of SDH reaction. 15 min ischemia. × 200

zdejmowanej z półkuli kontralateralnej wykazywały zróżnicowany spadek intensywności fluorescencji (ryc. 6). Była ona najwyraźniej widoczna we włóknach unerwiających okolice rozgałęzień grubych tętnic, a także w miejscu odgałęzienia się naczyń o średnicy 25—50 μm. W po-

zostałych elementach sieci naczyniowej łącznie z tętniczkami przedkorowymi i anastomozami tętniczymi, fluorescencja wyznaczająca przebieg aksonów adrenergicznych ulegała osłabieniu prawie do całkowitego jej wygasania we włóknach unerwiających odcinki grubych tętnic leżące między odchodzącymi od nich odgałęzieniami. Podobne osłabienie intensywności fluorescencji obserwowano również w zachowanych aksonach po stronie usuniętego zwoju. W tej grupie zwierząt zwracało także uwagę pojawienie się skupisk drobnych, fluoryzujących ziarnistości w miejscach odchodzenia odgałęzień. Podobne, zazwyczaj liniowo rozmieszczone ziarnistości widoczne były w niektórych tętniczkach przedkorowych, początkowych odcinkach tętniczek promienistych oraz w anastomozach.

U królików z obustronną sympatektomią nie stwierdzono obecności włókien adrenergicznych w ścianach naczyń opony miękkiej. Jedynie u kilku zwierząt, od których materiał do badań pobierano dokładnie w 3 tyg. po operacji, można było sporadycznie obserwować krótkie odcinki aksonów z wybitnie osłabioną intensywnością fluorescencji, nie pozwalającą na wykonanie dokumentacji fotograficznej. Podobne odnerwienie współczulne naczyń opony widoczne było także u królików, które przeżyły 20—25 min po przebytym 15-minutowym niedokrwieniu. Jednakże w tej grupie doświadczalnej dodatkowo zwracało uwagę pojawienie się typowej dla amin katecholowych zielonej fluorescencji zlokalizowanej w tworach przylegających do ścian naczyń. Przypominały one ciała komórek trudnych do zidentyfikowania w obrazie mikroskopowo-fluorescencyjnym.

Badania morfometryczne. Przeprowadzona analiza morfometryczna (tab. 1) wykazała, że u królików kontrolnych 23,00 ± 6,25% powierzchni naczyń tętniczych opony miękkiej pokrywają włókna cholinergiczne. Wartość ta nad obiema półkulami mózgu zwierząt z jednostronną sympatektomią ulegała tylko nieznacznym zmianom, które w porównaniu z kontrolą nie wykazywały znamienności statystycznej. Wzrost aktywności acetylocholinoesterazy obserwowany w oponie półkuli kontralateralnej w okresie poischemicznym znajdował odbicie w pomiarach morfometrycznych wskazujących na zwiększenie powierzchni zajętej przez sploty przywspółczulne do 25,90 ± 6,02%, $p < 0,05$. Po stronie ipsilateralnej widoczne w obrazie histochemicznym rozluźnienie sieci włókien cholinergicznych zmniejszało tę powierzchnię do 18,35 ± 4,14%, $p < 0,01$.

W grupie zwierząt z obustronną sympatektomią bez niedokrwienia powierzchnia ta była najmniejsza i wynosiła 12,70 ± 6,66%, $p < 0,01$, co znajdowało swój wyraz w odczynie na AChE ujawniającym w splotach włókna grube oraz zmniejszoną w porównaniu do kontroli ilość aksonów średniej grubości. W tej samej grupie doświadczalnej w okresie poniedokrwiennym obserwowano przyrost powierzchni zajętej przez sploty przywspółczulne do 16,85 ± 6,79%, $p < 0,01$.

Tabela 1. Powierzchnia zajęta przez wegetatywne sploty nerwowe w stosunku do powierzchni tętnic opony miękkiej królika (%)
Table 1. Surface occupied by vegetative nerve plexi in relation to the surface of pial arteries in rabbit (%)

Rodzaj doświadczenia Type of experimental	Włókna cholinergiczne Cholinergic fibers			Włókna adrenergiczne Adrenergic fibers		
	Zwierzęta kontrolne Control animals	Zwierzęta doświadczalne Experimental animals	p	Zwierzęta kontrolne Control animals	Zwierzęta doświadczalne Experimental animals	p
Jednostronna sympatektomia (strona nie operowana) Unilateral sympathectomy (nonoperated side)	23,08±4,83* (40)	23,00±6,25 (40)	< 0,05	20,24±4,91 (80)	14,75±4,36 (60)	< 0,01
Jednostronna sympatektomia (strona operowana) Unilateral sympathectomy (operated side)		22,68±4,97 (40)	< 0,05		–	–
Jednostronna sympatektomia i stan poischemiczny (strona nie operowana) Unilateral sympathectomy and postischemic state (nonoperated side)		25,90±6,02 (40)	< 0,05		13,13±3,08 (60)	< 0,01
Jednostronna sympatektomia i stan poischemiczny (strona operowana) Unilateral sympathectomy and postischemic state (operated side)		18,35±4,14 (40)	< 0,01		–	–
Obustronna sympatektomia Bilateral sympathectomy		12,70±6,66 (20)	< 0,01		–	–
Obustronna sympatektomia i stan poischemiczny Bilateral sympathectomy and postischemic state		16,85±6,79 (20)	< 0,01		–	–

* – $\bar{X}\pm SD$.
W nawiasach liczba odczytanych siatek morfometrycznych.
In parentheses – number of morphometric readings.
p – prawdopodobieństwo.
probability.

Badania morfometryczne układu adrenergicznego prowadzono wyłącznie u zwierząt z jednostronnie usuniętym zwojem, ponieważ obustronna sympatektomia prowadziła do współczulnego odnerwienia naczyń opony miękkiej. Trudno było również przeprowadzić taką analizę przy jednostronnej sympatektomii w półkuli ipsilateralnej, mimo obecności w niektórych naczyniach pojedynczych aksonów adrenergicznych. Ujęcie ich w morfometrii dostarczyłoby danych odnośnie tylko do nieznacznej liczby tętnic, co przeczy charakterowi tych badań ujmujących sieć naczyniową jako całość.

W grupie zwierząt kontrolnych, włókna adrenergiczne zajmowały 20,24 ± 4,91% powierzchni naczyń. W 3-4 tyg. po jednostronnym usunięciu zwoju, w oponie półkuli kontralateralnej powierzchnia ta malała do 14,75 ± 4,63%, $p < 0,01$ i ulegała dalszemu zmniejszeniu w okresie poniedokrwiennym do wartości 13,13 ± 3,8%, $p < 0,01$.

Dehydrogenaza bursztynianowa (SDH), dehydrogenaza mleczanowa (LDH) i adenozynotrójfosfataza (ATP-aza). Aktywność tych enzymów u zwierząt kontrolnych oraz zachodzące w niej zmiany w trakcie niedokrwienia OUN i w krótkich okresach poischemicznych opisano w poprzedniej pracy (Gadamski i wsp., 1980). W obecnych badaniach zwracano uwagę na ewentualne różnice w jakości i dynamice tych zmian pojawiających się w identycznych stanach patologicznych u zwierząt z jedno- i obustronnie usuniętym zwojem szyjnym górnym.

We wczesnych okresach niedokrwienia u królików z jedno- i obustronną sympatektomią, mimo nieznacznego spadku aktywności SHD, odczyn histochemiczny ujawniał wyraźnie układ komórek mięśni gładkich w ścianach tętnic bez względu na ich grubość (ryc. 7). Wyraźniejsze obniżenie aktywności enzymu widoczne było w 15 min niedokrwienia. Prowadziło ono do nieujawniania się w odczynie histochemicznym włókien mięśniowych w większości grubych naczyń, podczas gdy w pozostałych elementach sieci tętniczej obserwowano słabo widoczne komórki mięśniowe leżące pojedynczo lub w niewielkich skupiskach (ryc. 8). W 20–25 min po niedokrwieniu aktywność SDH ulegała wzmożeniu i wydawała się wyższa od spotykanej w kontroli (ryc. 9).

Zmiany w intensywności odczynu histochemicznego wykazywała również dehydrogeneza mleczanowa. Wyższa aktywność tego enzymu w niedokrwieniu ulegała tylko nieznacznemu spadkowi w okresie poischemicznym. Zwracało uwagę odcinkowe rozmieszczenie skupisk mięśni gładkich zwłaszcza w naczyniach średniej grubości (ryc. 10). Fragmenty tętnic leżące między tymi odcinkami były negatywne w odczynie na LDH. Charakterystyczną cechą dla okresu poischemicznego u zwierząt z jedno- i obustronną sympatektomią było pojawienie się wysokiej aktywności enzymu w astrocytach. Skupiska tych komórek przylegały do cienkich i średniej grubości żył i tętnic (ryc. 11), a ich

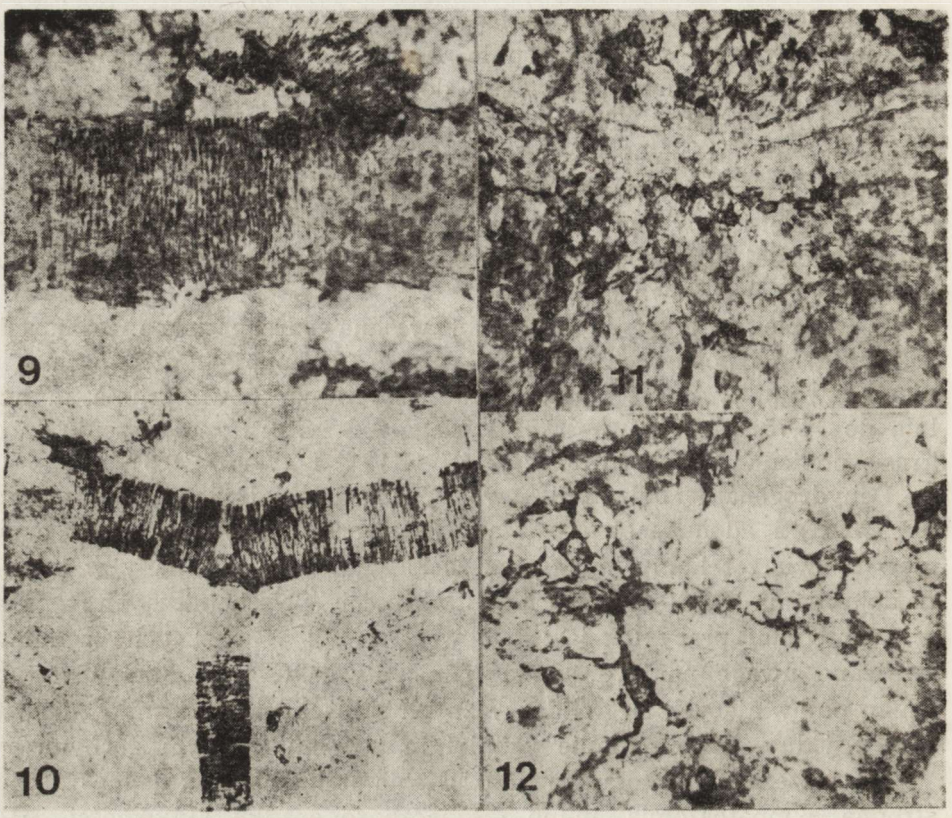

Ryc. 9. Obustronna sympatektomia i stan poischemiczny. Wzrost aktywności SDH w skupiskach mięśniówki gładkiej w naczyniach grubych i średnich. Pow. 200 ×

Fig. 9. Bilateral sympathectomy and postischemic state. Increased SDH activity in muscle agglomerations in thick, and medium thick vessels. × 200

Ryc. 10. Jednostronna sympatektomia (strona operowana). Wysoka aktywność LDH w 15 min niedokrwienia. Pow. 100 ×

Fig. 10. Unilateral sympathectomy (operated side). High LDH activity. 15 min ischemia. × 100

Ryc. 11. Obustronna sympatektomia i stan poischemiczny. Intensywna reakcja na LDH w skupiskach astrocytów przylegających do naczyń krwionośnych. Pow. 100 ×

Fig. 11. Bilateral sympathectomy and postischemic state. Intensive LDH reaction in groups of astrocytes adjacent to blood vessels. × 100

Ryc. 12. Obustronna sympatektomia i stan poischemiczny. W odczynie na LDH wyraźnie widoczne astrocyty, których wypustki przylegają do ściany naczynia. Pow. 400 ×

Fig. 12. Bilateral sympathectomy and postischemic state. LDH reaction in astrocyte adjacent to blood vessels. × 400

wypustki znajdowały zakończenie w ścianach naczyniowych (ryc. 12).

Umiarkowana aktywność adenozynotrójfosfatazy, obserwowana w tętnicach średniej grubości we wczesnej fazie niedokrwienia (ryc. 13) ulegała wyraźnemu spadkowi w 15 minucie jego trwania (ryc. 14). W okresie poischemicznym wzmagająca się aktywność tego enzymu

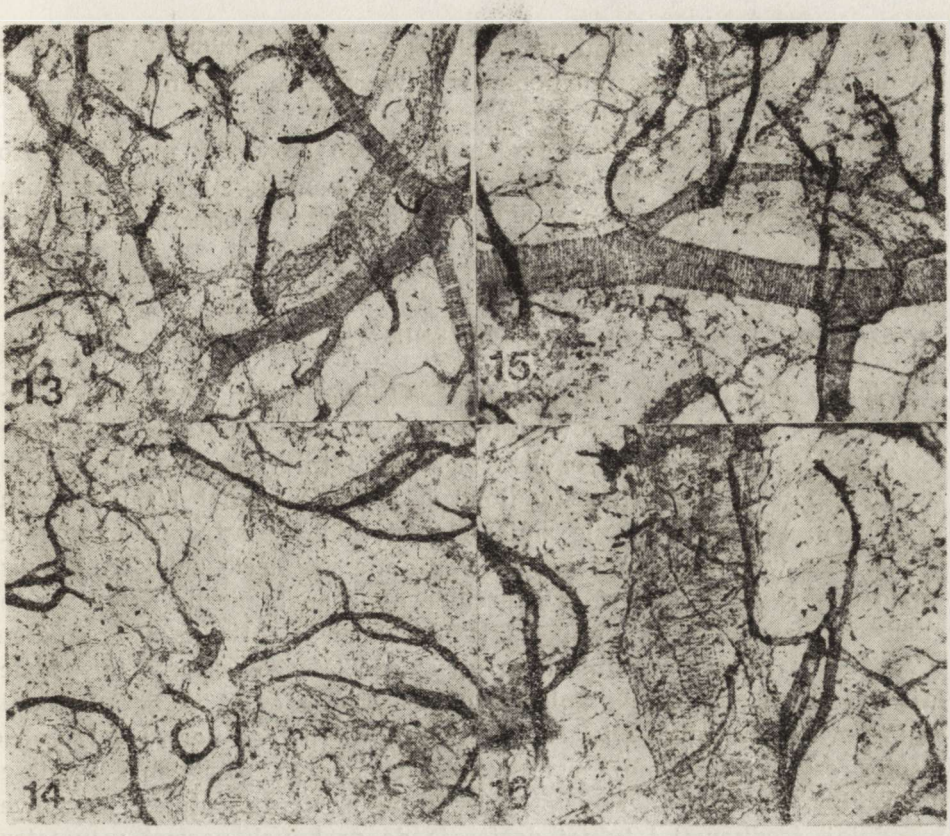

Ryc. 13. Jednostronna sympatektomia bez niedokrwienia (strona operowana). Wysoka aktywność ATP-azy w tętniczkach przedkorowych i promienistych oraz umiarkowana aktywność tego enzymu w tętnicach średniej grubości. Pow. 100 ×

Fig. 13. Unilateral sympathectomy without ischemia (operated side). High ATPase activity in precortical and radial arterioles and moderate activity in medium thick arteries. × 100

Ryc. 14. Jednostronna sympatektomia (strona operowana). Spadek aktywności ATP-azy w naczyniach średniej grubości w 15 min niedokrwienia. Pow. 100 ×

Fig. 14. Unilateral sympathectomy (operated side). Decreased ATPase activity in medium thick arteries. 15 min ischemia. × 100

Ryc. 15. Obustronna sympatektomia i stan poischemiczny. Wyraźny wzrost aktywności ATP-azy w mięśniówce gładkiej tętnic średniej grubości. Pow. 100 ×

Fig. 15. Bilateral sympathectomy and postischemic state. Marked increase of ATPase activity in smooth muscles of medium thick arteries. × 100

Ryc. 16. Obustronna sympatektomia i stan poischemiczny. Intensywny odczyn na ATP-azę wyznaczający przebieg pojedynczych włókien nerwowych w ścianach grubych tętnic opony. Pow. 100 ×

Fig. 16. Bilateral sympathectomy and postischemic state. ATPase reaction indicating the route of individual nerve fibers in thick pial arterial walls. × 100

wyznaczała wyraźnie układ okrężnej warstwy mięśniówki gładkiej równomiernie rozmieszczonej w przebiegu naczyń tętniczych (ryc. 15). W tym samym okresie, ale wyłącznie u zwierząt z obustronnie usuniętym zwojem, odczyn na ATP-azę ujawniał w niektórych grubych tętnicach przebieg nielicznych włókien nerwowych (ryc. 16). Szczególnie

wysoka aktywność enzymu w tętniczkach przedkorowych i promienistych pozostawała niezmieniona we wszystkich badanych grupach zwierząt.

W przypadku wszystkich trzech badanych enzymów nie stwierdzono żadnych różnic w ich aktywności w oponie miękkiej po stronie usuniętego i zachowanego zwoju, a także u zwierząt z obustronną sympatektomią.

OMÓWIENIE

Wyniki poprzednich badań (Gadamski, Baramidze, 1979), oraz spostrzeżenia z obecnie przeprowadzonych doświadczeń, potwierdzają obecność bogatego unerwienia cholinergicznego tętnic opony miękkiej królika, które w warunkach prawidłowych zajmuje niemal 1/4 powierzchni naczyń. Wartości tej nie zmieniała istotnie jednostronna sympatektomia, lecz wyraźnie obniżało ją obustronne usunięcie zwojów. Zjawisko to trudno wytłumaczyć w oparciu o dane anatomiczne dotyczące pochodzenia aksonów przywspółczulnych. Njaważniejszym ich źródłem wydaje się nerw pośrednio-twarzowy, od którego aksony te oddzielają się w obrębie zwoju kolankowego i biegną dalej w nerwie skalistym powierzchownym większym. Część włókien tego nerwu dołącza do tętnicy szyjnej wspólnej, a następnie do naczyń pierścienia tętniczego Wilizjusza. Stąd nerwy przywspółczulne, drogą tętnicy mózgowej przedniej, środkowej i tylnej docierają do drobnych naczyń wewnątrzmózgowych, a poprzez ich gałęzie oponowe również do naczyń opony miękkiej. Obok innych możliwych dróg osiągania tętnic opony przez włókna przywspółczulne, w dyskusji nad otrzymanymi wynikami można również brać pod uwagę aksony, które biorą początek z neuronów zwoju szyjnego górnego wykazujących dodatnią reakcję na acetylocholinoesterazę. Jeżeli istotnie istnieje i takie źródło pochodzenia włókien przywspółczulnych, to jednostronne usunięcie zwoju szyjnego górnego powinno powodować zauważalne rozluźnienie gęstości splotów w oponie po stronie ipsilateralnej.

Wobec niemożliwości uzasadnienia spostrzeganych zmian w oparciu o przesłanki anatomiczne należy ich szukać w mechanizmach autoregulacyjnych. W rozważaniach tych można sugerować następujący pogląd: jeżeli obustronna sympatektomia prowadzi do całkowitego odnerwienia współczulnego naczyń opony (zostało to wykazane w przeprowadzonych badaniach), to normalne napięcie układu przywspółczulnego, charakterystyczne dla zwierząt zdrowych, wywoływałoby nadmierną aktywację mechanizmów naczynioruchowych działających w kierunku rozszerzenia naczyń. Taki stan rzeczy pogłębiałby zaburzenia w przepływie krwi nie tylko w sieci naczyń opony, lecz również w korze mózgu.

Zmniejszenie powierzchni zajętej przez sploty włókien cholinergicznych do 12,70 ± 6,66% u zwierząt z obustronną sympatektomią można więc traktować jako działanie kompensacyjne, którego mechanizm nie jest bliżej znany. Rozluźnienie gęstości utkania splotów nie może być oczywiście traktowane jako zmniejszenie ilości lub całkowity brak w ich przebiegu acetylocholiny, co uniemożliwia ujawnienie tych włókien w stosowanej metodzie histochemicznej. Należy tutaj podkreślić, że obserwowane w obrazie mikroskopowym rozluźnienie splotów było spowodowane zanikaniem w ich sieci aksonów cienkich i średniej grubości, a więc tych elementów, które jako włókna preterminalne i zakończenia nerwowe wchodzą w bezpośredni kontakt z efektorem mięśniowym ściany naczynia. Spostrzeżenie to dodatkowo przemawia za uruchomieniem mechanizmów kompensacyjnych. U zwierząt nie poddanych po obustronnej sympatektomii niedokrwieniu OUN, mechanizmy te w tętnicach pozbawionych komponentu współczulnego działają raczej na zasadzie zwolnienia transportu acetylocholiny wzdłuż włókien przywspółczulnych, a nie na zasadzie hamowania jej syntezy. Pogląd taki można traktować wyłącznie jako hipotezę, bowiem dla konkretnego jego poparcia konieczne jest udowodnienie czy brak zakończeń adrenergicznych w naczyniach opony (po obustronnej sympatektomii), a tym samym brak noradrenaliny mógłby rzeczywiście wpływać na poziom acetylocholiny w zakończeniach cholinergicznych. Doniesienia dotyczące tego zagadnienia są bardzo skąpe. Można tutaj jedynie przytoczyć wyniki badań mikroskopowo-elektronowych Lindvalla i wsp. (1975), w których nie stwierdzili oni obecności zakończeń cholinergicznych w naczyniach wewnątrzmózgowych po sympatektomii.

Za szukaniem możliwości wyjaśnienia otrzymanych przez nas wyników w podstawach funkcjonowania mechanizmów autoregulacyjnych oraz w możliwości ich wzajemnego na siebie oddziaływania przemawiają również dane uzyskane w grupie zwierząt, u których po jednostronnej sympatektomii wywoływano 15-minutowe niedokrwienie OUN, a materiał do badań pobierano w 20—25 min po niedokrwieniu. Czas ten wybrano celowo, wychodząc z założenia, że wystarcza on na zapoczątkowanie procesów odnowy, a jednocześnie jest zbyt krótki dla pełnego powrotu do normy funkcji metabolicznych i neurotransmisyjnych w ścianach naczyń krwionośnych. Uważano ponadto, że tak dobrane warunki doświadczenia umożliwiają obserwację działania mechanizmów autoregulacyjnych zaangażowanych w usuwaniu patologicznych następstw niedokrwienia OUN przy ograniczonej sympatektomią możliwości ich działania.

W okresie poischemicznym u zwierząt z jednostronnie usuniętym zwojem, włókna cholinergiczne w oponie nad półkulą kontralateralną zajmowały 25,90 ± 6,02% powierzchni naczyń. Wartość ta po stronie ipsilateralnej wynosiła 18,35 ± 4,14%. Przedstawione dane świadczą

o odmiennej gęstości utkania splotów przywspółczulnych nad przeciwległymi półkulami mózgu, co również można traktować jako wynik kompensacji działającej jednakże na odmiennej zasadzie niż w przypadku obustronnej sympatektomii u królików nie poddanych niedokrwieniu. Większe nagromadzenie produktu końcowego reakcji w przebiegu włókien cholinergicznych nad półkulą kontralateralną świadczy o wzmożeniu procesów hydrolizy acetylocholiny, a tym samym o wysokim poziomie nagromadzenia tego neurotransmitera. Obniżanie napięcia układu współczulnego w naczyniach po stronie zachowanego zwoju może więc wiązać się bezpośrednio z hamującym wpływem dużych ilości acetylocholiny na uwalnianie noradrenaliny przez współczulne zakończenia nerwowe. Tak pojmowane działanie mechanizmów autoregulacyjnych, które po stronie zachowanego zwoju uniemożliwiają uwalnianie noradrenaliny, natomiast po stronie usuniętego zwoju hamują transport acetylocholiny prowadziłoby w efekcie do zapewnienia podobnego stanu homeostazy nad obiema półkulami. Spostrzeżenia te są w pewnej sprzeczności z danymi dotyczącymi zwierząt z jednostronną sympatektomią, nie poddawanych niedokrwieniu OUN, u których gęstość splotów przywspółczulnych po stronie usuniętego i zachowanego zwoju była podobna i nie różniła się statystycznie znamiennie od kontroli. Łączy się to prawdopodobnie z tym, że zwierzęta te przeżywały 3–4 tyg. w określonych warunkach środowiskowych. Były one ponadto prawie zupełnie pozbawione możliwości poruszania się, co w sumie być może nie stanowi dostatecznego bodźca do uruchomienia takiego poziomu funkcjonowania mechanizmów autoregulacyjnych, który dawałby się zauważyć przy określonej czułości stosowanych przez nas metod.

Możliwość wzajemnego oddziaływania na siebie komponentów wegetatywnych znajduje uzasadnienie w wynikach badań mikroskopowo-elekronowych (Nelson, Rennels, 1969; Iwayama i wsp., 1970; Nielsen i wsp., 1971; Lindvall i wsp., 1975). Jest rzeczą godną uwagi, że mimo niezaprzeczalnego neurogennego wpływu układu cholinergicznego na przepływ mózgowy (Vasquez, Pures, 1977) doniesienia na ten temat są skąpe. Wynika to przynajmniej z trzech przyczyn: a) brak dokładnego poznania zakończeń włókien cholinergicznych unerwiających naczynia mózgowe, co utrudnia podjęcie eksperymentów polegających na przecinaniu nerwów lub stymulacji; b) brak przekonywających danych, że włókna te rzeczywiście unerwiają naczynia wewnątrzmózgowe; c) trudności podjęcia badań farmakologicznych *in vivo* ze względu na wrażliwość licznych systemów efektorowych na leki cholinotropowe. Mimo tych utrudnień wiadomo obecnie, że zakończenia aksonów adrenergicznych i cholinergicznych tworzą ścisłe związki funkcjonalne (Nielsen i wsp., 1971; Edvinsson i wsp., 1972), co sugeruje możliwość ich wzajemnego oddziaływania sprowadzającego się do kontroli jednego sys-

temu przez drugi. Wiadomo również, że zakończenia nerwowe obu komponentów wegetatywnych leżą w bezpośrednim sąsiedztwie komórek mięśni gładkich i są od nich oddzielone przestrzenią 80–100 nm. Przemawia to za udziałem tych zakończeń w pobudzaniu efektorów mięśniowych ściany naczynia.

Istotnym spostrzeżeniem przeprowadzonych badań, znajdujących potwierdzenie w poprzedniej pracy (Gadamski i wsp., 1980), jest naprzemienne rozmieszczenie w przebiegu tętnic opony miękkiej skupisk mięśniówki gładkiej wykazujących odmienną reakcję w odczynie na LDH i SDH. Fakt ten skłania do przypuszczeń o istnieniu w tych tętnicach dwóch rodzajów włókien mięśniowych, które nawet w warunkach tlenowych zużywają odmienne substraty energetyczne (węglowodany w naczyniach o wysokiej aktywności fosforylaz oraz mleczan w przypadku wzmożonego odczynu na LDH).

W podsumowaniu należy zwrócić uwagę na znaczne trudności w określeniu metodami histochemicznymi właściwości metabolicznych mięśniówki gładkiej w poszczególnych elementach sieci naczyniowej, a w tym w jej odcinkach aktywnych (Gadamski, Baramidze, 1979). O właściwościach tych mogą przesądzić liczne czynniki: bogactwo unerwienia, specyfika pobudzania przez dyfuzję neurotransmiterów uwalnianych przez zakończenia nerwowe oraz przez naczynioaktywne substancje osocza, a także sugerowane przez nas występowanie dwóch rodzajów włókien mięśniowych czerpiących energię z hydrolizy odmiennych substratów.

VEGETATIVE INNERVATION AND THE ACTIVITY OF SOME ENZYMES IN PIA MATER IN RABBITS WITH UNI- AND BILATERALLY REMOVED UPPER CERVICAL GANGLION

Summary

The study deals with the vegetative innervation of arteries and the succinate dehydrogenase (SDH), lactate dehydrogenase (LDH) and adenosine triphosphatase (ATPase) activity in rabbit pia mater. The pial fragments were derived from control rabbits and from experimental animals with uni- and bilaterally removed upper cervical ganglion. In the case of experimental animals the material was taken 3 weeks after sympathectomy, either directly or following 15 min ischemia and retransfusion. Morphometric examinations revealed a decreased density of the texture of sympathetic plexi in pial vessels on the side contralateral to the removed ganglion and a complete disappearance of innervation on the ipsilateral side. The decrease of texture density also involved the parasympathetic plexi, in particular in animals with bilateral sympathectomy.

Histochemical tests disclosed a drop of the SDH activity following 15 min ischemia and an increase in the postischemic period. The high LDH activity apparent in ischemia underwent a very insignificant decrease in the postischemic period. The ATPase activity was distinctly below control in the 15th min of ischemia and showed an increase in the postischemic period. The three enzyme activities appeared unaffected by sympathectomy, either uni- or bilateral.

PIŚMIENNICTWO

1. Edvinsson L., Nielsen K. C., Owman Ch., Sporrong B.: Cholinergic mechanism in pial vessels. Histochemistry, electron microscopy and pharmacology. Z. Zellforsch., 1972, 134, 311—325.
2. El-Badawi A., Schenk F. A.: Histochemical methods for separate, consecutive and simultaneous demonstration of acetylcholinesterase and norepinephrine in cryostat sections. J. Histochem. Cytochem., 1967, 15, 580—588.
3. Falck B., Owman Ch.: A detailed methodological description of the fluorescence method for the cellular demonstration of biogenic monoamines. Acta Univ. Lund., 1965, II, 7, 5—23.
4. Gadamski R., Baramidze D. G.: Unerwienie wegetatywne opony miękkiej królika w warunkach normy i w niedokrwieniu ośrodkowego układu nerwowego. Neuropat. Pol., 1979, 17, 505—521.
5. Gadamski R., Szumańska G., Baramidze D. G.: Aktywność niektórych enzymów w ścianach naczyń tętniczych opony miękkiej królika w warunkach prawidłowych i w niedokrwieniu. Neuropat. Pol., 1980, 18, 569—580.
6. Hess R., Scarpelli D. G., Pearse A. G.: The cytochemical localization of oxidative enzymes. II Piridine nucleotide linked dehydrogenase. J. Biophys. Biochem. Cytol., 1958, 4, 753—760.
7. Holmstedt B.: A modification of the thiocholine method for the determination of cholinesterase. II. Histochemical application. Acta Physiol. Scand., 1957, 40, 331—357.
8. Iwayama T., Furness J. B., Burnstock G.: Dual adrenergic and cholinergic innervation of the cerebral arteries of the rat. Circ. Res., 1970, 26, 635—646.
9. Karnovsky M. J., Roots L.: A direct-coloring thiocholine technique for cholinesterases. J. Histochem. Cytochem., 1964, 12, 219—221.
10. Lindvall O., Björklund A.: The glyoxylic acid fluorescence histochemical method: A detailed account of the methodology for the visualization of central catecholamine neurons. Histochemistry, 1974, 39, 97—127.
11. Lindvall M., Cérvos-Navarro J., Edvinsson L., Owman Ch., Stenevi U.: Nonsympathetic perivascular nerves in the brain: Origin and mode of innervation studied by fluorescence and electron microscopy combined with stereotaxic lesions and sympathectomy. W: Blood flow and metabolism in the brain. Red. A. M. Harper, W. B. Jennett, J. D. Miller, J. O. Rowan. Churchill Livingstone, Edinburgh 1975, 1.7—1.9.
12. Mchedlishvili G. I.: Experimental model of controllable circulatory hypoxia (ischemia) of cerebral hemispheres. Neuropat. Pol., 1973, 11, 249—263.
13. Nelson E., Rennels M.: Neuromuscular contacts in intracranial arteries of the cat. Science (Wash.), 1969, 167, 301—302.
14. Nielsen K. C., Owman Ch., Sporrong B.: Ultrastructure of the autonomic innervation apparatus in the main pial arteries of rats and cats. Brain Res., 1971, 27, 25—32.
15. Novikoff A. B.: Electron transport enzymes biochemical and tetrazolium studies. I. Intern. Congress of Biochem. Cytochem. Pergamon Press, Oxford, London, New York, Paris 1963, 465—481.
16. Torack R. M., Barrnett R. J.: The fine structural localization of nucleoside phosphates activity in the blood-brain barrier. J. Neuropath. exp. Neurol., 1964, 23, 46—59.
17. Torre J. C., Surgeon J. W.: A methodological approach to rapid and sensitive monoamine histofluorescence using a modified glyoxylic acid technique. The SPG method. Histochemistry, 1976, 49, 81—93.

18. Wachstein M., Meisel F.: Histochemistry of hepatic phosphatases of a physiologic pH. Am. J. Clin. Pathol., 1957, 27, 13—23.
19. Vasquez J., Purves M. J.: Studies on the dilatator pathway to cerebral blood vessels. Neurogenic control of the brain circulation. W: Proc. Intern. Symp. Wenner-Gren Center, Stockholm, 1977. Red. Ch. Owman, L. Edvinsson. Pergamon Press, Oxford, New York, Toronto, Sydney, Paris, Frankfurt 1977, 59—73.

Adres autorów: Zespół Neuropatologii Centrum Medycyny Doświadczalnej i Klinicznej PAN, ul. Dworkowa 3, 00—784 Warszawa

NEUROPAT. POL., 1982, 20, 1—2
PL ISSN 0028—3894

ZOFIA ADAMCZEWSKA-GONCERZEWICZ

ROZWÓJ NERWU WZROKOWEGO KRÓLIKA W ŚWIETLE BADAŃ LIPIDOWYCH

STRESZCZENIE PRACY HABILITACYJNEJ

Nerw wzrokowy, będący integralną częścią ośrodkowego układu nerwowego, dzięki swej jednorodnej strukturze pozwala na obiektywizację danych biochemicznych, a jednocześnie na ścisłą ich korelację z badaniami morfologicznymi.

Nieliczni autorzy w pracach poświęconych składowi lipidowemu w rozwijającym się nerwie wzrokowym podkreślali nierównomierność przyrostu poszczególnych klas lipidów (Banik i wsp., 1968; Matheson, 1971; Detering, Wells, 1976; Adamczewska-Goncerzewicz, 1977). Na uzyskane wyniki wpływała, wzrastająca stale w okresie rozwoju, proporcja zawartej w nerwie wzrokowym mieliny.

O charakterze zmian w mielinie można dowiedzieć się o wiele więcej badając ją jako wyizolowaną frakcję. Kilka prac poświęconych temu problemowi (McBrinn, O'Brien, 1969; Ishibe, Yamamoto, 1979; Trapp i wsp., 1980) stanowiło jedynie prezentację wybranych etapów ontogenezy.

Stąd też wydało się celowe podjęcie próby kompleksowej analizy zmian lipidowych znamiennych dla procesu mielinizacji, uwzględniającej korelację ilościowych oraz jakościowych przesunięć lipidów w nerwie wzrokowym i pochodzącej z niego frakcji mielinowej. Ponadto, w celu bardziej precyzyjnego określenia zmian lipidowych w mielinizacji, podjęto analizę ilościowego różnicowania zawartości związków sterolowych w nerwie wzrokowym z uwagi na znaczenie głównego ich przedstawiciela — cholesterolu dla struktury osłonki mielinowej.

MATERIAŁ I METODY

Badania przeprowadzono na królikach rasy Szynszyl, płci obojga. Zwierzęta doświadczalne do badań całego nerwu wzrokowego podzielono na 6 grup wiekowych: 8, 18, 30, 48, 100 i 150—180 dni życia pozapłodowego, a dla wyizolowanej frakcji mielinowej z nerwu na 7 grup:

18, 26, 30, 34, 48, 100 i 150—180 dni. Frakcję mielinową wyodrębniano z nerwu wzrokowego przez ultrawirowanie w nieciągłym gradiencie gęstości sacharozy według metody Nortona i Poduslo (1973a). Kontrolę czystości frakcji mielinowej przeprowadzono przy użyciu mikroskopu elektronowego. Oznaczanie przyrostu mieliny i szczytu mielinizacji w nerwie wzrokowym królika przeprowadzono w grupie zwierząt w wieku: 18, 21, 24, 27, 30, 33, 36, 40, 43, 45, 60, 100 i 150—180 dni życia pozapłodowego metodą analizy wagowej podanej przez Nortona i Poduslo (1973b). Obojętne lipidy i galaktolipidy rozdzielano z całego nerwu i mieliny za pomocą chromatografii kolumnowej na Florisilu o ziarnie 100—120 mesh, według metody podanej przez Svennerholma (1964) i Kishimoto (1965). Cerebrozydy, sulfatydy i cholesterol rozdzielano za pomocą jednokierunkowej wstępującej chromatografii cienkowarstwowej na żelu krzemionkowym G według metody podanej przez Svennerholma (1964), a fosfolipidy za pomocą dwukierunkowej chromatografii cienkowarstwowej, według sposobu podanego przez Singha i wsp. (1971). Do ilościowego oznaczania zawartości cerebrozydów, sulfatydów oraz cholesterolu stosowano metody podane przez Svennerholma (1956) i Sperry i Webba (1950), a do oznaczania ilości fosfolipidów stosowano metodę podaną przez Bartletta (1959). Rozdział, oznaczanie oraz identyfikację wolnych steroli w całym nerwie wzrokowym oraz istocie białej półkul mózgu wykonano przy użyciu spektrometru mas firmy JEOL typ DMS-D 100, sprzężonym z chromatografem gazowym firmy JEOL typ IGC-20. Spektrometr mas był sterowany przez system danych z mikrokomputerem firmy JEOL typ IMA-231. Rozdział wolnych steroli prowadzono na kolumnie wypełnionej 3% OV-17 na nośniku Gas-Chrom Q o ziarnie 100—120 mesh. Ocena ilościowa chromatogramów była oparta na obliczaniu powierzchni pól przez wyznaczanie czasu retencji i wysokości piku. Rozdzielone w ten sposób wolne sterole bezpośrednio przekazywano do spektrometru mas w celu otrzymania widma mas (identyfikacja). W każdej grupie wiekowej przeprowadzono po 6 badań, a wyniki przedstawiono w postaci średnich ± odchylenie standardowe. Przy opracowaniu statystycznych wyników stosowano test Duncana oraz współczynnik korelacji liniowej Pearsona.

Uzyskane wyniki badań biochemicznych rozpatrywano w powiązaniu z morfologicznymi wykładnikami mielinizacji włókien nerwowych.

WYNIKI

Podczas dojrzewania całego nerwu wzrokowego następował systematyczny wzrost bezwzględnej ilości niemal wszystkich składników lipidowych. Największe wskaźniki wzrostu dotyczyły obu frakcji galaktolipidowych (cerebrozydów i sulfatydów), cholesterolu, plazmalogenu i sfingomielin.

Przyrost poszczególnych składników lipidowych był jednak nierównomierny. W całym nerwie wzrokowym w 8 dniu życia pozapłodowego, na chromatogramach cienkowarstwowych wykazano ślady cerebrozydów i sulfatydów, jednakże ilościowo nieoznaczalne. Stąd dominującymi lipidami w tym okresie były fosfolipidy. Najbardziej charakterystyczną zmianą we wszystkich okresach rozwoju nerwu był wzrost frakcji galaktolipidowej od śladowych ilości w 8 dniu życia pozapłodowego do około 35% w 180 dniu, z jednoczesnym spadkiem odsetka całkowitych fosfolipidów, w tym frakcji fosfatydylocholiny z około 40% w 8 dniu życia do 11% w grupie zwierząt dorosłych. Badania składu molowego wykazały, że z wyjątkiem najwcześniejszego okresu (8 dzień po urodzeniu), cholesterol był dominującym składnikiem lipidowym we wszystkich badanych okresach rozwoju nerwu. U zwierząt 18—30-dniowych kolejne miejsca po cholesterolu zajmowały cerebrozydy, fosfatydylocholina i plazmalogen. W późniejszych okresach rozwoju, podobnie jak i w grupie zwierząt dorosłych, plazmalogen zajął pozycję fosfatydylocholiny, umiejscawiając się na trzecim miejscu po cholesterolu i cerebrozydach. Analiza stosunków molowych pomiędzy poszczególnymi klasami lipidowymi wykazała, że podczas rozwoju całego nerwu wzrokowego królika można wyróżnić dwa okresy. Pierwszy, wczesny, od 8 dnia życia, charakteryzujący się szybkim odkładaniem galaktolipidów z poziomu zero i niewykrywalnym stosunkiem molowym galaktolipidów do fosfatydylocholiny (GL/FC) i cerebrozydów do fosfatydylocholiny (CE/FC) do stosunku molowego odpowiednio 1,4 i 1,0 dla GL/FC i CE/FC w 18 dniu życia pozapłodowego. W drugim okresie, powyżej 50 dnia życia, w grupie zwierząt 10-dniowych i dorosłych powyższy stosunek molowy był bardzo wysoki i wynosił odpowiednio 2,9 i 2,2. W 30 dniu życia pozapłodowego wysoki był stosunek molowy cholsterolu do fosfatydylocholiny (CH/FC), który z wartości 2,9 w tym okresie zmieniał się do wartości 4,4 u zwierzęcia dorosłego.

Mielina izolowana metodą Nortona i Poduslo (1973 a) w obrazie mikroskopowo-elektronowym wykazywała obecność licznych typowych blaszek mielinowych. Metodą wagową wykazano, że ilość mieliny w nerwie wzrokowym jest funkcją logarytmiczną wieku pozapłodowego i wyraża jej bezwzględny przyrost w procesie dojrzewania. Liniowy przyrost mieliny rozpoczynający się w 18 dniu, a postępujący aż do 180 dnia życia pozapłodowego, jest procesem rozciągającym się w czasie daleko poza okres aktywnej mielinogenezy, przypadającej na 26—35 dzień. Szczyt mielinizacji w nerwie wzrokowym przypadał na 30 dzień życia królika i wynosił 0,62 mg na dzień na nerw. W okresie tworzenia się osłonki mielinowej nerwu wzrokowego królika wzrastała zawartość prawie wszystkich lipidiów mieliny. Największe wskaźniki wzrostu dotyczyły cholesterolu oraz frakcji galaktolipidowej, w tym z dużym bezwzględnym przyrostem cerebrozydów i sulfatydów. U królików pomię-

dzy 18 a 48 dniem życia następował bardzo wolny bezwzględny przyrost fosfatydylocholiny, a w grupie zwierząt 100-dniowych i dorosłych, bardzo znaczny spadek tego fosfolipidowego składnika. Skład molowy wykazał, że w okresie tworzenia się osłonki mielinowej, głównym lipidem we wszystkich badanych grupach wiekowych był cholesterol. Po nim, już we wczesnych okresach rozwoju mieliny drugą pozycję zajmowały cerebrozydy, a w grupie zwierząt 100-dniowych i dorosłych trzecią pozycję zajmował plazmalogen. W osłonce mielinowej stosunek molowy GL/FC był znacznie wyższy niż w całym nerwie wzrokowym. W 18 dniu życia wynosił aż 3,7 i zmieniał się do wartości 5,5 i 9,3 w grupie królików 100-dniowych i dorosłych. Na szczycie mielinizacji (30 dzień) stosunek molowy cholesterolu do cerebrozydów (CH/CE był największy. Wysoki był również stosunek molowy cholesterolu do fosfatydylocholiny (CH/FC), zwłaszcza w późniejszych okresach rozwoju.

Techniką chromatografii gazowej-spektrometrii mas rozdzielono i zidentyfikowano po raz pierwszy w rozwijającym się nerwie wzrokowym królika następujące wolne sterole: cholesterol, desmosterol, 4,4-dwumetylo-5α-cholest-8,24-dien-3β-ol o c.cz. 412, 4α, 14α-dwumetylo-5α-cholest-7-en-3β-ol o c.cz. 414, 4,4,14α-trójmetylo-5α-cholest-8,24-dien-3β-ol o c.cz. 426 (lanosterol) oraz pochodną sterolu — cholesten o c.cz. 368. Skład steroli rozwijającego się nerwu wzrokowego królika porównano z istotą białą półkul mózgu tego samego zwierzęcia w takich samych okresach rozwoju ontogenetycznego. Wykazano, że skład steroli nerwu wzrokowego różni się nie tylko od składu dojrzałego nerwu, ale również od niedojrzałej istoty białej. W obu tkankach dominującym sterolem we wszystkich okresach rozwoju był cholesterol. W 8 i 18 dniu życia stwierdzono względnie wysoką zawartość lanosterolu, stanowiącą około 1/4 całkowitych steroli, podczas gdy lanosterol istoty białej nie przekraczał 1/10 całkowitych steroli. Dwa dwumetylosterole o c.cz. 412 i 414 stanowiły największy procent w dwóch pierwszych okresach rozwoju nerwu (8 i 18 dzień), a w istocie białej tylko w 18 dniu życia zwierzęcia. Zawartość procentowa desmosterolu w nerwie wzrokowym była największa w grupie zwierząt 18-dniowych, a w istocie białej w grupie 8-dniowej. W dojrzałym nerwie wzrokowym oraz w dojrzałej istocie białej mózgu można było wykryć tylko trzy sterole: cholesterol, desmosterol i pochodną sterolu — cholesten.

OMÓWIENIE

Zmiany w składzie lipidowym w okresie dojrzewania nerwu wzrokowego były przedstawione dotychczas jedynie w sposób fragmentaryczny (Detering, Wells, 1976; Banik i wsp., 1968; Adamczewska-Goncerze-

wicz, 1977). W toku rozwoju nerwu wzrokowego różnych ssaków wzrasta zawartość prawie wszystkich lipidów. Wzrost ten jednakże nie jest równomierny dla różnych klas, a także dla poszczególnych lipidów. Co więcej, istnieją znaczne różnice w ilościowym udziale poszczególnych związków w całej puli lipidowej. Porównania te nie mogą być zbyt ścisłe ze względu na różne gatunki zwierząt doświadczalnych, wykazujących odmienny przebieg dojrzewania nerwu. Wykazany w badaniach własnych systematyczny wzrost zawartości prawie wszystkich lipidów, wraz z nieproporcjonalnym wzrostem galaktolipidów i plazmalogenu w rozwijającym się nerwie wzrokowym, wydaje się odbiciem zmian, zachodzących podczas dojrzewania nerwu we wszystkich jego elementach, a więc zarówno w mielinie, w aksonach, jak i w komórkach oligodendrogleju. Cerebrozydy i sulfatydy są jednak najbardziej dynamicznie wzrastającymi lipidami, a odkładanie się ich podczas rozwoju i mielinizacji decyduje według Nussbauma i wsp. (1969) o fizycznej stabilności błony mielinowej. To szczególne odkładanie się galaktolipidów i plazmalogenu w nerwie wzrokowym królika między 8 a 180 dniem życia dobrze ilustrują zmiany w stosunkach molowych, zachodzące pomiędzy poszczególnymi lipidami (Adamczewska-Goncerzewicz, 1977). Szczególnie wysokie stosunki molowe GL/FC, CE/FC i CH/FC, które według Nortona i Poduslo (1973b) są czułymi wskaźnikami w procesie rozwoju i mielinizacji, zmieniały się znacznie podczas dojrzewania nerwu i mogą świadczyć o strukturalnych zmianach w nim zachodzących we wszystkich badanych okresach rozwoju. Te zmieniające się i wysokie stosunki molowe mogą być także dowodem, że dojrzewaniu nerwu towarzyszy selektywna wymiana fosfatydylocholiny i fosfatydyloetanoloaminy na cholesterol, cerebrozydy i plazmalogen. Przyrost typowych składników lipidowych — galaktolipidów — w okresie wczesnym, a plazmalogenu w późnym okresie rozwoju, może być bezpośrednim następstwem zwiększania się ilości osłonek w dojrzewającym nerwie, powodujących odkładanie się nowo uformowanej mieliny, podczas gdy zmiany zachodzące w późniejszych okresach dojrzewania mogą być odbiciem strukturalnego przekształcania się samej osłonki mielinowej z formy „niedojrzałej", podobnej składem do błony glejowej (Aschworth, 1966), w formę „dorosłą".

Powyższe wnioski, wynikające z badania całego nerwu wzrokowego, zostały lepiej udokumentowane w analizie jego frakcji mielinowej. Metoda wagowa określająca przyrost mieliny wykazała, że proces ten jest ilościowo uchwytny już w 18 dniu życia pozapłodowego, a największy dzienny przyrost, czyli szczyt mielinizacji przypada na 30 dzień życia zwierzęcia. Zjawisko to jest zgodne z wynikami badań morfologicznych Skoffa i wsp. (1976) oraz Wendera i wsp. (1979), dowodzących możliwości syntezy specyficznych lipidów błon mielinowych przez oligodendroblasty. Jednocześnie wykazany metodą wagową liniowy przyrost mie-

liny aż do 180 dnia życia potwierdza opinie Horrocksa (1968; 1973) i Adamczewskiej (1978), że proces ten rozciąga się w czasie, daleko poza okres aktywnej mielinogenezy. Procesowi temu towarzyszy bezwzględny przyrost stabilizujących błonę mielinową galaktolipidów oraz cholesterolu, który według Banika i wsp. (1968) ma być ilościowym wskaźnikiem masy mieliny.

Z kolei, analiza składu molowego, jak i stosunków molowych pomiędzy poszczególnymi klasami lipidów, wykazała jakościową różnicę błony mielinowej wcześniejszego w porównaniu z późniejszym okresem dojrzewania (Adamczewska-Goncerzewicz, 1980). Zamiana miejscami plazmalogenu z fosfatydylocholiną wśród dominujących klas lipidowych, wzrost stosunku molowego CH/CE oraz stale wzrastający i bardzo wysoki stosunek molowy GL/FC charakteryzowały proces dojrzewania mieliny. Jeden z aspektów tych zmian jakościowych może być wyjaśniony przez możliwość selektywnej wymiany lipidów (w szczególności fosfatydylocholiny i fosfatydyloetanoloaminy na cerebrozydy i plazmalogen) w uformowanej już osłonce mielinowej, postulowaną przez Jungawala i Davisona (1971) oraz Ishibe i wsp. (1977).

Uzyskane wyniki stanowią pierwsze systematyczne opracowanie składu lipidowego frakcji mielinowej nerwu wzrokowego królika. Poprzednio były wykonywane fragmentaryczne badania mieliny nerwu wzrokowego na innych gatunkach zwierząt: dorosłego wołu (MacBrinn i O'Brien, 1969), dorosłego królika (Ishibe i Yamamoto, 1979) i kijanki (Trapp i wsp., 1980). Wszystkie te badania, wykonywane metodami chromatografii cienkowarstwowej, wykazały ilościową dominację cholesterolu podczas wszystkich okresów mielinizacji. Natomiast dalsza analiza ilościowego różnicowania zawartości związków sterolowych w nerwie wzrokowym, w porównaniu z istotą białą mózgu w tych samych okresach ontogenezy okazała się możliwa jedynie przy zastosowaniu bardziej czułej metody. Zastosowana w badaniach nerwu wzrokowego technika chromatografii gazowej-spektrometrii mas (Adamczewska-Goncerzewicz, Trzebny, 1981) umożliwiła po raz pierwszy wyodrębnienie i zidentyfikowanie, poza cholesterolem, szeregu innych steroli, tak w rozwijającym się nerwie wzrokowym, jak i w istocie białej półkul mózgu. Ponadto, ogólna tendencja zmian składu sterolowego podczas dojrzewania jest identyczna w obu tkankach, co potwierdzają prace dotyczące całego mózgu (Ramsey i wsp., 1971; Ramsey, Nicholas, 1972; Rostas, 1975). Przy stałej dominacji cholesterolu udział innych steroli (lanosterol, desmosterol i dwumetylosterole o c.cz. 412 i 414) spadał systematycznie w miarę dojrzewania nerwu. Występowały jednak w poszczególnych okresach rozwoju znaczne różnice odsetkowe (zwłaszcza dotyczące lanosterolu) składu sterolowego nerwu wzrokowego w porównaniu z istotą białą półkul mózgu. Świadczyć to może o jakościowo różnych przemianach strukturalnych dokonujących się w obu tkankach

w okresie dojrzewania. Wytłumaczeniem tej różnicy mogą być z jednej strony odmienności topograficzne — większa ilość elementów niemielinowych oraz późniejsza mielinizacja istoty białej półkul mózgu (Adamczewska, 1982; Pankrac, 1980). Z drugiej strony na różnicę tę wpłynąć może, potwierdzony badaniami Davisona (1972), fakt istnienia wymiany steroli pomiędzy różnymi błoniastymi strukturami podkomórkowymi. Niemniej różnice te zanikały całkowicie pod koniec okresu dojrzewania i skład sterolowy obu tkanek stawał się identyczny.

Występujące w nerwie wzrokowym oraz istocie białej półkul mózgu obok cholesterolu inne związki sterolowe, wydają się jego naturalnymi prekursorami, a proces ich przekształcania się w cholesterol jest jednym z wykładników dojrzewania ośrodkowego układu nerwowego.

WNIOSKI

1. W nerwie wzrokowym oraz w wyizolowanej z niego frakcji mielinowej występuje w czasie ontogenezy systematyczny wzrost bezwzględnej ilości prawie wszystkich składników lipidowych.

2. Nierównomierny przyrost poszczególnych lipidów nerwu wzrokowego wypływa z jego wzbogacania się w swoiste lipidy mielinowe, przy czym dla wczesnego okresu ontogenezy charakterystyczny jest wzrost galaktolipidów, a dla późnego — plazmalogenu. Zjawiska te można powiązać kolejno z przyrostem bezwzględnej ilości mieliny, a następnie z przekształcaniem się osłonki mielinowej w formę dojrzałą.

3. Podczas rozwoju antogenetycznego stwierdza się bezwzględny liniowy przyrost mieliny, czemu towarzyszy stwierdzany w analizie frakcji mielinowej nerwu wzrokowego bezwzględny przyrost stabilizujących błonę mielinową galaktolipidów i cholesterolu. Miarą dojrzałości błony mielinowej jest stale wzrastający i ostatecznie bardzo wysoki stosunek molowy GL/FC, CH/FC i Plaz/FE.

4. Dominującemu lipidowi mieliny — cholesterolowi — towarzyszy w procesie dojrzewania nerwu wzrokowego pięć pośrednich związków sterolowych, będących jego bezpośrednimi prekursorami, a proces ich przekształcania się w cholesterol jest jednym z wykładników dojrzewania ośrodkowego układu nerwowego.

PIŚMIENNICTWO

1. Adamczewska-Goncerzewicz Z.: Lipid composition of the rabbit optic nerve during ontogenic development. Folia Biol. (Kraków), 1977, 25, 415—423.
2. Adamczewska Z.: Myelin lipids in the developing rat brain. Neuropat. Pol., 1978, 1, 11—23.
3. Adamczewska-Goncerzewicz Z.: Changes in the myelin lipids of the rabbit optic nerve during ontogenic development. Neuropat. Pol., 1980, 2, 169—180.
4. Adamczewska-Goncerzewicz Z., Trzebny W.: Free sterol composition of the

rabbit optic nerve and cerebral white matter during ontogenic development. J. Neurochem., 1981, 36, 1378—1382.
5. Aschworth L. E.: Plasma membranes: phospholipid and sterol content. Science, 1966, 151, 210—211.
6. Banik N. L., Blunt M. J., Davison A. N.: Changes in the osmiophilia of myelin and lipid content in the kitten optic nerve. J. Neurochem., 1968, 15, 471—475.
7. Bartlett G.: Phosphorus assay in column chromatography. J. Biol. Chem., 1959, 234, 466—468.
8. Davison A. N.: Metabolism of myelin lipids in the developing brain. Biochem. Soc. Symp., 1972, 35, 129—139.
9. Detering N., Wells E.: The non-synchronous synthesis of myelin components during early stages of myelination in the rat optic nerve. J. Neurochem., 1976, 26, 253—257.
10. Horrocks L. A.: Composition of mouse brain myelin during development J. Neurochem., 1968, 15, 483—488.
11. Horrocks L. A.: Composition and metabolism of myelin phosphoglycerides during maturation and aging. W: Neurobiological aspects of maturation and aging. Elsevier, Amsterdam 1973, 383—395.
12. Ishibe T., Yamamoto A., Nishikawa M.: Regional differences in sphingolipid composition in the nervous system. Neurochem. Res., 1977, 2, 344—351.
13. Ishibe T., Yamamoto A.: Regional differences in lipid composition in rabbit nervous tissue. J. Neurochem., 1979, 32, 1665—1670.
14. Jungawala F. B., Davison A. N.: The turnover of myelin phospholipids in the adult and developing rat brain. Biochem. J., 1971, 123, 683—689.
15. Kishimoto Y., Davies W. E., Radin N. S.: Turnover of fatty acids of rat brain gangliosides, glycerophosphatides, cerebrosides, and sulfatides as a function of age. J. Lipid Res., 1965, 6, 525—531.
16. MacBrinn M. C., O'Brien J. S.: Lipid composition of optic nerve myelin. J. Neurochem., 1969, 16, 7—12.
17. Matheson D. F.: Evidence in support of centripedal gradient in myelination in the rat optic nerve. Exp. Neurol., 1971, 32, 195—205.
18. Norton W. T., Poduslo S. E.: Myelination of rat brain: method of myelin isolation. J. Neurochem., 1973a, 21, 749—757.
19. Norton W. T., Poduslo S. E.: Myelination in rat brain: changes in myelin composition during brain maturation. J. Neurochem., 1973b, 21, 759—773.
20. Nussbaum J. L., Nescovic N., Mandel P.: A study of lipid composition in brain in the "Jimpy" mouse, a mutant with myelin deficiency. J. Neurochem., 1969, 16, 927—934.
21. Pankrac J.: Odkładanie się mieliny w rozwijającym się mózgu szczura ze szczególnych uwzględnieniem późnego okresu dojrzewania, Neuropat. Pol., 1982, 20, 25—29.
22. Ramsey R. B., Aexel R. T., Nicholas H. J.: Formation of methyl sterols in brain cholesterol biosynthesis. J. Biol. Chem., 1971, 216, 6393—6400.
23. Ramsey R. B., Nicholas H. J.: Brain lipids. Adv. Lipid Res., 1972, 10, 143—232.
24. Rostas J. A. P., McGregor A., Jefferey P. L., Austin L.: Transport of cholesterol in the chic optic system. J. Neurochem., 1975, 24, 295—302.
25. Singh H., Spritz N., Geyer B.: Studies of brain myelin in the "quaking mouse". J. Lipid Res., 1971, 12, 473—481.
26. Skoff R. P., Price D. L., Stocks A.: Electron microscopic autoradiographic studies of gliogenesis in rat optic nerve. I. Cell proliferation. J. Comp. Neurol., 1976, 169, 291—312.

27. Sperry W., Webb M.: A revision of the Schoenheimer-Sperry method for cholesterol determination. J. Biol. Chem., 1950, 187, 97—106.
28. Svennerholm L.: The quantitative estimation of cerebrosides in nervous tissue. J. Neurochem., 1956, 1, 42—53.
29. Svennerholm L.: The distribution of lipids in the human nervous system. J. Neurochem., 1964, 11, 839—859.
30. Trapp B. D., McIntyre L. J., Quarles R. H., Nonakat G., Moser A., Moser H. W., Webster H. F.: Biochemical characterisation of myelin isolated from the central nervous system of Xenopus tadpoles. J. Neurochem., 1980, 34 (5), 1241—1246.
31. Wender M., Kozik M., Śniatała-Kamasa M., Mularek O., Pankrac J.: Neuroglia of the optic nerve in the course of myelination. J. Hirnforsch., 1979, 29, 191—200.

Adres autorki: Klinika Neurologii AM, ul. Przybyszewskiego 49, 60—355 Poznań

SPIS TREŚCI
CONTENTS

M. Wender, M. Kozik, O. Mularek: Histochemistry of neuroglial enzymes in the developing rabbit optic nerve 1
M. Śniatała-Kamasa: Ultrastructural picture of the optic nerve in rabbit during ontogenetic development 11
J. Pankrac: Myelin formation in developing rat brain with particular reference to the late maturation period 25
A. Goncerzewicz, W. Biczysko, W. Citowicki: Wallerian degeneration in the myelinating rabbit optic nerve 31
A. Goncerzewicz: Electron microscopic study of astrocytic reaction in Wallerian degeneration of the rabbit optic nerve 47
P. Kozłowski: Pathomechanism of periventricular white matter necrosis in newborns (Preliminary report) 61
J. Lehman: Polymicrogyria and porencephaly after intrauterine cytomegaly virus infection 71
M. Dąmbska, D. Maślińska: Effect of Dichlorfos (DDVP) intoxication of rabbit brain 77
Z. Kraśnicka: Effect of serum from patients with uremic syndrome and of exogenous urea and creatinine on organotypic nerve tissue culture . . 85
Z. Stelmasiak: Effect of ischemia on monoamine metabolism. Brain monoamine metabolites in cerebrospinal fluid of patients with recent cerebral infarction 97
W. Jänisch, D. Schreiber, H. Gerlach: Aneurysms of the basal arteries as the cause of intracerebral circulatory disturbances 107
J. Dąbrowska: Choroid plexuses in cerebral atherosclerosis (Preliminary communication) 113
H. Hager, P. Zimmermann: Morphology and cytometry of sural nerve in Tangier disease 123
M. Gallai: Peroneal muscular atrophy. Electronmicroscopic studies . . . 129
H. Weinrauder, S. Krajewski: Location of specific antigens in brain by immunofluorescence in homo- and heterologous systems 137
J. Juraniec, R. E. Steiner, E. G. Jones: Some connections of the basal nucleus of Meynert in the squirrel monkey (Saimiri Sciureus) 143
R. Warzok, H. Warzok: The influence of hypoxia on the induction of experimental brain tumors in rats 151
J. Szymaś, W. Biczysko, P. Gabryel, H. Prokopanov: Histological features of meningiomas with their ultrastructural aspects 155
J. Alwasiak, G. Hajdukiewicz, M. Karasek, K. Marek, M. Majak, W. Papierz: Some aspects of the ultrastructure of gliomas 169
M. Majak, J. Alwasiak, W. Papierz, M. Pruszczyński: Types of growth and spread of brain lymphomas 175

II-ND POLISH-SCANDINAVIAN NEUROPATHOLOGICAL SYMPOSIUM. ABSTRACTS 183
H. Weinrauder, Z. Kraśnicka, B. Gajkowska: Wpływ surowicy antyglejowej na pozaustrojową hodowlę móżdżku noworodka szczura 207
M. Wender, M. Śniatała-Kamasa, A. Piechowski: Myelin of the optic nerve in rats chronically intoxicated with triethyl tin sulfate (TET) . . . 223
J. Szczech, M. Kontek: Zmiany morfologiczne w mózgu szczura po doświadczalnym zatruciu bromfenwinfosem (Ipofos-IPO 62) 239
Z. Kraśnicka, K. Olszewska: Wpływ etylonitrozomocznika (ENU) na organotypową hodowlę tkanki nerwowej (Badania w mikroskopie świetlnym i elektronowym) 253
B. Gajkowska: Ultrastruktura układu przysadkowo-nadnerczowego szczura w stresie wywołanym unieruchomieniem 277
R. Gadamski, D. G., Baramidze, G. I. Mchedlishvili, Z. T. Gordeładze: Unerwienie wegetatywne oraz aktywność niektórych enzymów w naczyniach opony miękkiej królików z jedno- i obustronnie usuniętym zwojem szyjnym górnym 285
Z. Adamczewska-Goncerzewicz: Rozwój nerwu wzrokowego królika w świetle badań lipidowych (Streszczenie pracy habilitacyjnej) 305
Komunikaty 106, 112
J. Dymecki: Dział kroniki i informacji 136, 150, 174

Zakład Narodowy im. Ossolińskich — Wydawnictwo. Wrocław 1983. Nakład: 650 egz. Objętość: ark. wyd. 21,70, ark. druk. 19,75, ark. A_1 - 26. Papier ilustracyjny kl. III, 70 g, 70 × 100. Oddano do składania 6 VII 1982. Podpisano do druku 28 I 1983. Druk ukończono w lutym 1983. Wrocławska Drukarnia Naukowa. Zam. 1225/82. H-11. Cena zł 120.—

Cena zł 120,—

Indeks 36668